AD-A087 135 ARMY ENGINEER WATERWAYS EXPERIMENT STATION VICKSBURG--ETC F/G 13/11
FIELD TESTS OF PLASTIC PIPE FOR AIRPORT DRAINAGE SYSTEMS.(U)
DEC 79 W J HORN DOT-FA75WAI-536
UNCLASSIFIED WES/TR/GL-79-24 FAA-RD-79-86 NL

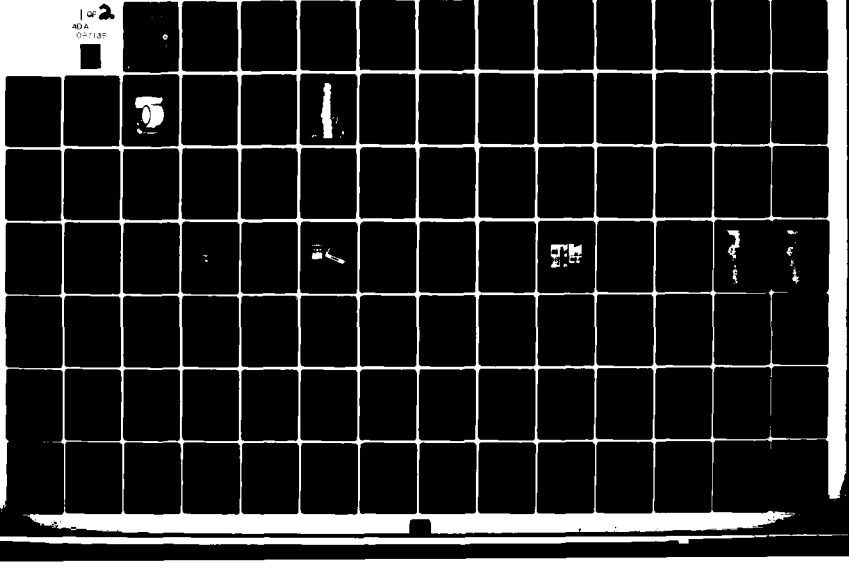

Report No. FAA-RD-79-86
WES TR GL-79-24

LEVEL II

12

FIELD TESTS OF PLASTIC PIPE FOR AIRPORT DRAINAGE SYSTEMS

Walter J. Horn

U. S. Army Engineer Waterways Experiment Station
Geotechnical Laboratory
P. O. Box 631, Vicksburg, Miss. 39180

DECEMBER 1979
FINAL REPORT

Prepared for

DEPARTMENT OF DEFENSE
DEPARTMENT OF THE ARMY
Office, Chief of Engineers
Washington D. C. 20314

U. S. DEPARTMENT OF TRANSPORTATION
FEDERAL AVIATION ADMINISTRATION
Systems Research & Development Service
Washington, D. C. 20591

80 8 04 000

NOTICES

This document is disseminated under the sponsorship of the Department of Transportation in the interest of information exchange. The United States Government assumes no liability for its contents or use thereof.

The United States Government does not endorse products or manufacturers. Trade or manufacturers' names appear herein solely because they are considered essential to the object of this report.

Technical Report Documentation Page

1. Report No.	2. Government Accession No.	3. Recipient's Catalog No.
FAA-RD-79-86		

4. Title and Subtitle	5. Report Date
FIELD TESTS OF PLASTIC PIPE FOR AIRPORT DRAINAGE SYSTEMS	December 1979
	6. Performing Organization Code
7. Author(s) Walter J. Horn	8. Performing Organization Report No. WES TR GL-79-24
9. Performing Organization Name and Address U. S. Army Engineer Waterways Experiment Station Geotechnical Laboratory P. O. Box 631, Vicksburg, Miss. 39180	10. Work Unit No. (TRAIS)
	11. Contract or Grant No. DOT-FA75WAI-536
12. Sponsoring Agency Name and Address	13. Type of Report and Period Covered Final Report October 1976 to March 1979
	14. Sponsoring Agency Code

15. Supplementary Notes
This study was sponsored by the Federal Aviation Administration, Systems Research and Development Service, under Interagency Agreement (IAA) No. DOT FA75WAI-536, March 1975, and the Office, Chief of Engineers, Facilities Investigation and Studies Program (O&M,A) project, "Use of Plastic Pipe for Drainage of Military Pavements."

16. Abstract

Airport designers are beginning to select plastic pipe as an alternative in the design of underdrains, storm sewers, culverts, and similar drainage elements at airports because plastic pipe is economical and easy to transport and install. This report provides information concerning the performance of buried plastic pipe under dynamic wheel loadings. Three types of plastic pipe - polyvinyl chloride (PVC) polyethylene (PE), and acrylonitrile-butadiene-styrene (ABS) - of different diameters were buried at different shallow depths at three separate test sites and were subjected to static and dynamic wheel loads.

The PVC pipe performed well under a range of loadings simulating highway and light- and medium-load aircraft traffic. Results for PE and ABS pipe followed. The report concludes that good pipe installation practices should be followed and that a compacted coarse-grained material should be used for bedding, haunching, and backfill to at least a depth of one pipe radius above the crown of the pipe. A cover depth of 12 in. is suggested for PVC pipe for highway 18-kip axle loads, 18 in. for heavier highway loadings and light aircraft traffic, and 24 in. of cover for PVC pipe subjected to medium-load aircraft. PE pipe should be protected with 18 in. of cover from 18-kip axle loads and with 24 in. of cover for heavier highway loads and light aircraft traffic. While 24 in. of cover seemed to be adequate cover for pipe subjected to medium-load aircraft, additional repetitive load tests are required in order to finalize a recommended safe cover depth.

17. Key Words	18. Distribution Statement
Plastic pipe Airport drainage Subsurface drainage	Document is available to the public through the National Technical Information Service, Springfield, Va. 22151.

19. Security Classif. (of this report)	20. Security Classif. (of this page)	21. No. of Pages	22. Price
Unclassified	Unclassified	180	

Form DOT F 1700.7 (8-72) Reproduction of completed page authorized

METRIC CONVERSION FACTORS

Approximate Conversions to Metric Measures

Symbol	When You Know	Multiply by	To Find	Symbol
		LENGTH		
in	inches	*2.5	centimeters	cm
ft	feet	30	centimeters	cm
yd	yards	0.9	meters	m
mi	miles	1.6	kilometers	km
		AREA		
in^2	square inches	6.5	square centimeters	cm^2
ft^2	square feet	0.09	square meters	m^2
yd^2	square yards	0.8	square meters	m^2
mi^2	square miles	2.6	square kilometers	km^2
	acres	0.4	hectares	ha
		MASS (weight)		
oz	ounces	28	grams	g
lb	pounds	0.45	kilograms	kg
	short tons (2000 lb)	0.9	tonnes	t
		VOLUME		
tsp	teaspoons	5	milliliters	ml
Tbsp	tablespoons	15	milliliters	ml
fl oz	fluid ounces	30	milliliters	ml
c	cups	0.24	liters	l
pt	pints	0.47	liters	l
qt	quarts	0.95	liters	l
gal	gallons	3.8	liters	l
ft^3	cubic feet	0.03	cubic meters	m^3
yd^3	cubic yards	0.76	cubic meters	m^3
		TEMPERATURE (exact)		
°F	Fahrenheit temperature	5/9 (after subtracting 32)	Celsius temperature	°C

*1 in = 2.54 (exactly). For other exact conversions and more detailed tables, see NBS Misc. Publ. 286, Units of Weights and Measures, Price $2.25, SD Catalog No. C13.10:286.

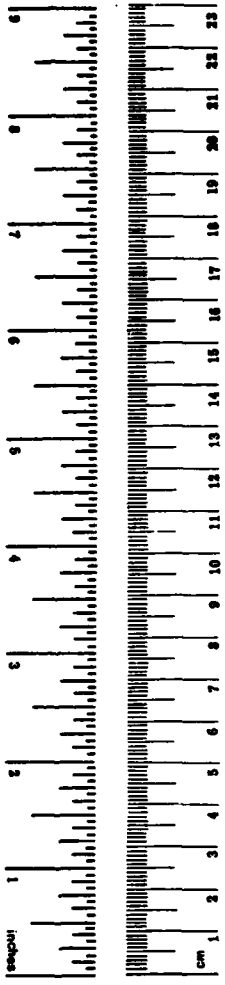

Approximate Conversions from Metric Measures

Symbol	When You Know	Multiply by	To Find	Symbol
		LENGTH		
mm	millimeters	0.04	inches	in
cm	centimeters	0.4	inches	in
m	meters	3.3	feet	ft
m	meters	1.1	yards	yd
km	kilometers	0.6	miles	mi
		AREA		
cm^2	square centimeters	0.16	square inches	in^2
m^2	square meters	1.2	square yards	yd^2
km^2	square kilometers	0.4	square miles	mi^2
ha	hectares (10,000 m^2)	2.5	acres	
		MASS (weight)		
g	grams	0.035	ounces	oz
kg	kilograms	2.2	pounds	lb
t	tonnes (1000 kg)	1.1	short tons	
		VOLUME		
ml	milliliters	0.03	fluid ounces	fl oz
l	liters	2.1	pints	pt
l	liters	1.06	quarts	qt
l	liters	0.26	gallons	gal
m^3	cubic meters	35	cubic feet	ft^3
m^3	cubic meters	1.3	cubic yards	yd^3
		TEMPERATURE (exact)		
°C	Celsius temperature	9/5 (then add 32)	Fahrenheit temperature	°F

PREFACE

The study reported herein was sponsored by the Federal Aviation Administration, Systems Research and Development Service, under Inter-Agency Agreement (IAA) No. DOT FA75WAI-536, March 1975, and the Office, Chief of Engineers, Facilities Investigation and Studies Program (O&M,A) project, "Use of Plastic Pipe for Drainage of Military Pavements."

This study was conducted under the overall supervision of Messrs. J. P. Sale, R. G. Ahlvin, R. L. Hutchinson, A. H. Joseph, and H. H. Ulery, Jr. This study was conducted by Dr. Walter J. Horn and Messrs. A. J. Bush III, H. G. Brown, and R. T. Sullivan of the Geotechnical Laboratory, U. S. Army Engineer Waterways Experiment Station (WES), during the period October 1976 to March 1979. This report was written by Dr. Horn.

COL John L. Cannon, CE, and COL Nelson P. Conover, CE, were Commanders and Directors of WES during the conduct of this study and preparation of this report. Mr. F. R. Brown was Technical Director.

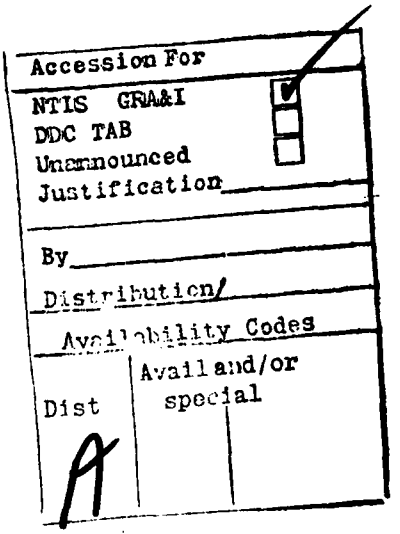

TABLE OF CONTENTS

	Page
INTRODUCTION	1
BACKGROUND	1
OBJECTIVES	2
SCOPE	2
DESCRIPTION OF PIPE TESTED	3
TEST SITE DESCRIPTION, PREPARATION, AND INSTALLATION OF PIPES	7
TEST SITE NO. 1, CIRCULAR TEST TRACK	7
TEST SITE NO. 2	23
TEST SITE NO. 3	26
INSTRUMENTATION SYSTEM	34
DISPLACEMENT TRANSDUCERS	34
DEFLECTOMETER	36
TESTING	39
LABORATORY TESTS	39
TRAFFIC TESTS	39
TEST SITE NO. 1	39
TEST SITE NO. 2	43
TEST SITE NO. 3	46
RESULTS	48
TEST SITE NO. 1	48
PVC PIPE	62
PE PIPE	71
ABS PIPE	72
TEST SITE NO. 2	72
PVC PIPE	77
PE PIPE	77
ABS PIPE	83
TEST SITE NO. 3	83
CONCLUSIONS	85
RECOMMENDATIONS	87
APPENDIX A: DYNAMIC AND PERMANENT PIPE DEFLECTIONS OF CTT	A-1
APPENDIX B: MEASURED DEFLECTOMETER DATA FOR PIPES AT TEST SITE NO. 2 FOR SIMULATED F-4 AND C-141 AIRCRAFT TRAFFIC AND FOR STATIC LOADS OF F-4 AND C-141 GEAR ASSEMBLIES	B-1

LIST OF ILLUSTRATIONS

Figure No.		Page
1	Dimensions of corrugations and wall thicknesses of PE pipe (1 in. = 2.54 cm)	4
2	Segments of each type of pipe investigated	6
3	Circular test track facility	8
4	Overall view of Circular Test Track facility	9
5	Subgrade classification data	11
6	CBR, density, and water content relationships for the subgrade and lean clay backfill	12
7	Layout of pipe installed in the Circular Test Track (Test Site No. 1)	13
8	Gradation curve of pea gravel backfill	15
9	Gradation curve for crushed stone base used at Circular Test Track	17
10	Gradation curve for aggregate used in the double-bituminous surface treatment of the Circular Test Track	18
11	Cross sections of pipe installed in the Circular Test Track	19
12	Layout of Test Site No. 2	25
13	Cross sections of pipe installed in Test Site No. 2	27
14	Details of installation of 12-in. PVC pipe at Test Site No. 3	33
15	Interior of PVC pipe with DCDT gages mounted in both the vertical and horizontal directions	35
16	Deflectometer and strain gage indicator	37
17	Parallel plate loading of PE pipe	41
18	Load cart simulating F-4 aircraft load	44
19	Load cart simulating C-141 aircraft load	45
20	Vertical deflection of 12-in. PVC pipe as a function of applied static load	51
21	Vertical deflection of 10-in. PVC pipe as a function of applied static load	52

Figure No.		Page
22	Vertical deflection of 6-in. PVC pipe in CTT as a function of applied static load	53
23	Vertical deflection of 10-in. PE pipe as a function of applied static load	54
24	Vertical deflection of 6-in. PE pipe in CTT as a function of applied static load	55
25	Vertical deflection of 4-in. PE and 4-in. PVC pipe in CTT as a function of the applied static load	56
26	Measured deflectometer data for 12-in. PVC pipe F1 of CTT (13-kip static load after 10,000 coverages; approximately 12,500 coverages of 18-kip axle load) . .	57
27	Measured deflectometer data for 10-in. PE pipe G1 of CTT (13-kip static load after 10,000 coverages; approximately 12,500 coverages of 18-kip axle load) . .	58
28	Typical oscillograph of dynamic load deflection	60
29	Variation of maximum value of dynamic load deflection with cover depth	61
30	Permanent deflection of 12-in. PVC pipe as a function of traffic (CTT)	64
31	Permanent deflection of 10-in. PVC pipe as a function of traffic (CTT)	65
32	Permanent deflection of 6-in. PVC pipe as a function of traffic (CTT)	66
33	Permanent deflection of 10-in. PE pipe as a function of traffic (CTT)	67
34	Permanent deflection of 6-in. PE pipe as a function of traffic (CTT)	68
35	Permanent deflection of 4-in.-diameter PE and PVC pipes	69
36	Permanent deflection of 15-in. ABS pipe as a function of traffic (CTT)	70
37	Summary of pipe deflections due to static loads at Test Site No. 2 (12-in. PVC pipe)	74
38	Summary of pipe deflections due to static loads at Test Site No. 2 (10-in. PE pipe)	75
39	Summary of pipe deflections due to static loads at Test Site No. 2 (15-in. ABS pipe)	76
40	Summary of permanent deflections of the 12-in. PVC pipe installed in Test Site No. 2	80

Figure No.		Page
41	Summary of permanent deflections of the 10-in. PE pipe installed in Test Site No. 2	81
42	Summary of permanent deflections of the 15-in. ABS pipe installed in Test Site No. 2	82
43	Permanent deflections of the 12-in. PVC pipe installed in Test Site No. 3	84

LIST OF TABLES

Table No.		
1	Total Permanent Deflection in Instrumented Pipes of Test Site No. 1 (CTT) at the Conclusion of Construction of the Test Site	24
2	Dry Density and Water Content of the Layers of the Pipe Trenches of Test Site No. 2	31
3	External Loading Properties of Pipe by Parallel Plate Loading	40
4	CTT Surface Elevations at the Center of the Traffic Lane Over Each Pipe	49
5	Summary of Pipe Deflections Resulting from Static Loads (Deflection/Pipe Interior Diameter) × 100	50
6	Summary of Permanent Pipe Deflection Data from Circular Test Track	63
7	Pipe Deflections Due to Static Loads on Pipe Installed in Test Site No. 2 (Percent of Internal Diameters)	73
8	Summary of Dynamic Load Response of Pipe Installed in Test Site No. 2	78
9	Summary of Permanent Pipe Deflections for the Pipe Installed in Test Site No. 2 (Percent of Internal Diameter)	79

INTRODUCTION

BACKGROUND

The potential economic benefit of plastic pipe, related to its light weight and associated ease of transportation and installation, has led to its wider use in recent years, particularly in agricultural and light construction applications. These same features of plastic pipe are now causing airport designers to consider plastic pipe as an alternative in the design of underdrains, storm sewers, culverts, and similar drainage elements at airports. With this increasing interest in using plastic pipe at airport sites comes the need for information concerning the performance of buried plastic pipe under dynamic loadings associated with airport traffic.

Many theoretical and experimental investigations have been conducted on the general subject of flexible pipes since 1941 when Professor M. G. Spangler* reported on the behavior of flexible pipe under earth loading. G. G. Harvey** gives a lengthy bibliography of the recently published works that have some bearing on the application of plastic pipe in airport pavements. Even though much work had been done with flexible pipe, there was a need for field tests to provide plastic pipe response data for shallow buried pipes under dynamic wheel loads, so that safe burial depths could be established. Therefore, in October 1976 the U. S. Army Engineer Waterways Experiment Station (WES) initiated a field study of plastic pipes for airport drainage systems. The work was sponsored by the Federal Aviation Administration (FAA) as part of an overall study entitled "Improved Criteria and Plastic Components for Airport Airside Drainage Systems." Additional support for the analysis and report writing phase of the study was received from the Office, Chief of Engineers, under an O&M,A project, "Use of Plastic Pipe for Drainage of Military Pavements."

---

* M. G. Spangler, "The Structural Design of Flexible Pipe Culverts," Bul 153, Iowa Engineering Experiment Station, Ames, Iowa, 1941.

** G. G. Harvey, "Plastic Pipe in Airport Drainage Systems," FAA-RD-77-38, U. S. Department of Transportation, Federal Aviation Administration, Washington, D. C., Jan 1977.

OBJECTIVES

The objectives of this study were to evaluate the performance of three types of plastic pipe at shallow burial depths subjected to dynamic wheel loads representative of the loads imposed upon buried pipes at airports and to develop tentative safe burial depths for each type of pipe tested.

SCOPE

The performance of three types of plastic pipes was determined by installing a number of pipes in three test sites and measuring the response of the pipes to a range of static and dynamic wheel loads. Pipe deflections were measured at various intervals of load applications. All pipes were installed in trenches with either lean clay or pea gravel as primary backfill. The pipes were installed at several cover depths to determine the minimum cover depth for each type of pipe for the tested loads.

DESCRIPTION OF PIPE TESTED

Three types of plastic pipe were used in the field tests. These were polyvinyl chloride (PVC), smooth-wall pipe of nominal diameters of 10 and 12 in.; polyethylene (PE), corrugated pipe with a nominal diameter of 10 in.; and acrylonitrile-butadiene-styrene (ABS), composite pipe of 15-in. nominal diameter. These three types were selected for study based upon the recommendations of an earlier study* in which they were found to be the most promising types of plastic pipes for airport drainage systems. Corrugated perforated PE tubing and perforated PVC sewer pipe were recommended for underdrains and the PVC and composite ABS sewer pipe were recommended for storm drains and small culverts.

The two sizes of PVC pipe tested were both PSM PVC nonpressure sewer pipe meeting ASTM D 3034-74. The 10-in. ID pipe had a standard dimension ratio (SDR) of 35 and the 12-in. ID pipe had an SDR of 42. Both pipes were purchased in 20-ft lengths.

The 10-in. corrugated and nonperforated PE pipe was purchased in 20-ft lengths. Harvey* gives a summary of the characteristics of the PE drainage pipe, and the dimensions of the corrugations and wall thickness are as shown on Figure 1.

The 15-in. ABS composite pipe investigated during the field tests was a double-wall pipe consisting of two thin concentric annular shells connected by diagonal plastic web elements that are continuous along the length of the pipe. The void area between the two shells is filled with a foam-mortar filler. The pipe was purchased in approximately 12-ft lengths.

Another plastic pipe field study** was conducted at WES simultaneously with the one reported herein. Small-diameter (4- and 6-in.) PVC and PE pipes were tested. When appropriate, the measured results of this study are included in this report.

---

* Harvey, op. cit., p. 1.

** A. J. Bush and R. T. Sullivan, "Dynamic Testing of Slotted Underdrain Pipe," FHWA-RD-79-501, U. S. Department of Transportation, Federal Highway Administration, Washington, D. C., Feb 1979.

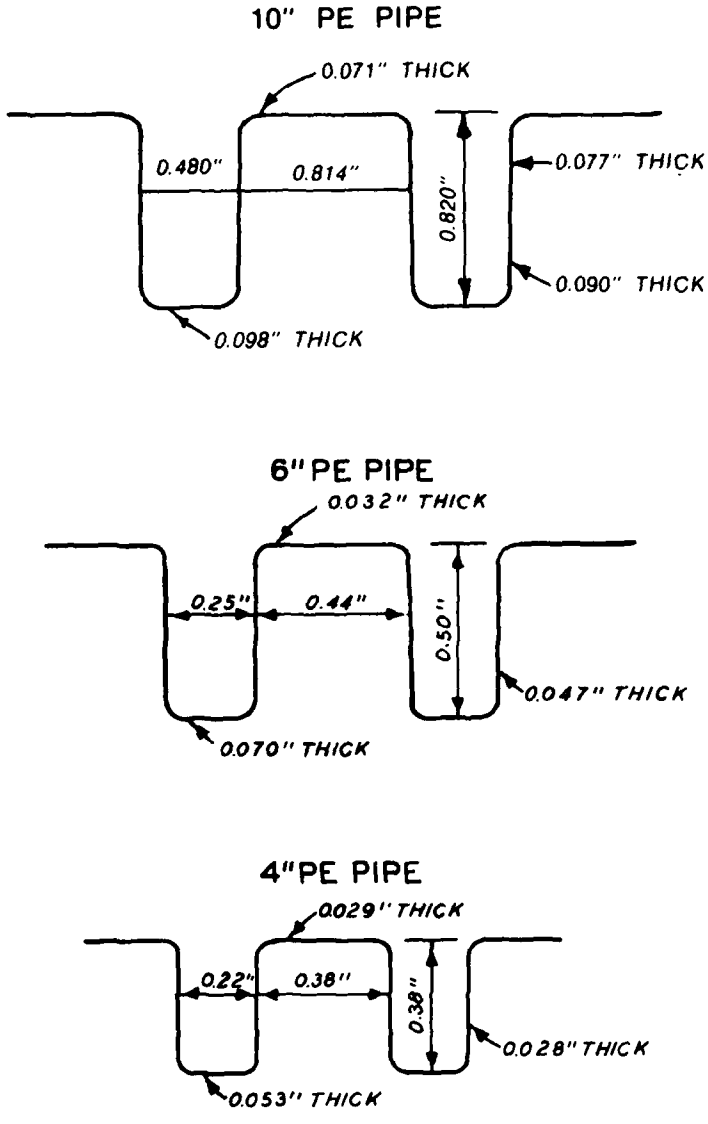

Figure 1. Dimensions of corrugations and wall thicknesses of PE pipe (1 in. = 2.54 cm)

Figure 2 contains a photograph of a sample of each size and type plastic pipe investigated during the reported and related studies.

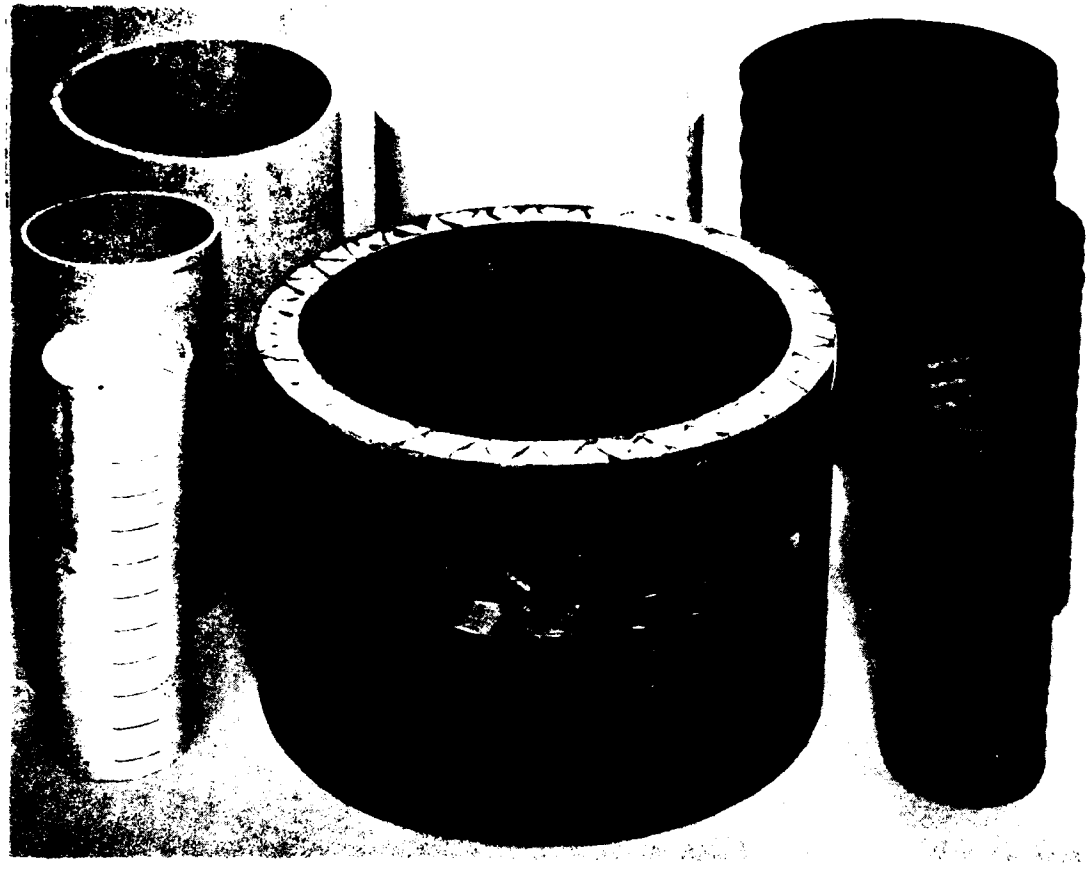

Figure 2. Segments of each type of pipe investigated

TEST SITE DESCRIPTION, PREPARATION, AND INSTALLATION OF PIPES

Three separate test sites were used during the field studies. The most productive, in terms of volume of data, was the WES Circular Test Track, hereafter referred to as Test Site No. 1 or the CTT. Thirty-two pipes were installed in this site and were loaded by a moving wheel load. Test Site No. 2 was the overrun area of a WES test section that utilized load carts capable of simulating aircraft gear load. Testing at this site became available well after the test plan was established for this project and near the completion of testing at the CTT. Additional field tests were conducted at this site because pipe deflection data for simulated aircraft loading conditions could be obtained at a fraction of the cost required to construct a test site dedicated exclusively to the plastic pipe study. Test Site No. 3 was of a very small scale relative to the two mentioned above. It consisted of the installation of one pipe in an existing test road at WES. The loading of this pipe was provided primarily by a military truck.

TEST SITE NO. 1, CIRCULAR TEST TRACK

The CTT consisted of a 21-ft-wide circular track contained within two concentric circular strips of concrete pavement, as shown on Figure 3. The interior radius of the test track was 28 ft and the outside radius was 49 ft. The outer strip of concrete was 7 ft wide and provided the surface for the propulsion unit. The inner circular strip of concrete provided the supporting surface for the idler bogie. The propulsion unit was attached to one end of a frame that pivoted about a concrete pedestal in the center of the track. The load cart and wheel were attached to this frame and could be traversed across the width of the track at a regulated rate while the frame revolved around the center of the track. The load cart is equipped with a dead-wheel assembly having 11.00-20 tires with a center-to-center spacing of 13.25 in. The load cart could accommodate a range of loads from 7,000 to 50,000 lb at maximum speeds of 15 to 40 mph depending upon the load. Figure 4 is a photograph of the CTT that shows the elements of the system described above.

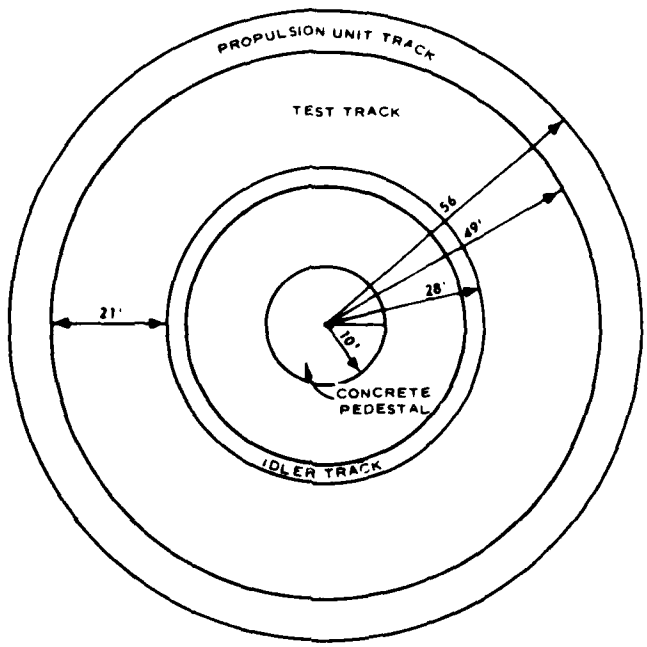

Figure 3. Circular Test Track facility

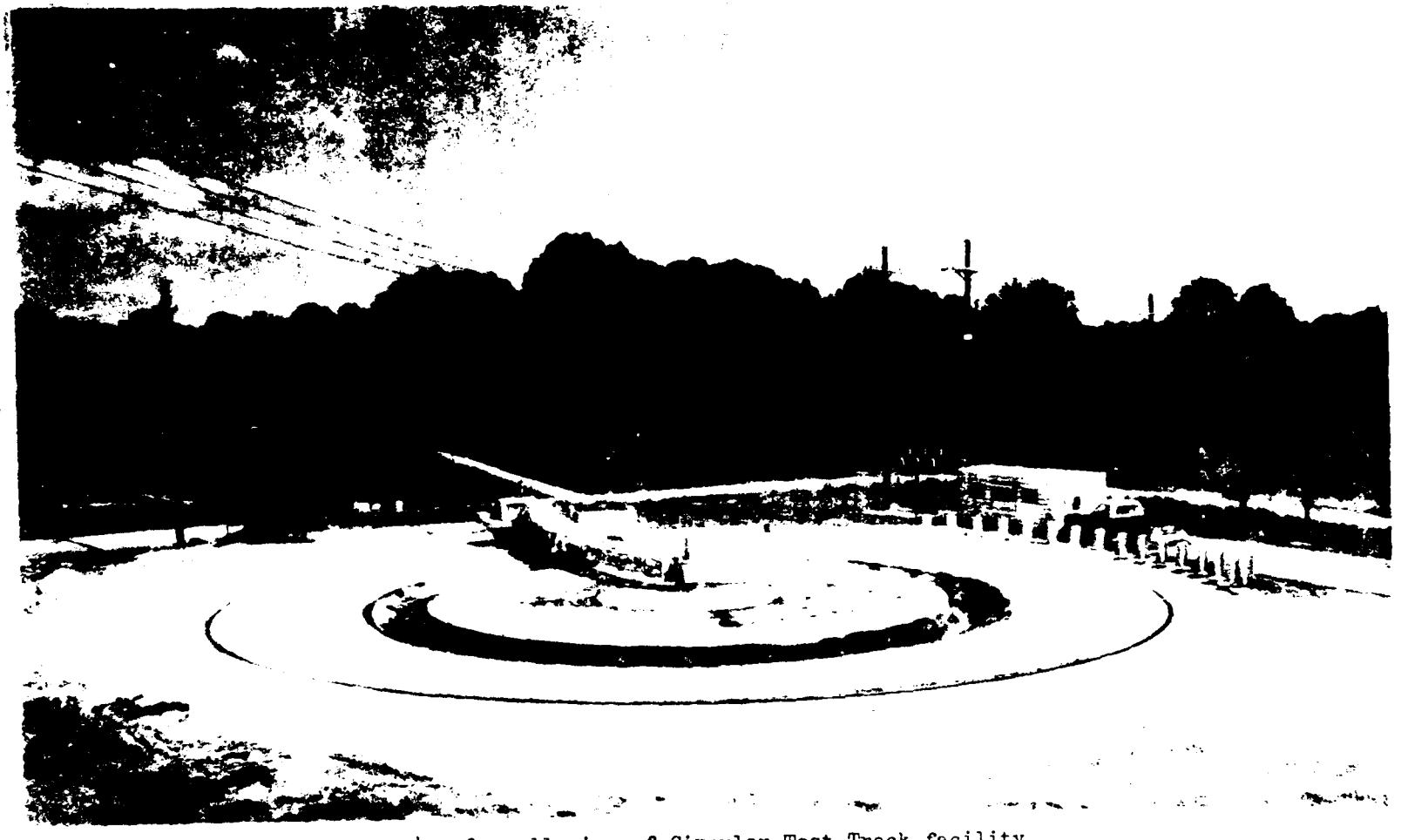

Figure 4. Overall view of Circular Test Track facility

The CTT was excavated to a depth of 26 in. The native lean clay (CL) found below 26 in. was compacted with a sheepsfoot roller. This compaction effort on the surface of the undercut resulted in an average dry density of 100.2 pcf, an average water content of 17.3 percent, and an average California Bearing Ratio (CBR) of 13.3. The water content of the lean clay was approximately 2 percent over optimum. Figure 5 shows the grain size distribution curve for the lean clay subgrade, and Figure 6 gives the CBR, density, and water content curves for the subgrade.

The elevation of the subgrade was brought up to the required depth by bringing in soil from a WES borrow area, which was the same as the material in the test track undercut. This was accomplished in three 8-in. lifts with each lift being compacted with the sheepsfoot roller pulled by a D-4 Caterpillar tractor. After compaction of the final lift, test pits were dug into the subgrade. Each pit was located between proposed locations of buried pipes so it would not disturb the conditions of these selected areas. Densities, CBR, and water content were measured in each test pit at the surface and at depths of 6, 12, and 24 in. Results from these pits indicated that the test site had an average CBR of 21, a water content of 16.8 percent, and a dry density of 100.5 pcf.

Figure 7 shows a layout of Test Site No. 1, showing the location of all the pipes installed in the CTT. Pipes labeled A through K, C1, F1, G1, H1, and K1 were the pipes used in this study. Their description, including type, diameter, type of backfill, nominal cover depth, and type of instrumentation, is given in Figure 7. Note that other plastic pipes were installed in the CTT during the period of testing These pipes, labeled 1 through 18, were part of a Federal Highway Administration (FHWA) sponsored study* to investigate the dynamic loading performance of plastic pipe underdrains. These field tests were conducted specifically for PE and PVC pipes with diameters of 4 and 6 in. The performance results for these pipes are included in this report to

---

* Bush and Sullivan, op. cit., p. 3.

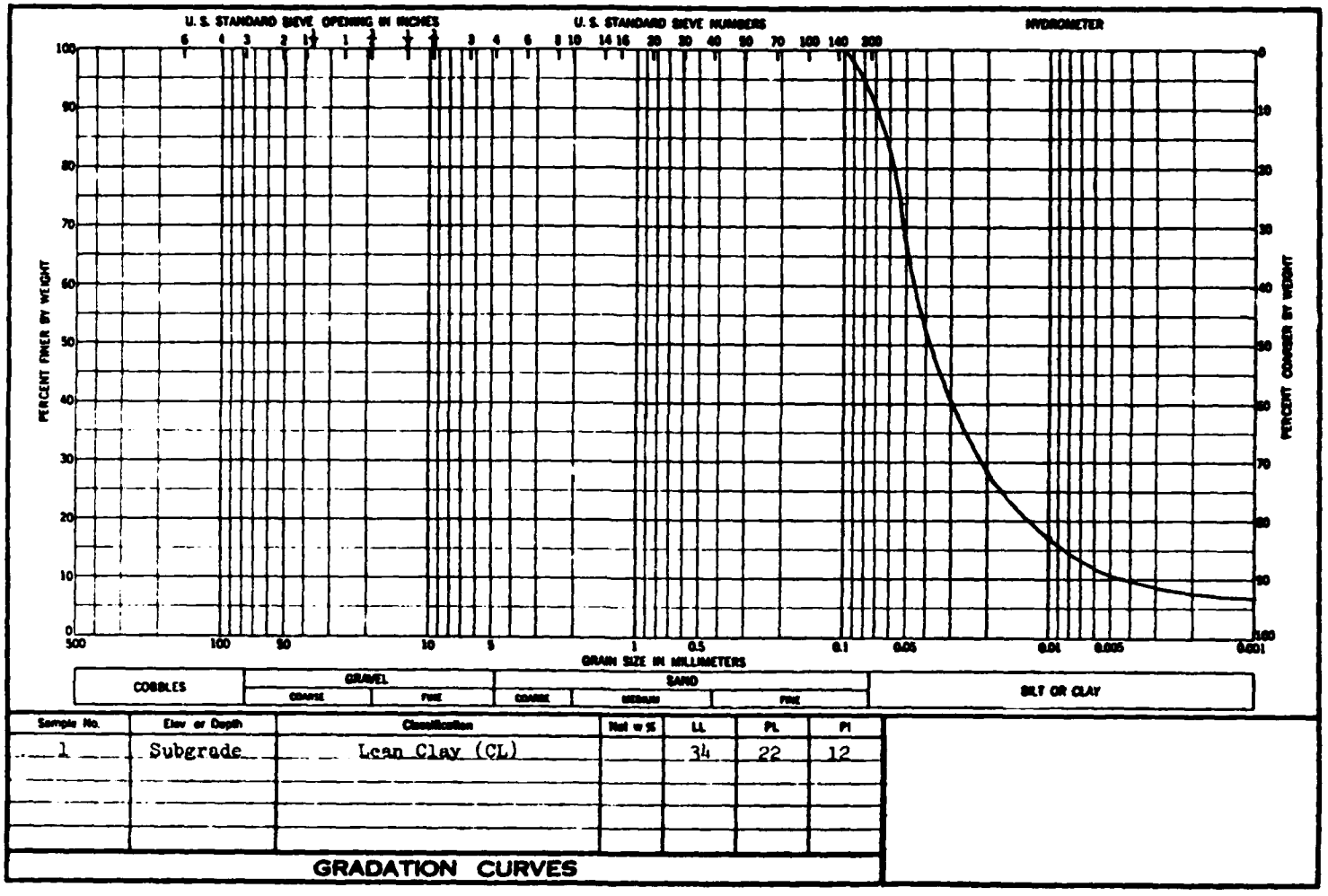

Figure 5. Subgrade classification data

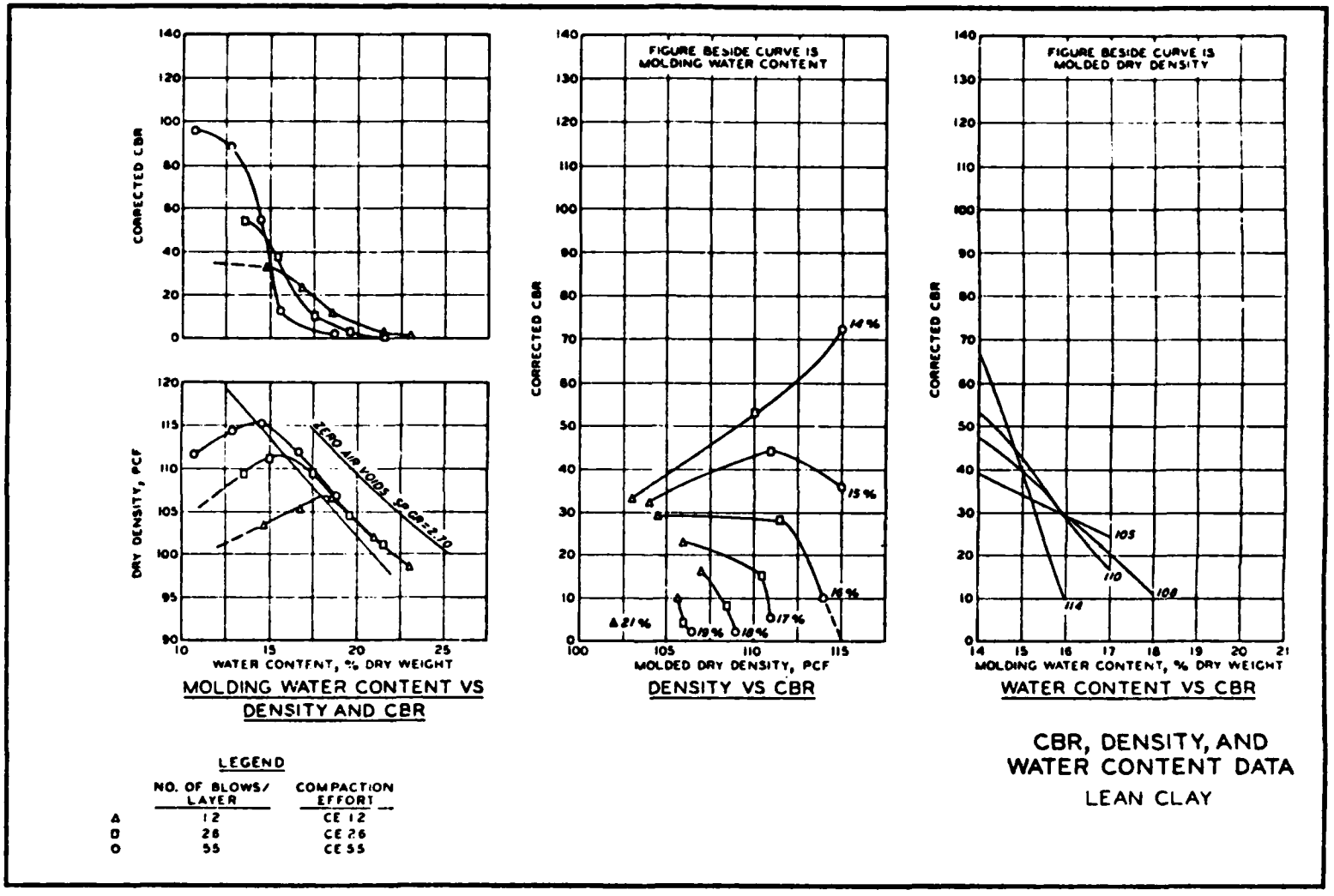

Figure 6. CBR, density, and water content relationships for the subgrade and lean clay backfill

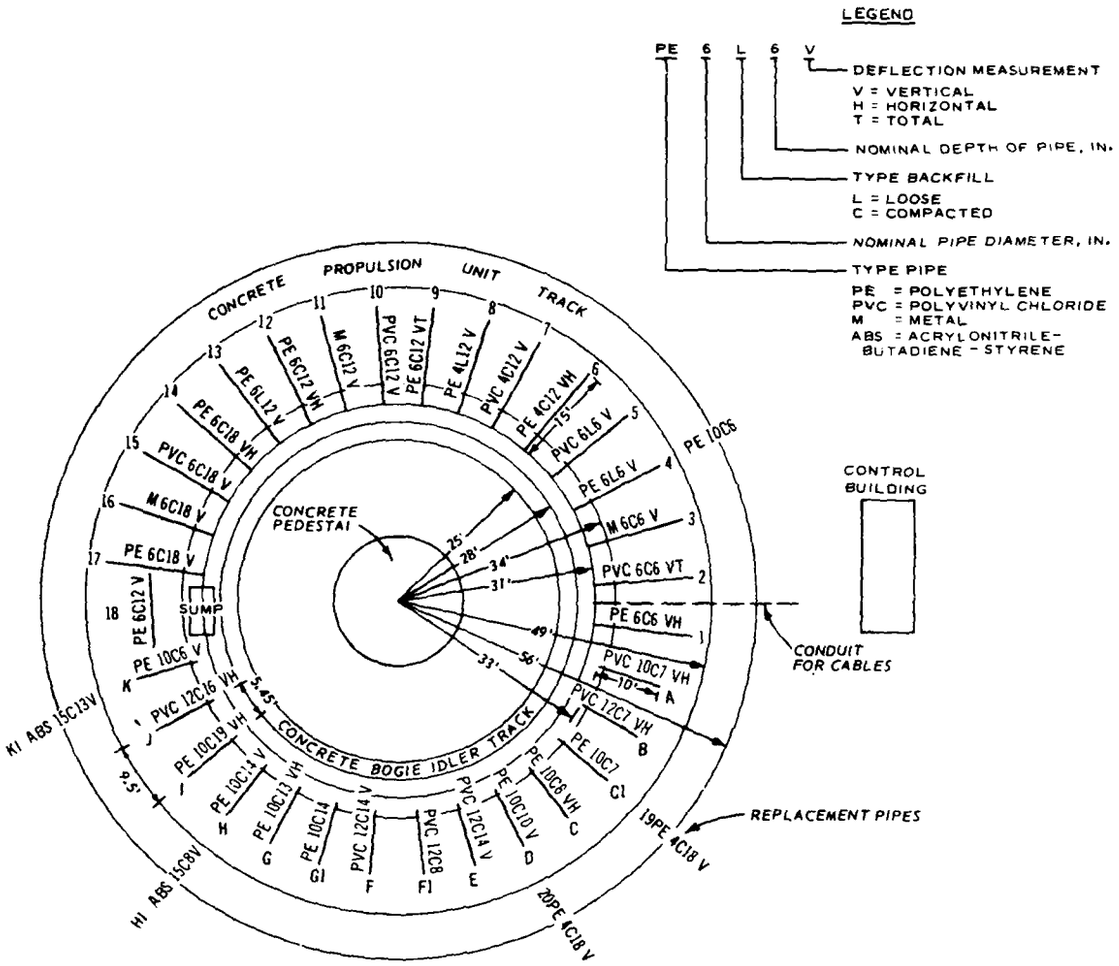

Figure 7. Layout of pipe installed in the Circular Test Track (Test Site No. 1)

provide data for the smaller pipe diameters. All pipe installations except No. 18 were laid out with an average distance of 7 ft between pipes at the center of the pipe length. Pipe 18 was installed longitudinally to traffic. All pipes were placed at a 2-percent slope to the inside radius of the track where a surface drain trench was constructed to remove excess water.

Basically, the same procedure was followed to install the pipes at all three test sites. Trenches were excavated by backhoe to a depth that would satisfy the top of the pipe elevations required by each of the installations. The width of each trench was 18 in. for the smaller (4- and 6-in.) pipes and 24 in. for all other pipes. With the trench at the appropriate depth, a layer of pea gravel approximately 4 to 6 in. deep was placed in the bottom of the trench and compacted with a small vibratory plate compactor. Figure 8 contains the gradation curve for the pea gravel. The average dry density of the pea gravel after compaction was 98.7 pcf. A groove was formed in the pea gravel and the pipe was carefully placed in the groove so that the pipe was in contact with the pea gravel over the lower one-sixth of its circumference. The pipes were positioned within the trench so that gages (in the case of Test Site No. 1) were in the proper location, and several elevation measurements were made along the top of the pipe to ensure that it was placed at the proper depth and had the proper slope.

Backfill material was placed around the pipe to the depth of the pipe spring line and compacted by hand. Elevations were again measured along the length of the pipe to ensure proper burial depth. The backfill material was then placed in the trench to the depth of the crown of the pipe and compacted by hand. Final elevation measurements were then taken along the length of the pipe and recorded. The remainder of the embedment material was placed in the trench to a depth of 6 in. above the crown of the pipe, when possible, and compacted using the small vibratory plate compactor. The remainder of the backfill material was then placed in 4- to 6-in. lifts in the trench and compacted with the vibratory plate compactor.

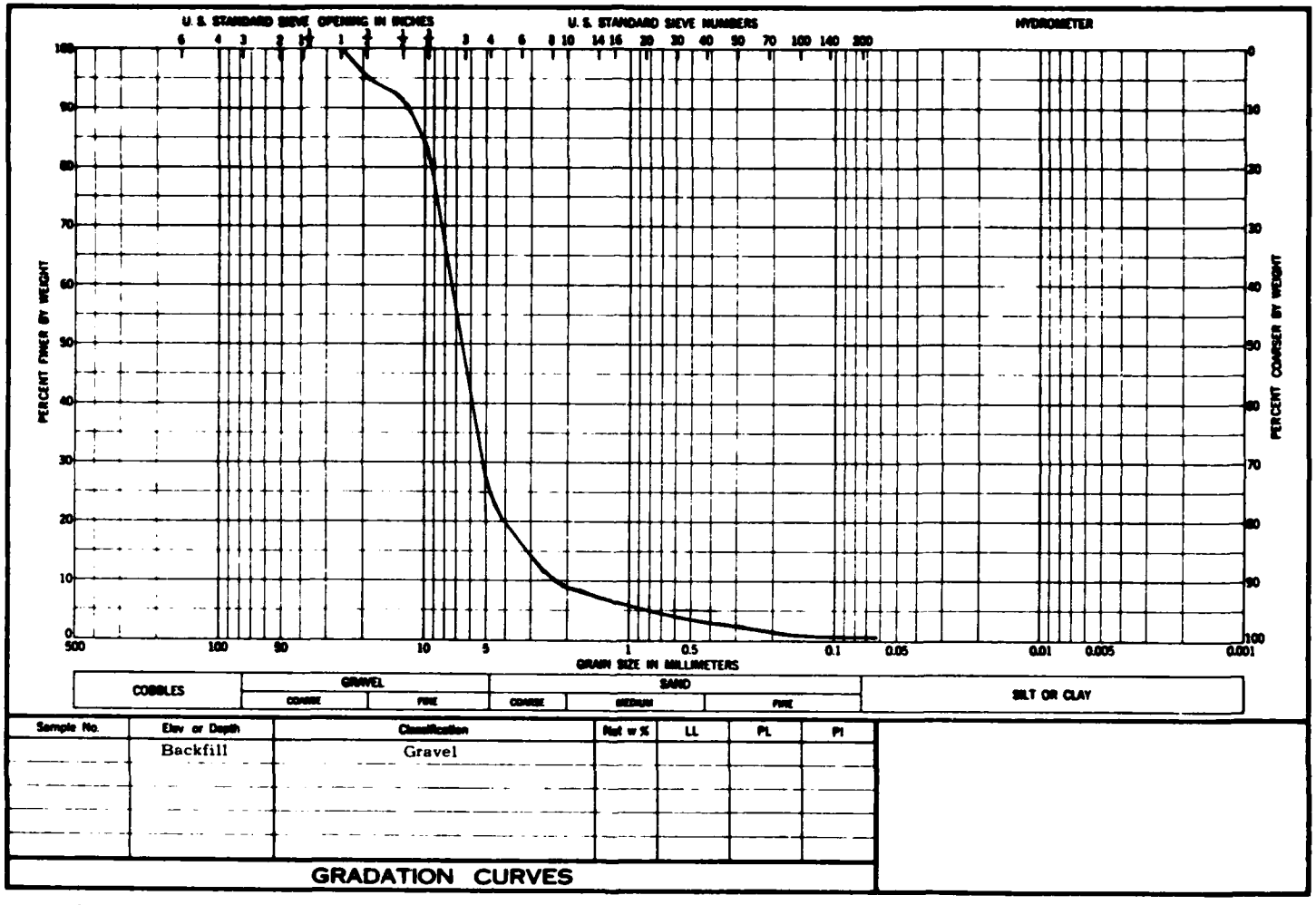

ENG FORM 1 MAY 63 2087

Figure 8. Gradation curve of pea gravel backfill

A base course was then installed on the CTT test site. A crushed stone (limestone) with the gradation curve of Figure 9 was used as the base material. Grade stakes were set at regular intervals on both the inner and outer edges of the track at the required elevation to maintain the 2-percent slope and final grade of the surface. The crushed stone base was placed in one lift. To avoid disturbing the trenches with exposed pea gravel, all trucks dumped their loads of crushed stone at the outer edge of the CTT and a D-4 Caterpillar tractor was used to spread the crushed stone over the pipe installations. A motor grader was then used to grade the test track to a height slightly above the desired elevation. The base was compacted with 7 passes of a rubber-tired, self-propelled roller and 2 passes of an 8- to 10-ton steel-wheel roller. The rubber-tired roller had a weight of 30 tons on seven tires having a tire pressure of 90 psi. The track was graded again with the grader and recompacted with 8 passes of the rubber-tired roller and 3 passes of the steel-wheel roller. Dry densities of the base averaged 139.3 pcf with a water content of 5.3 percent.

A double-bituminous wearing course was applied to the base course of the CTT. The surface of the base and the drainage ditch of the CTT was sprayed with asphalt (RC-800) at the rate of 0.6 gal per sq yd using a trailer distributor. The crushed stone base absorbed more than expected; therefore, another application of 0.3 gal per sq yd was required. Crushed limestone was then spread on the surface. The size of the crushed stone of the first layer of bituminous treatment was 100 percent retained on the No. 4 screen with a maximum size of 1-1/2 in. The gradation curve for the crushed stone is presented as Curve 1 of Figure 10. The surface was then sprayed again with asphalt at the rate of 0.3 gal per sq yd and another course of stone with the gradation curve of Curve 2 of Figure 10 was applied. The grain size distribution of this stone was such that 100 percent passed the 3/4-in. screen and 100 percent was retained on the No. 200. The asphalt was allowed to cure and the double-bituminous treatment was subsequently rolled with the rubber-tired roller for 8 passes. Figure 11 contains the final installation cross sections of all pipes installed in the CTT along with the layer

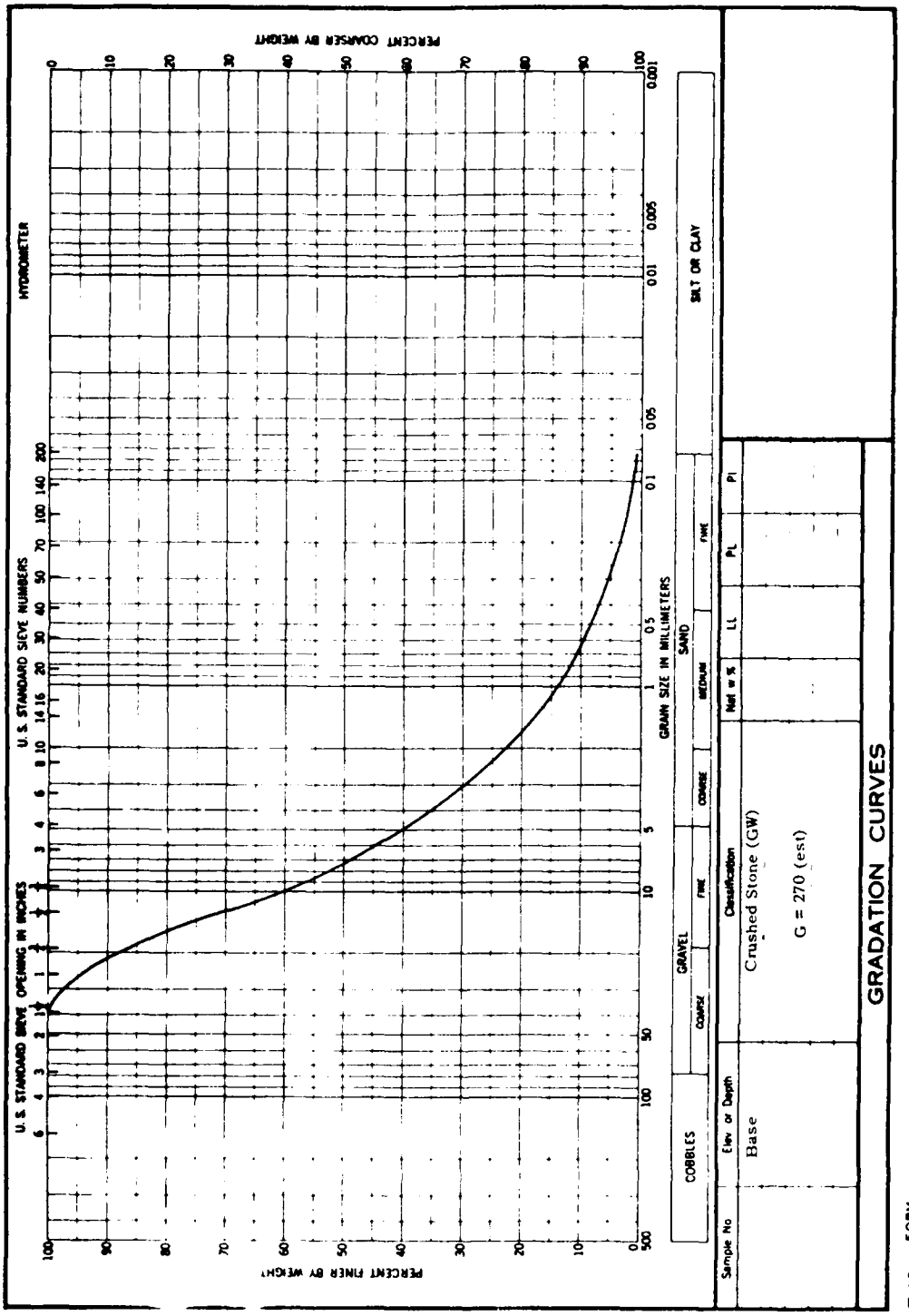

Figure 9. Gradation curve for crushed stone base used at Circular Test Track

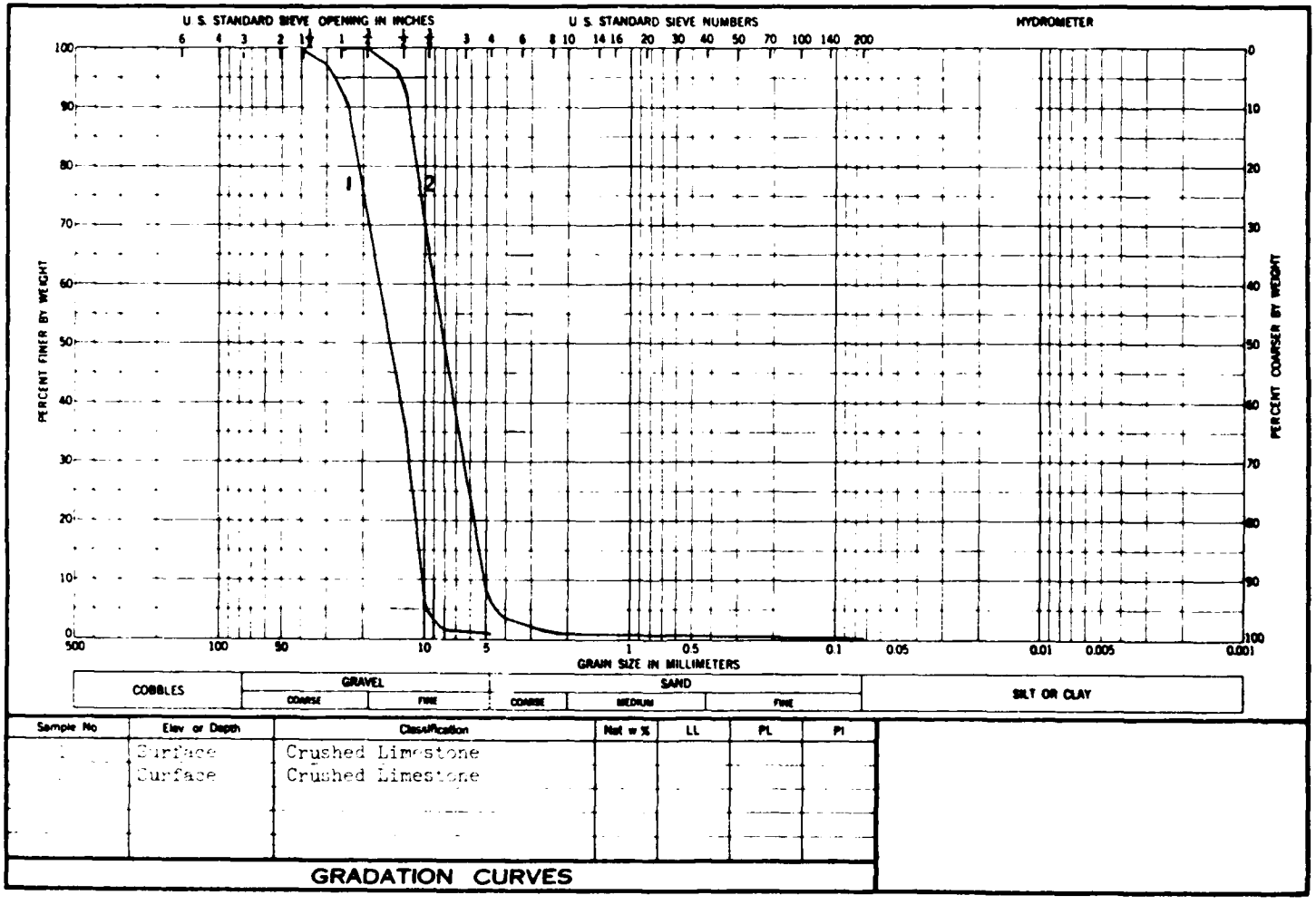

ENG FORM MAY 63 2087

Figure 10. Gradation curve for aggregate used in the double-bituminous surface treatment of the Circular Test Track

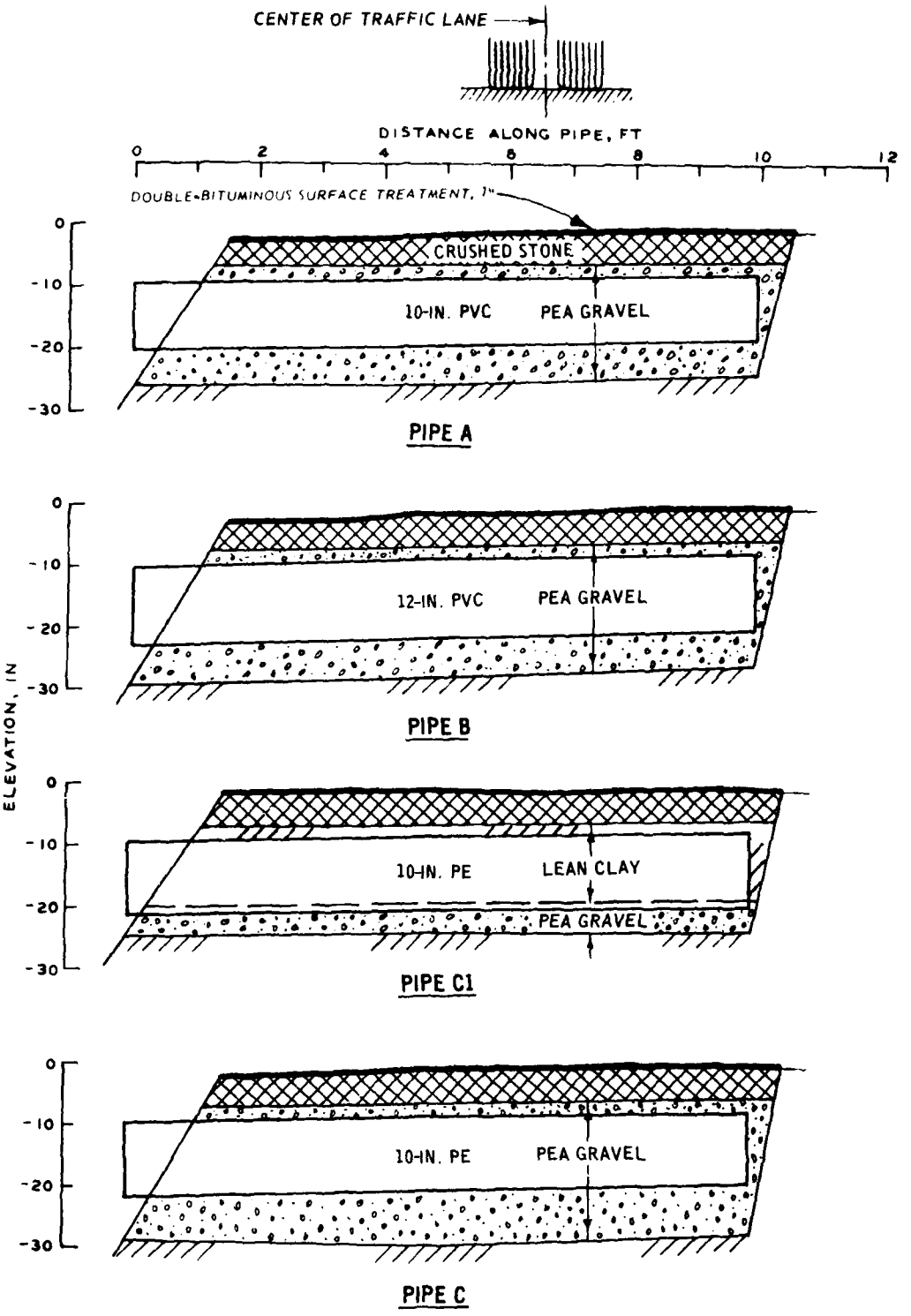

Figure 11. Cross sections of pipe installed in the Circular Test Track

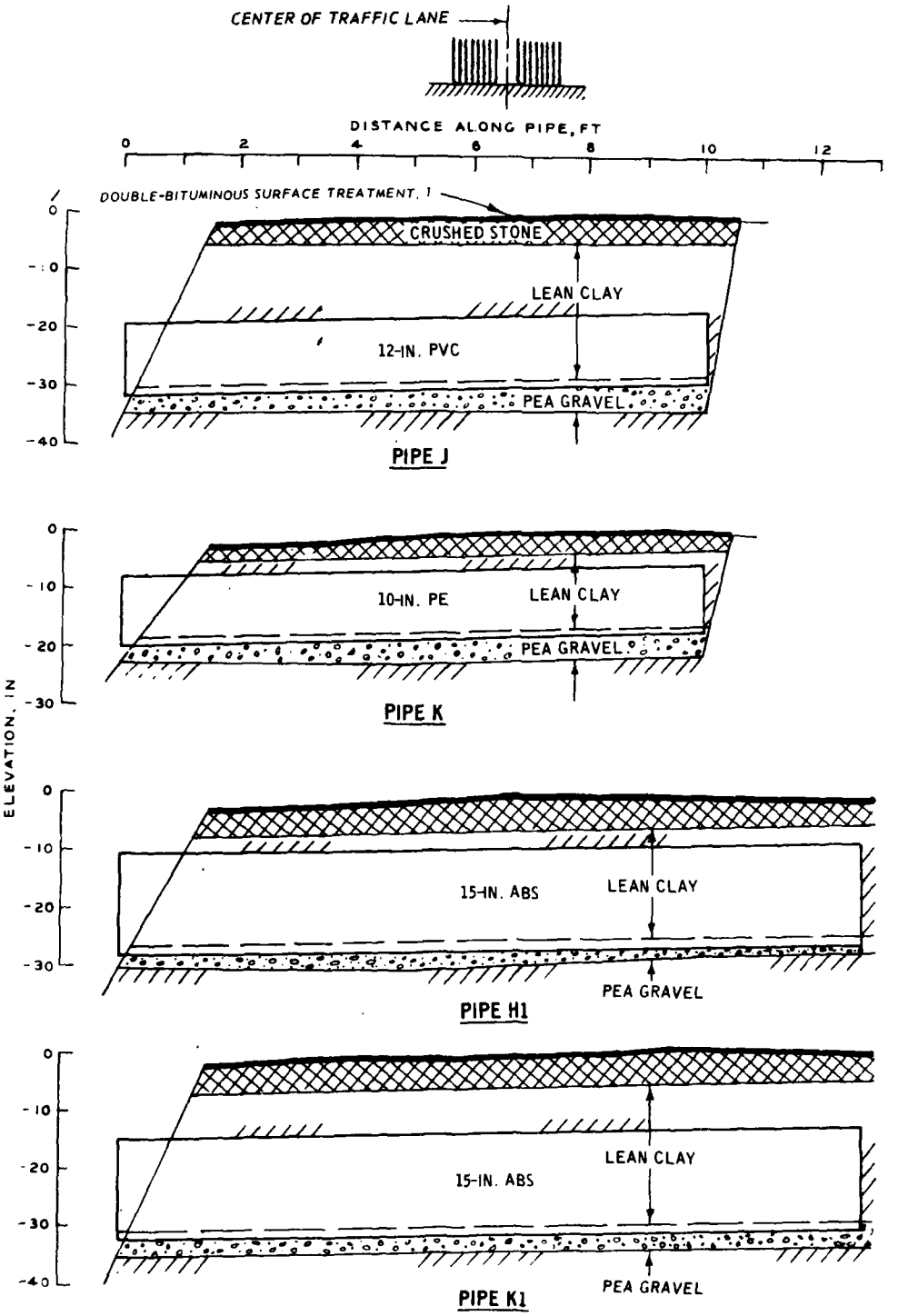

Figure 11 (Continued)

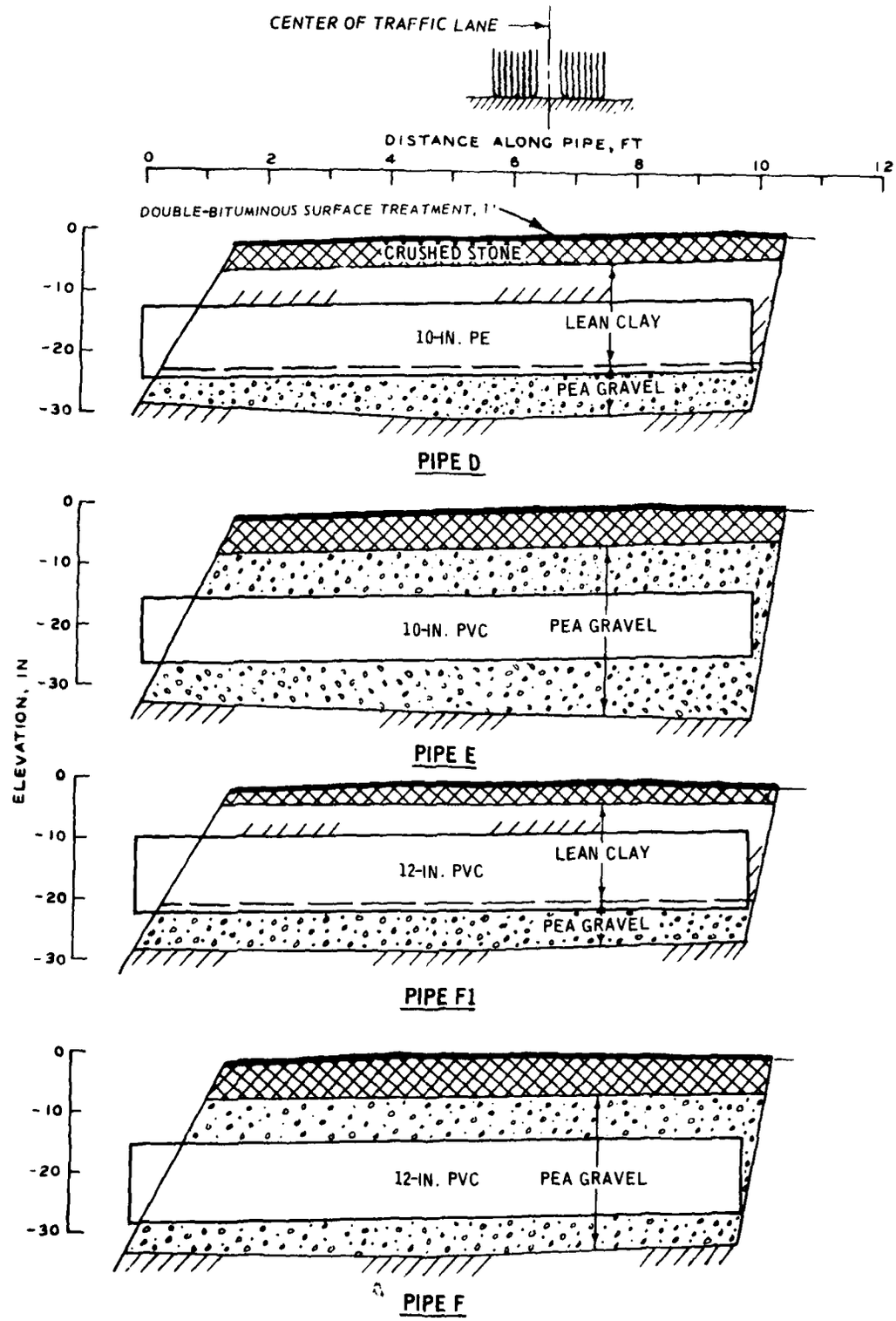

Figure 11 (Continued)

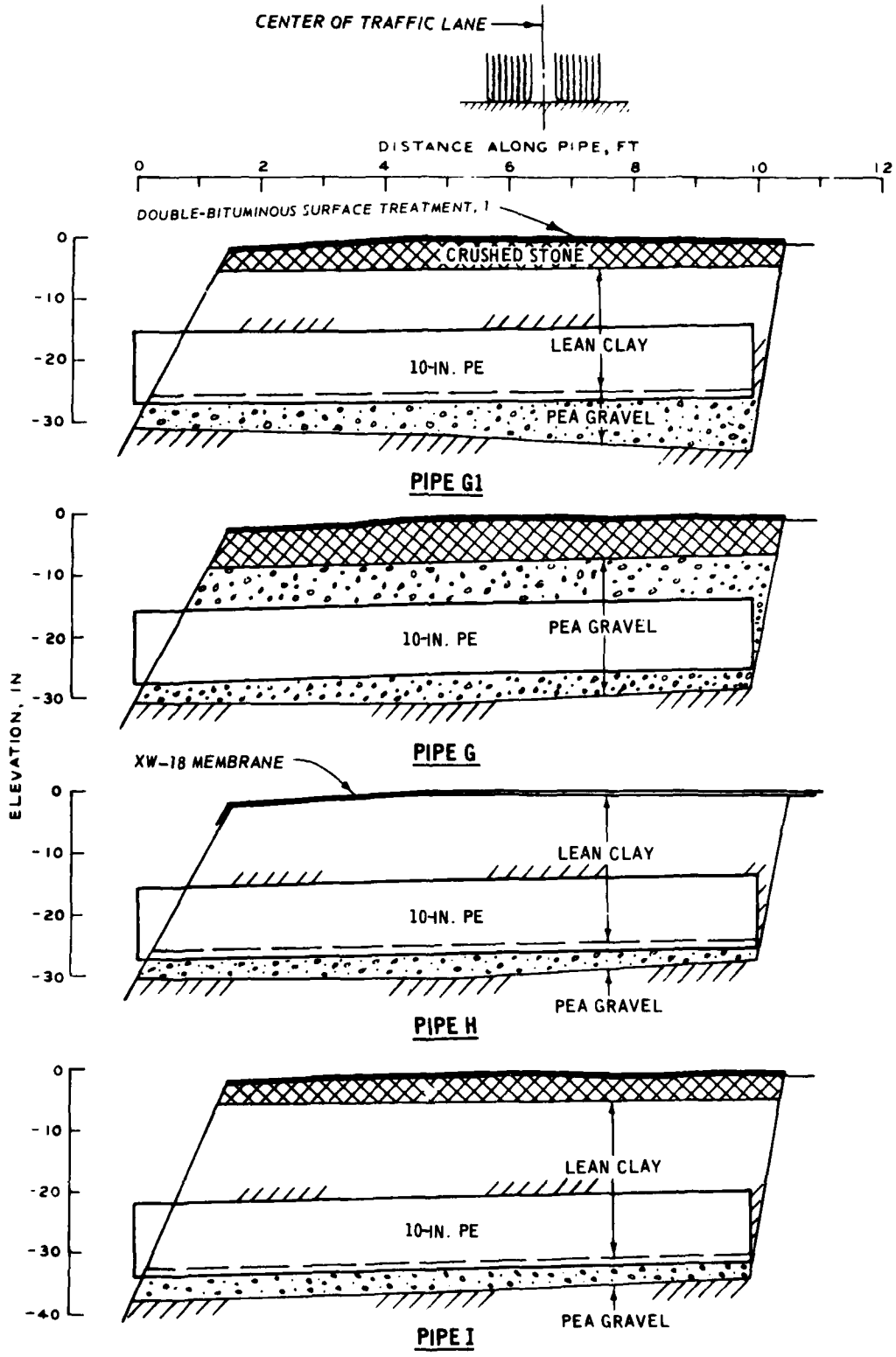

Figure 11 (Concluded)

thicknesses of the bedding, haunching, backfill, and surfacing materials.

Pipes H1 and K1 (and pipes No. 19 and 20 of the FHWA study) were installed after traffic had begun on the CTT. The installation procedure was the same as that for the pipes installed initially except that the crushed stone was placed over the trenches only and the area surrounding the pipe trenches was sprayed with asphalt to seal the surface from the penetration of water.

A record of permanent deflections of the pipe during construction phases was taken with the instrumentation system. Table 1 contains a summary of the permanent deflections of the pipe resulting from the construction of the test site.

TEST SITE NO. 2

The second test site used in this study was the overrun area of a field test section constructed to investigate the performance of pavement elements to aircraft loads. This site was chosen for the installation of plastic pipe primarily because it allowed the application of simulated aircraft traffic.

Four uninstrumented sections of each of the three types of pipe were buried at various depths within the 50-ft-wide test section. The installation in Test Site No. 2 was very similar to that of the CTT of Test Site No. 1. Figure 12 contains a layout of the test section showing the location of all pipes. Trenches were excavated by backhoe to a depth approximately 4 in. below the final elevation of the bottom of the pipe. An approximate 5-in. layer of pea gravel (identical to the pea gravel used at Test Site No. 1) was placed in each trench and compacted using a small vibratory plate compactor. A groove was formed in the center of the trench for the length of the pipe and the pipe was lowered into the groove. Care was taken to lightly shake the pipe until it was firmly seated in the groove in the pea gravel. Elevations of the top of the pipe were taken for the full length of the pipe and adjustments were made so that it was at the proper elevation and had a

Table 1

Total Permanent Deflection in the Instrumented Pipes of Test Site No. 1 (CTT) at the Conclusion of Construction of the Test Site

Pipe	Direction of Gage	Deflection in.	Deflection (% Internal Diameter)
A	Vertical	0.004	0.04
	Horizontal	0.004	0.04
B	Vertical	0.039	0.34
	Horizontal	0.068	0.58
C	Vertical	0.020	0.20
	Horizontal	0.099	0.99
D	Vertical	0.580	5.80
E	Vertical	0.036	0.37
F	Vertical	0.104	0.89
G	Vertical	0.051	0.51
	Horizontal	0.048	0.48
H	Vertical	0.523	5.23
I	Vertical	0.463	4.63
	Horizontal	0.343	3.43
J	Vertical	0.200	1.72
	Horizontal	0.187	1.61
K	Vertical	0.625	6.25

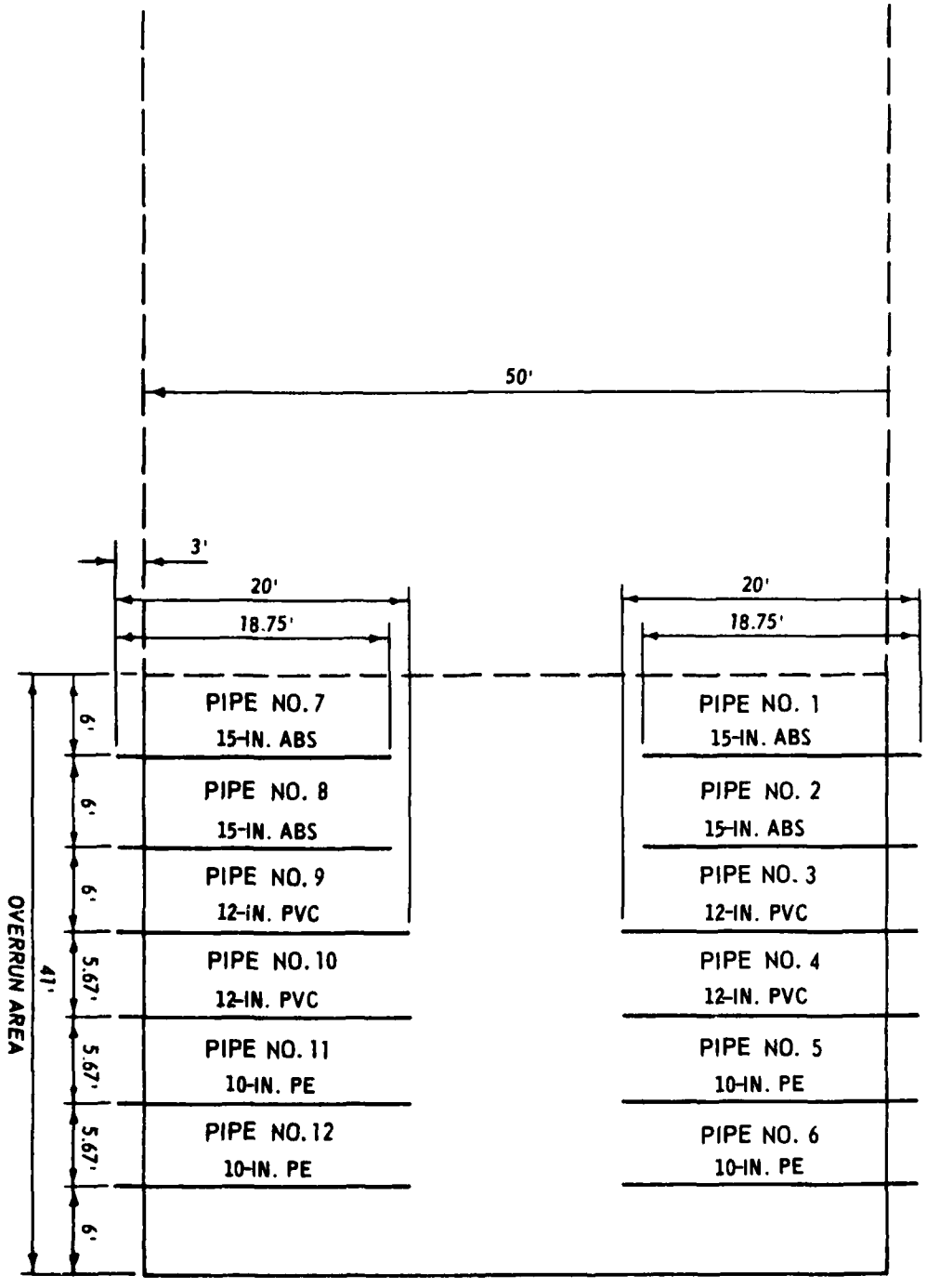

Figure 12. Layout of Test Site No. 2

1-percent slope. Pea gravel was then placed to the pipe crown and compacted by hand. Final elevations were then measured at the top of the pipe along its entire length. The final layer of pea gravel was then placed over the pipe to a depth of approximately 6 in. or to the top of the trench if it was less than 6 in. above the pipe. The vibratory compactor was used to compact this final layer of pea gravel. Crushed stone was used to complete the backfill to the top of the trenches in those trenches that had not been filled by the pea gravel. Again, the vibratory compactor was used to compact the crushed stone layer. An approximate 12-in. layer of crushed stone was then placed on the entire test site in 6-in. lifts and compacted with a vibratory steel-wheel roller. Figure 13 contains the final installation depths of all pipes and the layer thicknesses of embedment and backfill material.

Density and water content measurements were taken at each step during the installation of pipes. Drive cylinder samples were taken from the bottom of each trench for this purpose and a nuclear density device was used at the other locations. The results of these density and water content measurements are presented in Table 2.

TEST SITE NO. 3

The third test site was a road constructed at WES for another research program. One uninstrumented 12-in. PVC pipe was installed at this site.

A concrete saw was used to cut through the asphaltic concrete pavement of the existing road so that a 2-ft-wide trench could be cut diagonally across the road. The trench was approximately 40 ft long and had an average depth of 26.5 in. The existing pavement structure consisted of a 3-in. asphaltic concrete surface over a 6-in. layer of stabilized clay gravel (4 percent lime and 2 percent cement) over a compacted loess subgrade. Once the trench was excavated, drive cylinder samples were taken. A layer of sand bedding approximately 4 in. deep was placed in the trench and compacted with a hand tamper. The 12-in. PVC pipe was then lowered into the trench and carefully shaken to ensure continuous contact with the sand bedding over the entire length of the

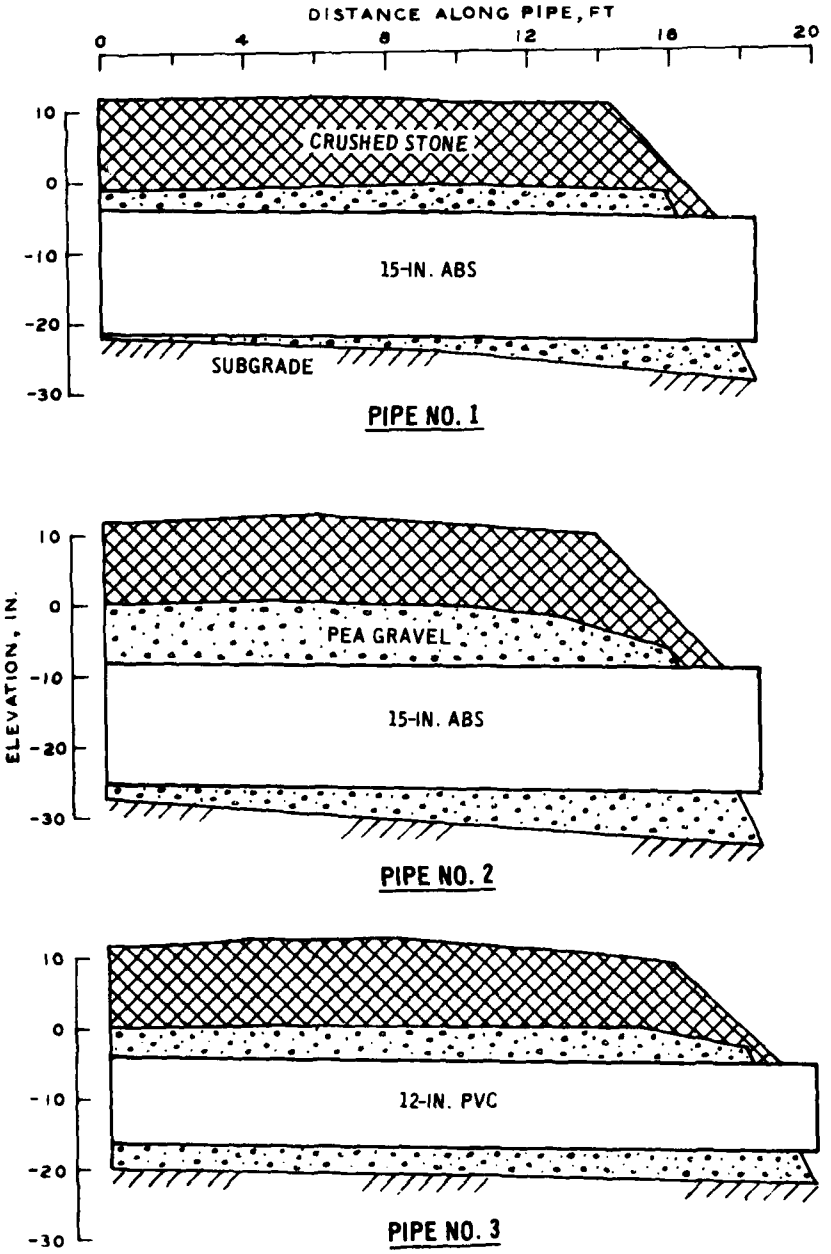

Figure 13. Cross sections of pipe installed in Test Site No. 2

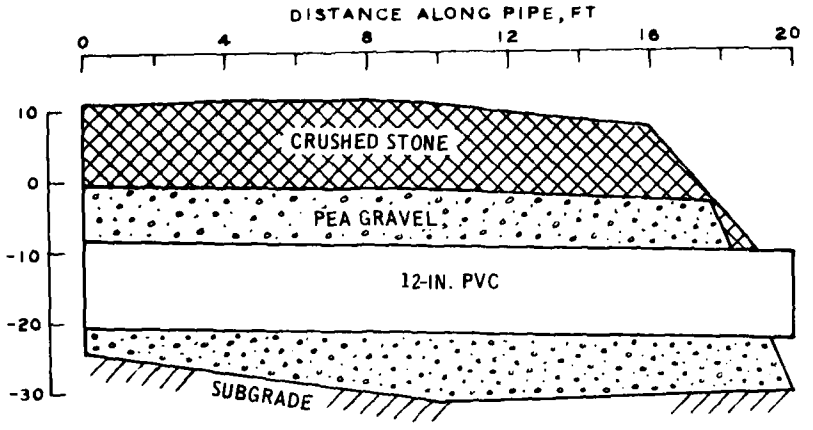

PIPE NO. 4

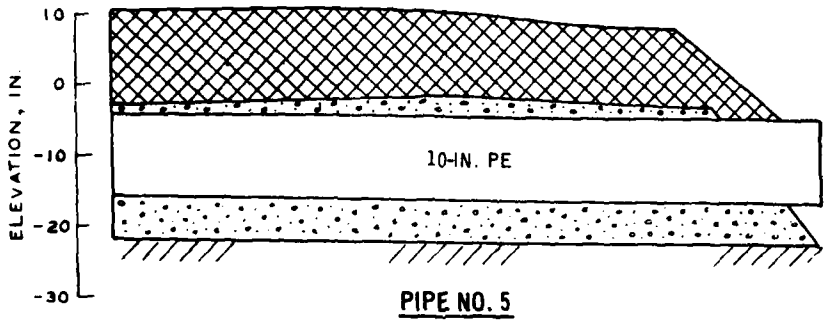

PIPE NO. 5

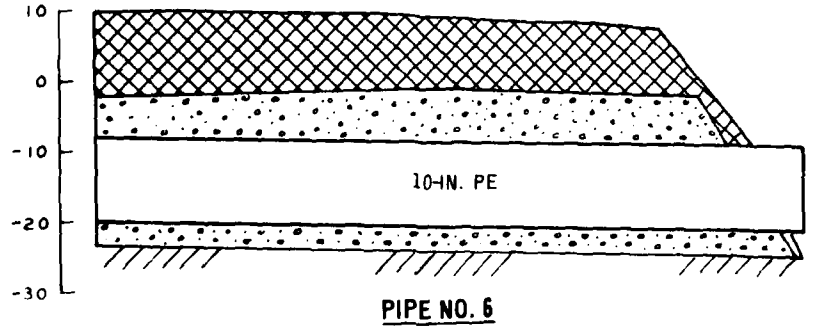

PIPE NO. 6

Figure 13 (Continued)

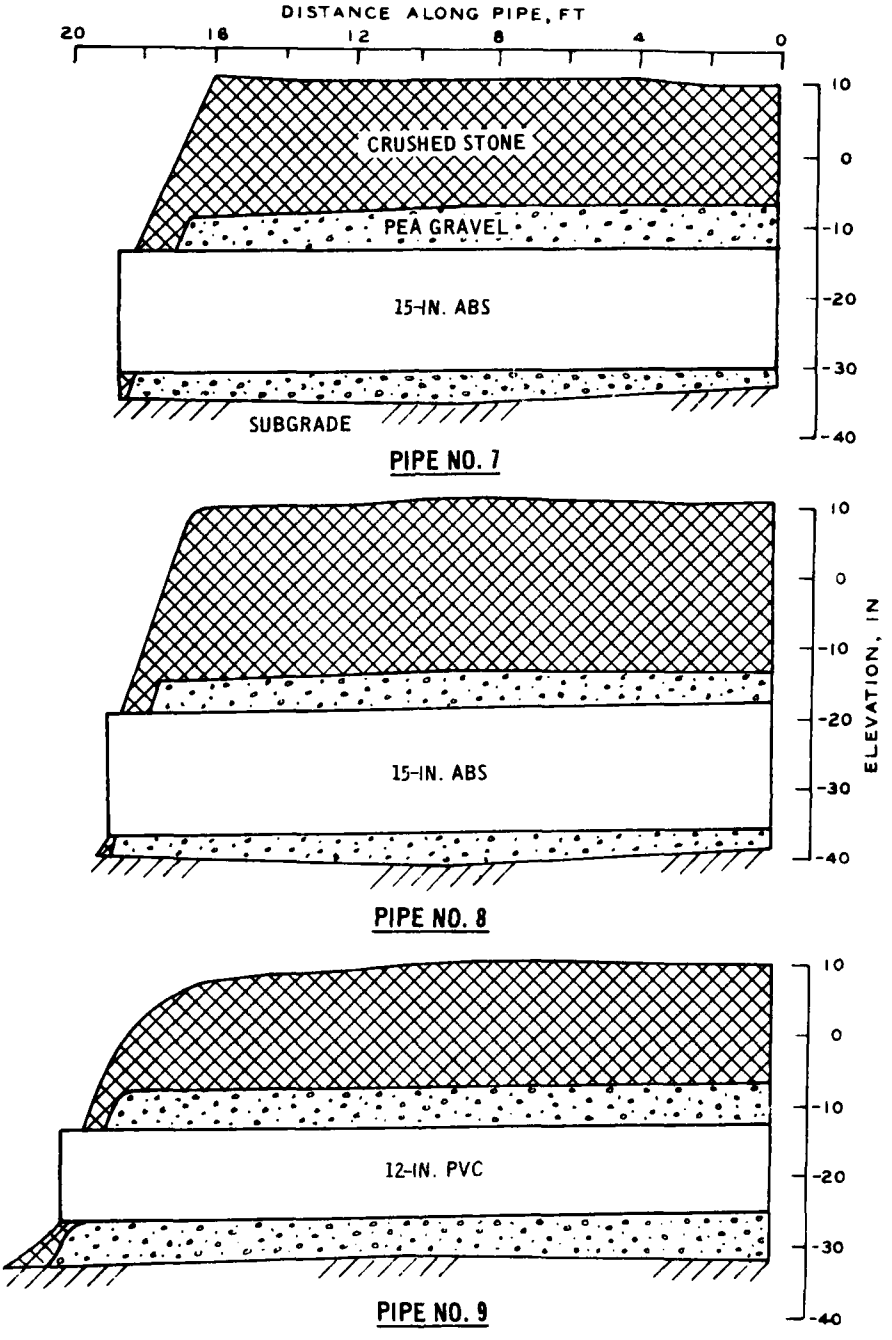

Figure 13 (Continued)

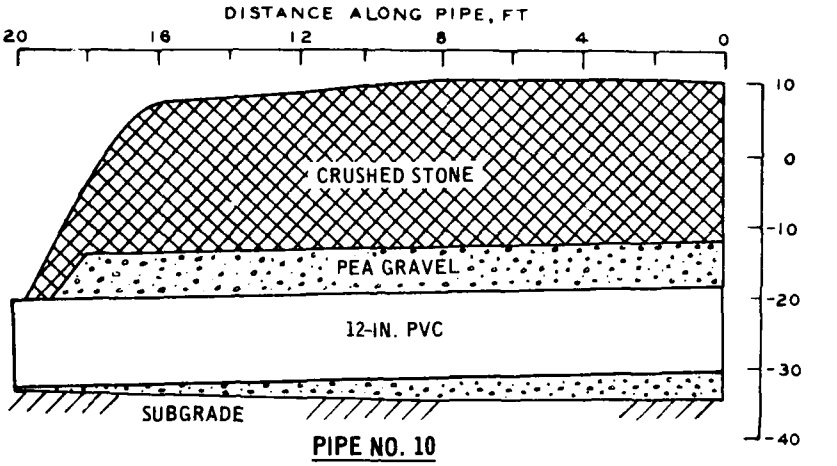

PIPE NO. 10

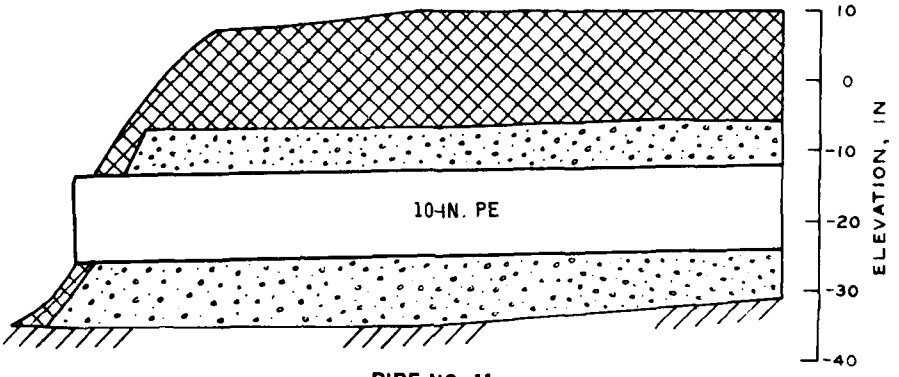

PIPE NO. 11

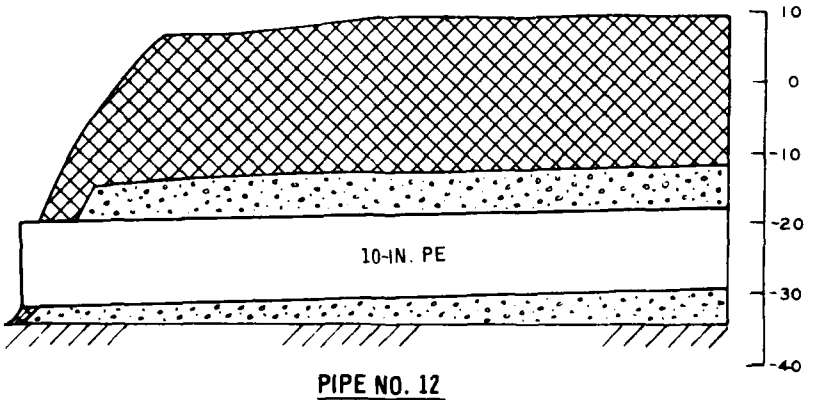

PIPE NO. 12

Figure 13 (Concluded)

Table 2

Dry Density and Water Content of the Layers of the Pipe Trenches of Test Site No. 2

Trench No.	Subgrade Density pcf	Subgrade W/C %	Top of Bedding Density pcf	Top of Bedding W/C %	Top of Pea Gravel Density pcf	Top of Pea Gravel W/C %	First Lift of Crushed Stone Density pcf	First Lift of Crushed Stone W/C %	Final Lift of Crushed Stone Density pcf
1	90.4	21.3	108.5	4.2	109.0	3.2	127.0	4.9	141.0
2	92.3	19.2	105.0	4.6	108.5	3.9	134.7	4.9	141.7
3	91.4	20.4	105.0	4.0	104.5	5.9	133.5	4.9	145.5
4	95.5	18.5	104.5	4.4	108.0	4.8	137.0	4.9	146.3
5	90.4	21.7	118.3	4.2	117.5	4.0	123.0	4.9	146.0
6	91.7	20.2	--	--	106.5	3.7	124.5	4.9	141.5
7	91.9	22.3	106.5	4.0	105.5	4.1	121.0	4.9	146.5
8	91.6	22.0	111.5	4.1	109.0	4.2	125.3	4.9	145.5
9	90.3	22.5	104.5	3.1	107.0	2.5	120.0	4.9	142.3
10	93.6	21.2	106.5	3.9	105.5	3.8	124.0	4.9	144.5
11	92.0	23.0	104.7	4.4	109.0	4.1	126.0	4.9	148.0
12	92.2	24.5	105.5	4.2	105.5	4.3	126.5	4.9	141.0

pipe. Sand was then placed around the pipe up to its spring line and compacted by hand. The elevation along the top of the pipe was then measured at several locations to ensure the pipe was at the proper depth and slope.

A loess material was used to backfill to the crown of the pipe and was compacted by hand. Final elevation measurements were taken along the top of the pipe and then loess was placed to a depth of 2 in. over the top of the pipe and compacted with a small vibratory plate compactor. Approximately 5 in. of stabilized clay gravel was then placed in the trench and compacted using a Wacker vibratory compactor as well as the vibratory plate compactor. The stabilized material was produced by combining 4 percent lime and 2 percent cement with clay gravel. Cold-mix asphalt was used to backfill the remainder of the trench (approximately 2.5 to 3 in.) to the level of the existing pavement system. The vibratory plate compactor was used to compact this final layer. Figure 14 contains two views of the pipe, showing the approximate thicknesses of all layers of the embedment backfill materials.

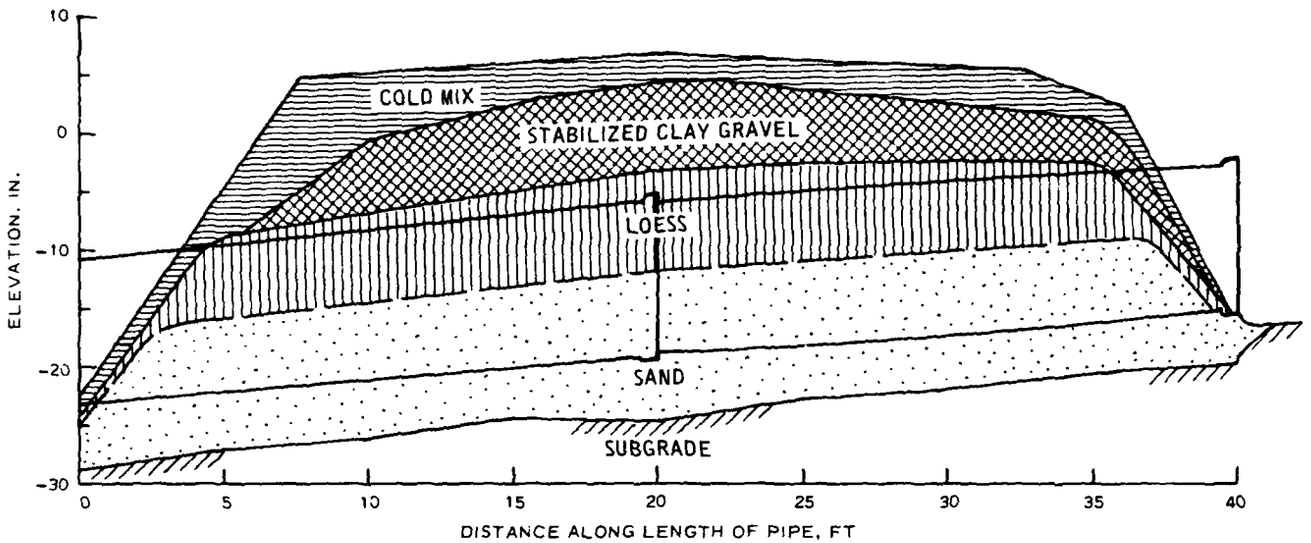

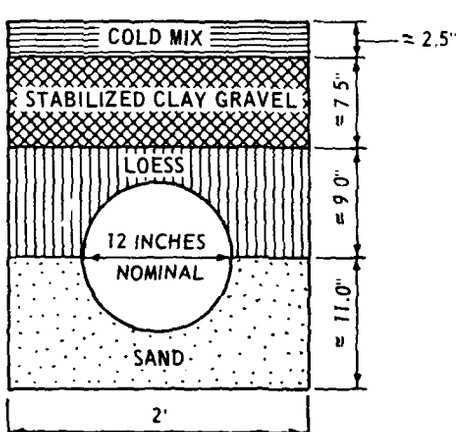

Figure 14. Details of installation of 12-in. PVC pipe at Test Site No. 3

INSTRUMENTATION SYSTEM

Most of the pipes installed in the CTT were instrumented with displacement transducers to electronically measure the change of the pipe interior diameter in the vertical and horizontal directions. Another device (hereafter called a deflectometer) was constructed to measure vertical pipe diameters and was used to measure the permanent and static deflections of uninstrumented pipes. The device was also used as a backup for pipe measurements in which the limits of the displacement transducer had been exceeded or failed. This deflectometer was the only measuring device used at Test Sites No. 2 and 3.

DISPLACEMENT TRANSDUCERS

Direct current linear displacement transducers (DCDT) were installed within the pipes to measure the variation of the vertical or horizontal pipe diameters. The DCDT is an electromechanical transducer that produces an electrical output proportional to the displacement of a rod-shaped magnetic core that is free to move within an array of cylindrical coils. When the magnetic core is displaced from its pull position, a differential voltage output is produced that varies linearly with the change in core position. When the core rod is moved in the opposite direction, a similar linear differential voltage is produced, but with a 180-deg phase shift. Figure 15 is a photograph of the interior of a PVC pipe with a DCDT installed vertically and another DCDT installed horizontally. The coils are contained within the cylindrical housing of the DCDT, which is securely mounted to the outside of the wall of the pipe. The magnetic core is the slender rod that projects from the larger cylindrical housing of the DCDT. It is attached to the wall of the pipe in a manner such that the gage passes through the center of the undeformed pipe. With this arrangement, the displacement of a point on one side of the pipe relative to a point on the opposite side of the pipe produces an electrical signal that can be calibrated; thus, the diameter of the pipe can be monitored. DCDT gages installed to measure the change in vertical diameter of the pipe were located so that

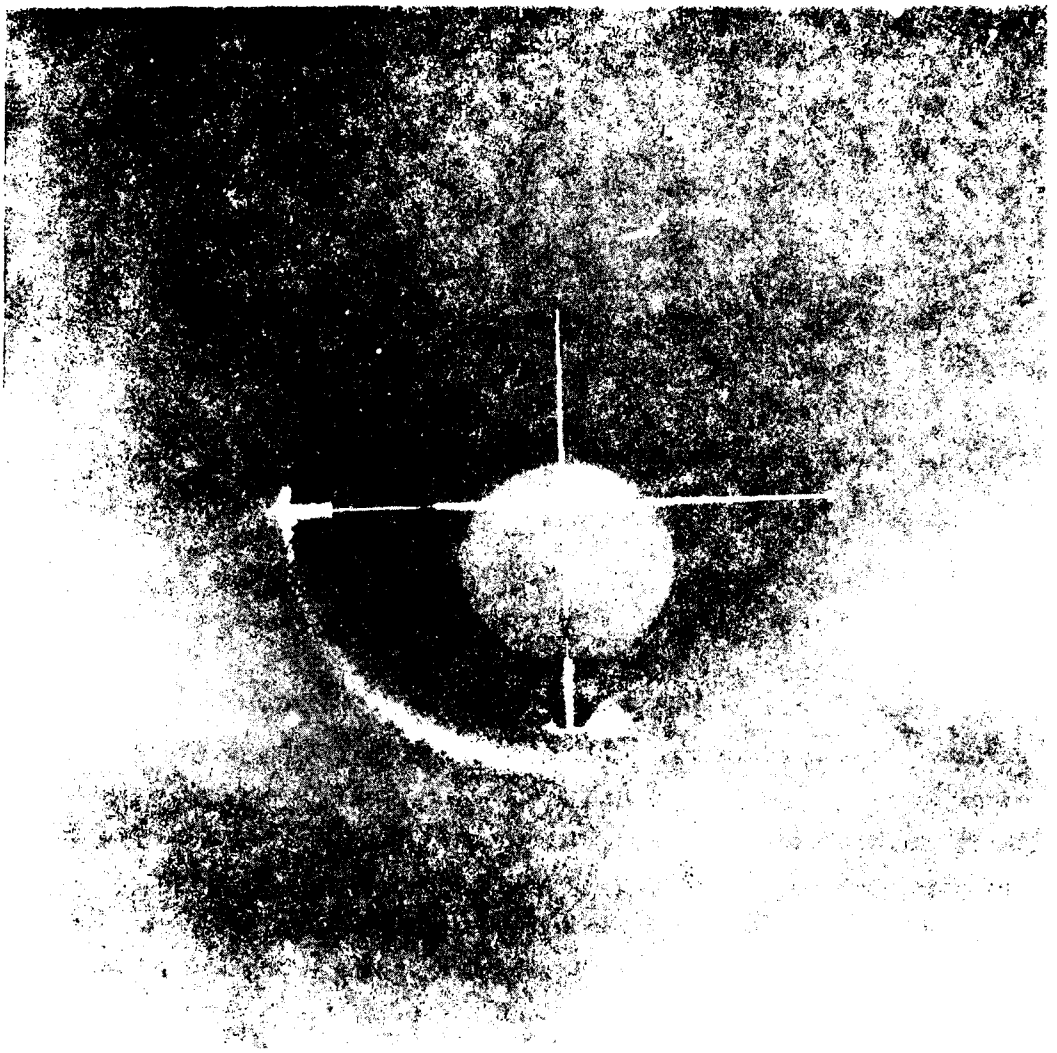

Figure 19. [illegible]
in both the vertical and [illegible]

they would be directly under the outside tire (the tire farthest from the center of the CTT) of the loading assembly when it was in the center of its traffic pattern. Horizontal DCDT gages were installed such that they were under the inside tire when the loading assembly was in the center of its traffic pattern.

DCDT gages were also installed in the CTT to measure the total movement of the pipe.* This was accomplished by attaching the magnetic core of the DCDT to a reference rod that was anchored by a 3-sq-in. plate installed at a depth of 5 ft below the surface of the track.

DCDT gages of two different gage lengths were used to instrument the pipes; one with a 1.5-in. range of travel and the other with a 0.75-in. range of travel. This was done to minimize the physical size of the gage and gage mount so that they could have only a minor effect on the deflection of the pipe. The gages were hand-wired to a signal conditioning system housed in a control building at the CTT site. Here the gages were powered, the output signals were amplified, and the hardcopy oscillograph outputs were produced.

DEFLECTOMETER

The description and plans for the deflectometer were obtained from the Plastic Pipe Institute, New York, New York, and it was constructed at WES. A photograph of the deflectometer along with a strain gage indicator is shown in Figure 16. Essentially the deflectometer was composed of a "sled" of two rails connected by a platform, with a long slender strip of spring steel rigidly clamped to the platform and strain-gaged near the clamped end. The sled was designed to slide along the bottom of the pipe such that the platform remained in a level horizontal plane and the free end of the spring steel maintained contact with the top of the pipe. The deflectometer was calibrated by measuring the voltage output of the strain gage as a function of the distance from the highest point of the spring steel to the horizontal platform of the deflectometer. Once the deflectometer was calibrated it was placed in the open end of a

---

* Bush and Sullivan, op. cit., p. 3.

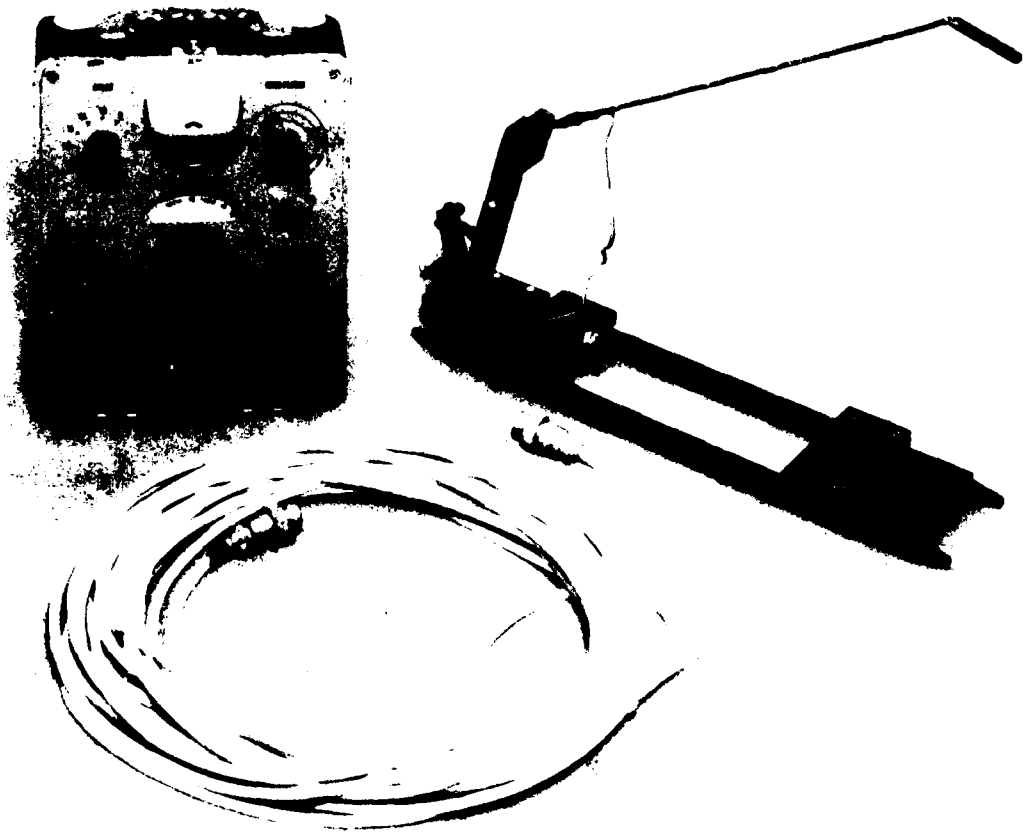

Figure 16. Deflectometer and strain gage indicator

pipe specimen and pushed through the pipe, stopping at those locations where deflection data were desired. At those points, the strain was read from the strain gage indicator and the calibration curves were used to convert the strain reading to a pipe diameter reading.

This initial arrangement proved to be unsatisfactory because measuring the deflection of the pipe at several locations along its length was such a time-consuming operation. Therefore, the deflectometer system was modified. The new system consisted of the original deflectometer with its gaged spring steel, but the strain gage indicator was replaced with an x-y plotter which produced a continuous line output from the input signal of the deflectometer strain gage and the signal from a displacement transducer that was added to the system. With this new system a continuous plot of the pipe diameter as a function of location along the pipe could be produced in the time that it took to pull the deflectometer through the pipe.

TESTING

LABORATORY TESTS

Laboratory tests were conducted as described in ASTM D 2412, "External Loading Properties of Plastic Pipe by Parallel-Plate Loading," to determine the pipe stiffness properties. Table 3 contains a summary of the results of the laboratory tests. Pipe stiffness data for 4- and 6-in.-diam PE and PVC pipe are given by Bush and Sullivan.* Each test result is the average of three tests. Figure 17 shows a typical test setup using PE pipe.

TRAFFIC TESTS

TEST SITE NO. 1

An initial static load of 7,000 lb on dual tires was applied at the completion of construction of Test Site No. 1 and the data were recorded and examined. The measured data indicated that all elements of the instrumentation system were operating properly, so 26 passes of channelized traffic were applied. Pipe deflections were monitored continuously during these early load applications. No extraordinary deflections were observed during these initial passes, so the load was increased to 9,000 lb and static load tests were conducted over each pipe. That is, pipe deflections were measured for a statically applied load of 9,000 lb placed directly over the gages installed in the pipes. Again, the pipe deflection data looked reasonable, and an additional 22 passes of channelized traffic with 9,000-lb load were applied. Static load data were then taken on four pipes with an 11,000-lb load. Based upon the results of these initial shakedown tests the load was reduced to 9,000 lb, the loading assembly was adjusted to apply a prescribed pattern of distributed traffic, and 8,000 coverages of the 9,000-lb dual-wheel load were applied.

The traffic distribution pattern selected for the tests was based

---

* Bush and Sullivan, op. cit., p. 3.

Table 3

External Loading Properties of Plastic Pipe*

by Parallel Plate Loading

(as Specified in ASTM D 2412)

Pipe Type in.	Average Specimen Length in.	Average Outside Diameter in.	D Average Inside Diameter in.	Average Wall Thickness in.	Δy Vertical Deflection in.	Percent Vertical Deflection Relative to Inside Diameter %	Average Load at Δy lb	F Distributed Load lb/in.	Pipe Stiffness F/Δy psi	Stiffness** Factor lb-in.^{2}/in.
10 PVC	5.875	10.45	9.71	0.369	0.486	5	292	49.702	102.27	1,743.82
					0.971	10	511	86.979	89.58	1,527.44
					2.910	30	910	154.894	53.23	907.63
12 PVC	5.980	12.50	11.71	0.394	0.586	5	254	42.475	72.48	2,167.63
					1.171	10	446	74.582	63.69	1,904.75
					3.513	30	866	144.816	41.22	1,232.75
10 PE	6.030	11.75	10.05	0.850	0.500	5	133	22.056	44.11	833.93
					1.000	10	204	33.831	33.83	639.58
					3.010	30	310	51.410	17.08	322.91
15 ABS	6.005	17.59	14.73	1.430	0.736	5	782	130.225	176.94	10,532.48
					1.473	10	580	96.586	65.57	3,903.10
					4.419	30				

* Average of three tests.

** Stiffness factor = $0.149\ (D/2)^3\ F/\Delta y$.

† Pipe failed prior to the 10 percent vertical deflection.

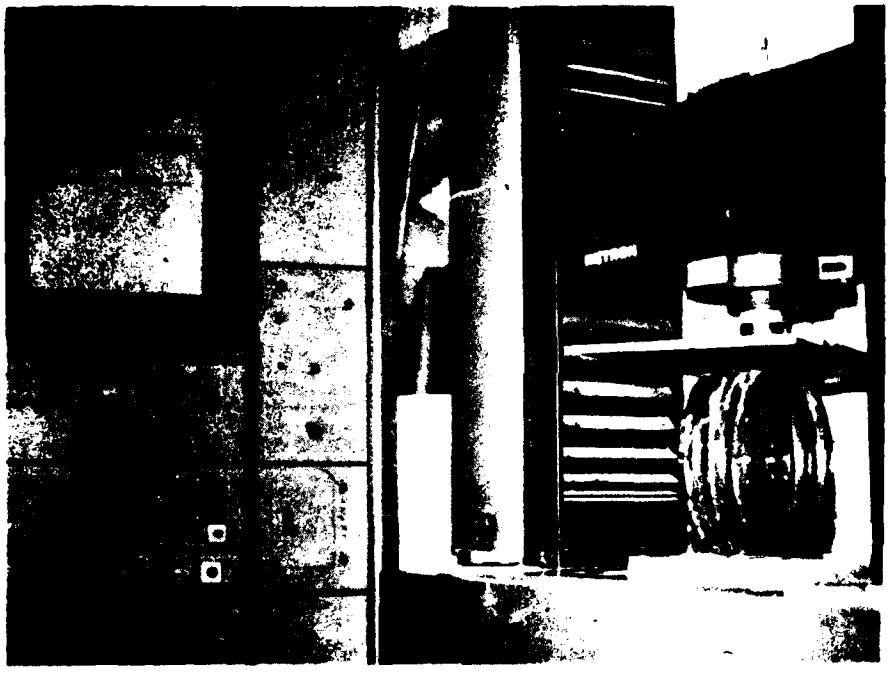

Figure 17. Parallel [illegible]

upon highway traffic distribution studies conducted in Texas* and Georgia.** In both studies the lateral distribution of highway truck traffic appeared to follow a normal distribution with a standard deviation of approximately 10 in. A combination of two distributions was used to simulate the actual traffic distribution. Most of the traffic (75 percent) was applied using a traffic distribution pattern in which the load wheels were cyclically traversed radially at a constant rate over a range of ±15 in. The remaining 25 percent of the traffic was applied in a similar manner, but the wheels were traversed over a range of ±5 in. The rate of radial displacement of the load was approximately 3 in. per revolution of the load rig.

Each pass of the load cart was the equivalent of approximately 0.46 coverages at the location of the DCDT gages with the ±15-in. distribution and 0.8 coverages with the ±5-in. distribution. A coverage is defined for these tests as a load application of any portion of a tire directly over the gages.

After the initial 8,000 coverages of the 9,000-lb load were applied to the test track, the load was increased in increments of 2,000 lb every 2,000 coverages. With this schedule of loading, 22,000 coverages were applied to the pipe segments, and the maximum applied load was 23,000 lb. This maximum loading represents an overload for highways and would simulate a loading equivalent to a light aircraft.

Static load tests were generally conducted at each increment of loading prior to the application of traffic at the new load level. Permanent pipe deflection data were measured each day prior to the application of traffic. Dynamic load deflections were also measured each day after a few passes of the load cart. Static load measurements were taken in the uninstrumented pipes with the deflectometer system described earlier.

---

* Charles J. Keese and Charles Pinnell, "Effect of Freeway Medians on Traffic Behavior," Highway Research Board, Bul 135, 1976, Washington, D. C.

** Personal communication with R. D. Barksdale, Georgia Institute of Technology, Atlanta, Ga., 1977.

Surface elevation measurements were taken over the length of each of the pipes at the 2000-lb load increments also. These measurements were used to determine the current approximate depth of cover of each pipe at any time during the field tests. Additional surface elevation measurements were taken when major repairs were performed.

TEST SITE NO. 2

Pipe deflections were measured using the deflectometer previously described. Deflection data were taken for static loads applied directly over the pipes and during dynamic loading of the pipes. Permanent deflections were also measured periodically with no load applied to the pipe.

Loads that were representative of aircraft loads were applied to the test section by two different load carts. The first load cart (Figure 18) applied a single-wheel load of 35,000 lb with a tire inflation pressure of 250 psi. This simulated the wheel load produced by an F-4 type aircraft. Traffic was applied in a distributed manner that was representative of the traffic pattern associated with F-4 ground operations.

The second load cart (Figure 19) used during the field tests at Test Site No. 2 simulated the load that would be applied by the C-141 aircraft. Using this load cart, a load of 144,000 lb was transmitted through 4 wheels (39.5- by 48-in. spacing) to the surface of the test site. Tire pressures of 180 psi were used on this load cart.

A distribution of traffic similar to that of aircraft ground traffic was designed for the tests with the C-141 load cart. When testing was actually begun, however, it was not possible to maneuver the load cart properly to maintain a traffic pattern. This was due to the rutting of the test site, mechanical problems, and maneuver space. Therefore, the traffic was generally applied in a channelized manner with any wander of the load being the result of the unintentional wander of the load cart, not a predetermined loading pattern.

The F-4 load cart was used for the initial loading of the pipe installed in Test Site No. 2. Static load, dynamic load, and permanent

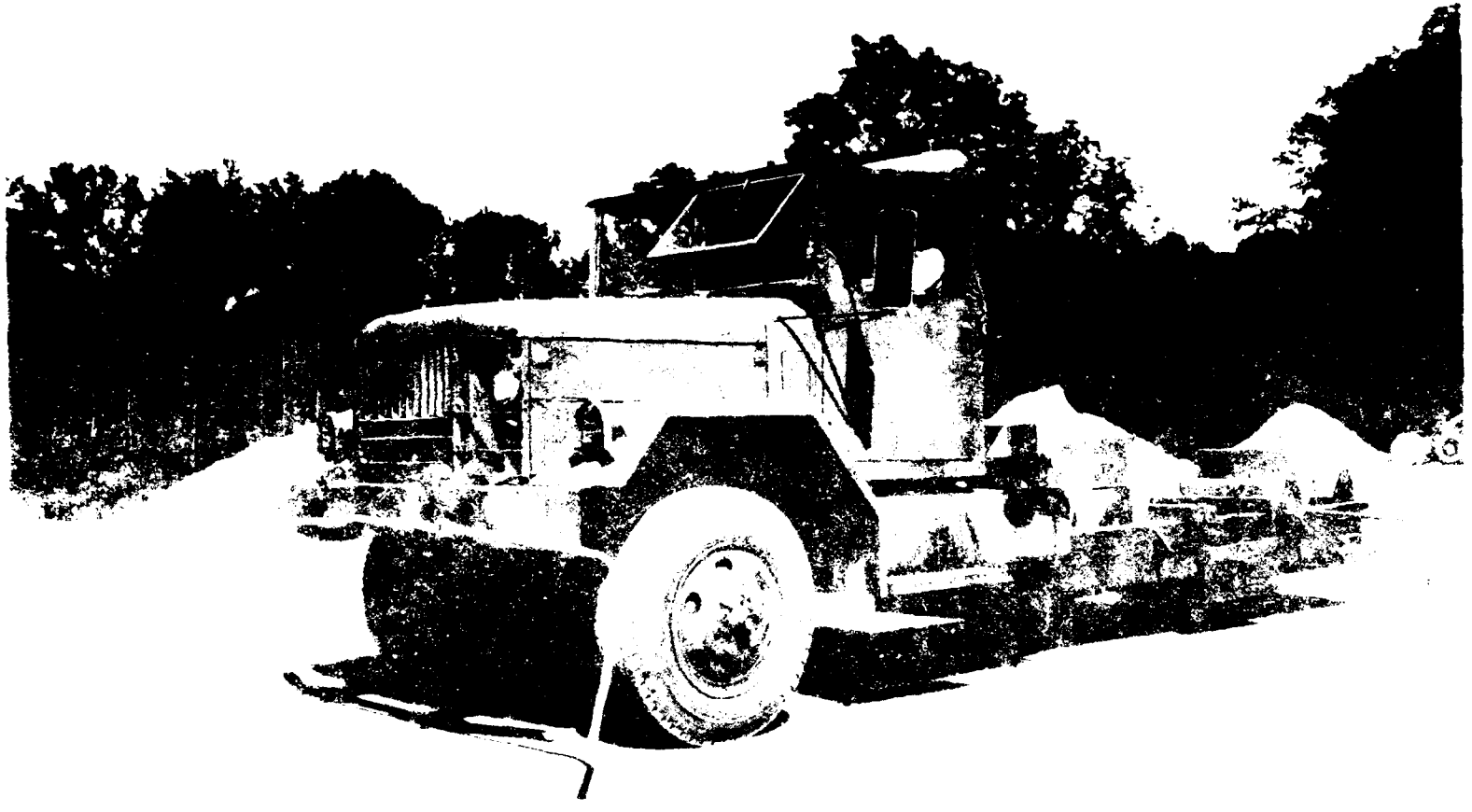

Figure 19. Load cart simulating C-141 aircraft load

pipe deflections were measured at various intervals during the subsequent tests. A total of 84 coverages of F-4 loading were applied to the twelve pipes installed in the test section.

All pipe deflection data were measured using the deflectometer in its final modified form. That is, the deflectometer signal and the signal of a displacement transducer were fed to an x-y plotter that produced a continuous plot of the pipe diameter as a function of its location along the length of the pipe.

The application of traffic with the C-141 load assembly was initiated immediately at the conclusion of the application of F-4 traffic. Significant problems that developed immediately after the initiation of C-141 traffic hampered all tests with the C-141 load. As mentioned previously, the surface rutting, the size of the test site, and mechanical difficulties made maneuvering of the C-141 assembly in a specific load pattern impossible. Static load, dynamic load, and permanent pipe deflection data were measured during the application of 10 coverages of C-141 traffic to half of the pipe specimens and 20 coverages to the other half. Again, the deflectometer arrangement used during the F-4 traffic was used during the application of simulated C-141 traffic.

TEST SITE NO. 3

The loading of the pipe installed in Test Site No. 3 was provided primarily by a military truck (M51 dump truck) along with passes of a personnel carrier (M113) and a few load applications of a military tank (M48A1). The M51 dump truck had a tire pressure of 70 psi. The loading was distributed by the natural wander of the vehicle. The total amount of test traffic was as follows:

Test Vehicle	Gross Weight lb	No. of Passes	Equivalent 18-kip Single-Axle Loads
M51	50,920	5,008	14,323
M51	41,145	1,750	6,125
M51	43,900	310	1,575
M51	48,699	1,040	12,120
M113	19,000	526	130
M48A1	103,210	20	50,000

Pipe deflections were measured at irregular intervals with the deflectometer described previously. The irregular interval of data collection was the result of the very small pipe response to the applied loading.

RESULTS

TEST SITE NO. 1

Data were collected during the field test conducted at the CTT in the form of surface elevations over the pipes, pipe deflections due to static loads, pipe deflections due to dynamic loads, and permanent deflections as a function of the number of load applications.

Table 4 contains a summary of the surface elevations at the center of the traffic lane directly over each pipe. These data demonstrate the deterioration of the surface above the pipes and the probable variations in the cover depth of each of the pipes. Note that major test site repair was accomplished after 14,000 coverages of traffic.

Table 5 contains a summary of static load pipe deflection. The deflections have been normalized with respect to the internal diameter of the individual pipes and are presented as a percentage of that diameter. The sign convention for pipe deflection is that a positive deflection represents an increase in the pipe diameter and, conversely, a negative deflection represents a decrease in the pipe diameter. It should be pointed out that the pipes were subjected to traffic between the various levels of load given in the table.

Figures 20 through 25 are comparison plots of vertical pipe deflection/static load relationships for each of the types of pipe under investigation. These curves were prepared to show the influence of the depth of cover and backfill material on the response of the pipe. Note that the data for Figures 22, 24, and 25 were obtained from the final report of the FHWA study* that was conducted concurrently with the one reported herein. Figures 26 and 27 contain plots of the change of pipe diameter due to a static load of 13 kips (13,000 lb) for the uninstrumented pipes F1 and G1. Data for both of these pipes were measured with the deflectometer after approximately 12,500 coverages of an equivalent 18-kip axle load.

---

* Bush and Sullivan, op. cit., p. 3.

Table 4

Surface Elevations at the Center of the Traffic Lane over Each Pipe (CTT)

Pipe	Coverages														
	0	126	707	2,000	2,892	5,339	8,038	10,000	12,000	14,000	14,000	16,000	18,000	20,000	22,000
A	-1.4	-1.6	-1.8	-1.6	-2.1	-2.0	-1.8	-2.1	-2.2	-2.8	-0.2	-0.9	-2.5	-1.2	-2.6
B	-1.4	-1.7	-1.8	-1.0	-1.3	-1.5	-2.4	-1.8	-1.7	-2.5	+0.1	-0.4	-1.5	-0.9	-2.43
C1	-1.2	-3.4*	--	--	--	--	--	--	--	--	--	--	--	--	--
C	-0.6	-1.0	-1.8	-1.7	-1.7	-1.3	-1.7	-1.4	-1.8	-1.7	+0.1	-0.5	-0.1	-0.5	-2.0
D	-0.9	-1.5	-2.0	-1.0	-1.1	--	--	--	--	--	--	--	--	--	--
E	-0.8	-1.0	-1.4	-1.3	-1.5	-1.0	-1.4	-1.4	-1.8	-1.3	+0.7	+0.3	+0.4	-0.1	0.0
F1	-0.4	-3.5	--	-1.1	-2.3	-1.0	-1.3	-1.4	-1.7	-1.8	-0.1	-0.2	-0.1	+0.1	0.0
F	-0.4	-0.9	-1.5	-1.5	-1.6	-1.1	-1.5	-1.5	-1.8	-2.0	+0.3	-0.1	-0.1	-0.3	-1.85
G1	-0.3	-1.6	-2.3	-1.3	-1.8	-0.8	-1.1	-1.9	-1.2	-1.8	0.0	-0.2	-1.7	-0.9	-1.5
G	-0.8	-1.2	-1.6	-2.5	-1.7	-2.0	-2.1	-2.0	-2.2	-2.3	-0.1	-0.4	-0.6	-0.4	-1.5
H	-0.7	-1.3	-0.7	-1.9	-2.5	--	--	--	--	--	--	--	--	--	--
H1**	-0.8	--	-1.3	--	-2.0	-1.9	-2.2	-3.0	--	--	--	--	--	--	--
I	-0.9	-2.4	-1.3	-1.7	-2.0	-1.2	-1.4	-1.6	-1.9	-2.8	-0.4	-0.9	-1.7	-1.4	-2.15
J	-1.1	-1.7	-1.7	-1.6	-1.8	-2.2	-2.5	-1.6	-1.9	-2.4	-0.6	-1.2	-3.1	-2.0	-3.0
K	-0.5	-3.1†	--	--	--	--	--	--	--	--	--	--	--	--	--
K1**	-1.2	--	-1.6	--	-1.9	-1.4	-1.7	-2.8	-1.1	-2.1	--	-2.7	--	--	--

* Elevation of C1 at 50 coverages was -1.85 in.

** Actual coverage levels for H1 and K1 were: 0; 1,449; 4,148; 6,110; 8,110; 10,110; 12,110; 14,110; 16,110; and 18,110.

† Elevation of K at 50 coverages was -1.30 in.

Table 5

Summary of Pipe Deflections Resulting from Static Loads

(Deflection/Pipe Interior Diameter) × 100

Pipe Gage	Static Load, lb								
	7,000	9,000	11,000	13,000	15,000	17,000	19,000	21,000	23,000
AV	-0.49	-0.46	-1.03	-0.89	-1.20	-1.48	-1.08	-0.53	-0.20
AH	+0.47	+0.40	--	--	--	--	--	--	--
BV	-0.48	-0.88	-1.06	-1.44	-1.35	-2.07	-1.32	-0.63	-0.96
BH	+0.42	+0.460	+0.96	+1.22	+1.28	+1.58	+1.06	+0.54	--
CV	-1.02	-0.76	-1.44	-1.28	-1.98	-1.84	-1.76	-2.05	-1.80
CH	+0.38	+0.20	+0.38	+0.44	+0.68	+0.56	+0.64	+0.82	+0.56
DV	-1.08	--	--	--	--	--	--	--	--
EV	-0.26	-0.59	-0.68	-0.52	-1.01	-0.94	-0.96	-0.99	-1.03
FV	-0.18	-0.11	-0.60	-0.54	-0.84	-0.98	-0.78	-0.86	-0.67
F1*	--	-2.58	-0.62	-0.26	--	--	--	--	--
GV	-0.42	-0.78	-0.71	-1.00	-1.41	-1.20	-1.20	-1.22	-1.40
G1*	--	--	-0.80	-1.10	--	--	--	--	--
GH	+0.14	+0.16	+0.24	+0.40	+0.52	+0.44	+0.44	+0.45	+0.62
HV	-0.82	--	--	--	--	--	--	--	--
IV	-0.45	-0.50	--	--	--	--	--	--	--
IH	+0.46	+0.3	--	--	--	--	--	--	--
JV	-0.35	-0.61	-1.05	-1.29	-1.25	-1.08	-1.03	-0.88	-1.02
JH	+0.42	+0.75	+1.04	+1.27	+1.27	+1.35	+1.20	+1.33	+1.39
KV	-3.00	--	--	--	--	--	--	--	--
HV1	--	--	--	--	--	--	--	--	--
KV1	--	--	-0.52	-0.43	-0.57	-0.89	-0.70	-0.86	-1.44

* Deflectometer data.

NOTE: Positive value of deflection represents an increase of diameter.

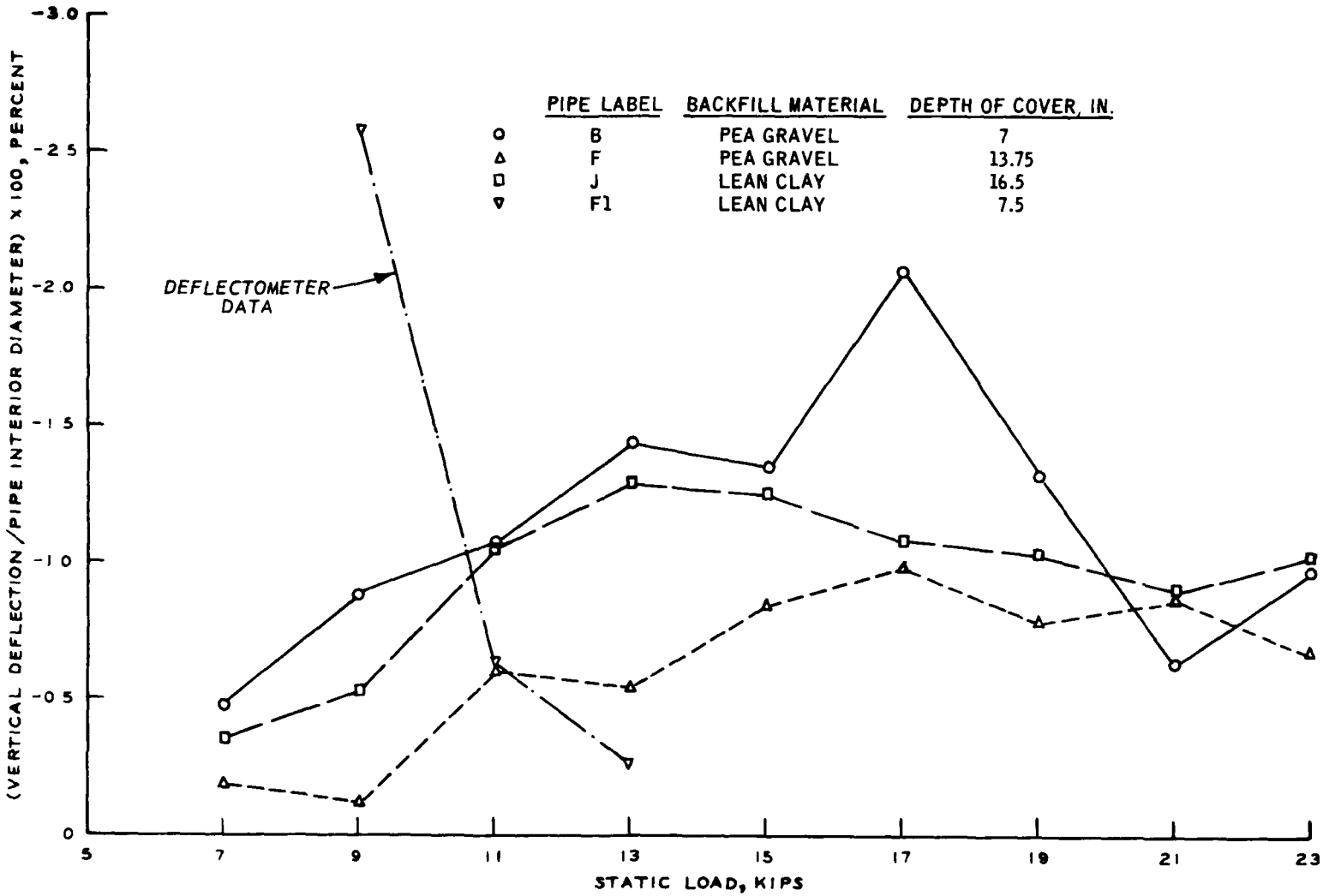

Figure 20. Vertical deflection of 12-in. PVC pipe as a function of applied static load

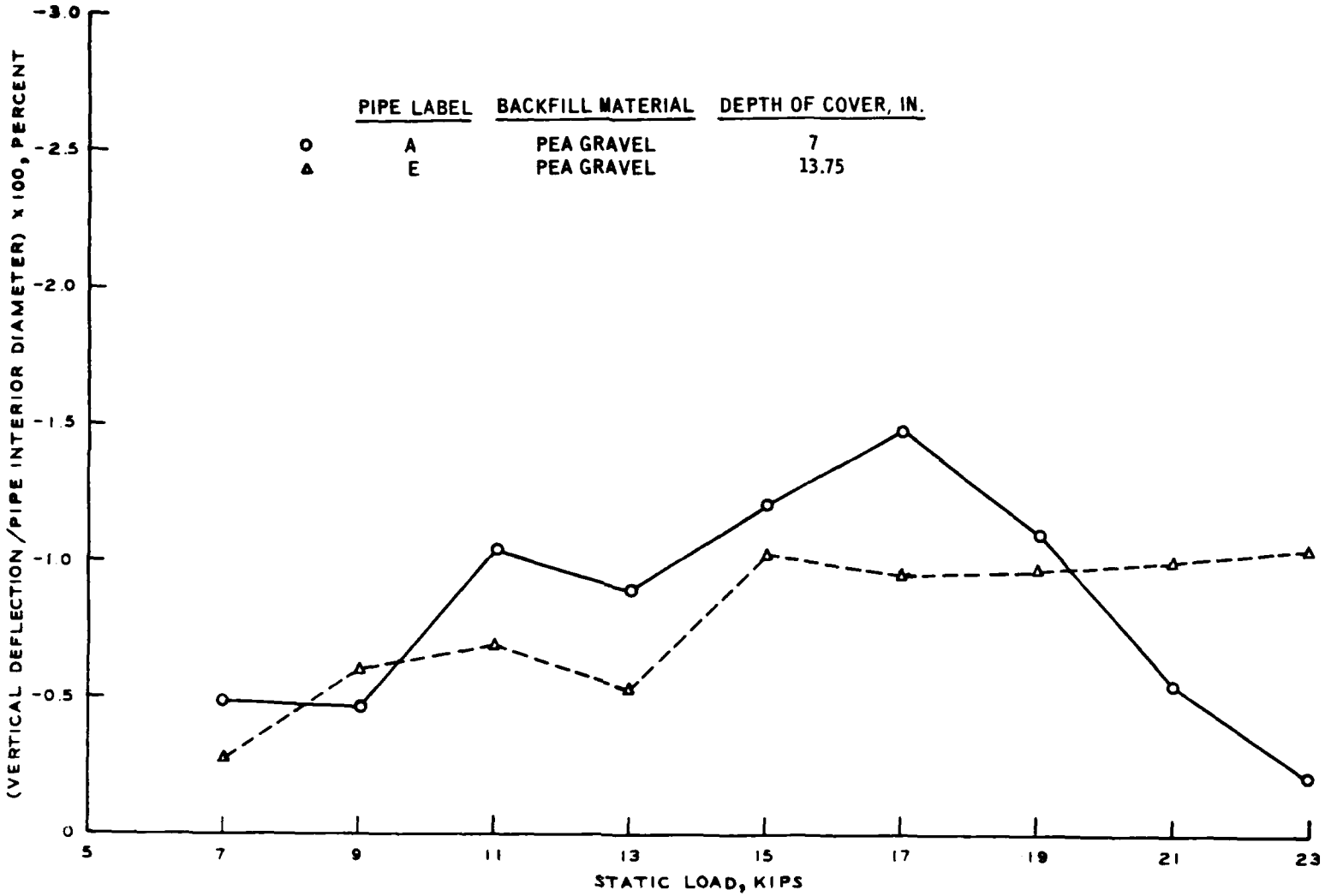

Figure 21. Vertical deflection of 10-in. PVC pipe as a function of applied static load

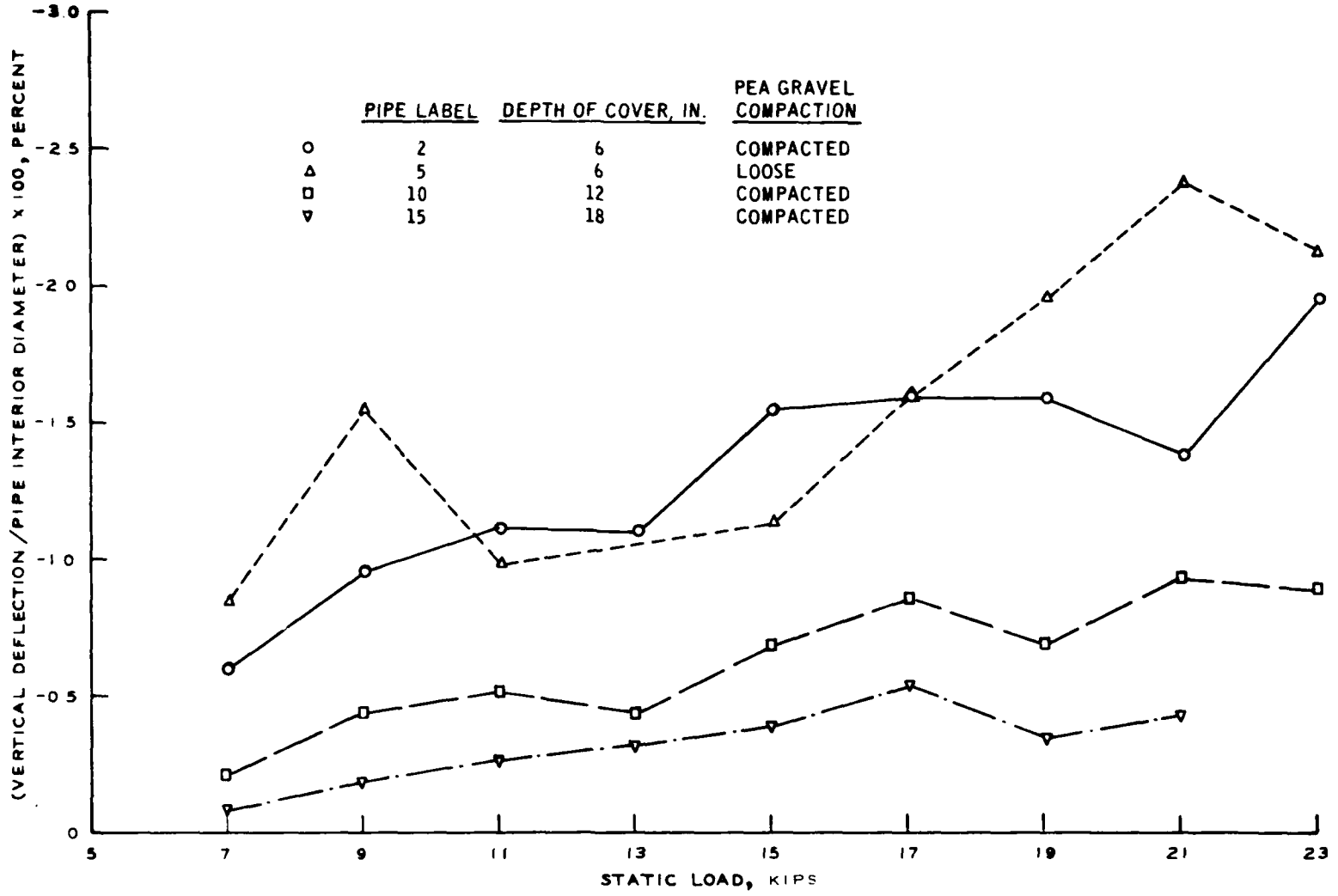

Figure 22. Vertical deflections of 6-in. PVC pipe in CTT as a function of applied static load

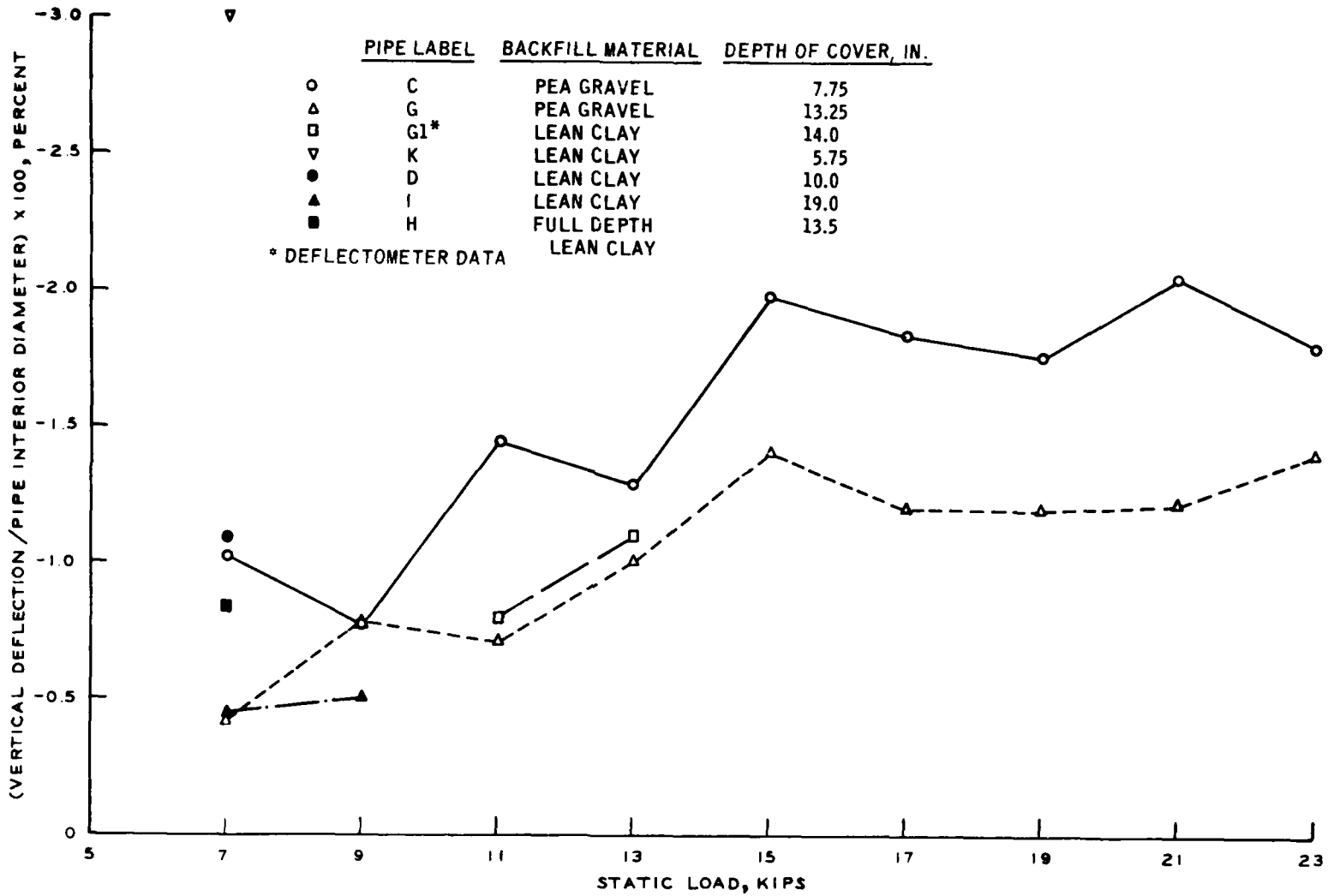

Figure 23. Vertical dèflection of 10-in. PE pipe as a function of applied static load

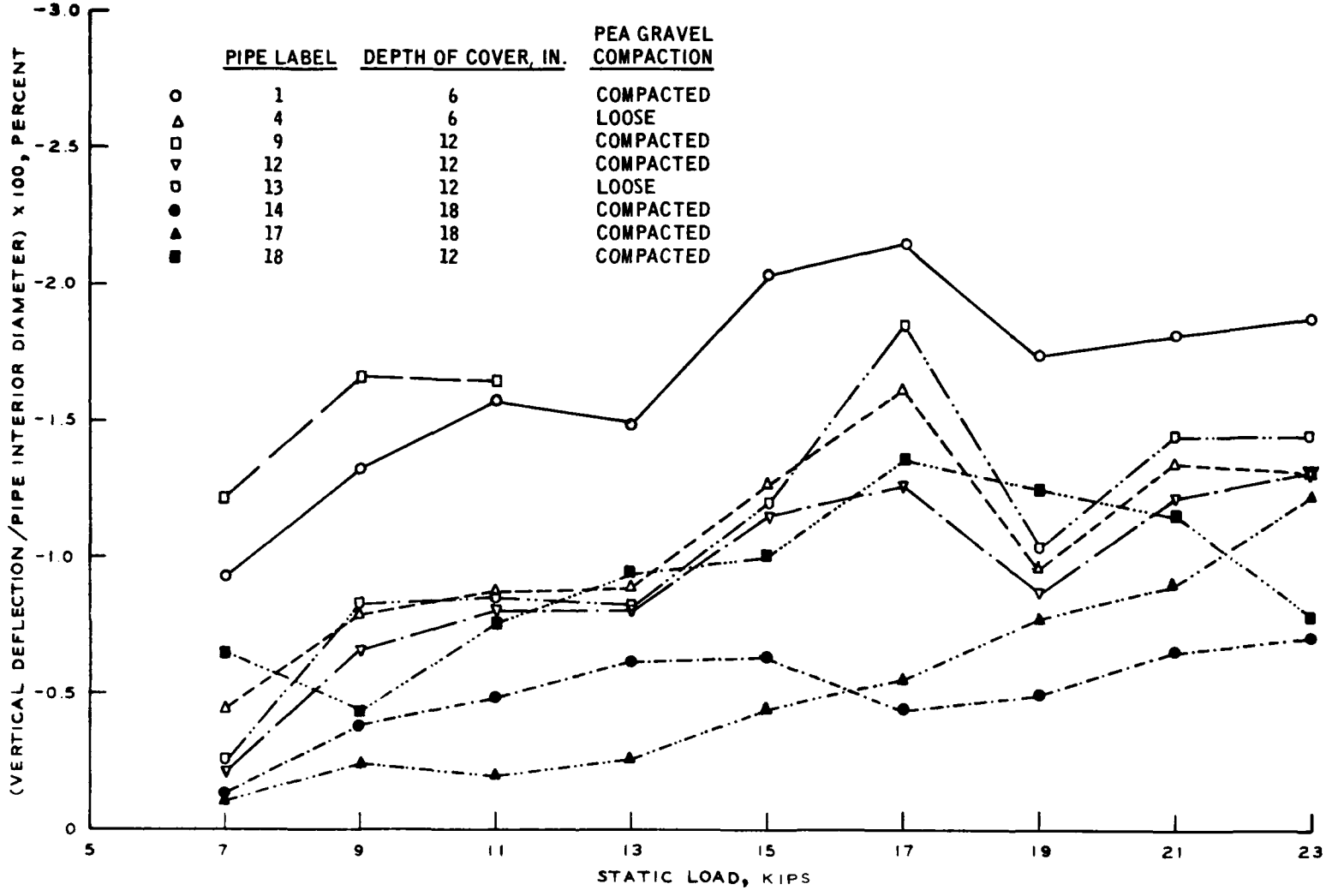

Figure 24. Vertical deflection of 6-in. PE pipe in CTT as a function of applied static load

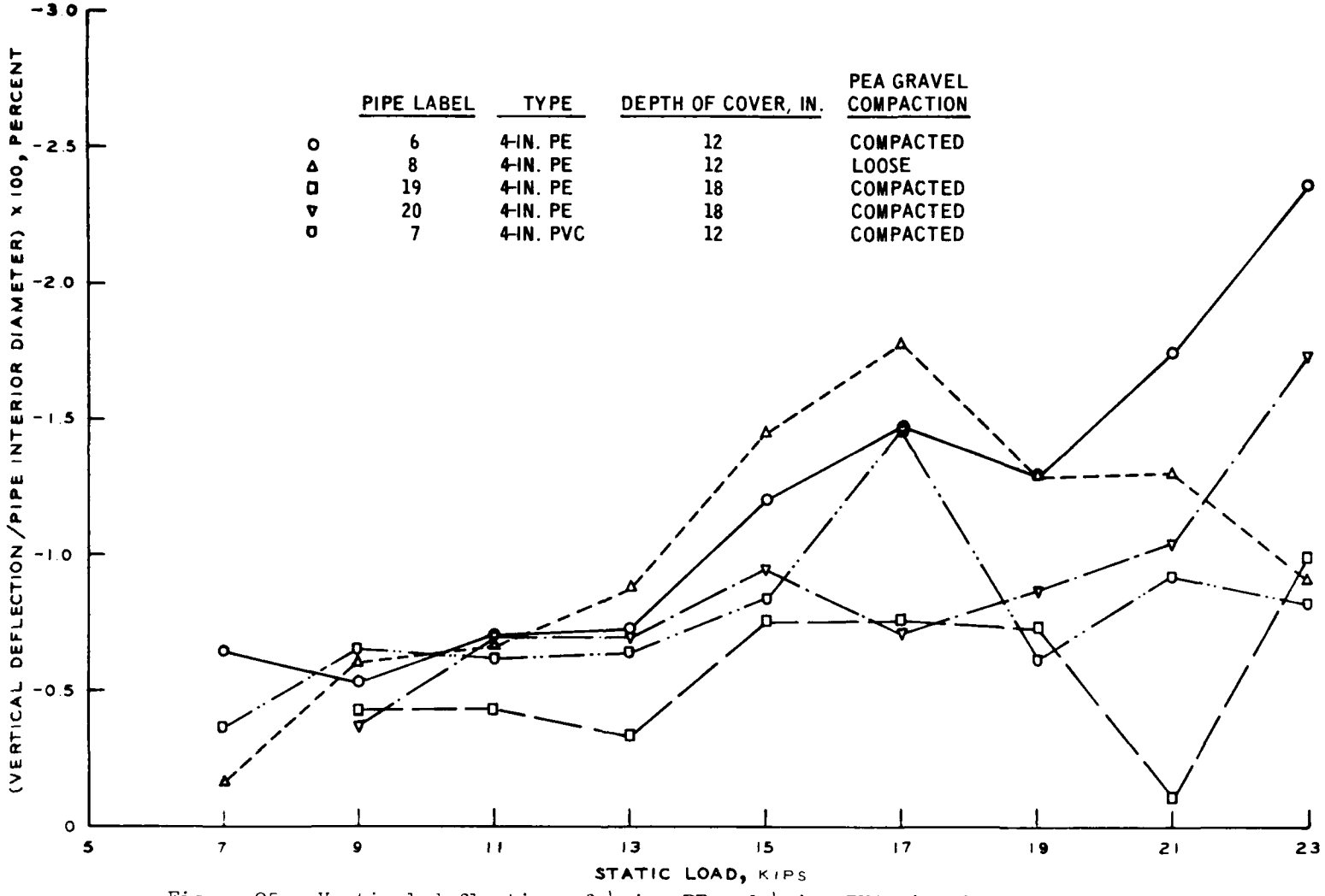

Figure 25. Vertical deflection of 4-in. PE and 4-in. PVC pipe in CTT as a function of the applied static load

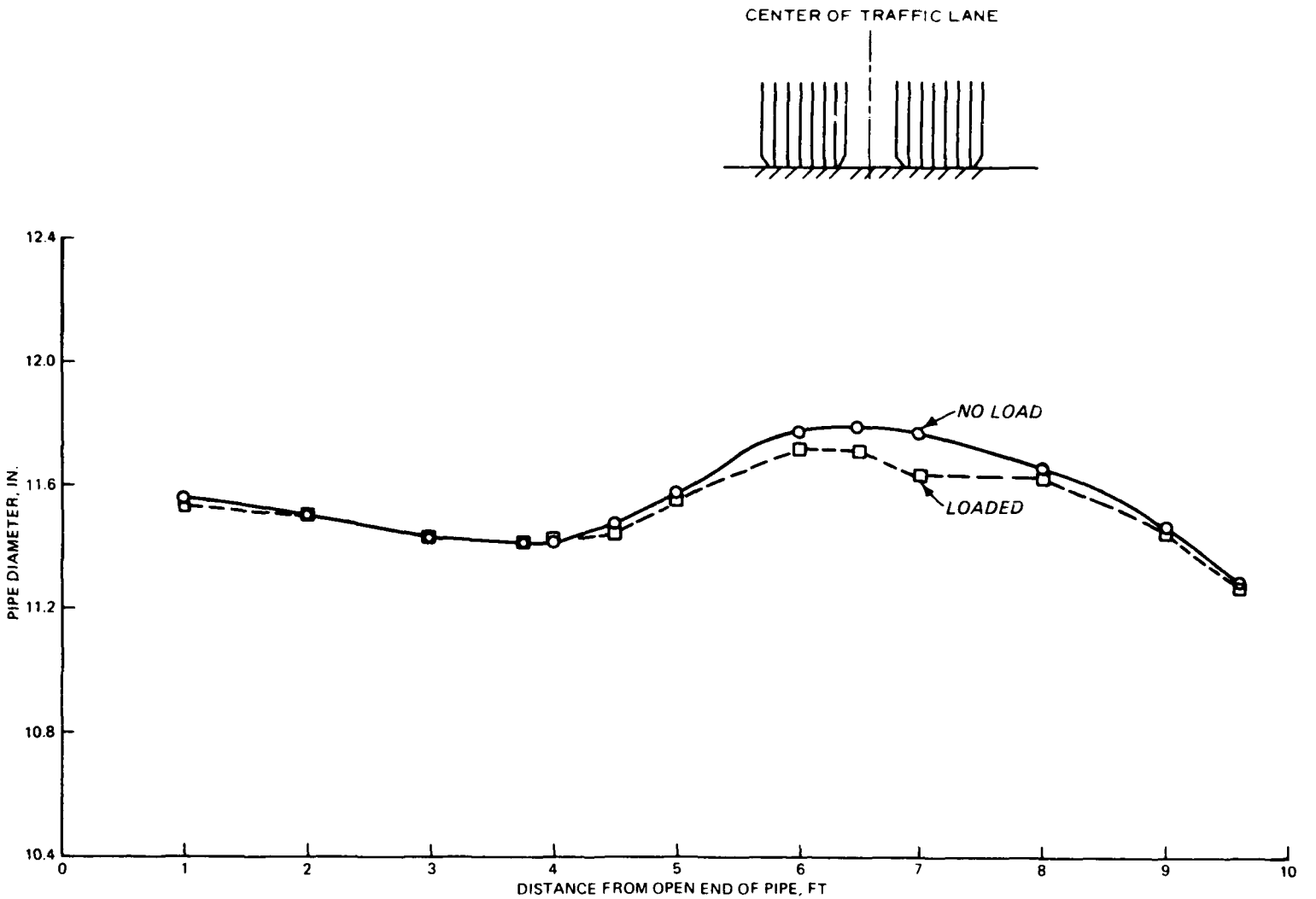

Figure 26. Measured deflectometer data for 12-in. PVC pipe F1 of CTT (13-kip static load after 10,000 coverages; approximately 12,500 coverages of 18-kip axle load)

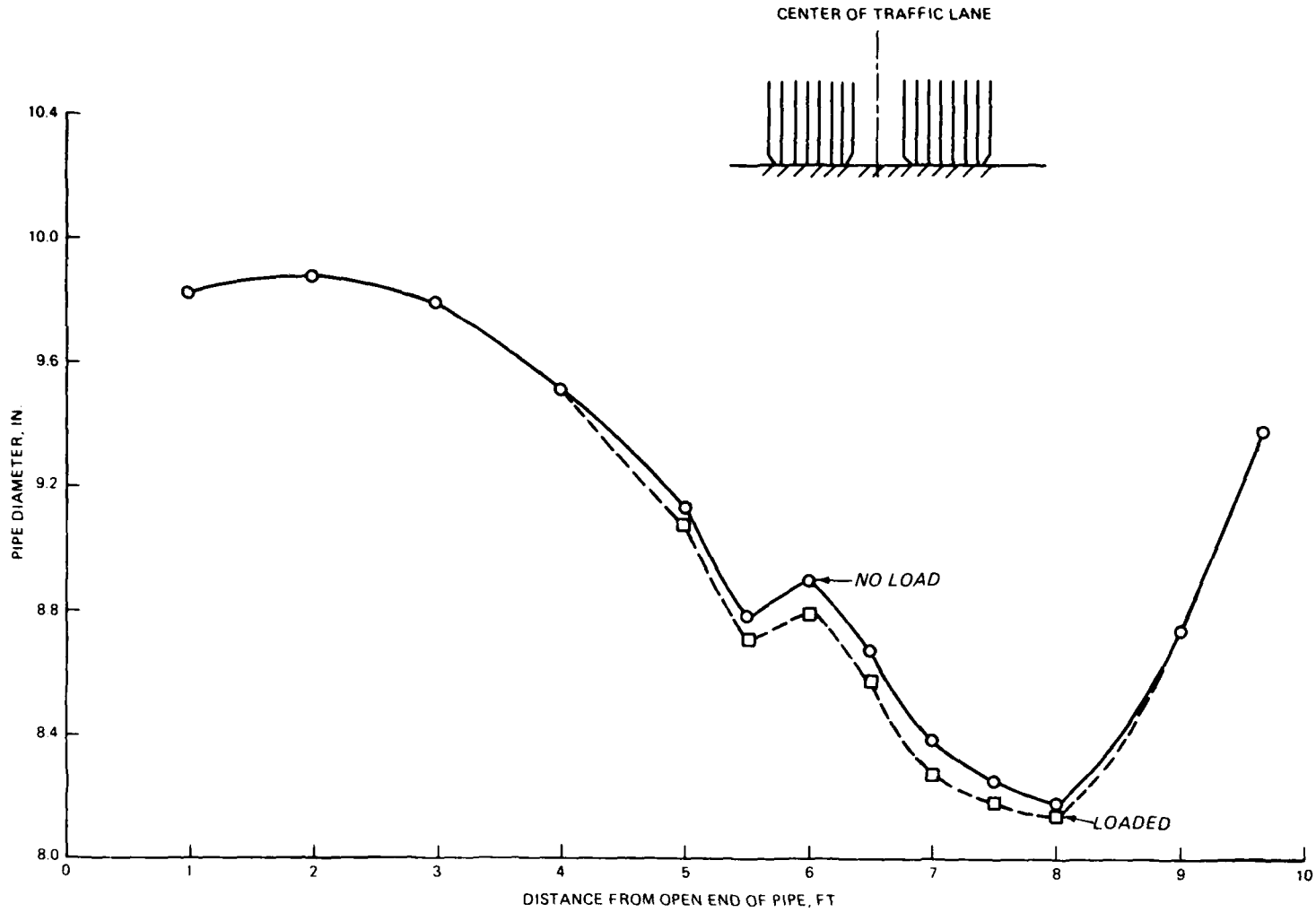

Figure 27. Measured deflectometer data for 10-in. PE pipe G1 of CTT (13-kip static load after 10,000 coverages; approximately 12,500 coverages of 18-kip axle load)

In general, the magnitude of the pipe deflections due to static loads was very small for the load range applied during the field tests at Test Site No. 1. In fact, the magnitude of deflection was always less than 2.5 percent and less than 1.5 percent for a great majority of the pipes. The results of the static load tests also show that the pipe deflections did not increase proportionally with the applied static load, which would support the idea that the pipe-soil system gets stiffer with traffic. In general, static pipe deflections increase with load to a maximum value and from that point show a gradual decrease with additional applied load. Generally, the static deflection of the pipe varied inversely with the depth of cover for those pipes with the same backfill material. Pipes installed with a clay backfill had greater deflections due to static loads than pipes installed at the same cover depth with pea gravel backfill. As would be expected, horizontal pipe deflections are less than vertical pipe deflections.

Figure 28 contains a typical oscillograph output for pipe response to dynamic loading. Figures A1 through A14 of Appendix A contain the pipe deflections at a point in the pipe as a result of the application of dynamic loads directly above the point. These data have been plotted as pipe deflections (normalized with respect to pipe internal diameter) as a function of load applications (coverages). The applied load as a function of coverage level is also shown at the top of each plot. In these plots the absolute value of pipe deflections has been plotted; thus, the vertical deflections are shown as positive values. The magnitudes of the pipe deflections due to dynamic loads were very small, with the majority of values being near 1 percent of the internal pipe diameter. The dynamic load deflections, in general, increase to a maximum value of deflection and then begin a decrease with additional traffic. This maximum value of deflection appears to vary inversely with the depth of cover, as shown in Figure 29. Finally, the dynamic load deflection data indicate no significant difference between the deflections of the different types of pipes for the same number of load applications.

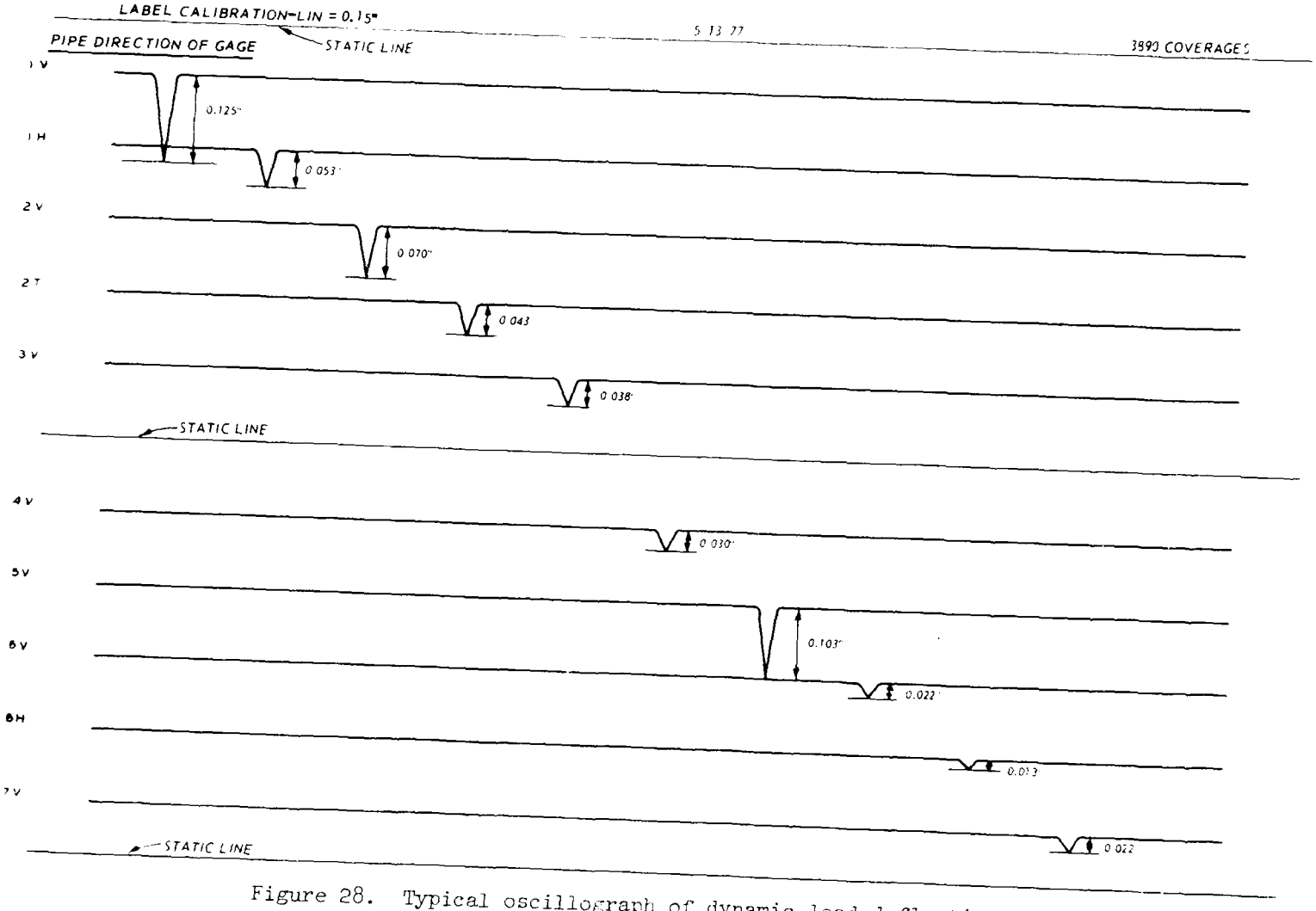

Figure 28. Typical oscillograph of dynamic load deflection

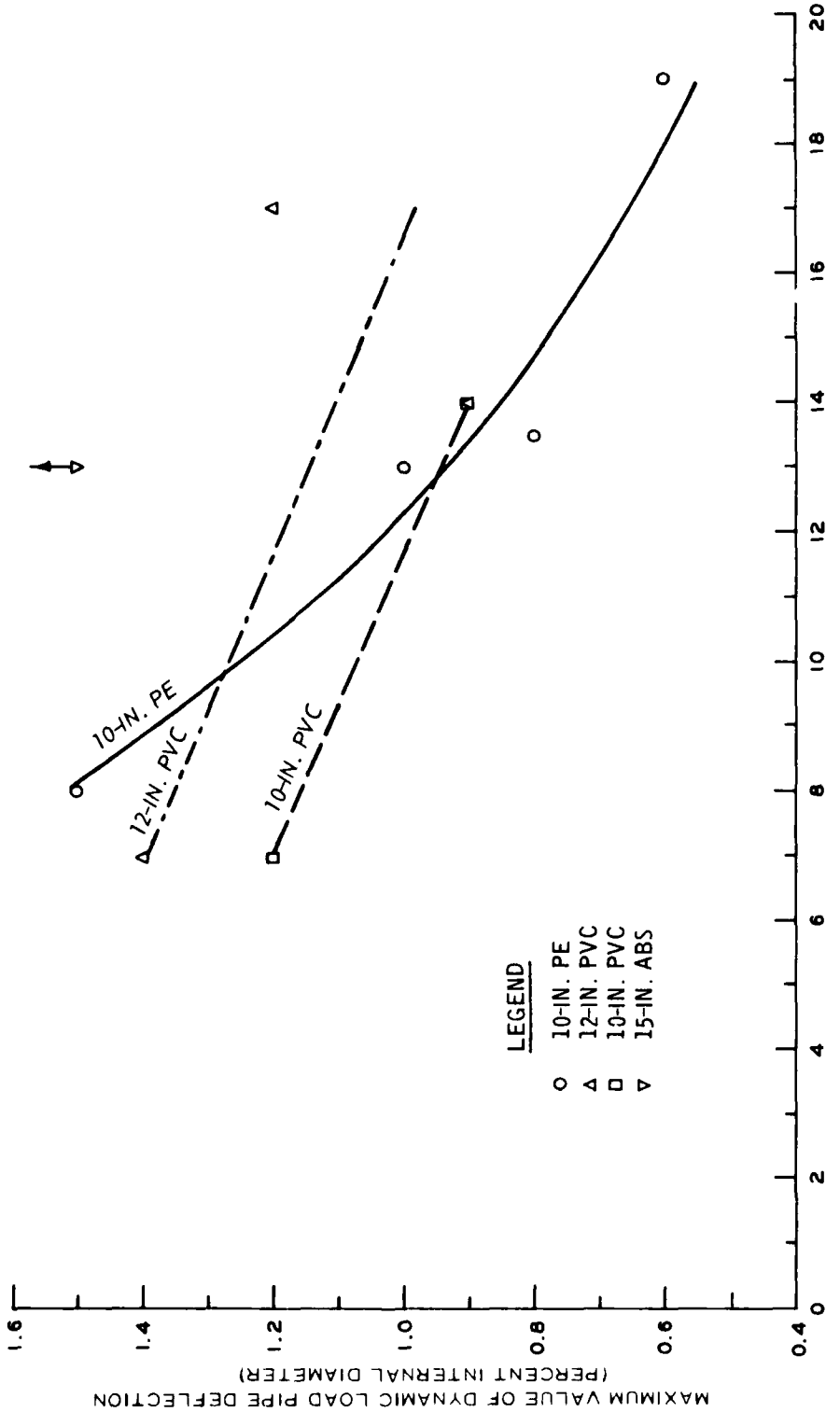

Figure 29. Variation of maximum value of dynamic load deflection with cover depth

Figures A15 through A35 of Appendix A contain plots of the permanent pipe deflection as a function of equivalent coverages of an 18-kip axle load. The actual coverage levels were converted to equivalent coverages* of an 18-kip axle load using the equivalent curve of Figure A36 of Appendix A. Again, pipe deflections are presented in terms of percentage of internal pipe diameter.

Table 6 contains a summary of permanent pipe deflections in which the zero level of the data of Figures A15 through A35 have been adjusted to account for the initial compaction of the pipe backfill material. These same data are presented in Figures 30 through 36 as curves of permanent pipe deflection as a function of equivalent coverages of an 18-kip axle load for each of the types of pipe under investigation. Also presented are similar results from Bush and Sullivan* for the smaller pipe sizes (4- and 6-in. PE and PVC).

The limit of acceptable permanent deflection for plastic pipes is a subject of some controversy. This limit ranges between a low of 5 percent to a high of 12 percent, depending upon the source and the approach selected. An acceptable deflection limit of 5 percent permanent deflection is probably the most common limit and was used throughout this report to establish the point at which the plastic pipes are considered to have failed. Pipe deflections were measured following the failure of the pipes (permanent deflection greater than the 5-percent limit) until the pipes had deflected to the point that they hampered the testing of other pipes, at which time they were removed from the test site.

The permanent deflection data at the CTT yield the following observations, which are listed according to the type of pipe.

PVC PIPE

a. The 10- and 12-in. PVC pipes performed very well for all depths of cover in both the pea gravel and lean clay backfill.

b. Both the 12-in. PVC pipe installed at a cover depth of 13.75 in. and the one installed at 7 in. with pea gravel

* Bush and Sullivan, op. cit., p. 3.

Table 6

Summary of Permanent Pipe Deflection Data from Circular Test Track

(Test Site No. 1)

Pipe ID	Type/Nom. Diam.	Depth of Cover in.	Type of Backfill	Load Applications (×1000 Coverages)								
				0	12.5	25	50	100	200	300	400	End of Testing
A	PVC/10	7	Gravel	0	-0.70	-0.80	-0.75	-0.850	-0.25	+0.125	+0.225	+0.250
B	PVC/12	7	Gravel	0	-1.4	-1.55	-0.9	-0.74	-1.05	-0.64	0.0	+0.120
C1	PE/10	7	Clay	0	Failed after 126 coverages of 18-kip axle load							
C	PE/10	7.75	Gravel	0	-1.5	-2.0	-2.25	-2.85	-2.95	-2.4	+0.700	+0.700
D	PE/10	10	Clay	0	Failed after approximately 600 coverages of 18-kip axle load (deflection = 16.5%)							
E	PVC/10	13.75	Gravel	0	-0.80	-0.80	-0.85	-0.50	-0.60	-0.425	--	-0.225
F1	PVC/12	7.5	Clay	0	Deflectometer data for <13,000 coverages of 18-kip axle load (+1.2% maximum)							
F	PVC/12	13.75	Gravel	0	-0.35	-0.45	-0.70	-0.75	-0.40	-0.30	--	-0.35
G1	PE/10	14	Clay	0	Deflectometer data for <13,000 coverages of 18-kip axle load (5% deflection at 600 coverages, 15.4% deflection at 12,850 coverages)							
G	PE/10	13.25	Gravel	0	-8.1	-9.2	-9.6	-10.0	-9.5	-10.0	--	-11.2
H	PE/10	13.5	Clay	0	Failed after approximately 2400 coverages of equivalent 18-kip axle load (deflection = -11.3%)							
I	PE/10	19	Clay	0	Failed after approximately 7000 coverages of equivalent 18-kip axle load (deflection = -15.0%)							
J	PVC/12	16.5	Clay	0	-3.4	-3.7	-4.4	-5.0	-4.9	-4.72	--	-4.72
K	PE/10	5.75	Clay	0	Failed after approximately 71 coverages of equivalent 18-kip axle load (deflection = -9.76%)							
H1	ABS/15	8.5	Clay	0	Failed after approximately 4000 coverages of equivalent 18-kip axle load (deflection = - 9.77%)							
K1	ABS/15	13.0	Clay	0	0.0	0.0	-0.125	-0.125	-1.250	-5.375	--	-10.88

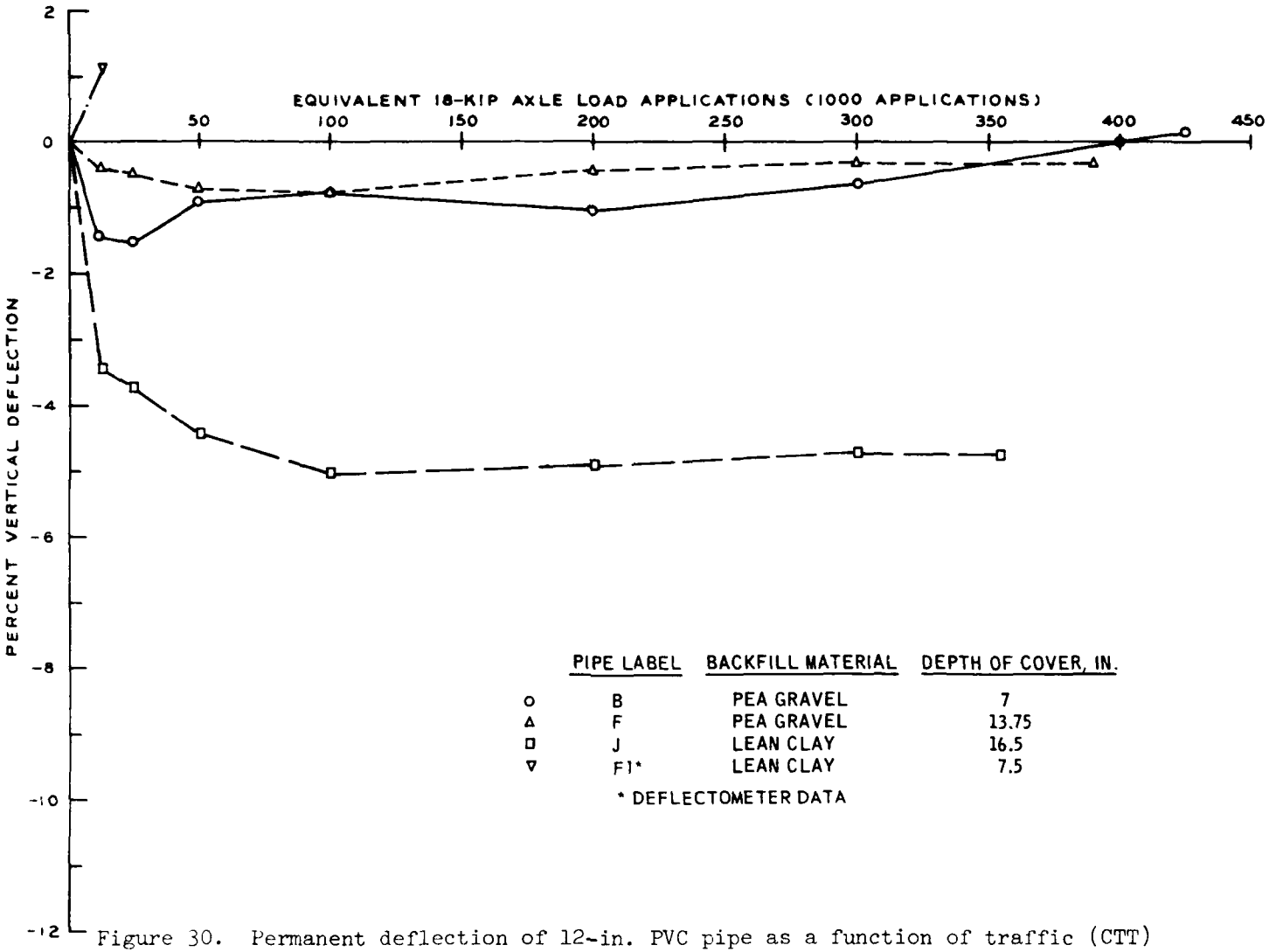

Figure 30. Permanent deflection of 12-in. PVC pipe as a function of traffic (CTT)

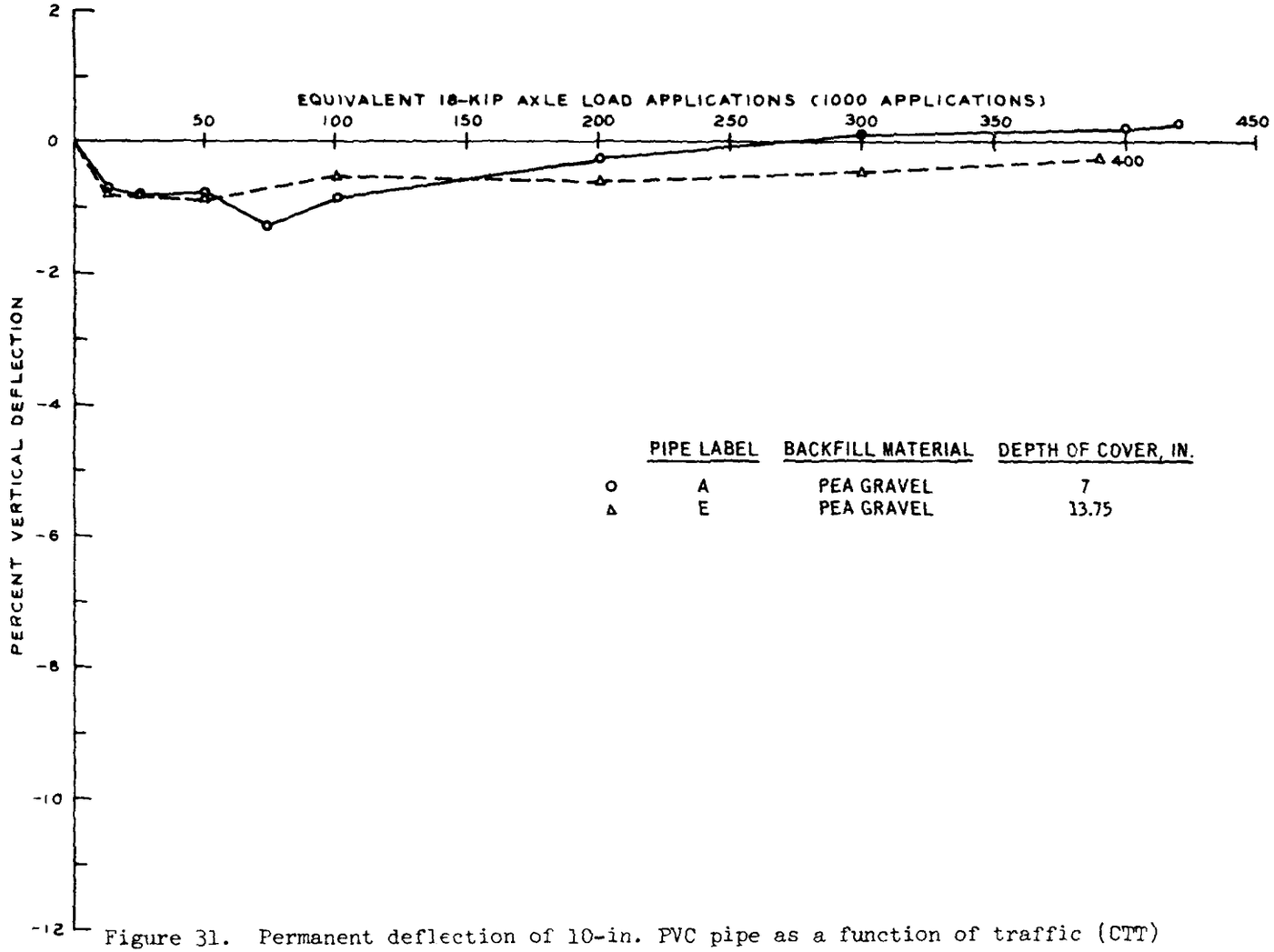

Figure 31. Permanent deflection of 10-in. PVC pipe as a function of traffic (CTT)

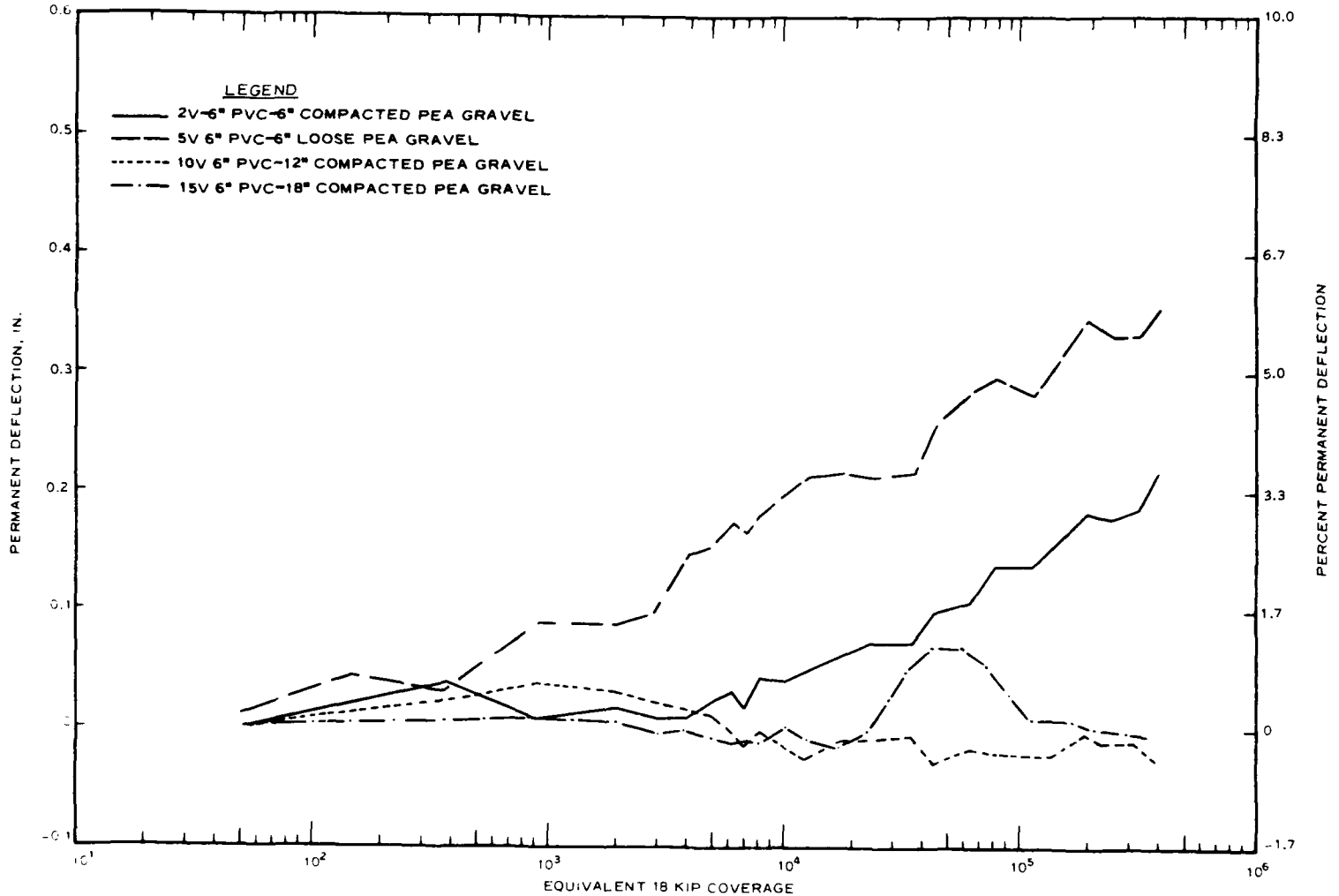

Figure 32. Permanent deflection of 6-in. PVC pipe as a function of traffic (CTT)

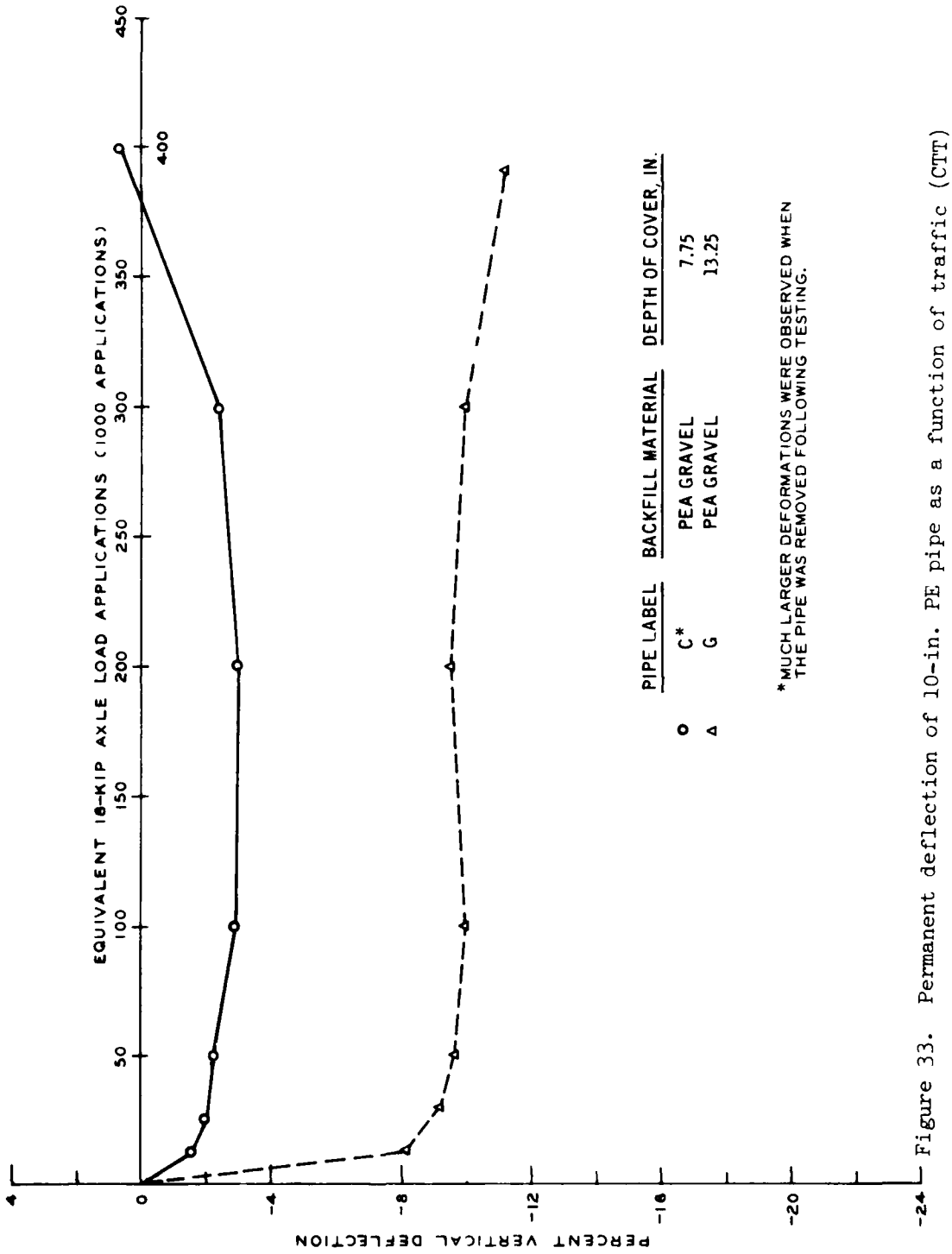

Figure 33. Permanent deflection of 10-in. PE pipe as a function of traffic (CTT)

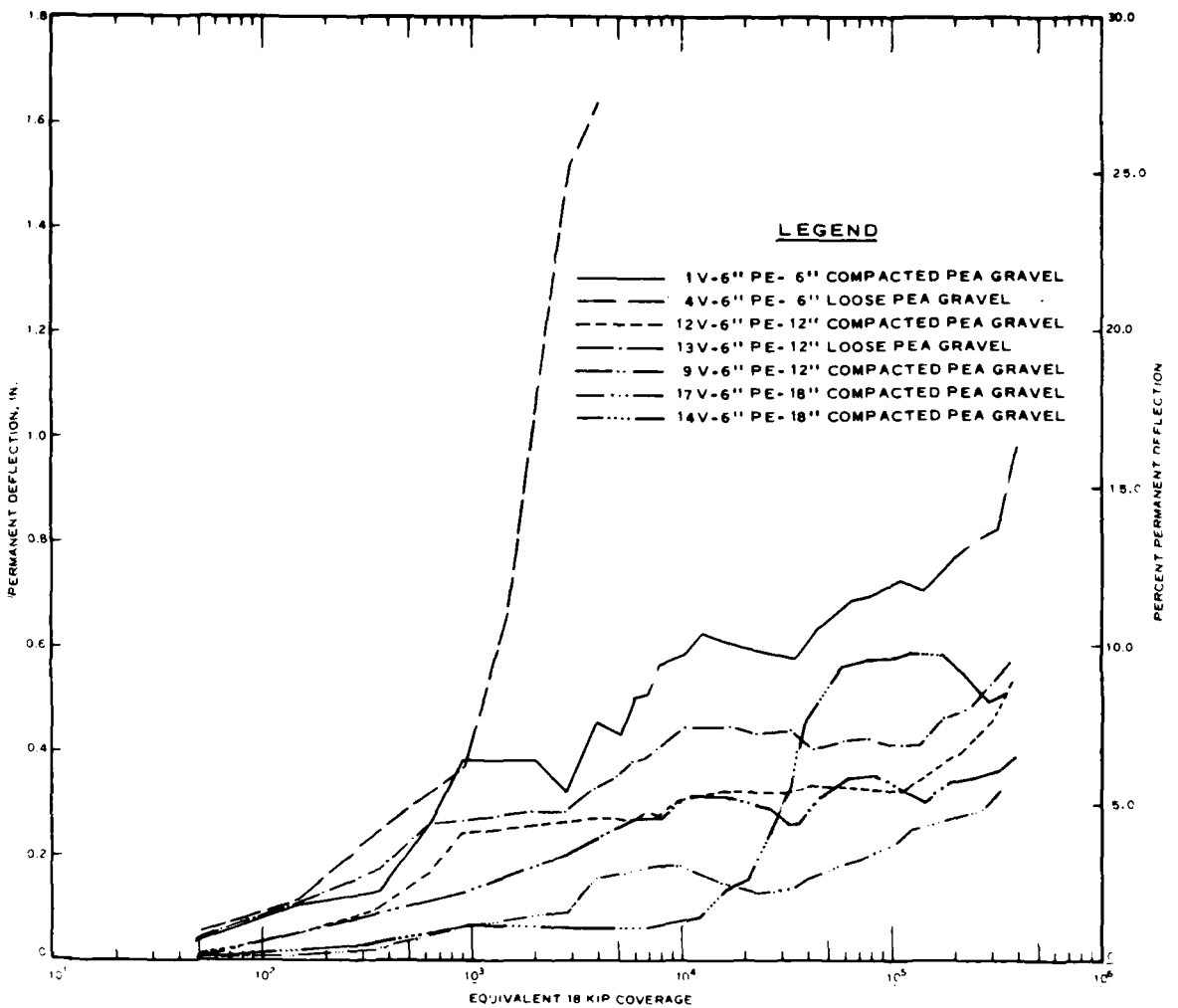

Figure 34. Permanent deflection of 6-in. PE pipe as a function of traffic (CTT)

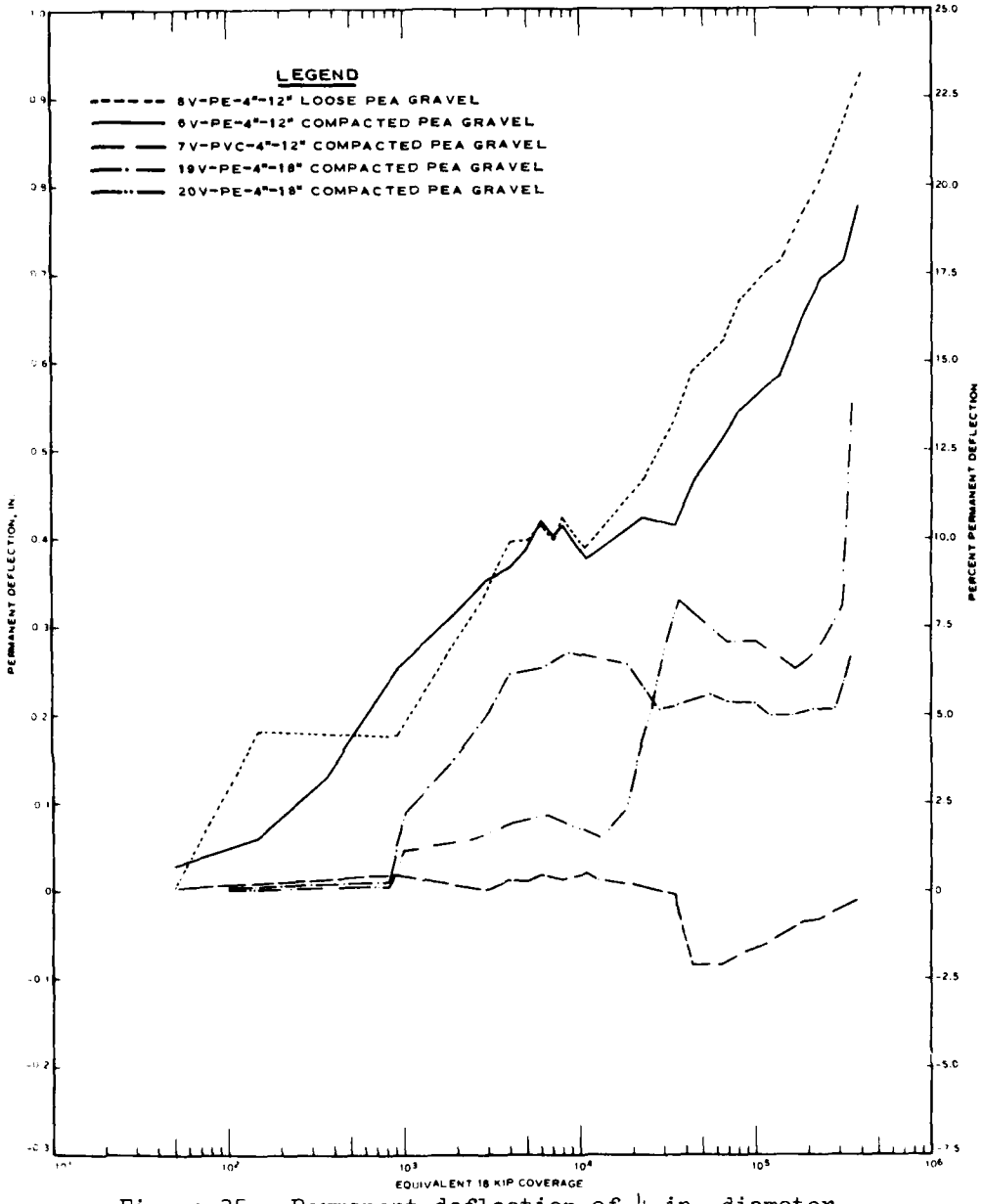

Figure 35. Permanent deflection of 4-in.-diameter PE and PVC pipes

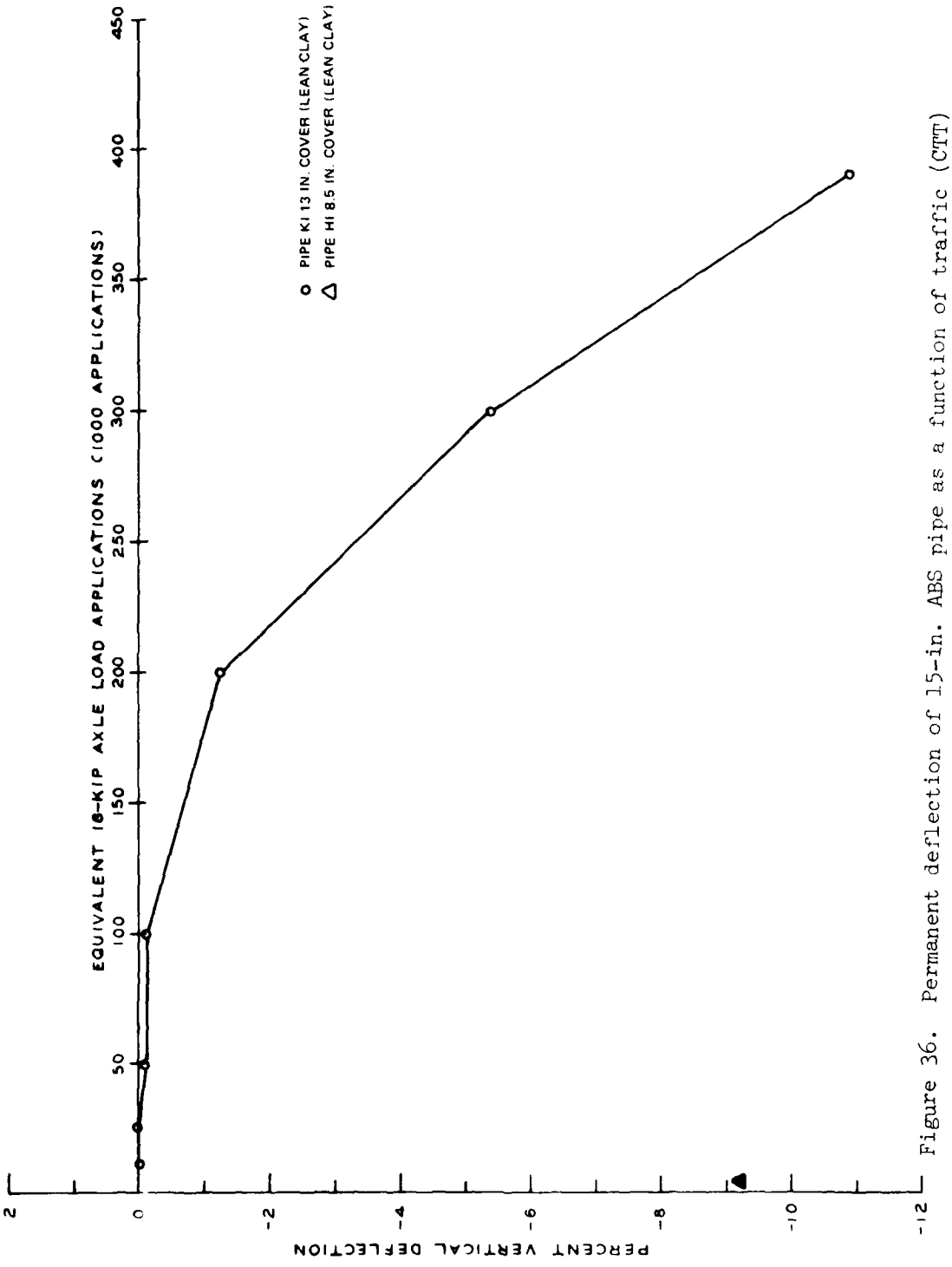

Figure 36. Permanent deflection of 15-in. ABS pipe as a function of traffic (CTT)

backfill had very small permanent deflections (less than 2 percent) after 400,000 applications of equivalent 18-kip axle loads.

c. The 12-in. PVC pipe with a cover depth of 16.5 in. and a lean clay backfill reached a maximum deflection of approximately 5 percent after 100,000 equivalent 18-kip axle loads and remained at that level for the remainder of the field tests.

d. Both the 10-in. PVC pipes installed with pea gravel backfill, one at 7-in. cover depth and the other at 13.75-in. cover depth, had maximum permanent deflections of less than 1 percent throughout the field tests at the CTT.

e. Of the four 6-in. PVC pipes installed (all with pea gravel bedding and backfill), the two installed at the 6-in. cover depth had permanent deflections that exceeded 5 percent but neither had a permanent deflection greater than 8 percent at the conclusion of testing. The other two 6-in. PVC pipes were installed at 12 and 18 in. of cover and had permanent deflections that did not exceed 3 percent before testing was terminated.

f. The one 4-in. PVC pipe installed with 12 in. of cover had a maximum permanent deflection in the vertical direction of approximately 2.5 percent.

PE PIPE

a. Of the two 10-in. PE pipes with pea gravel bedding and backfill, surprisingly the pipe installed at a depth of 7.75 in. appeared to develop a much smaller permanent deflection than the one installed with a 13.25-in. depth of cover. The shallower pipe had an indicated maximum vertical permanent deflection of approximately 3 percent, while the deeper pipe had a maximum permanent deflection of 11 percent. The deflection of both pipes seemed to stabilize after approximately 75,000 equivalent 18-kip axle load coverages and maintain that level of permanent deflection through approximately 300,000 equivalent 18-kip axle load coverages. At that point the permanent deflection of the deeper pipe began to slowly increase while the permanent deflection of the shallow buried pipe began to decrease. When the shallow pipe was removed at the completion of testing, it appeared to have deflected considerably more than the 3 percent maximum indicated by its gage in the vertical direction, and it appeared as though the pipe had rotated during the testing such that the vertical gage was no longer vertical. In fact, it appeared that the gage could have rotated in the direction of oncoming traffic by as much as 30 to 45 deg. Of course, this would influence the magnitude of the deflection indicated by the gage since it would

not be sensing the maximum change in pipe diameter. This probably accounts for the discrepancy between the electronically measured deflection of the shallow pipe and the observed deflection.

b. The six 10-in. PE pipes installed with pea gravel bedding but with a lean clay backfill material did not perform well. In fact, all six pipes failed very early in the tests. The pipe at the 5.75-in. depth survived approximately 71 equivalent 18-kip axle load coverages, the one at the 19-in. cover depth lasted through 7,000 coverages, and those at depths of cover of 7, 10, and 13.5 in. survived equivalent 18-kip axle load coverage levels of 216, 600, and 2,400, respectively. The 10-in. PE pipe installed with 14 in. of cover carried 10,000 equivalent 18-kip axle load coverages but had a permanent deflection of approximately 15 percent.

c. All of the 4- and 6-in. PE pipes installed with cover depths of 6, 12, or 18 in. had exceeded 5 percent deflection prior to the completion of the tests.

ABS PIPE

Both of the 15-in. ABS pipes were installed with lean clay backfill. The one with 8.5 in. of cover failed after approximately 4,000 coverages with a permanent deflection of approximately 10 percent. The pipe with 13 in. of cover had approximately 2 percent permanent deflection through 200,000 equivalent 18-kip axle load coverages, but started to deteriorate rapidly from that point. It had exceeded a permanent deflection of 5 percent by 300,000 equivalent 18-kip axle load coverages and had exceeded 10 percent before 400,000 coverages.

TEST SITE NO. 2

Figures B1 through B53 of Appendix B contain the measured deflectometer data for all of the pipes of this site for various levels of simulated F-4 and C-141 traffic and for static loads of the F-4 and C-141 gear assemblies. All subsequent figures and tables related to pipe response to static loads or permanent deflection are based upon the data presented in these figures.

Table 7 contains a summary of the pipe deflections as a function of static loads of the F-4 and C-141 load assemblies after various levels of applied traffic. These same data are presented in graphical form in Figures 37 through 39 for the three types of pipe investigated.

Table 7

Pipe Deflections Due to Static Loads on Pipes Installed in Test Site No. 2

(Percent of Internal Diameters)

Pipe No.	Pipe Type	Depth of Cover in.	P4				C-141	
			0	10	54	86	0	10
1	ABS	15.5	-1.49	-3.11	--	--	-1.96	--
2	ABS	20.5	-0.78	--	-1.42	-1.59	-2.03	--
3	PVC	17.00	-0.86	--	-1.72	-1.55	-3.23	--
4	PVC	20.5	-0.77	--	-1.55	-1.12	-2.32	--
5	PE	15	-1.29	--	-4.76	-3.57	-3.37	>-32
6	PE	18.0	-1.49	--	-1.69	-1.69	-2.87	--
7	ABS	24.0	-1.35	--	-1.28	--	-1.42	- 1.55
8	ABS	28.0	-0.57	--	-0.91	-0.71	-0.47	- 1.62
9	PVC	24.0	-0.95	--	-1.08	-0.77	-0.95	- 1.08
10	PVC	30.5	-0.69	--	-0.69	-0.60	-1.25	- 0.99
11	PE	24.0	-1.19	--	-1.09	-1.39	-1.78	- 1.59
12	PE	28.0	-1.49	--	-1.49	-0.79	-1.69	- 2.78

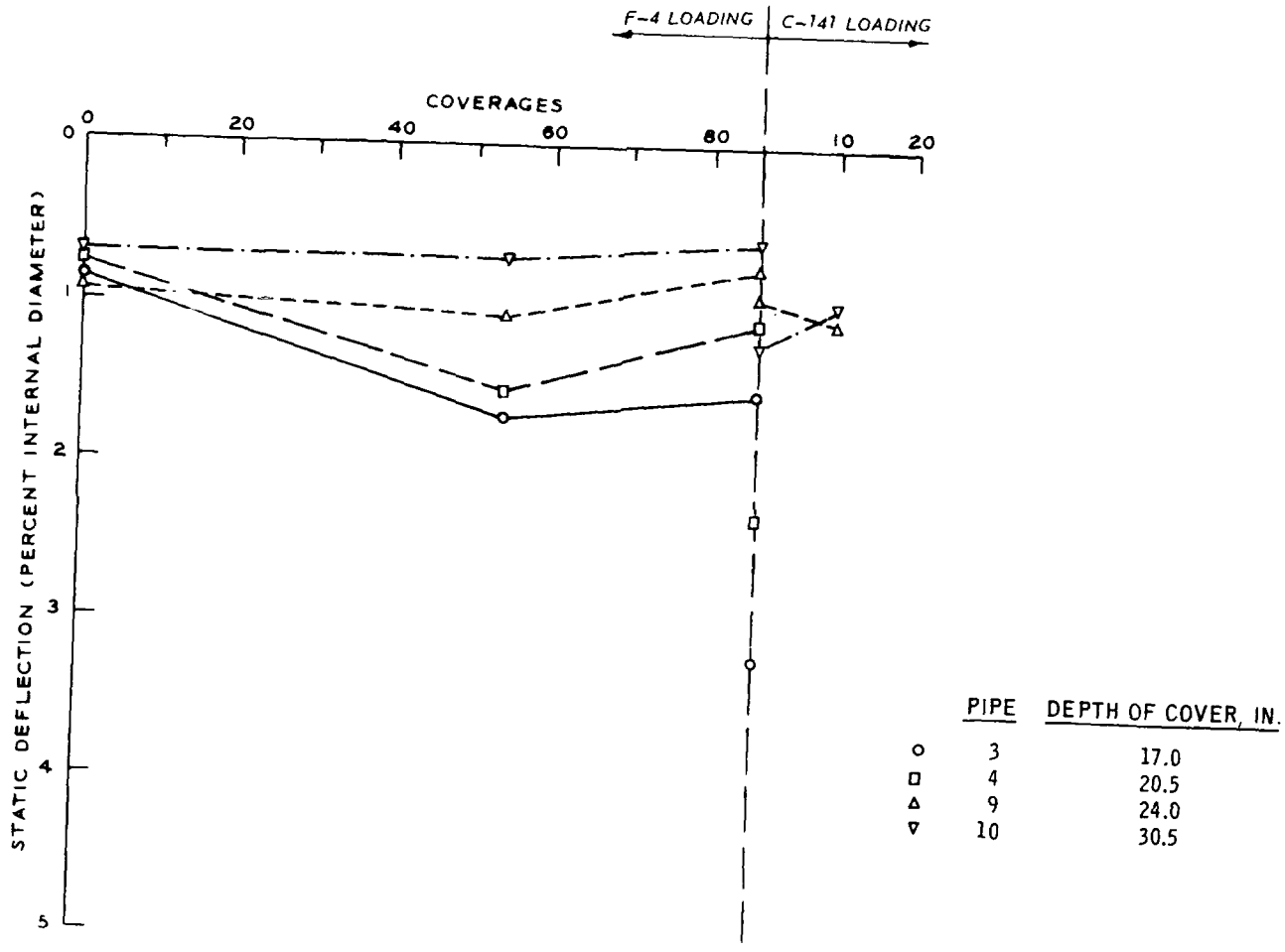

Figure 37. Summary of pipe deflections due to static loads at Test Site No. 2 (12-in. PVC pipe)

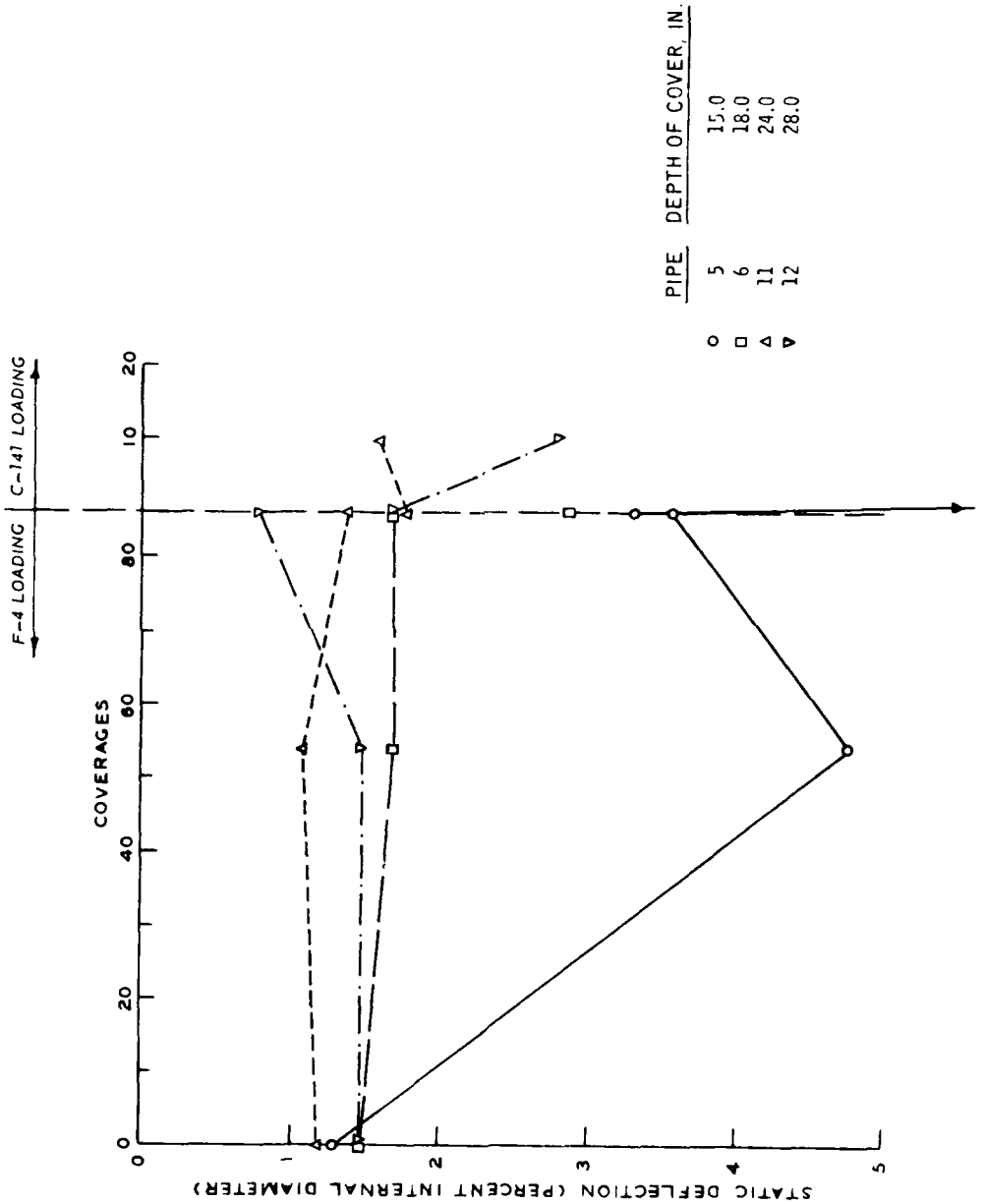

Figure 38. Summary of pipe deflections due to static loads at Test Site No. 2 (10-in. PE pipe)

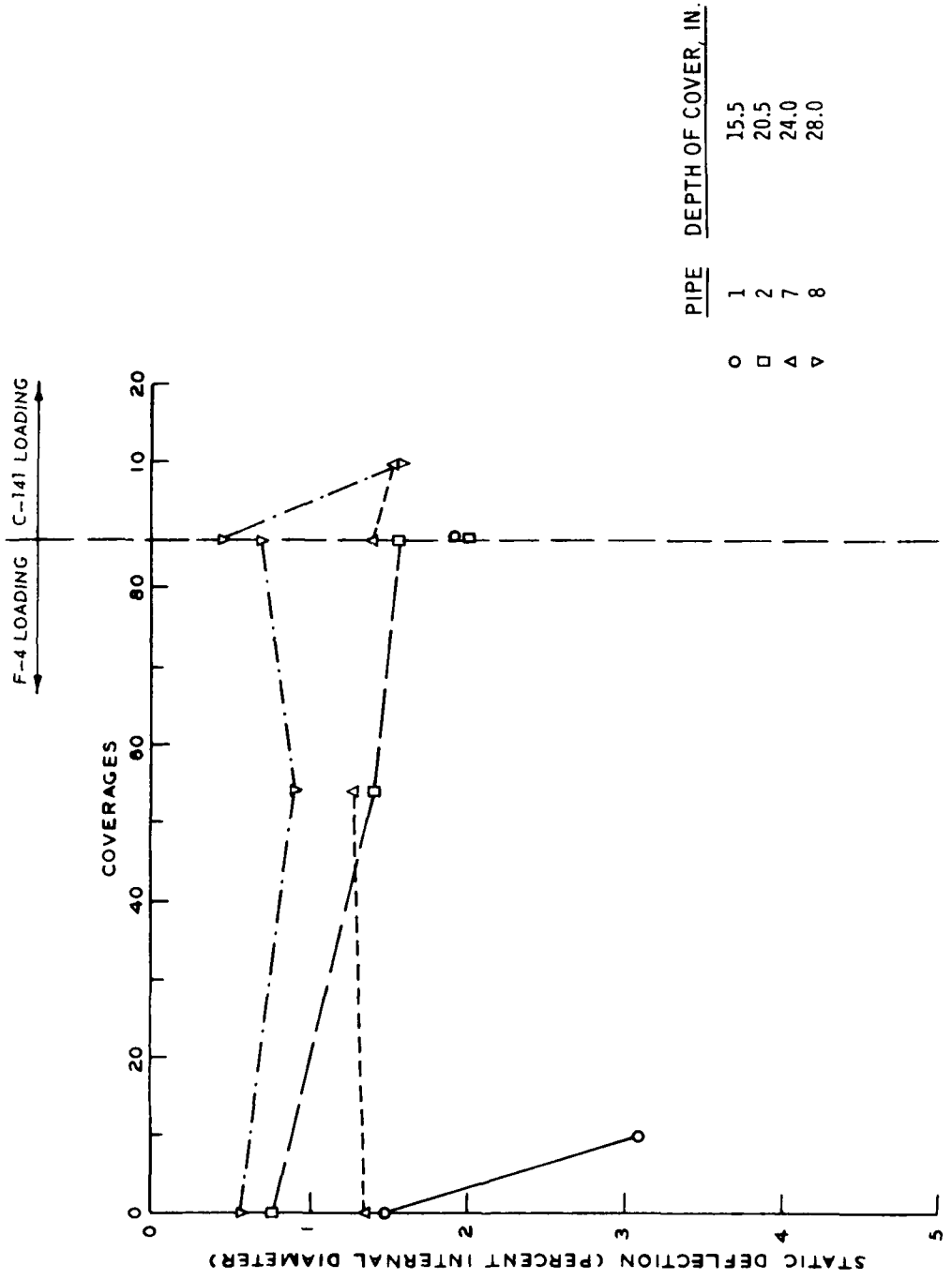

Figure 39. Summary of pipe deflections due to static loads at Test Site No. 2 (15-in. ABS pipe)

As was the case at Test Site No. 1, the pipe deflections due to static loads applied directly over the pipe were generally less than 3 percent. The one exception was the case of the 10-in. PE pipe with a cover depth of 15 in. which had a maximum deflection of approximately 32 percent for the C-141 static loading. With few exceptions the deflection due to static load varied inversely with the depth of cover.

Table 8 contains a summary of the response to dynamic loading of several of the pipes in the test site. Since only one deflectometer was available, only limited dynamic loading data were collected. Again, the dynamic deflections were very small, with the exception of the measured dynamic deflection of Pipe 3 (12-in. PVC) at a depth of 17.25 in. for the dynamic load simulating the C-141 loading.

Table 9 contains a summary of the permanent deflection of the pipes with respect to the level of applied traffic. These data are presented in graphical form in Figures 40 through 42 for the three types of pipe. Figures B38 through B53 of Appendix B contain summary plots of the permanent pipe deflection for the full measurable length of the pipe at various levels of applied traffic. A general trend noted for pipes in Test Site No. 2 was that pipes installed at deeper depths had larger permanent deflections than pipe at shallower depths. This trend is not considered fully developed because the deflection values were very small and few load repetitions were actually applied to the test site.

PVC PIPE

The PVC pipe performed very well under traffic. The maximum deflections in these pipes were less than 3 percent even for the case of the applied C-141 load.

PE PIPE

Permanent deflections significantly greater than 5 percent were measured in the 10-in. PE pipe with the least cover (15 in.), but the 5 percent deflection criterion was only slightly exceeded in the pipe with the greatest cover (28 in.) for the F-4 and C-141 loading. The PE pipe with 18-in. cover also had permanent deflections greater than 5 percent

Table 8

Summary of Dynamic Load Response of Pipe Installed in Test Site No. 2

Pipe No.	Load Assembly	Coverage Level F4/C-141	Maximum Dynamic Deflection (% Internal Diameter)
3	C-141	86/0	>-9
5	F4	20/0	-1.35
	F4	30/0	-2.51
	F4	54/0	-3.31
9	C-141	86/10	+0.79
	C-141	86/20	+1.2
11	F4	10/0	+0.6
	F4	54/0	+1.09
	F4	86/0	+1.19

Table 9

Summary of Permanent Pipe Deflections for the Pipes Installed in Test Site No. 2 (Percent of Internal Diameter)

Pipe No.	F4 Coverage Levels					C-141 Coverage Levels	
	0	10	28	54	86	10	20
1	0	0.71	--	--	--	--	--
2	0	--	--	-1.50	- 1.91	--	--
3	0	--	--	-0.68	- 1.02	+ 2.21	--
4	0	--	--	+0.78	+ 1.30	+ 1.93	--
5	0	--	--	+2.41	+12.04	>32	--
6	0	--	--	-2.51	- 3.34	- 7.74	--
7	0	--	--	-0.48	+ 0.48	- 1.44	-2.54
8	0	--	--	-1.55	- 1.55	- 2.44	-4.47
9	0	--	-1.30	-2.42	- 1.90	- 1.37	-2.23
10	0	--	-0.96	-1.56	- 0.78	- 2.63	-2.72
11	0	--	-2.65	-3.28	- 3.39	- 2.21	-4.11
12	0	--	-3.81	-4.87	- 6.89	- 4.15	-6.02

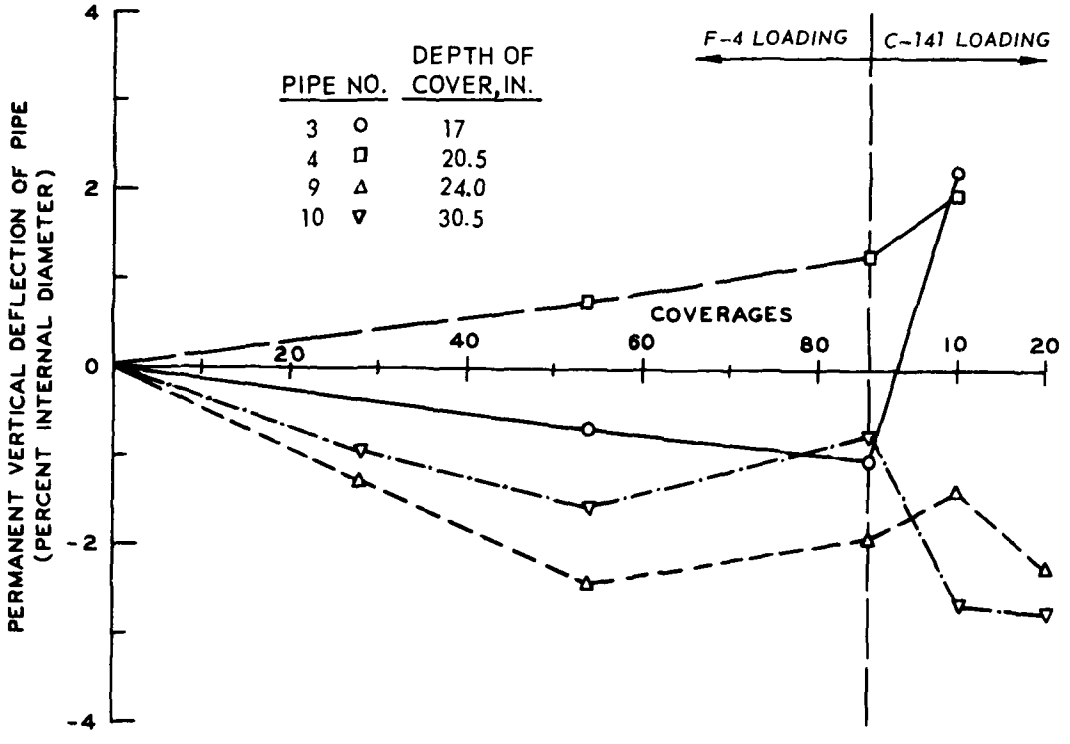

Figure 40. Summary of permanent deflections of the 12-in. PVC pipe installed in Test Site No. 2

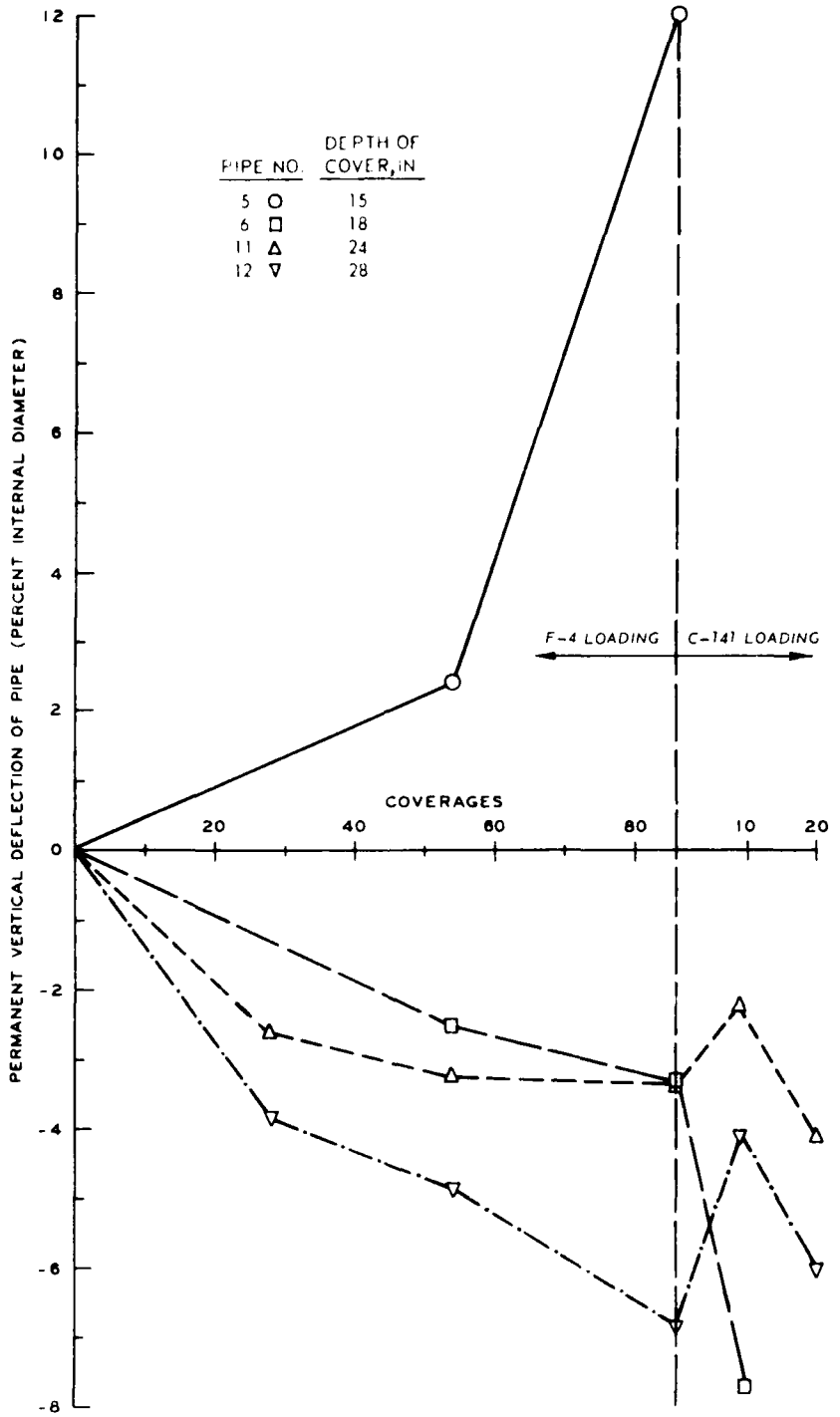

Figure 41. Summary of permanent deflections of the 10-in. PE pipe installed in Test Site No. 2

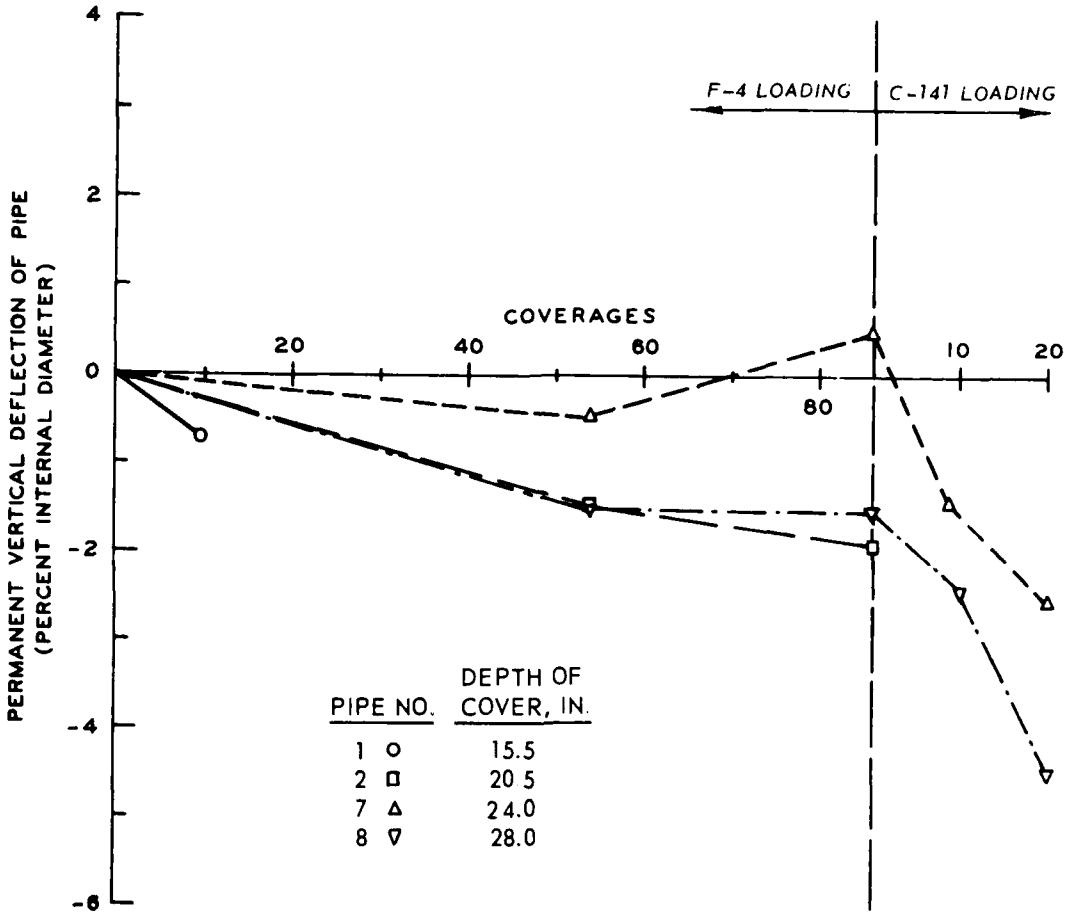

Figure 42. Summary of permanent deflections of the 15-in. ABS pipe installed in Test Site No. 2

once the C-141 loading was applied. The pipe installed at 24-in. depth performed satisfactorily under all loadings.

ABS PIPE

The permanent deflections of the four 15-in.-diam ABS pipes were all less than 5 percent for both the F4 and C-141 loadings. The actual coverage levels for the ABS pipes are also slightly less than those listed on the curves because of the previously mentioned problems encountered early in the field tests at Test Site No. 2.

TEST SITE NO. 3

Figure 43 contains a comparison of the internal diameter of the 12-in. PVC pipe as a function of the longitudinal distance along the pipe at two levels of applied traffic. It would appear that the maximum change of pipe diameter for the increment of applied Army truck traffic was approximately 1 percent. These data point out the very small measurable deflection for the 12-in. PVC pipe installed in Test Site No. 3. This pipe is part of a permanent drainage installation and will be observed periodically. Visual examination of the pipe and roadway surface over the pipe has indicated no structural deficiencies to date.

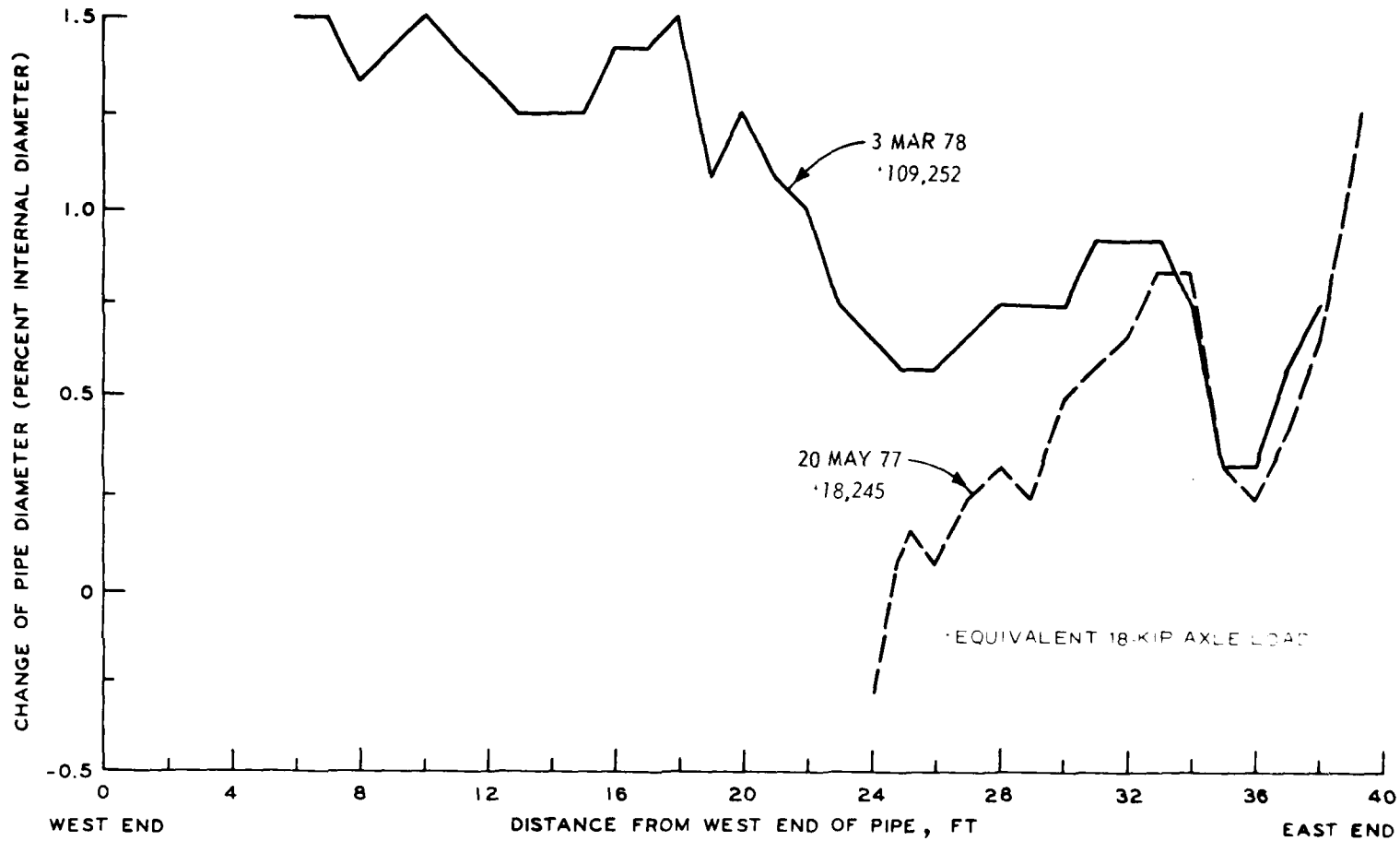

Figure 43. Permanent deflections of the 12-in. PVC pipe installed in Test Site No. 3

CONCLUSIONS

The following conclusions are based on the results of this and related studies and are applicable to only those types, sizes, and strengths of plastic pipe used in the studies.

a. Pipe deflections due to static loads and the deflections due to dynamic loads appear, in general, to approach a maximum value and then gradually to decrease with further increases in load repetitions.

b. There was no significant difference between static load and dynamic load deflections of pipe that performed well and those that performed poorly. Thus, for these tests, neither static load deflections nor dynamic load deflections were useful predictors of pipe performance.

c. Pipes installed with compacted pea gravel embedment material (bedding, haunching, and initial backfill) performed better than those pipes embedded in the lean clay material.

d. Certain results and trends were evident to some extent in the data that are thought contrary to the expected, e.g., a lengthening of vertical pipe diameter and larger deflections occurring at deeper depths than at shallow depths.

e. The PVC pipe installed in all three test sites performed well under a range of loadings representative of highway and light and medium aircraft. The permanent pipe deflection data from the CTT tests show that none of the PVC pipe had a permanent deflection greater than 5 percent. In Test Site No. 2, the permanent PVC pipe deflection did not exceed 3 percent under the simulated F-4 and C-141 aircraft load repetitions. Only about 1 percent permanent pipe deflection occurred under the Army truck loadings applied to the PVC pipe in Test Site No. 3.

f. For the very shallow burial depths, i.e., less than 12 in., the PE pipe experienced large early deflections and resultant failure. PE pipe installed with between 12 to 18 in. of cover with the compacted pea gravel backfill performed fairly well, with borderline failures being the predominant test result. Two 10-in. PE pipes were tested in Test Site No. 2 with cover depths of 24 and 28 in. Both pipes performed well; the pipe installed at 24-in. depth performed somewhat better than the one installed at 28 in. The 24-in. pipe did not fail and the one installed at 28-in. depth was a borderline failure (i.e., pipe deflection of 6 to 7 percent).

g. Six sections of ABS pipe were tested. The two shallow buried (8.5- and 13-in. cover) ABS pipes installed in the CTT both failed. The four ABS pipes in Test Site No. 2 all performed

well, with less than 5 percent permanent deflection occurring under the F-4 and C-141 loadings. From the CTT tests there was an indication that at initial stages of traffic only very small permanent deflection occurred, but with an increase in coverages the permanent pipe deflection increased rapidly to failure. Under the relatively limited amount of traffic applied to Test Site No. 2, this trend was not observed.

h. Results from this study can be used to develop preliminary recommendations for minimum cover depths for plastic pipe installed beneath unsurfaced and flexible pavement highways and airports. To develop complete pipe cover requirements for highway and airport usage additional field and laboratory tests and analytical studies using the full range of plastic pipe sizes and strengths available are required.

RECOMMENDATIONS

The following recommendations are suggested based upon the results and conclusions of this study.

a. Good pipe installation practices such as those proposed by Harvey* should be strictly adhered to when installing plastic pipe.

b. A compacted coarse-grained material should be used for the bedding, haunching, and backfill to at least a depth of one pipe radius above the crown of the pipe.

c. Until further traffic testing is accomplished, particularly simulated heavy aircraft loading, a cover height of 12 in. is recommended for PVC pipe when subjected to highway (18-kip axle loads), 18 in. for pipe subjected to heavier highway loadings and light aircraft traffic (gross weight not exceeding 30,000 lb), and 24 in. of cover is recommended for traffic of light to medium (300,000 lb gross weight) aircraft.

d. For highway loadings (18-kip axle loadings), a minimum depth of cover of 18 in. is recommended for PE pipe and 24 in. of cover is recommended for pipe subjected to heavier highway loadings and light aircraft (not exceeding 30,000 lb gross weight) traffic. More tests are needed to determine repetitive load effects and safe burial depths, particularly for pipe subjected to medium- to heavy-load aircraft.

e. While preliminary indications from these tests are that at least 24 in. of cover is required for adequate protection of ABS pipe under traffic conditions, additional tests are needed to better define repetitive load effects and safe burial depths.

---

* Harvey, op. cit., p. 1.

AD-A087 135 ARMY ENGINEER WATERWAYS EXPERIMENT STATION VICKSBURG--ETC F/G 13/11
FIELD TESTS OF PLASTIC PIPE FOR AIRPORT DRAINAGE SYSTEMS.(U)
DEC 79 W J HORN DOT-FA75WAI-536
UNCLASSIFIED WES/TR/GL-79-24 FAA-RD-79-86 NL

2 OF 2
ADA
087135

END
DATE FILMED
10-80
DTIC

APPENDIX A

DYNAMIC AND PERMANENT PIPE DEFLECTIONS OF CTT

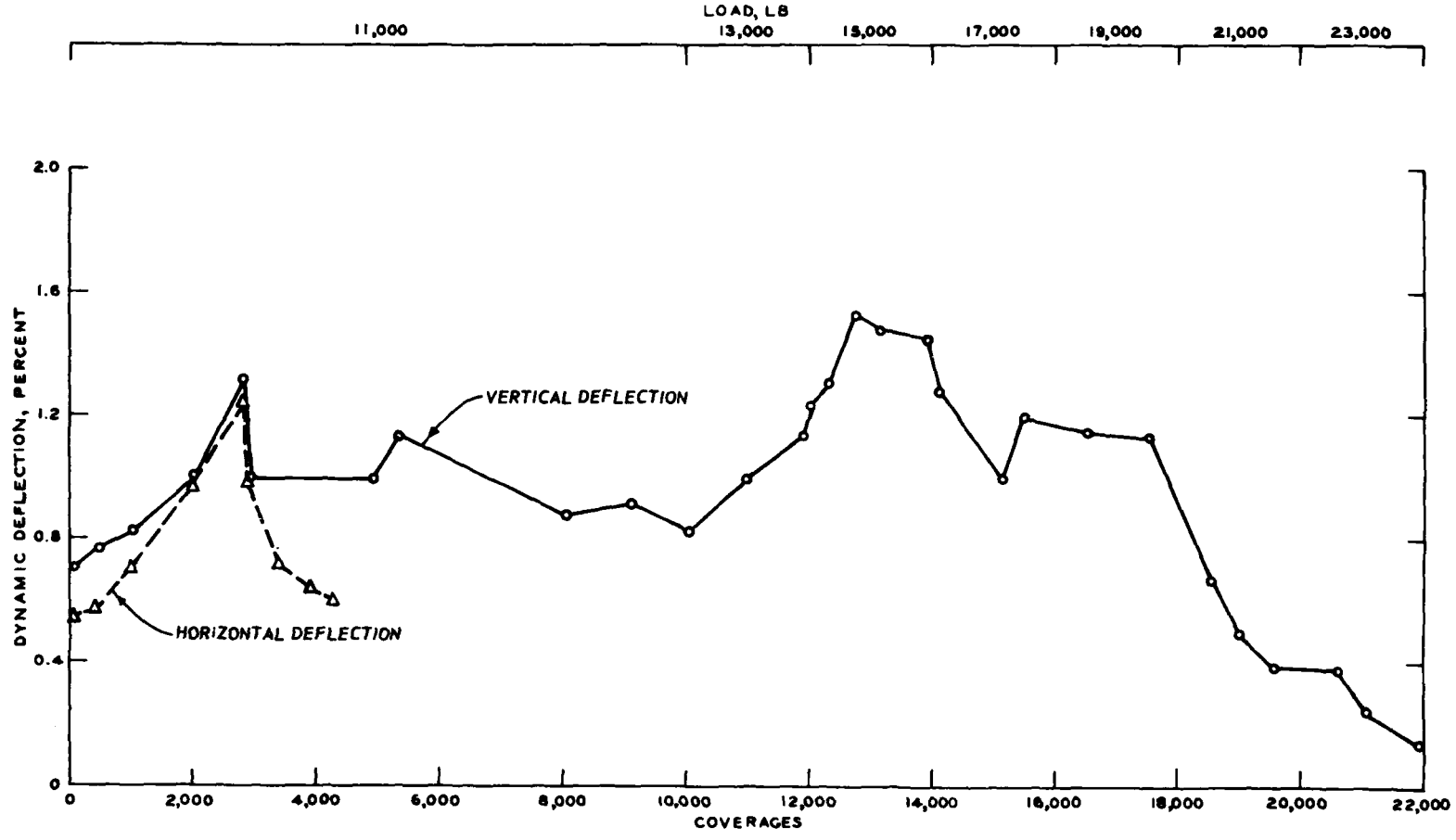

Figure A-1. Dynamic load deflection of pipe A of Test Site No. 1 (10-in. PVC; pea gravel backfill; 7-in. depth of cover)

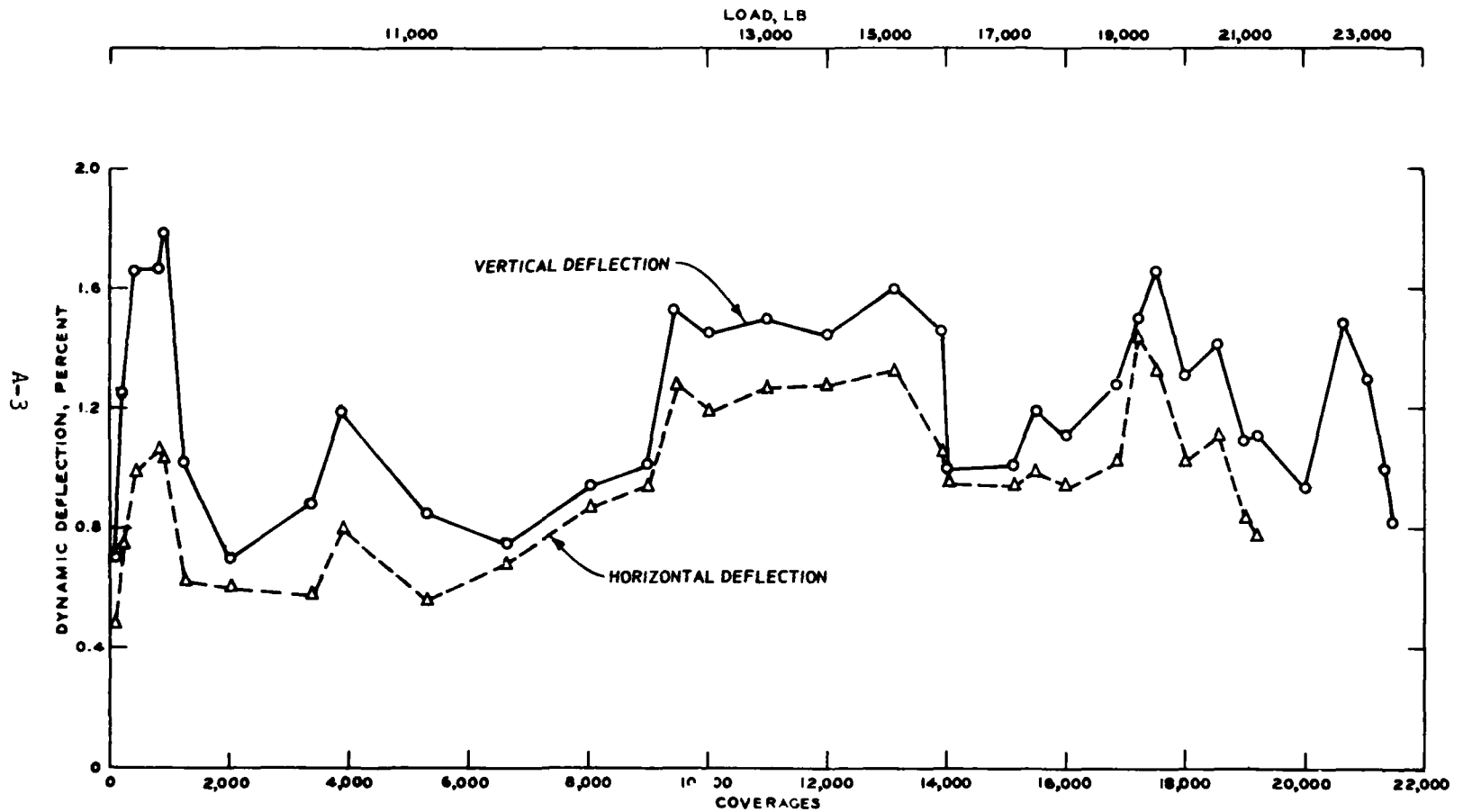

Figure A-2. Dynamic load deflection of pipe B of Test Site No. 1 (12-in. PVC; pea gravel backfill; 7-in. depth of cover)

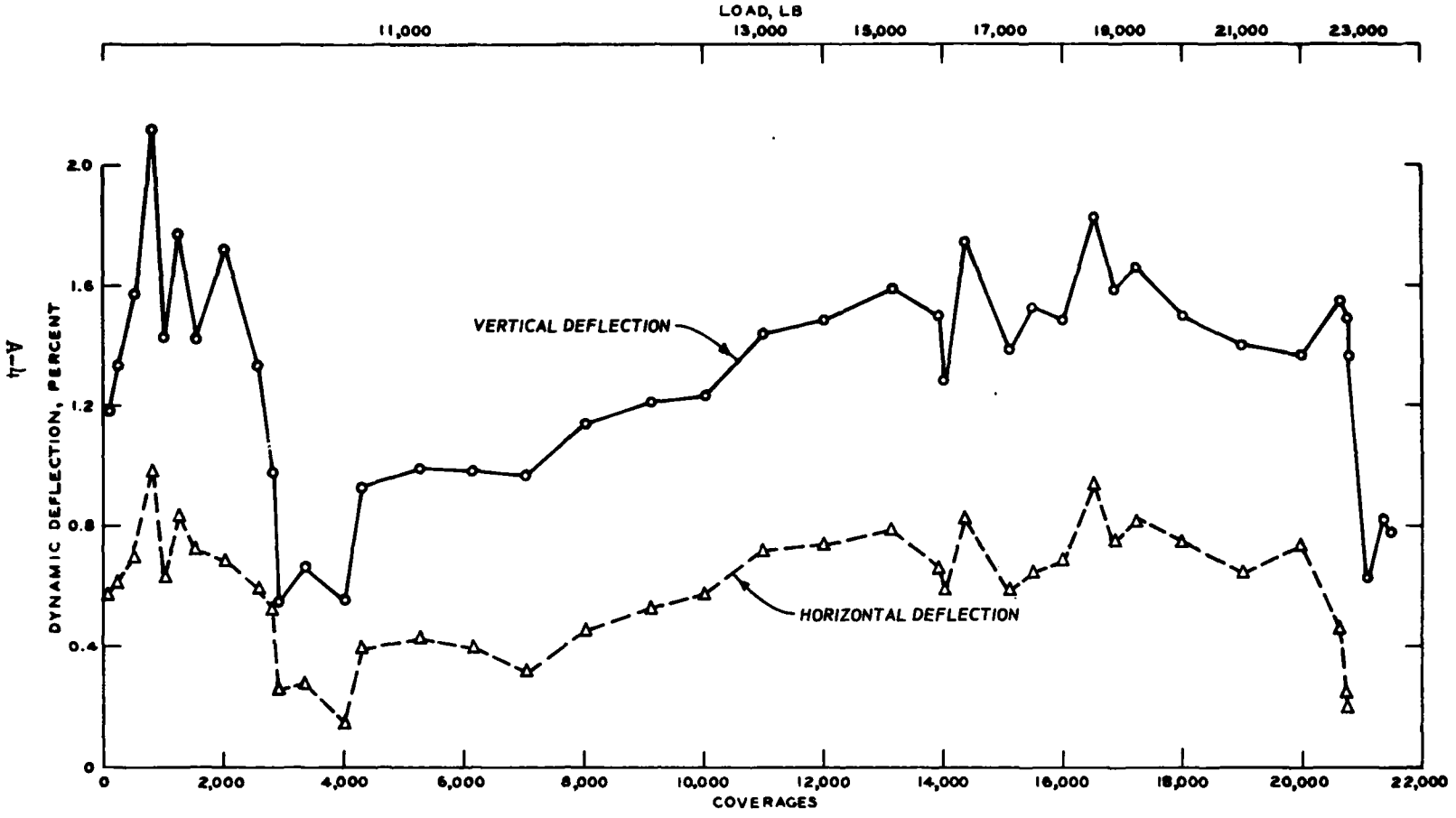

Figure A-3. Dynamic load deflection of pipe C of Test Site No. 1 (10-in. PE, pea gravel backfill; 7.75-in. depth of cover)

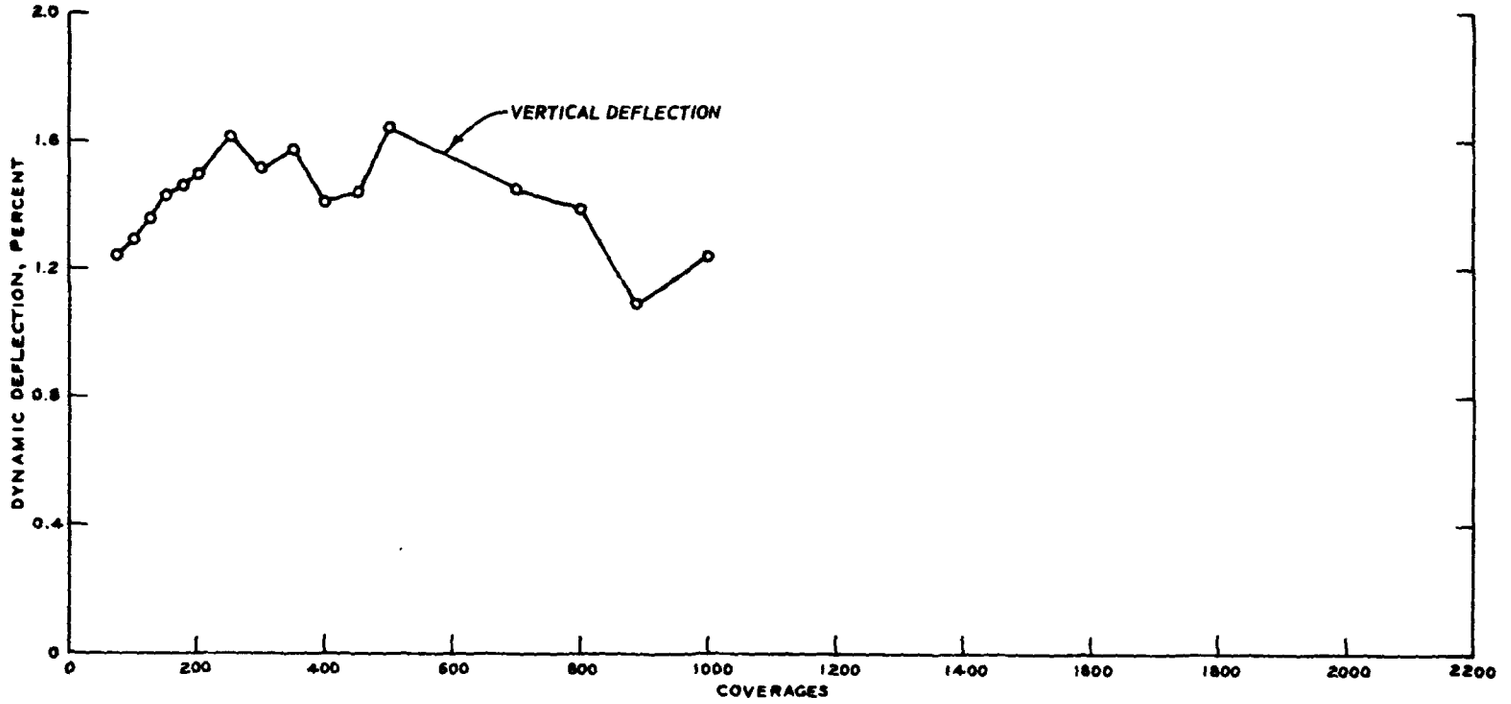

Figure A-4. Dynamic load deflection of pipe D of Test Site No. 1 (10-in. PE; lean clay backfill; 10-in. depth of cover)

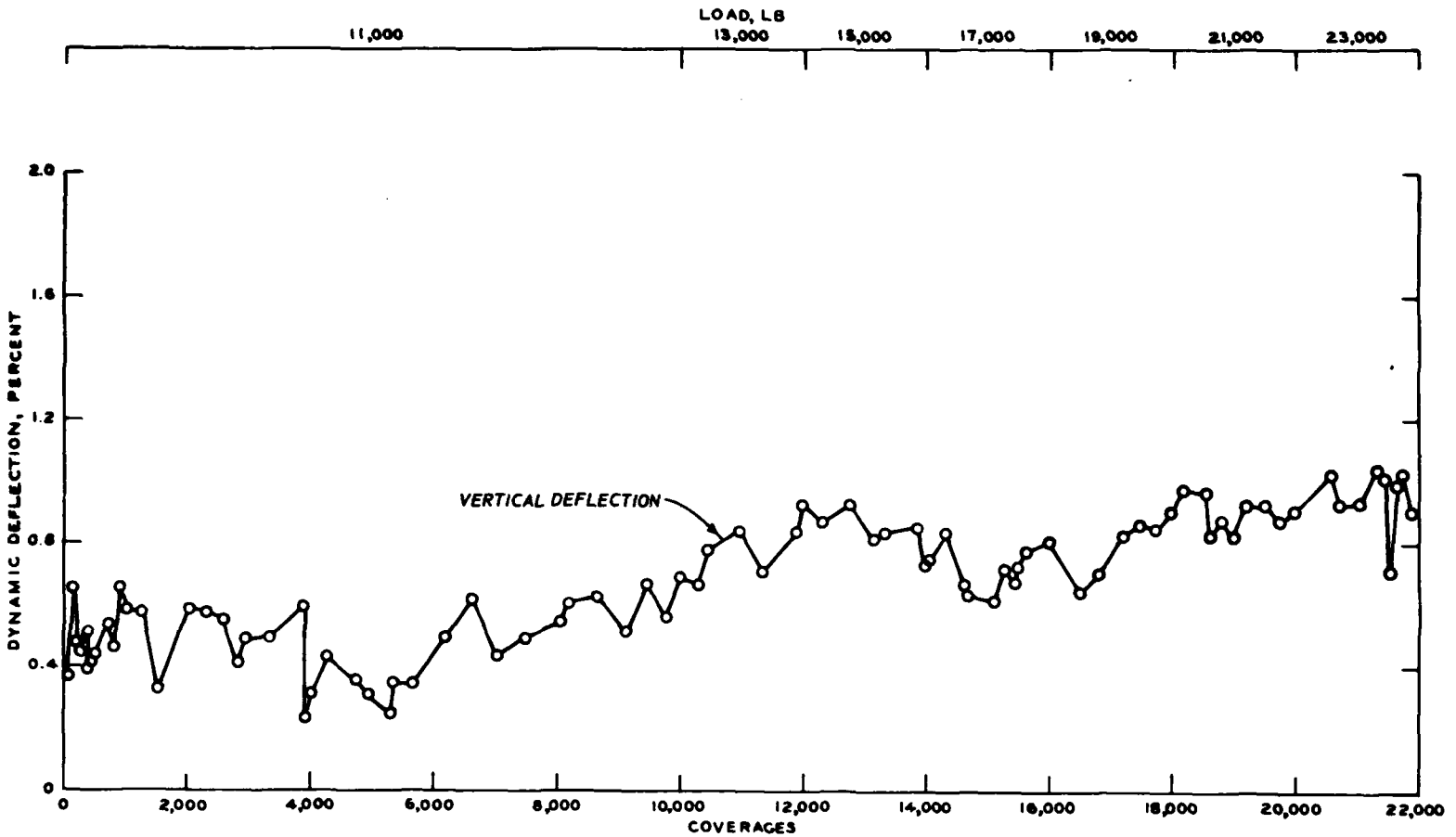

Figure A-5. Dynamic load deflection of pipe E of Test Site No. 1 (10-in. PVC; pea gravel backfill; 13.75-in. depth of cover)

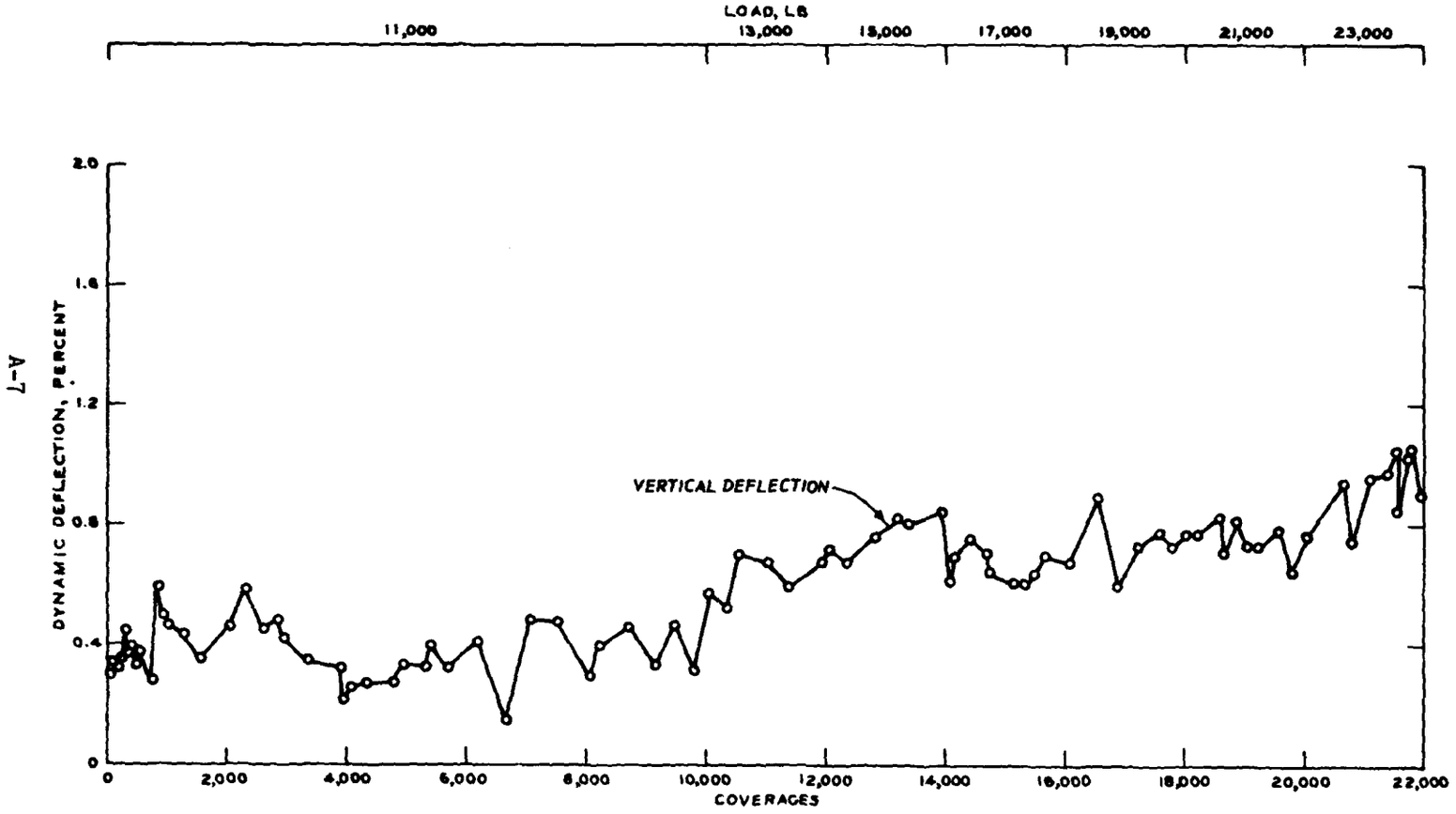

Figure A-6. Dynamic load deflection of pipe F of Test Site No. 1 (12-in. PVC; pea gravel backfill; 13.75-in. depth of cover)

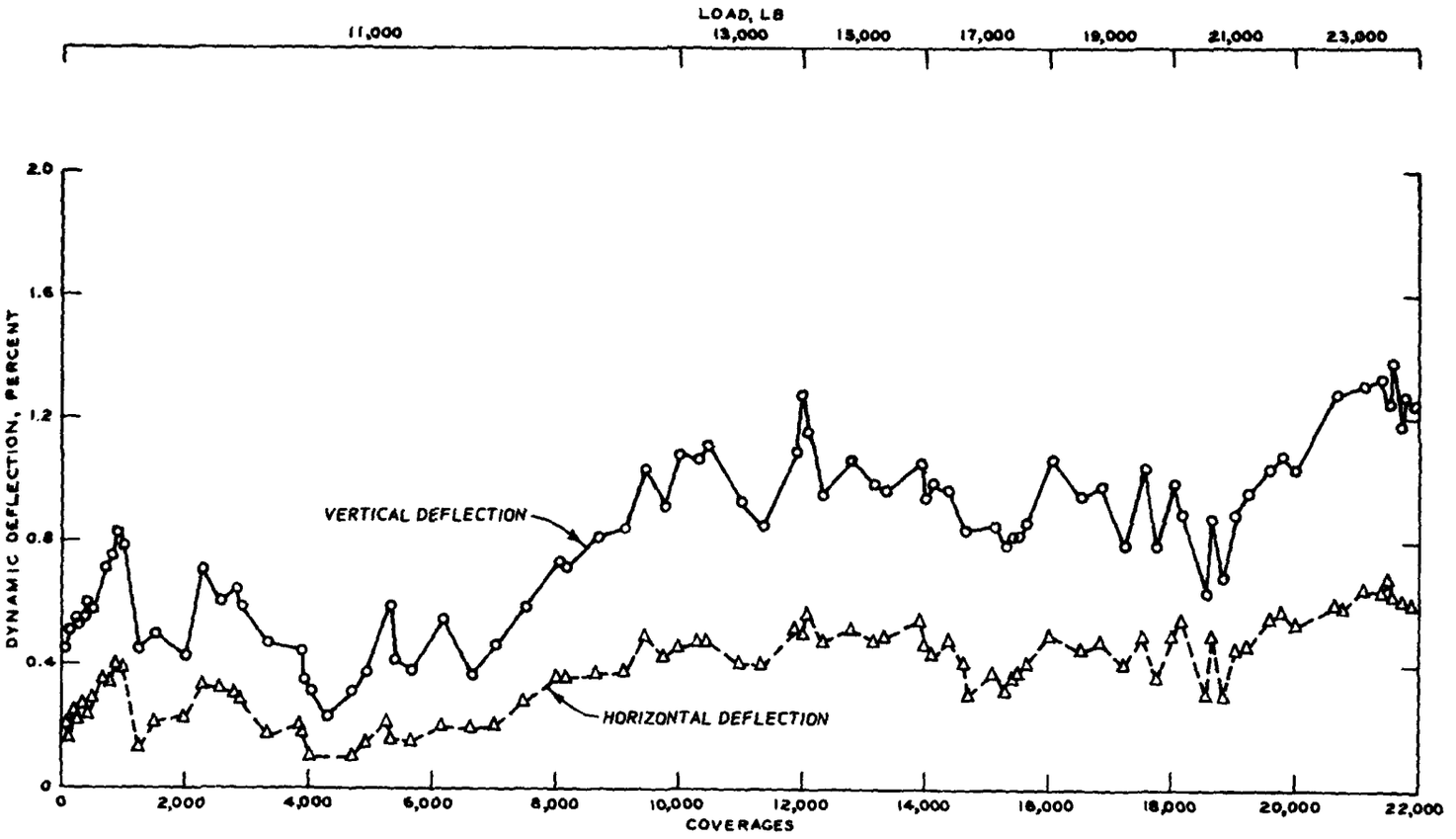

Figure A-7. Dynamic load deflection of pipe G of Test Site No. 1 (10-in. PE; pea gravel backfill; 13.25-in. depth of cover)

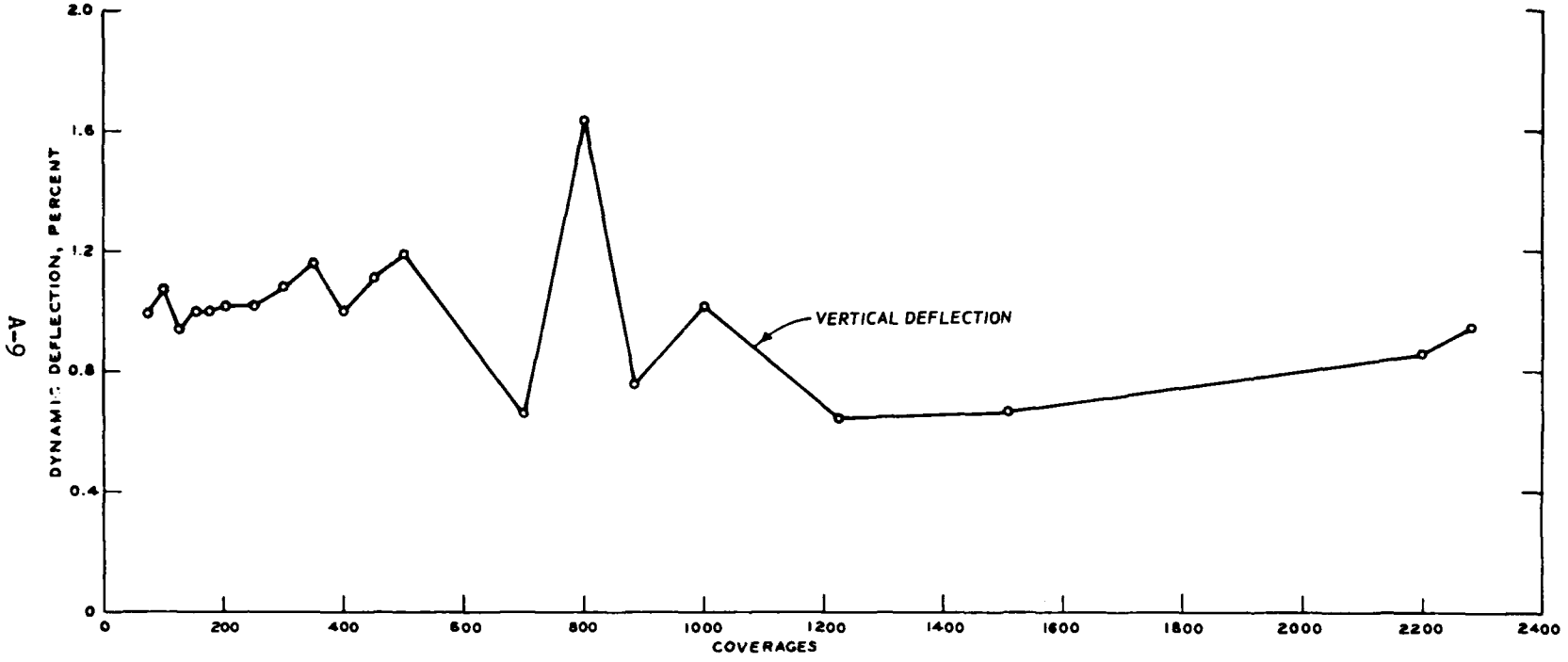

Figure A-8. Dynamic load deflection of pipe H of Test Site No. 1 (10-in. PE; full-depth lean clay; 13.5-in. depth of cover, 11,000-lb dynamic load)

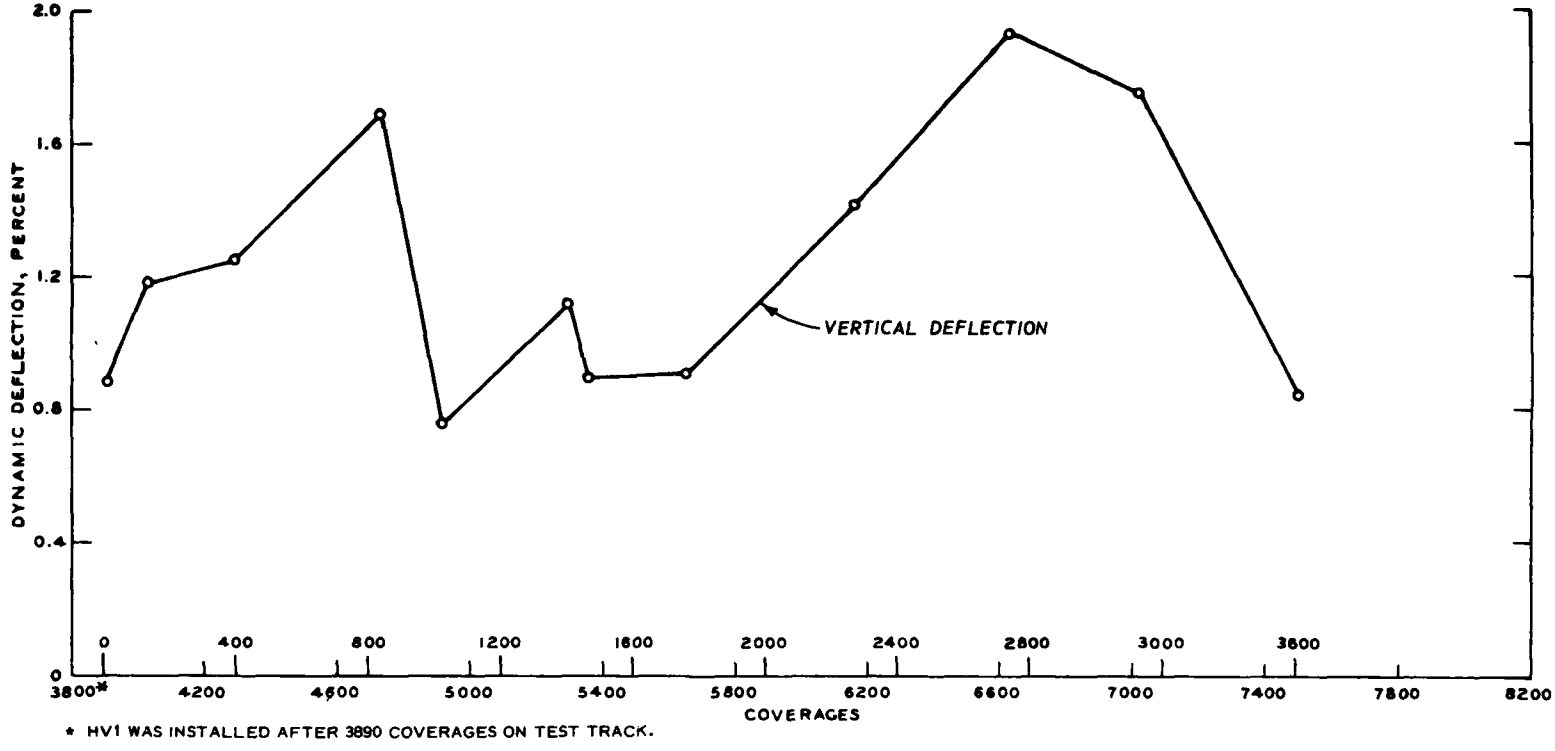

Figure A-9. Dynamic load deflection of pipe H1 of Test Site No. 1 (15-in. ABS pipe; lean clay backfill; 8.5-in. depth of cover; 11,000-lb dynamic load)

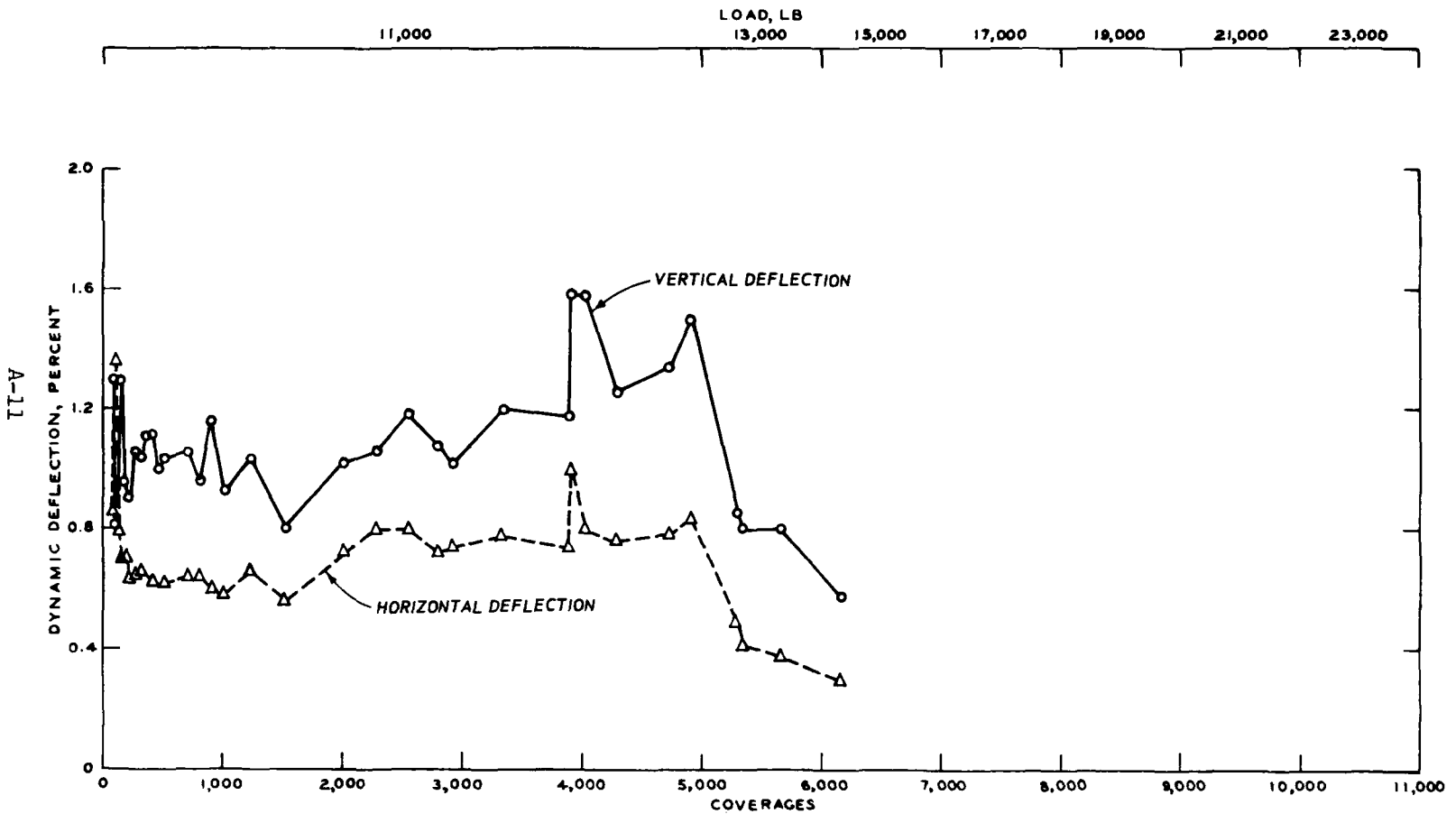

Figure A-10. Dynamic load deflection of pipe I of Test Site No. 1 (10-in. PE pipe; lean clay backfill; 19-in. depth of cover)

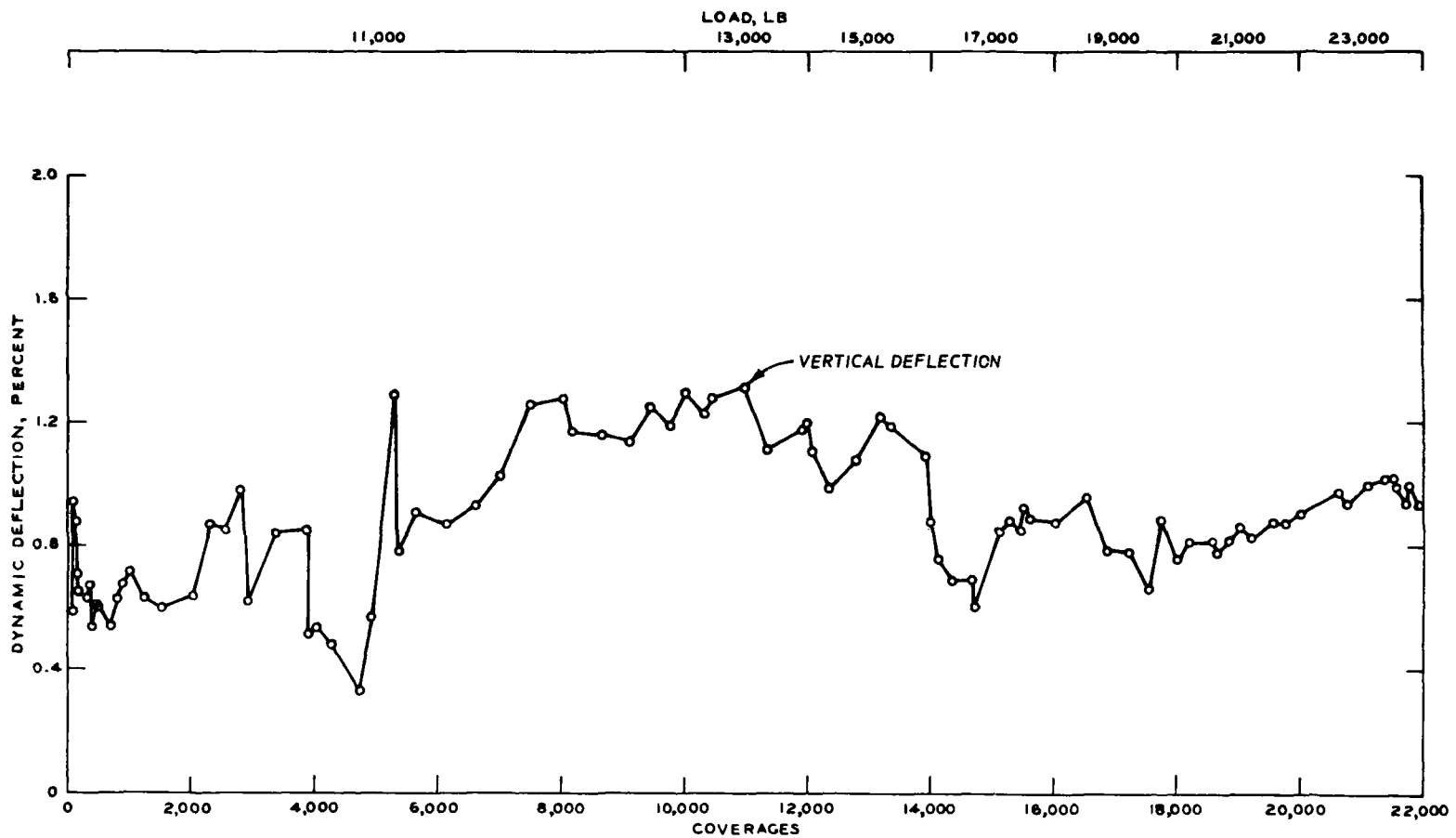

Figure A-11. Dynamic load deflection of pipe J of Test Site No. 1 (12-in. PVC pipe; lean clay backfill; 16.5-in. depth of cover)

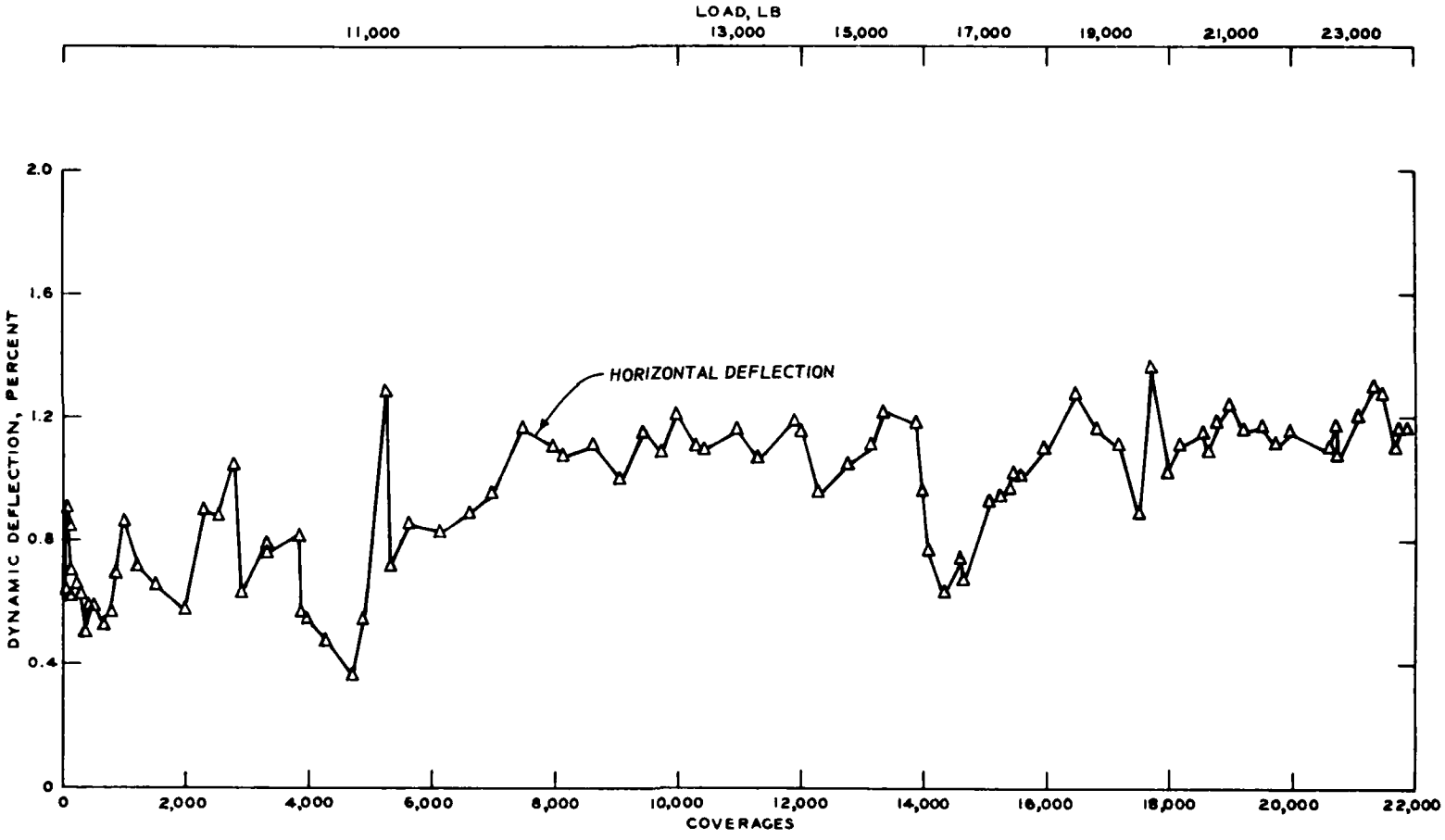

Figure A-12. Dynamic load deflection of pipe J of Test Site No. 1 (12-in. PVC pipe; lean clay backfill; 16.5-in. depth of cover)

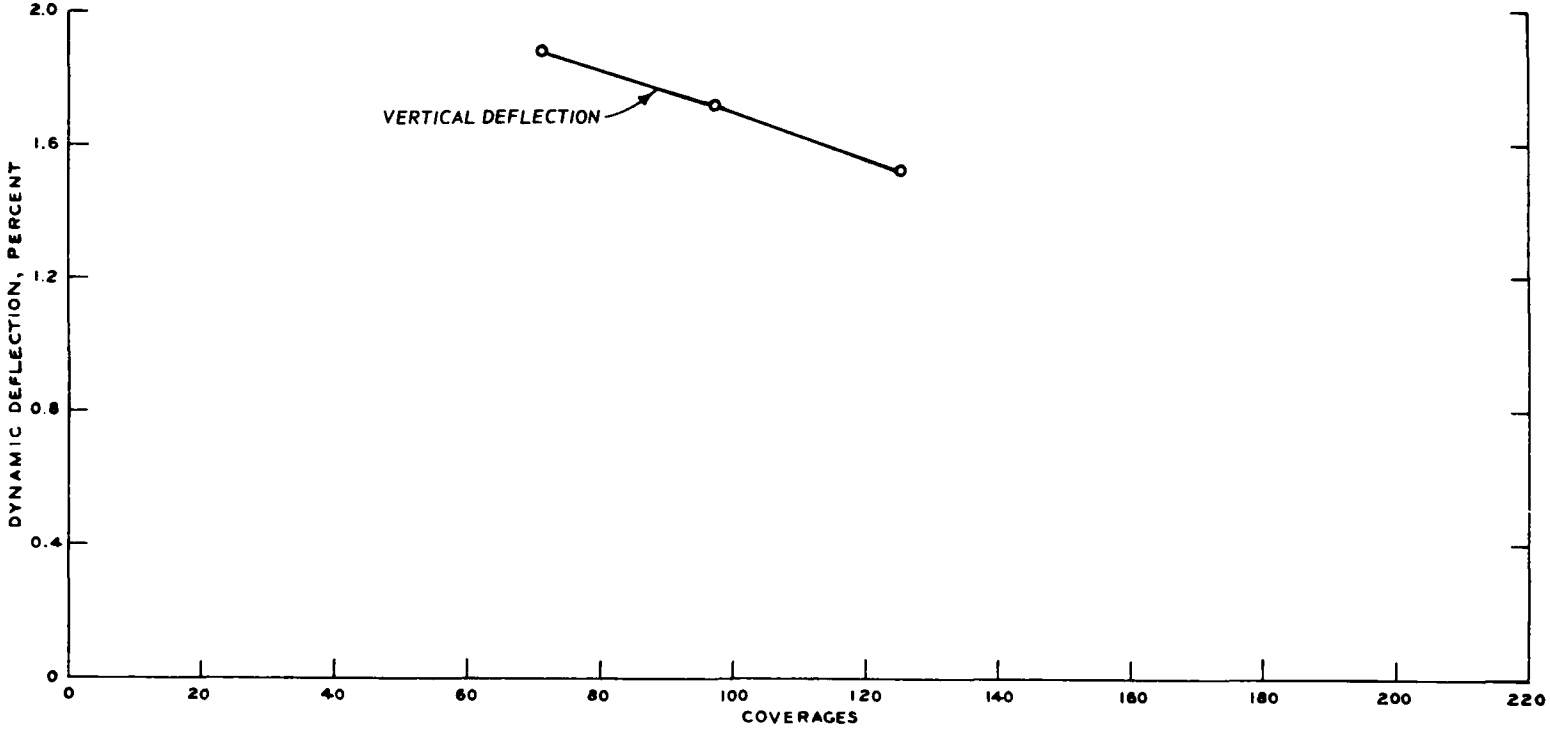

Figure A-13. Dynamic load deflection of pipe K of Test Site No. 1 (10-in. PE pipe; lean clay backfill; 5.75-in. depth of cover; 11,000-lb dynamic load)

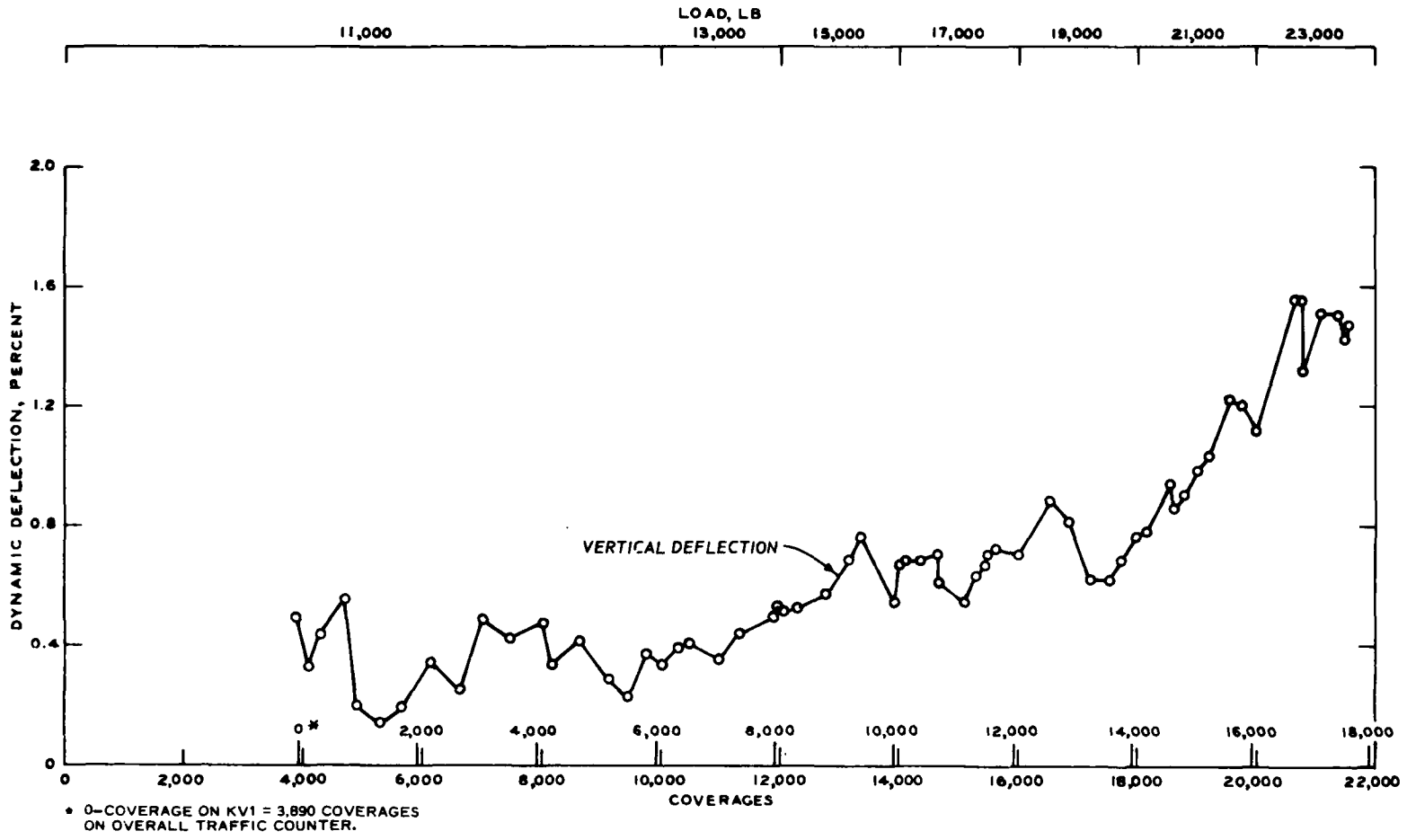

Figure A-14. Dynamic load deflection of pipe K1 of Test Site No. 1 (15-in. ABS pipe; lean clay backfill; 13.0-in. depth of cover)

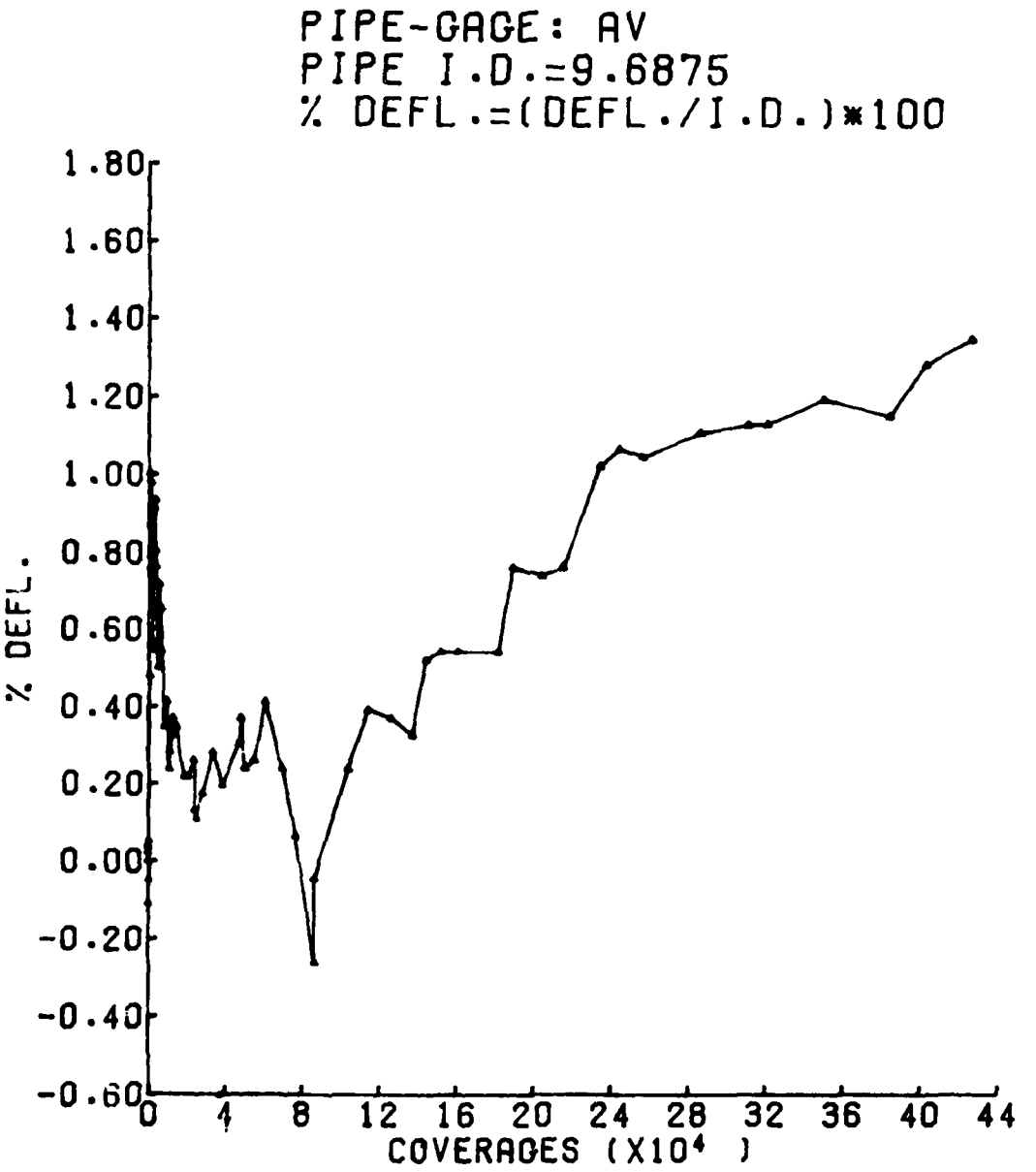

Figure A-15. Permanent deflection of pipe A in CTT as a function of equivalent coverages of an 18-kip axle load

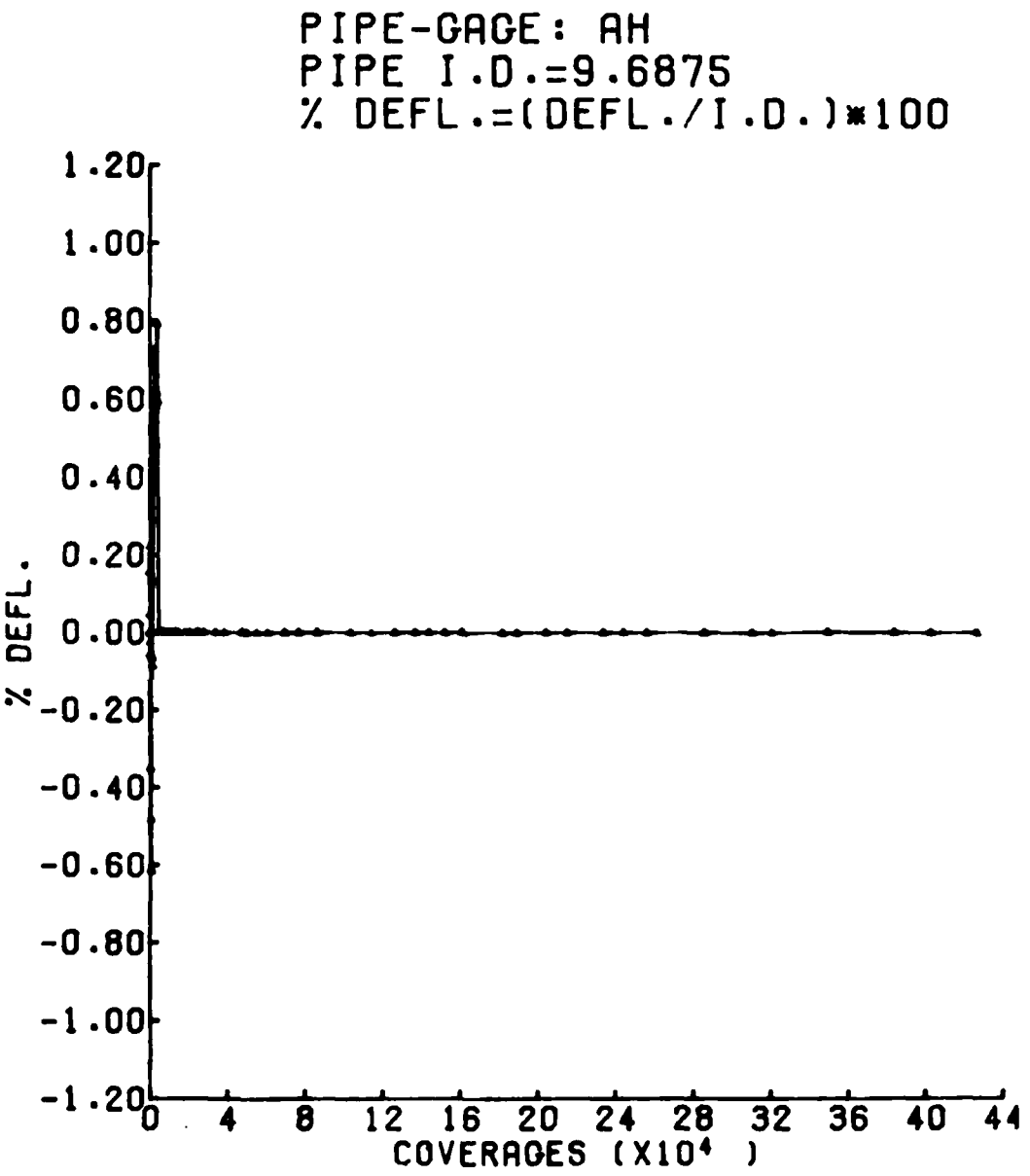

Figure A-16. Permanent deflection of pipe A in CTT as a function of equivalent coverages of an 18-kip axle load

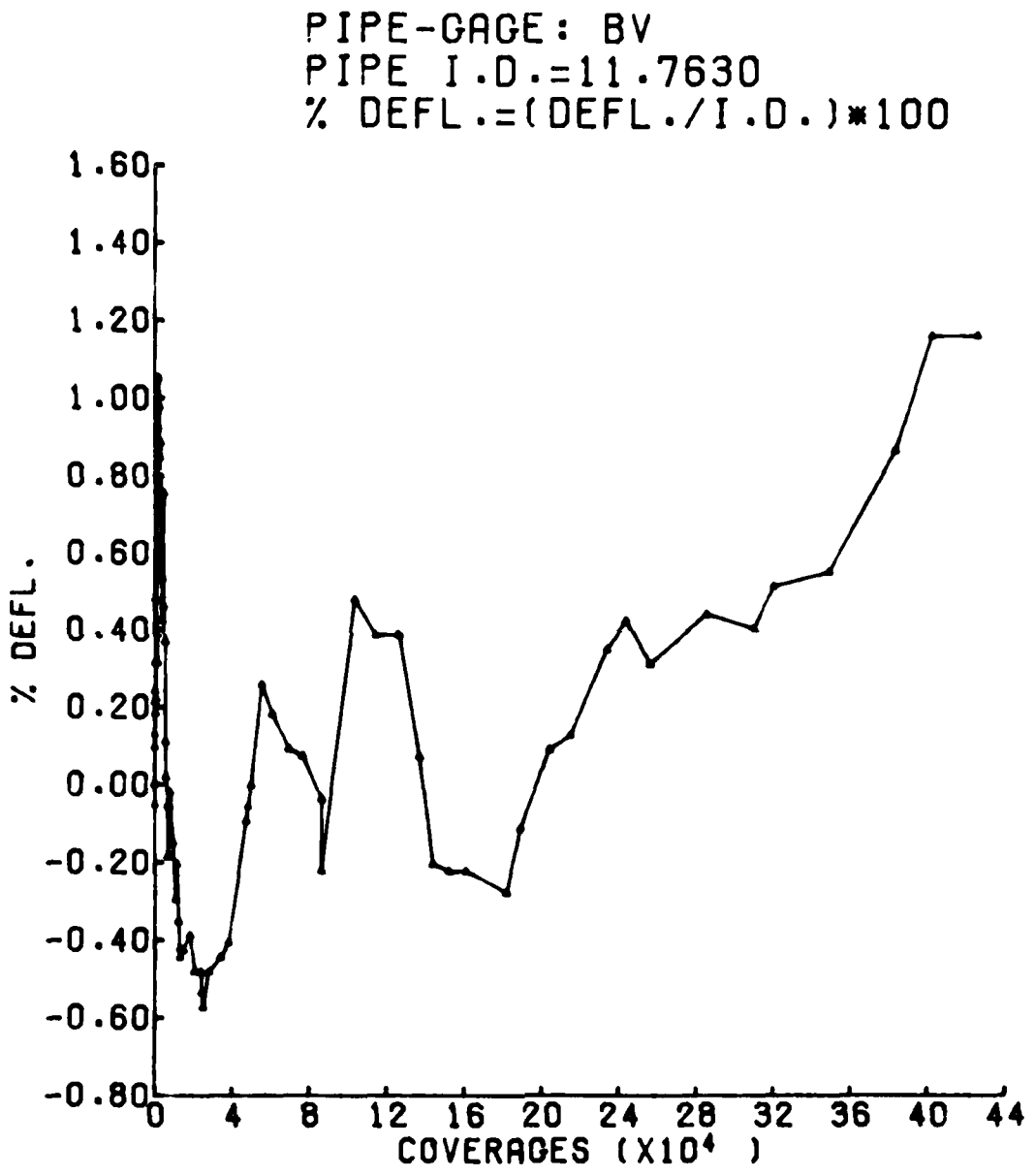

Figure A-17. Permanent deflection of pipe B in CTT as a function of equivalent coverages of an 18-kip axle load

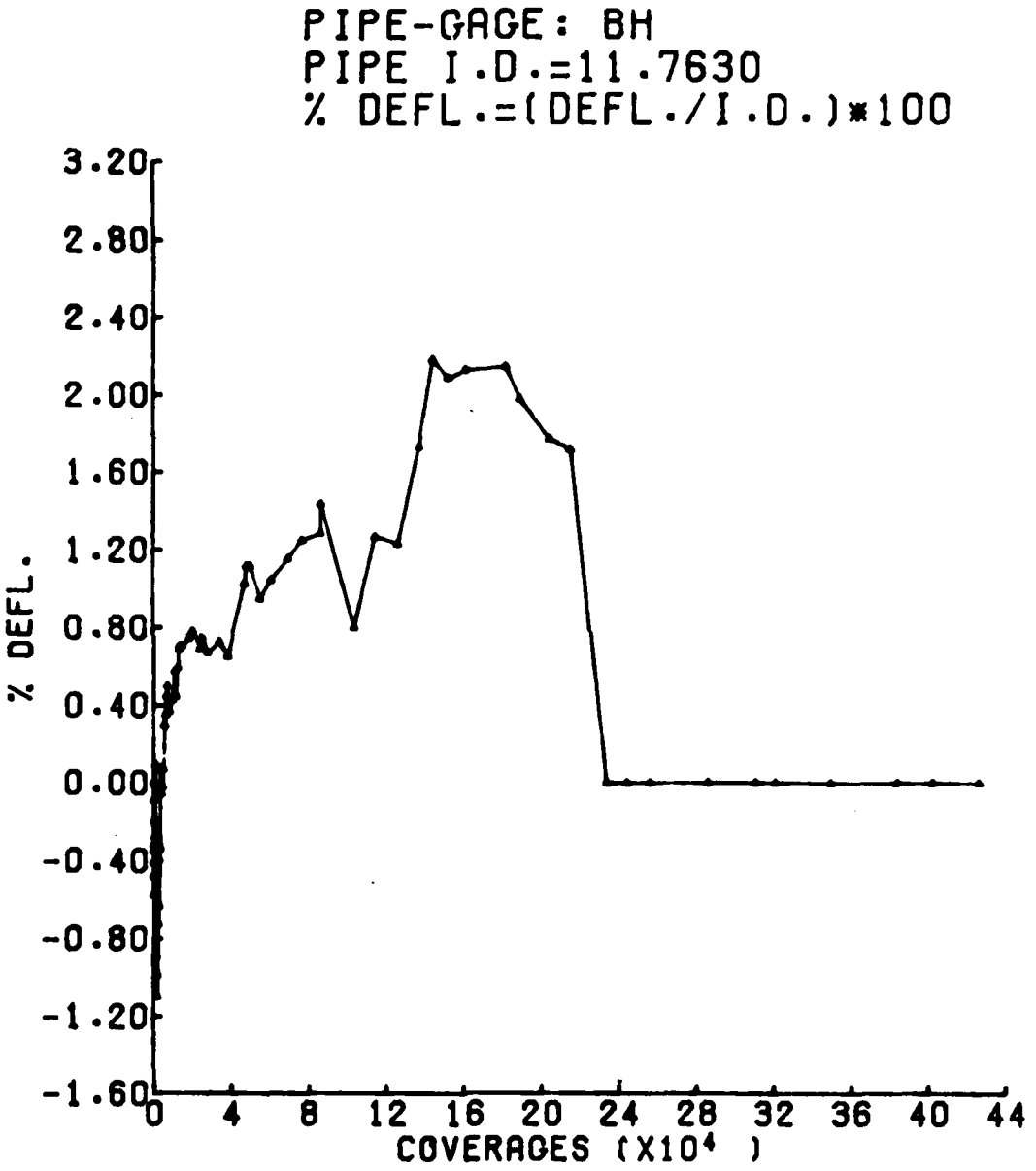

Figure A-18. Permanent deflection of pipe B in CTT as a function of equivalent coverages of an 18-kip axle load

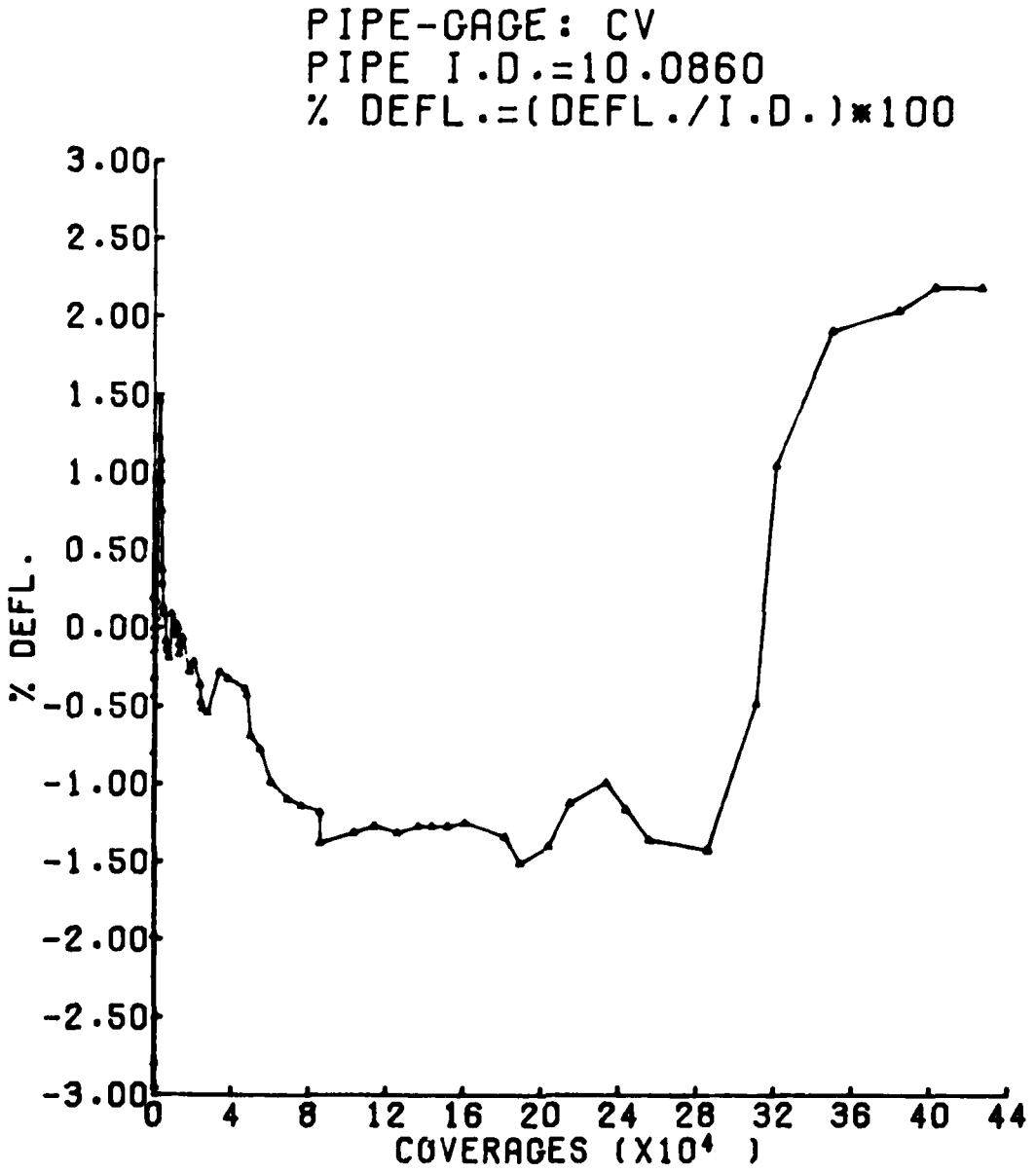

Figure A-19. Permanent deflection of pipe C in CTT as a function of equivalent coverages of an 18-kip axle load

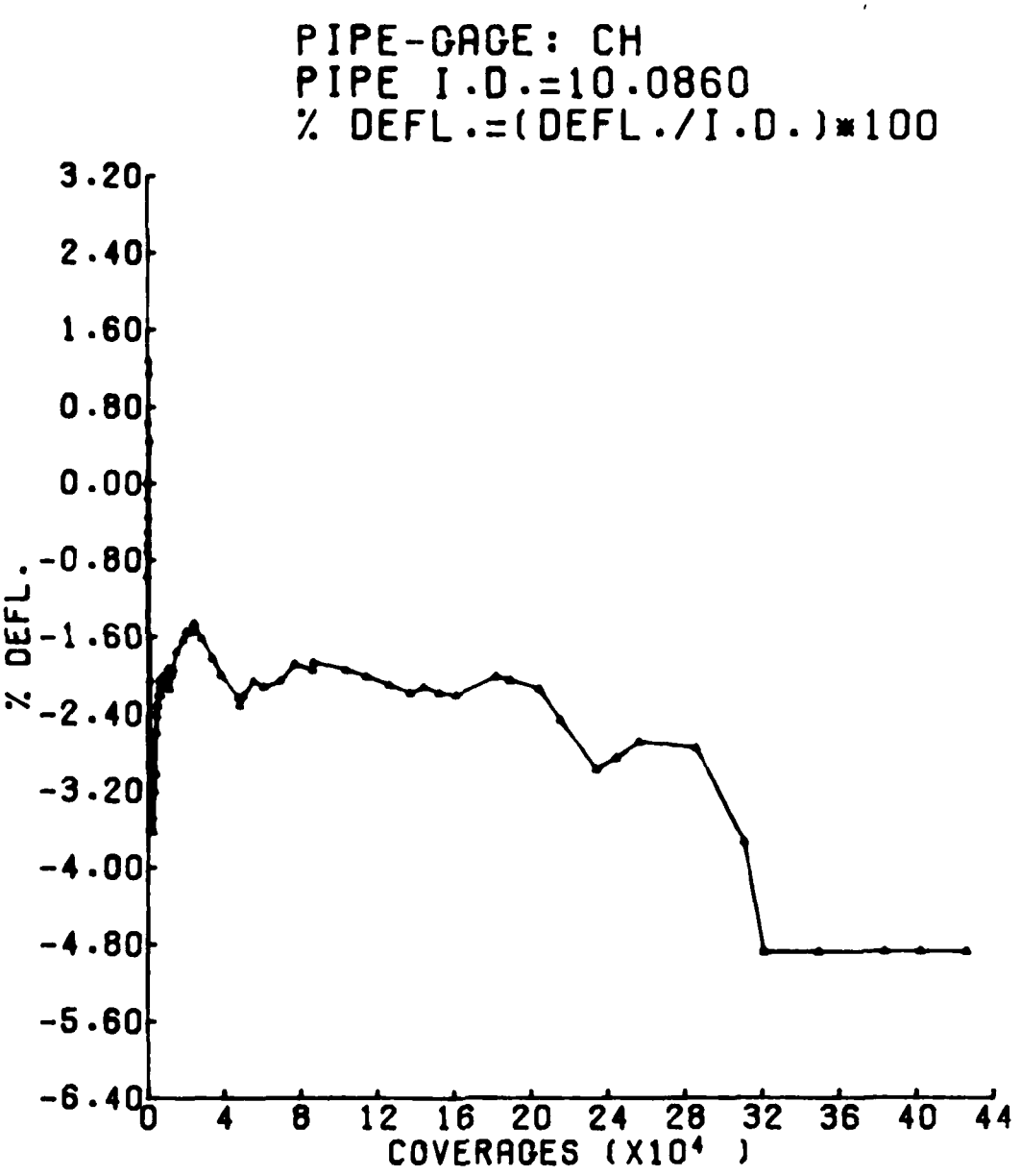

Figure A-20. Permanent deflection of pipe C in CTT as a function of equivalent coverages of an 18-kip axle load

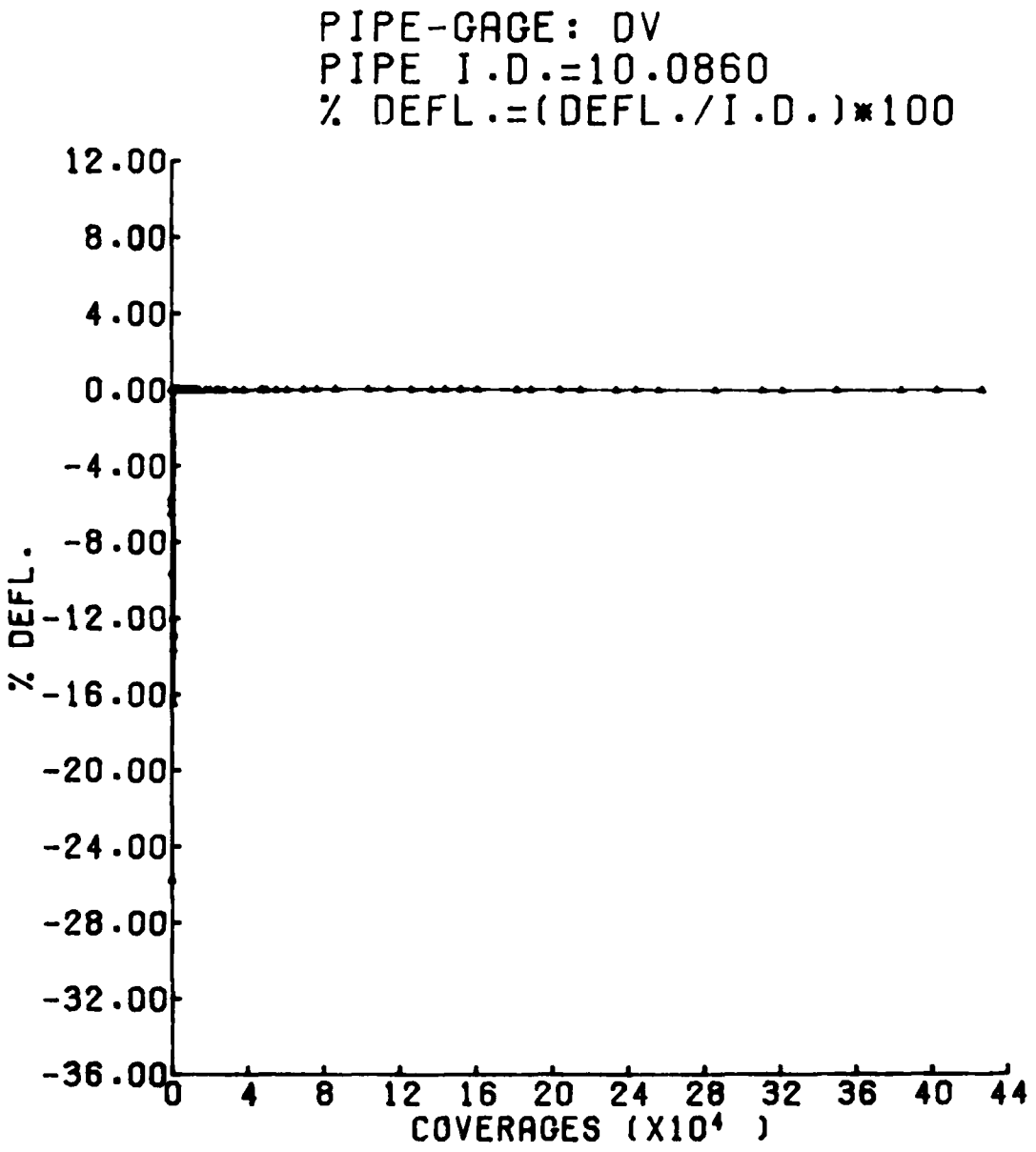

Figure A-21. Permanent deflection of pipe D in CTT as a function of equivalent coverages of an 18-kip axle load

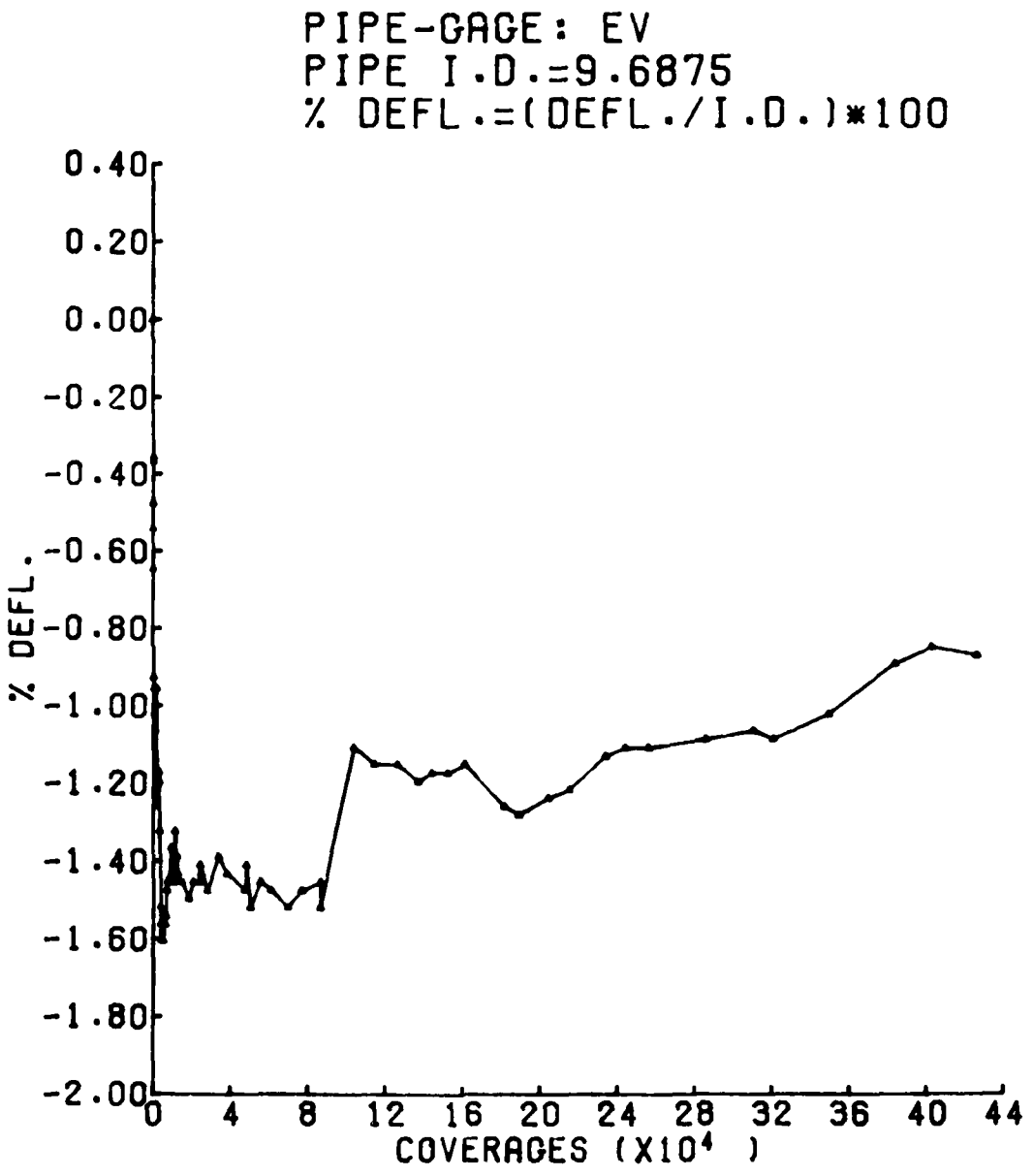

Figure A-22. Permanent deflection of pipe E in CTT as a function of equivalent coverages of an 18-kip axle load

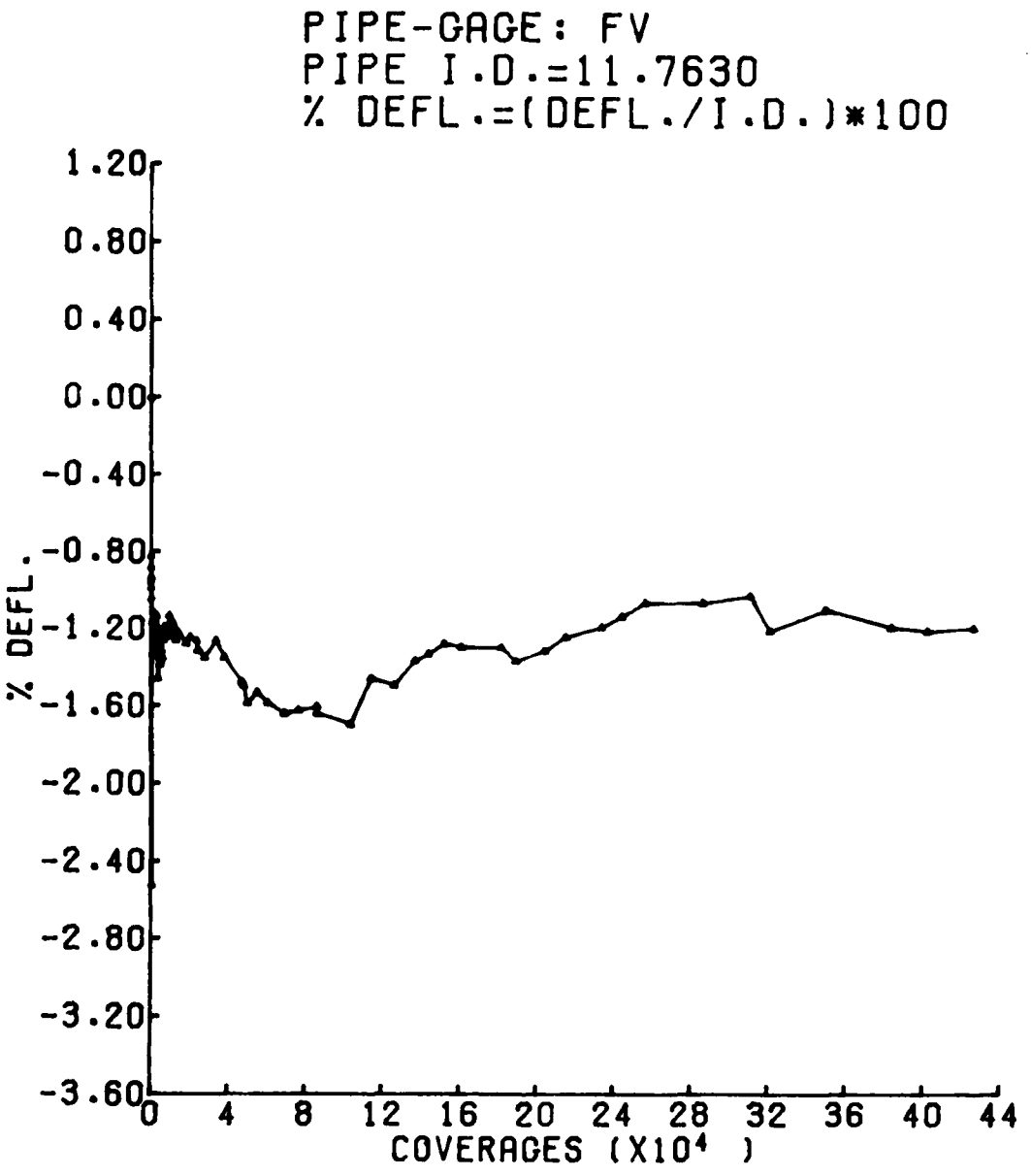

Figure A-23. Permanent deflection of pipe F in CTT as a function of equivalent coverages of an 18-kip axle load

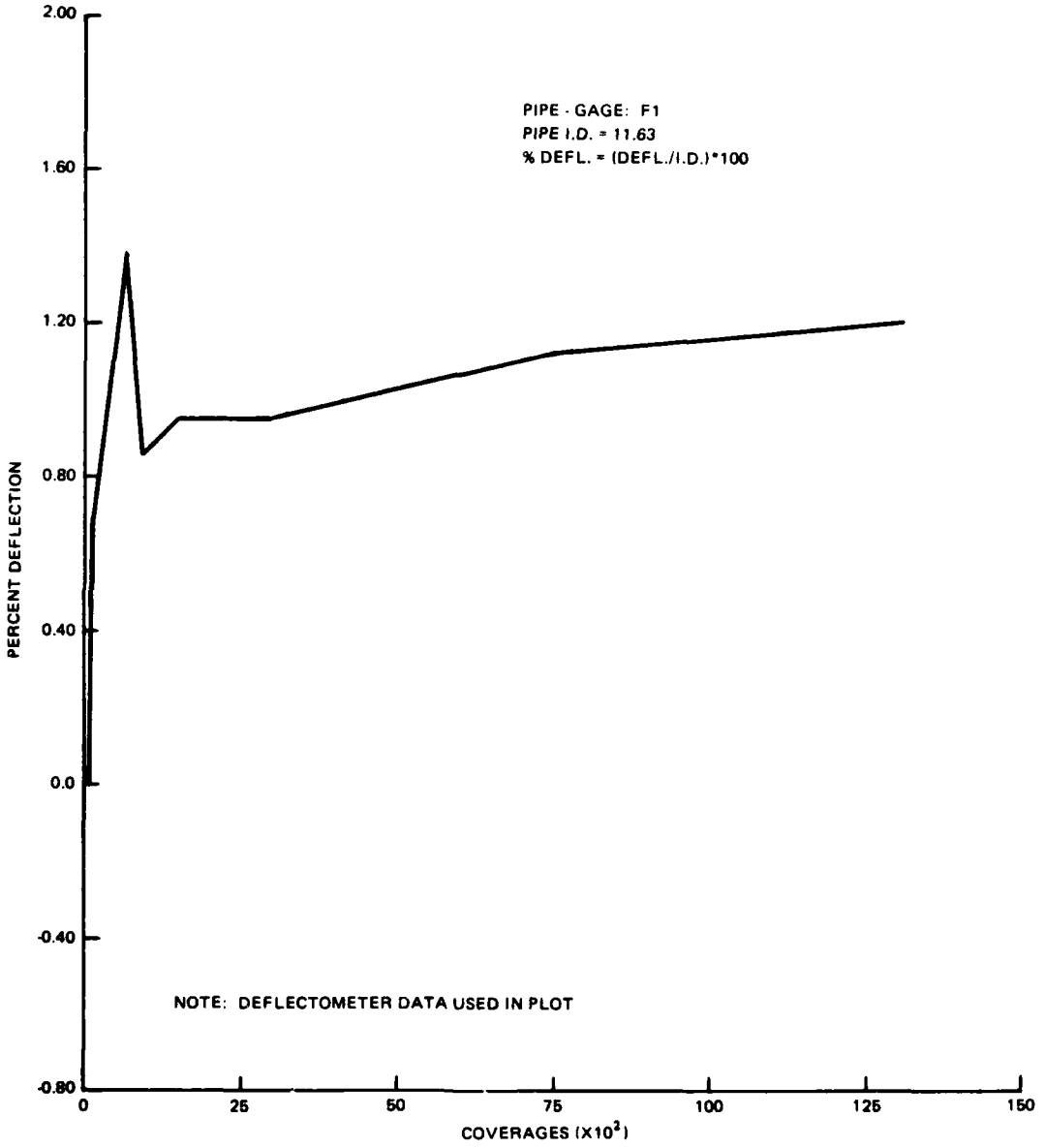

Figure A-24. Permanent deflection of pipe F1 in CTT as a function of equivalent coverages of an 18-kip axle load

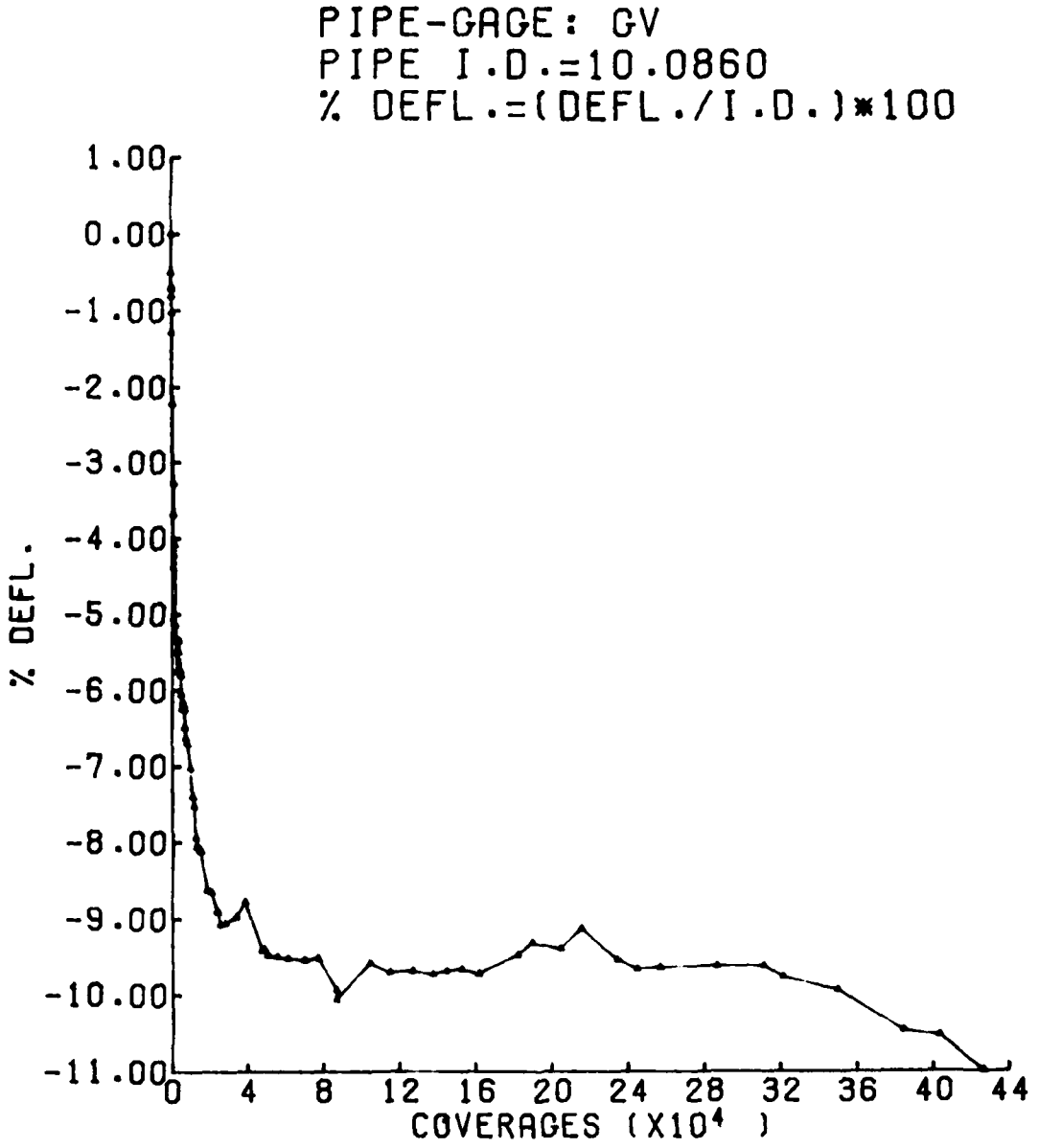

Figure A-25. Permanent deflection of pipe G in CTT as a function of equivalent coverages of an 18-kip axle load

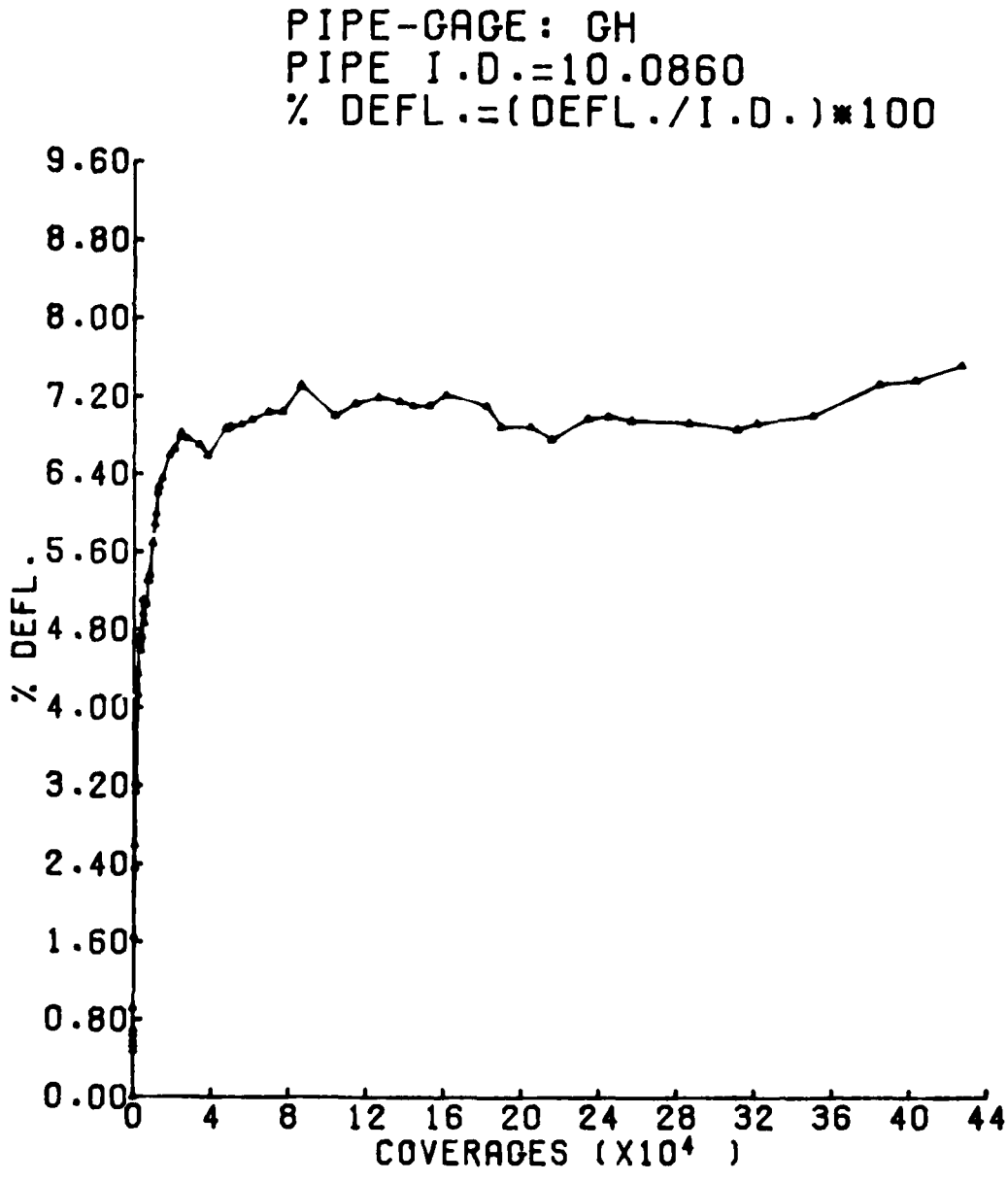

Figure A-26. Permanent deflection of pipe G in CTT as a function of equivalent coverages of an 18-kip axle load

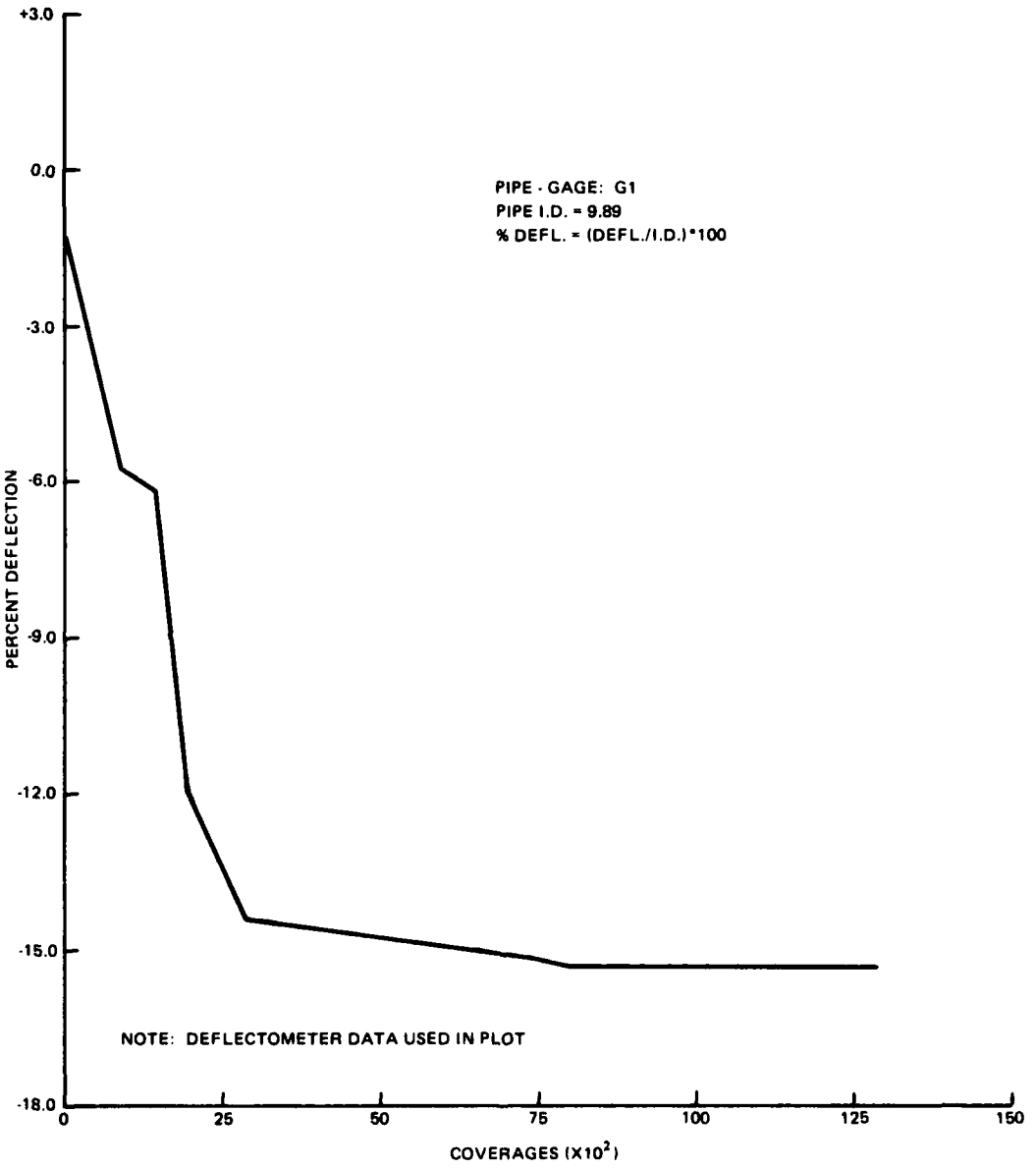

Figure A-27. Permanent deflection of pipe G1 in CTT as a function of equivalent coverages of an 18-kip axle load

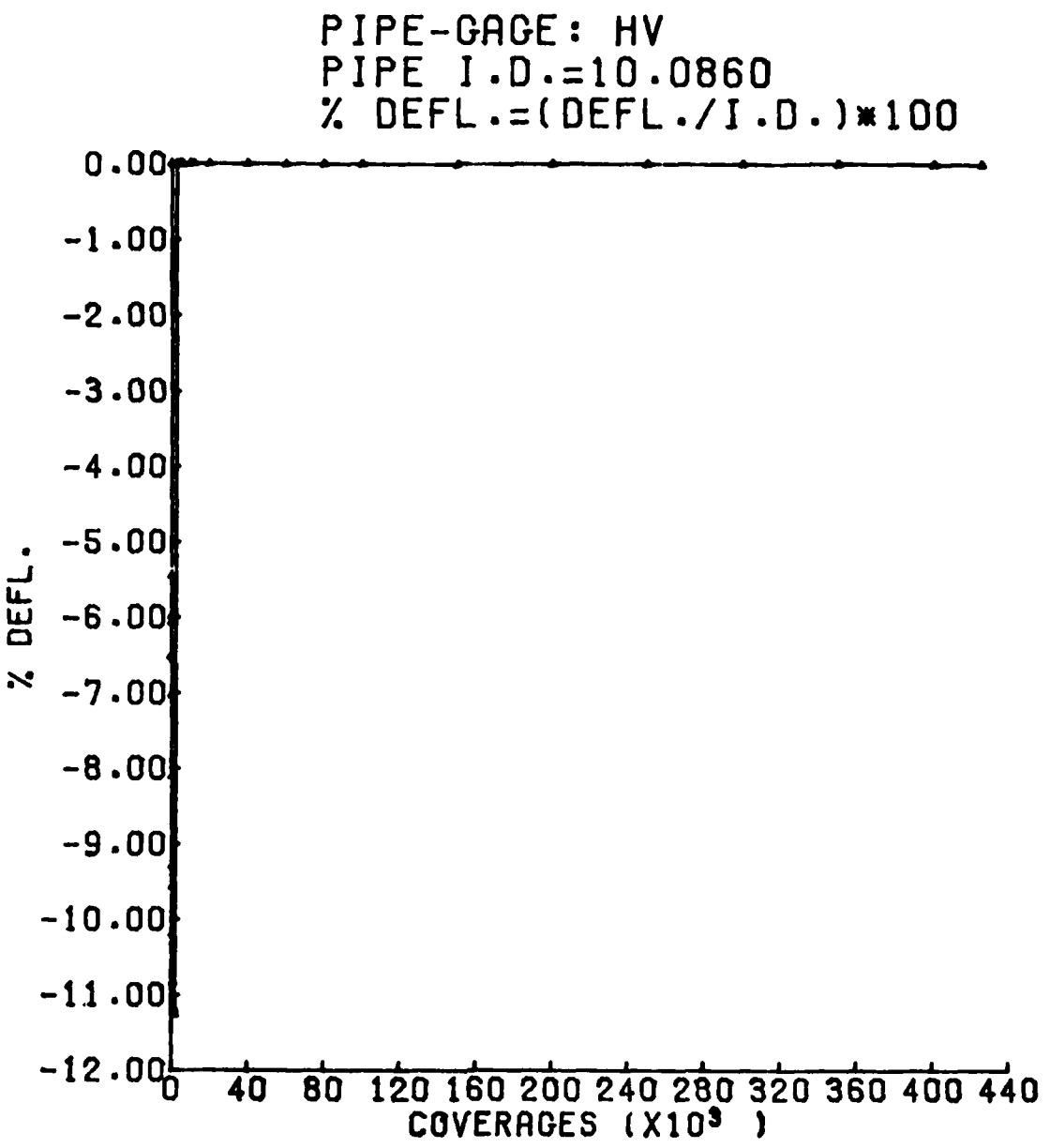

Figure A-28. Permanent deflection of pipe H in CTT as a function of equivalent coverages of an 18-kip axle load

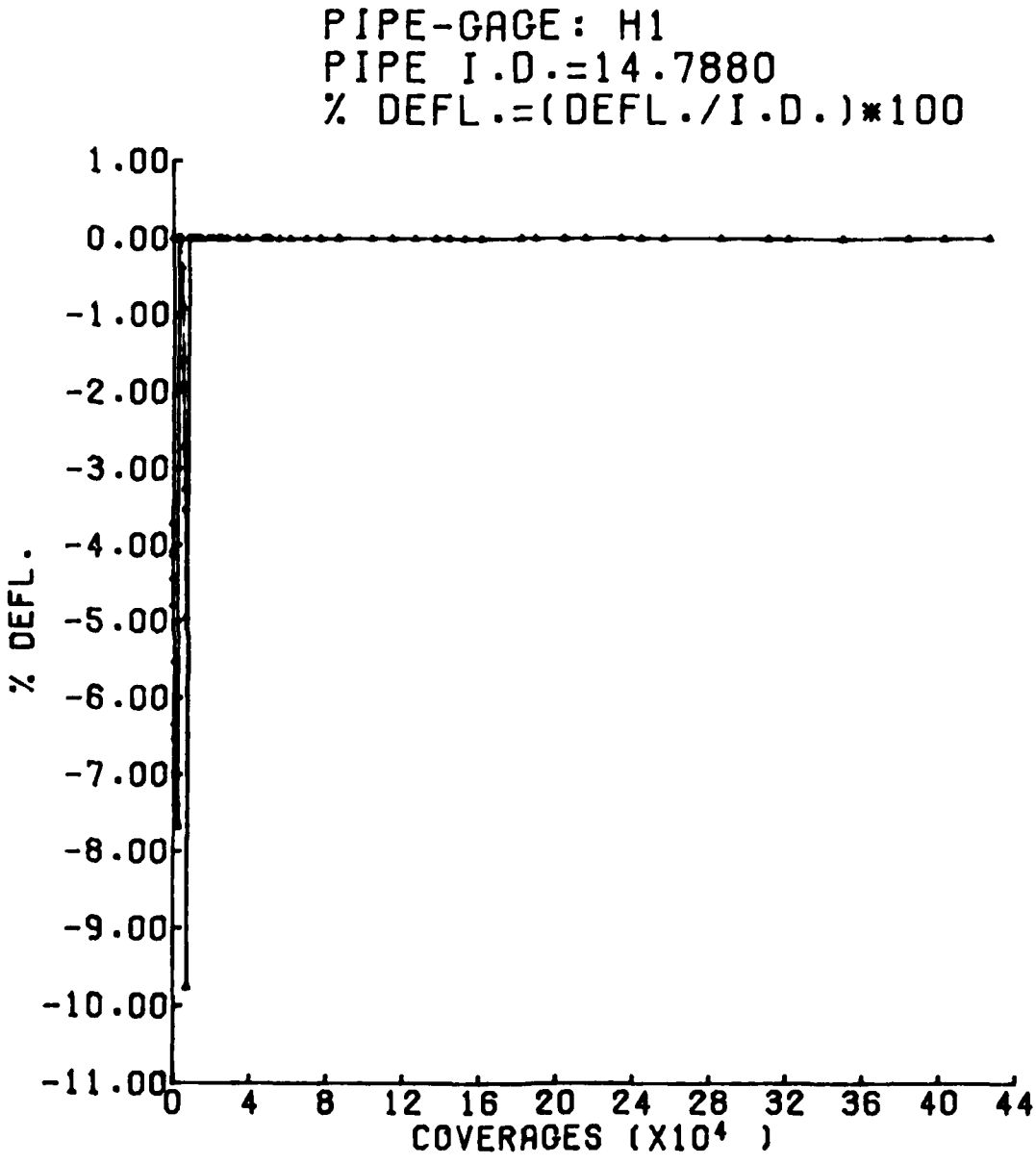

Figure A-29. Permanent deflection of pipe H1 in CTT as a function of equivalent coverages of an 18-kip axle load

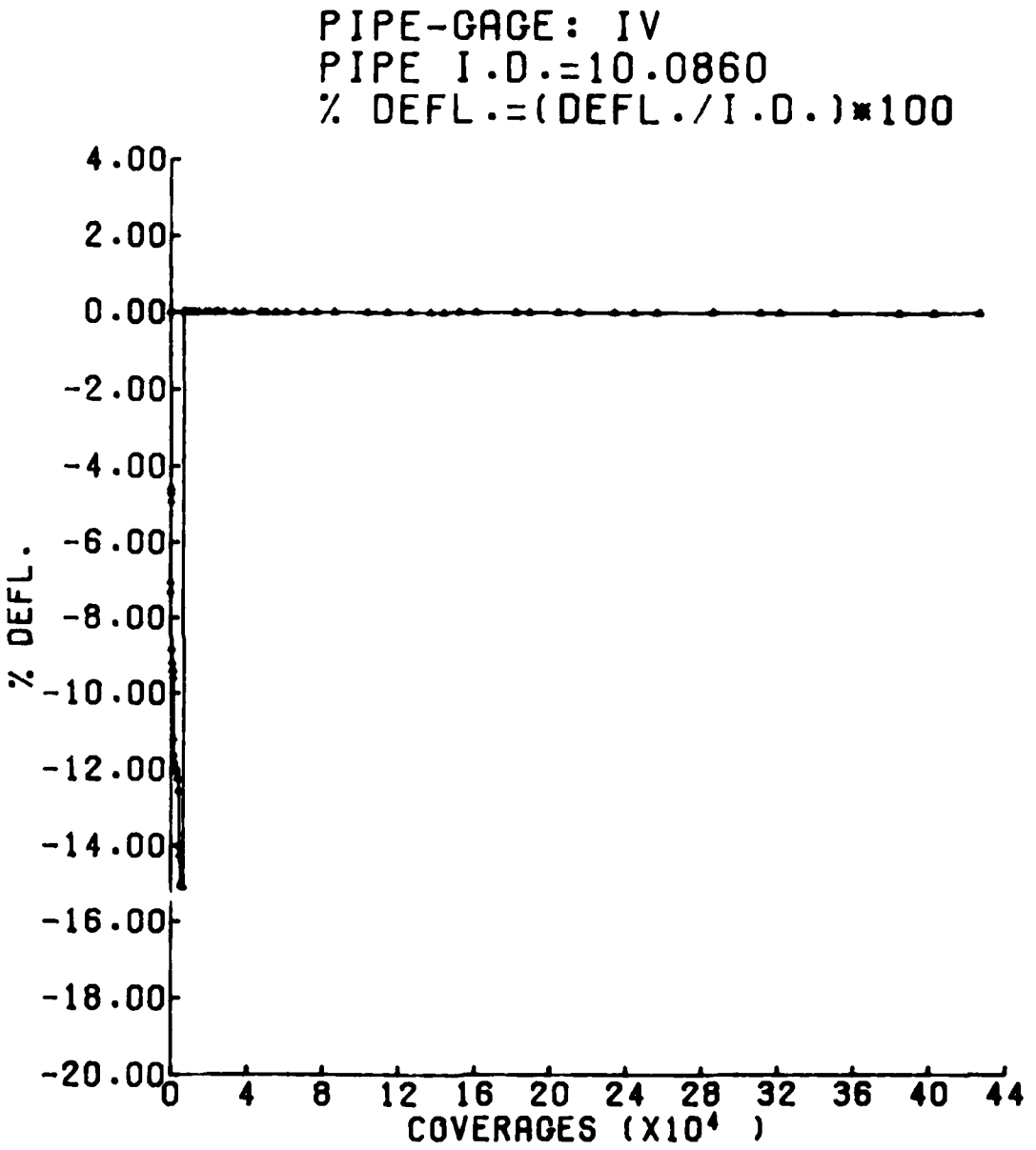

Figure A-30. Permanent deflection of pipe I in CTT as a function of equivalent coverages of an 18-kip axle load

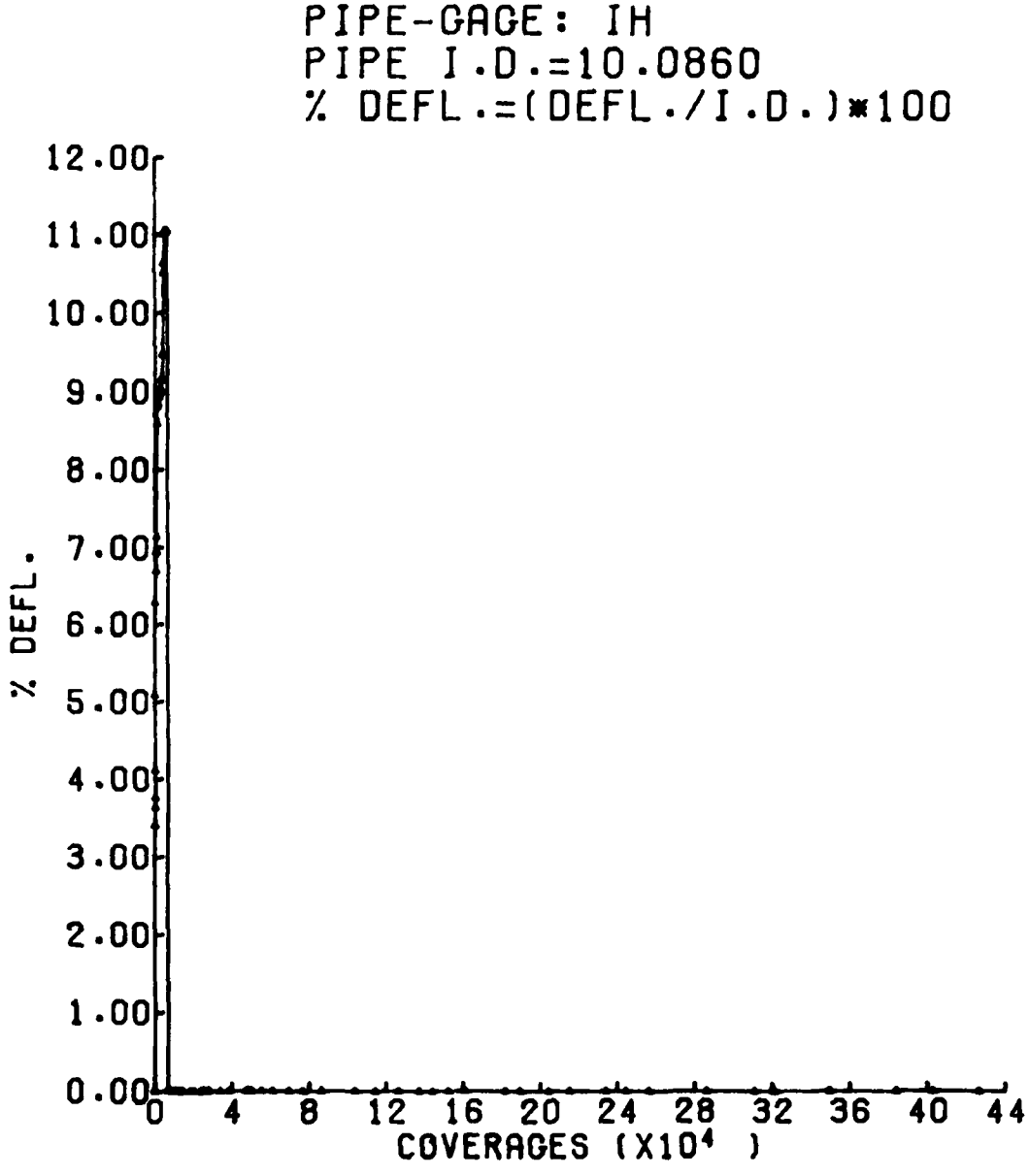

Figure A-31. Permanent deflection of pipe I in CTT as a function of equivalent coverages of an 18-kip axle load

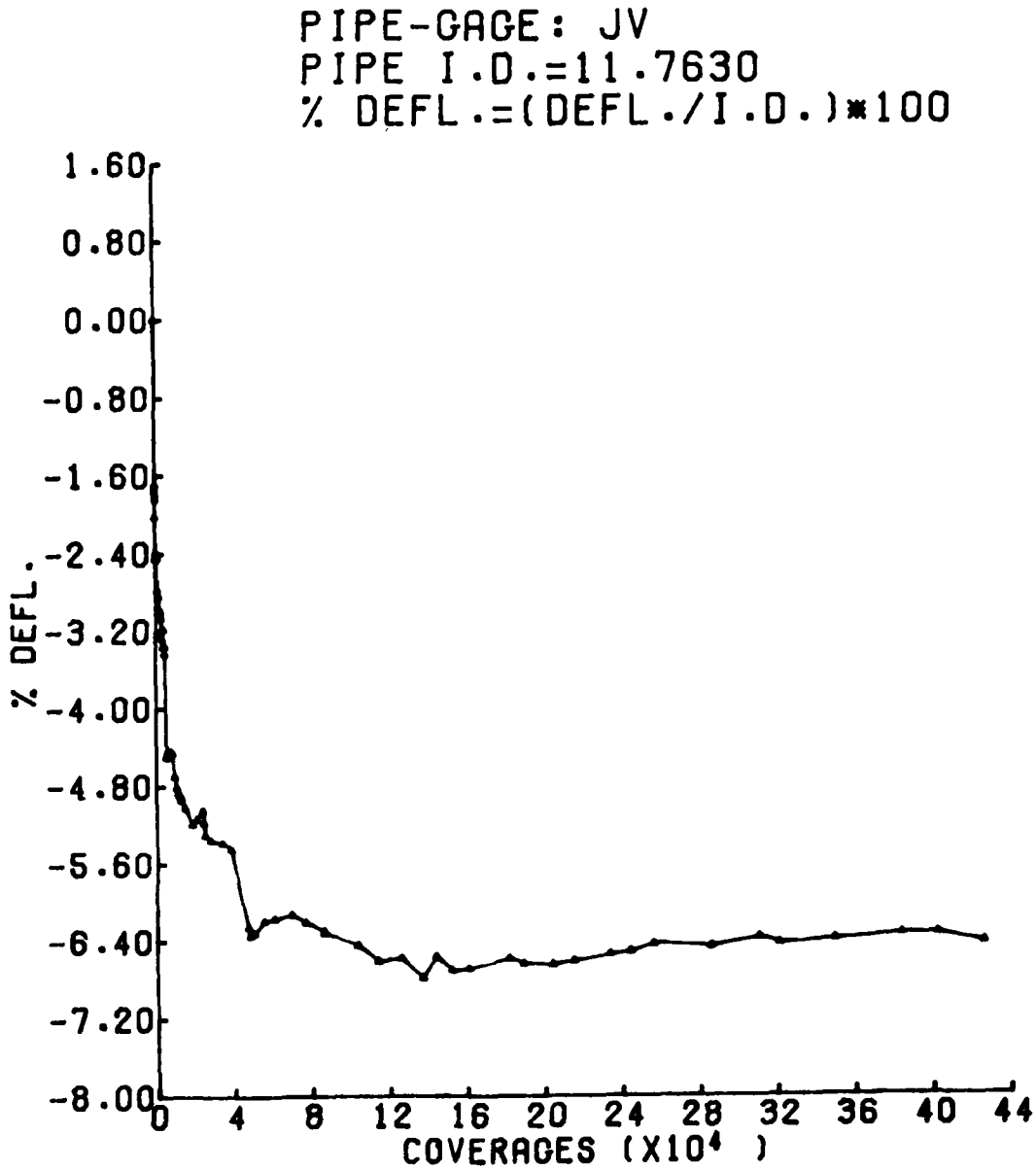

Figure A-32. Permanent deflection of pipe J in CTT as a function of equivalent coverages of an 18-kip axle load

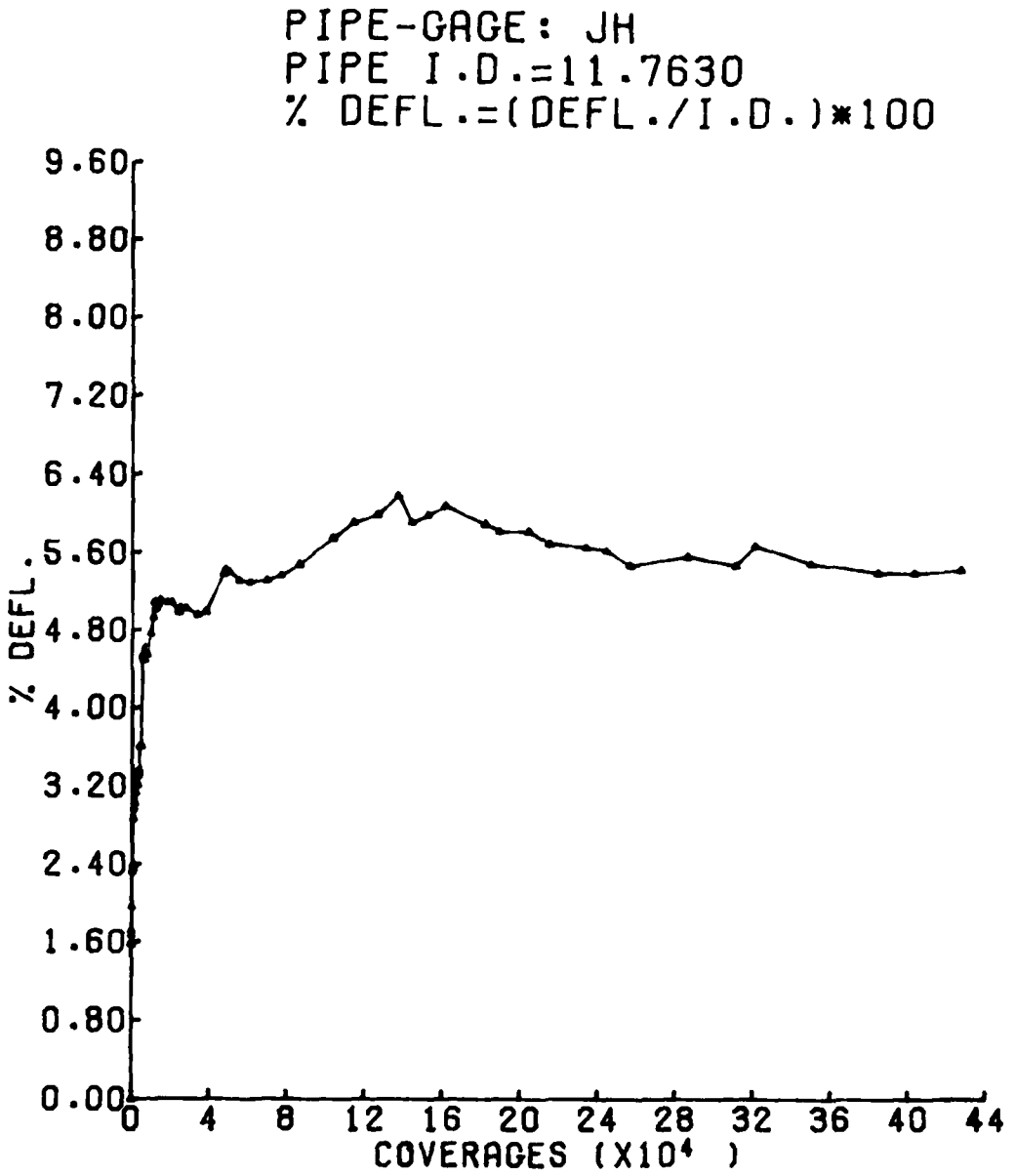

Figure A-33. Permanent deflection of pipe J in CTT as a function of equivalent coverages of an 18-kip axle load

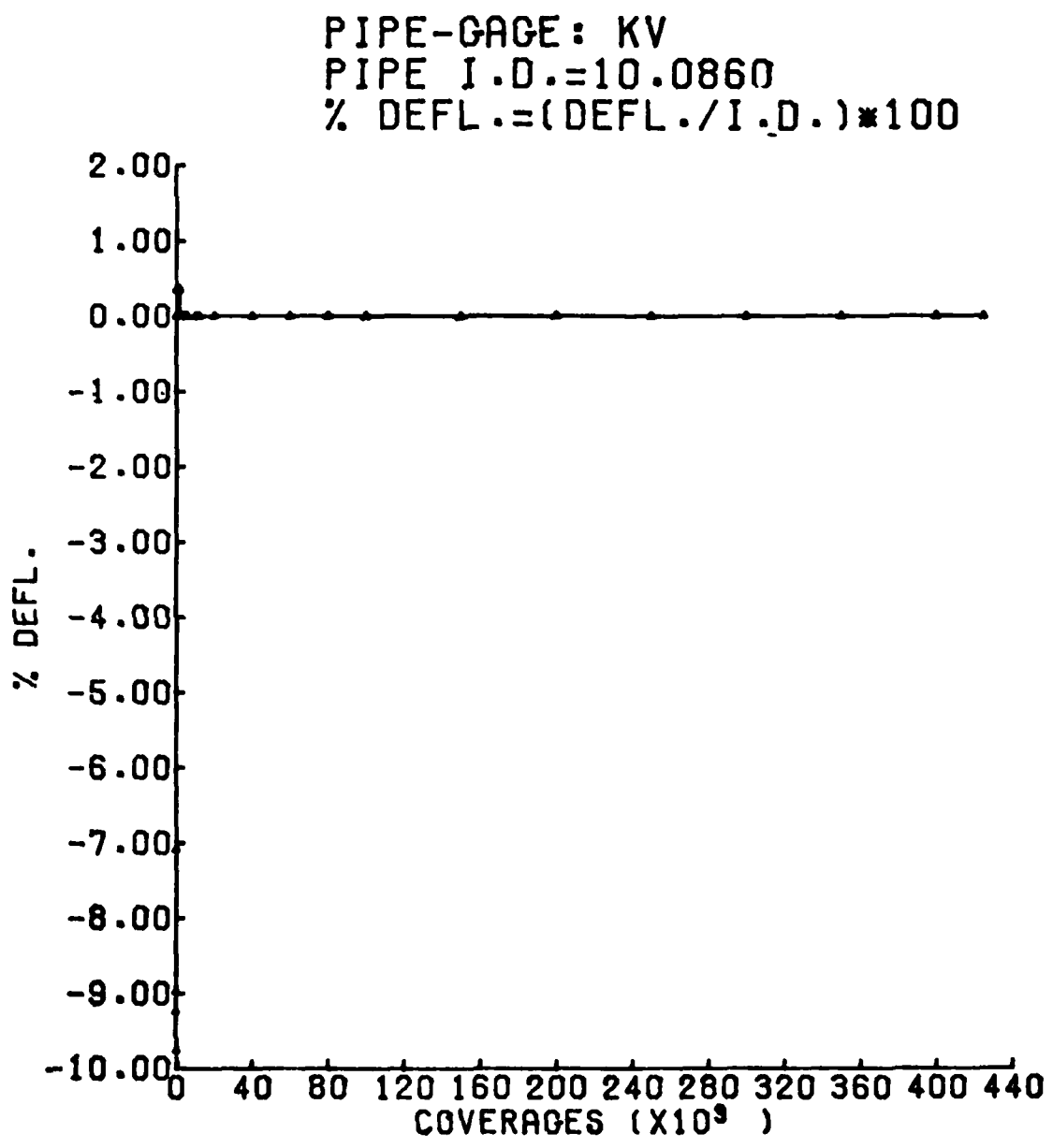

Figure A-34. Permanent deflection of pipe K in CTT as a function of equivalent coverages of an 18-kip axle load

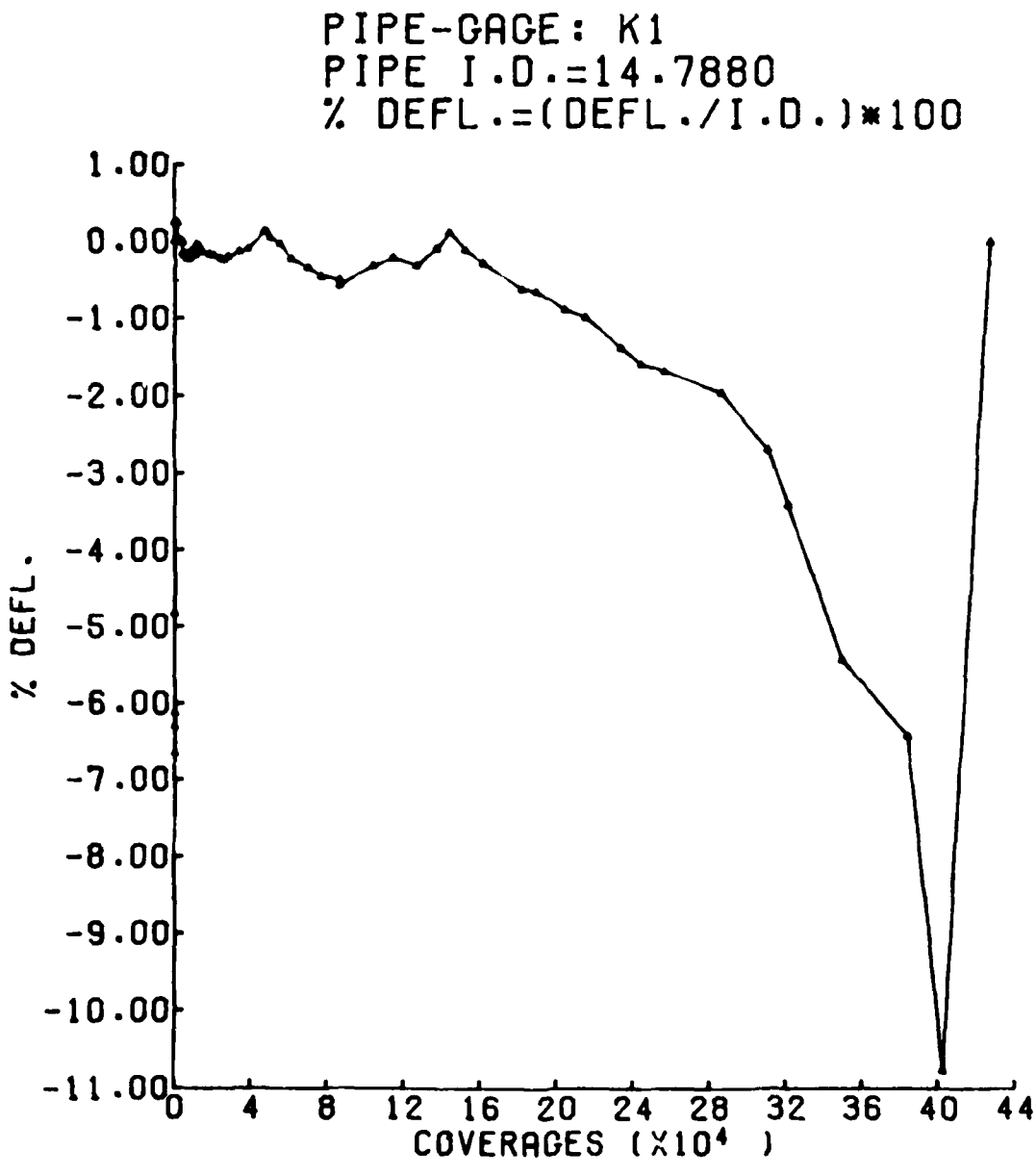

Figure A-35. Permanent deflection of pipe K1 in CTT as a function of equivalent coverages of an 18-kip axle load

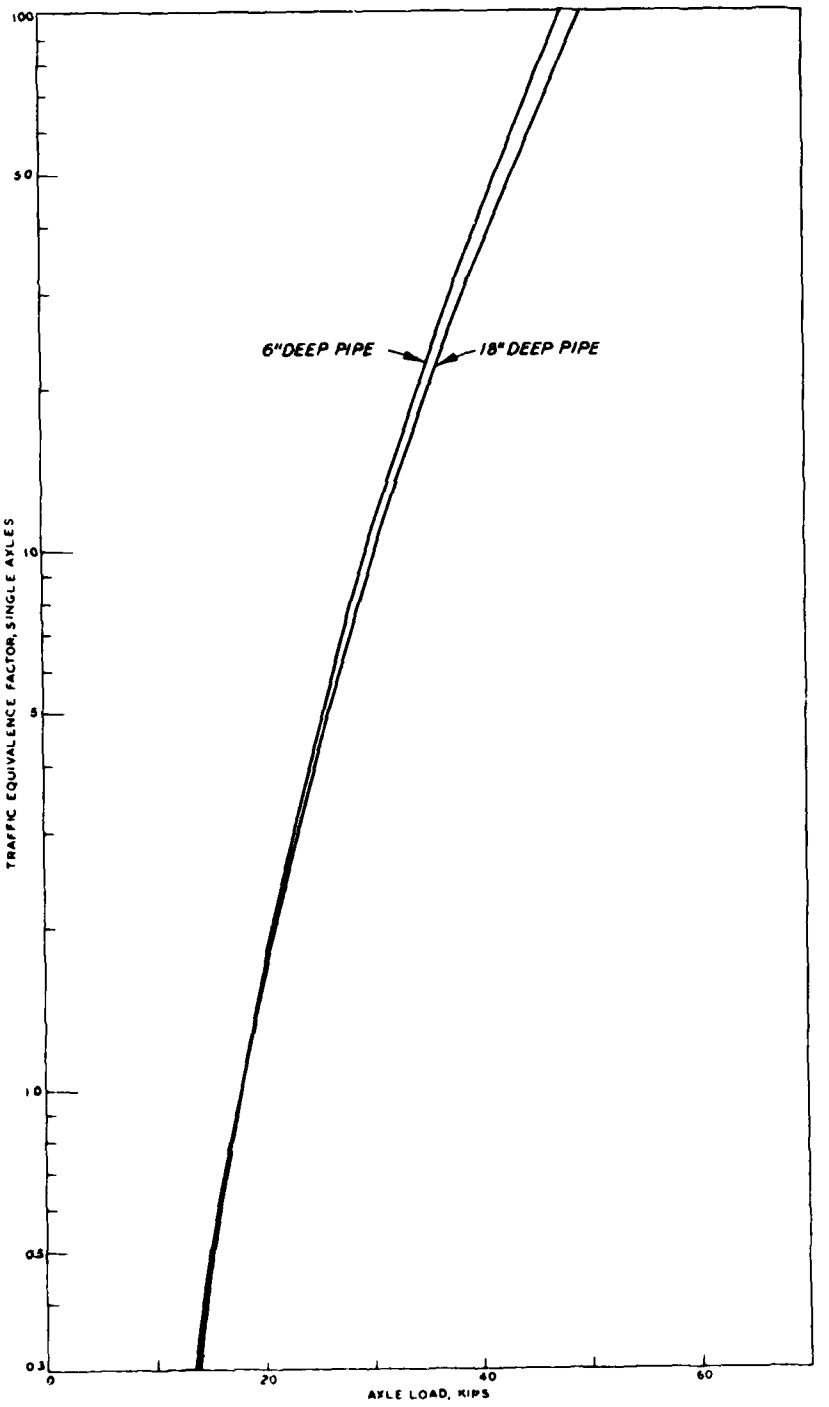

Figure A-36. Curve for converting to equivalent 18-kip coverages (1 in. = 2.54 cm; 1 kip = 0.4535 tonne)

APPENDIX B

MEASURED DEFLECTOMETER DATA FOR PIPES AT TEST SITE NO. 2 FOR SIMULATED F-4 AND C-141 AIRCRAFT TRAFFIC AND FOR STATIC LOADS OF F-4 AND C-141 GEAR ASSEMBLIES

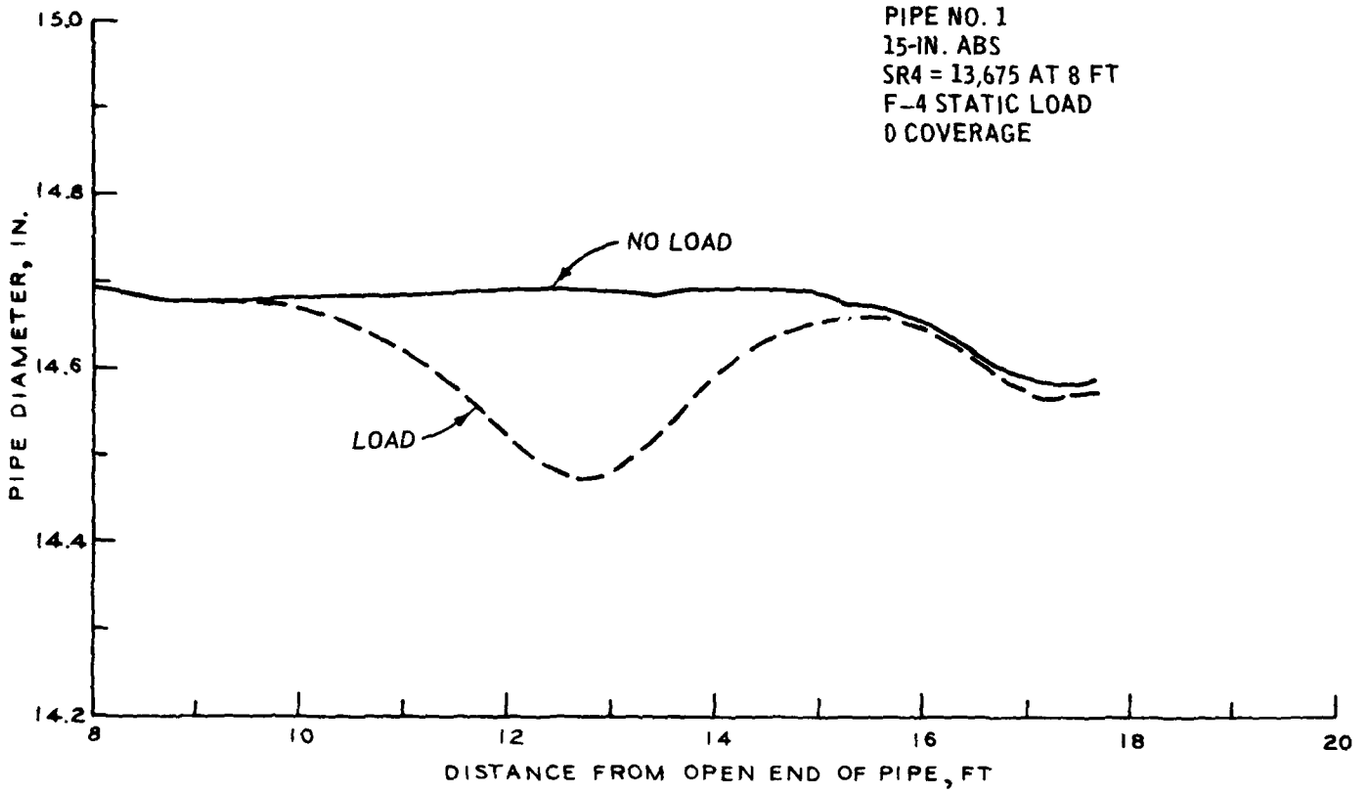

Figure B-1. Measured deflectometer data for pipe No. 1 of Test Site No. 2 (F-4 static load at 0 coverages of F-4 traffic)

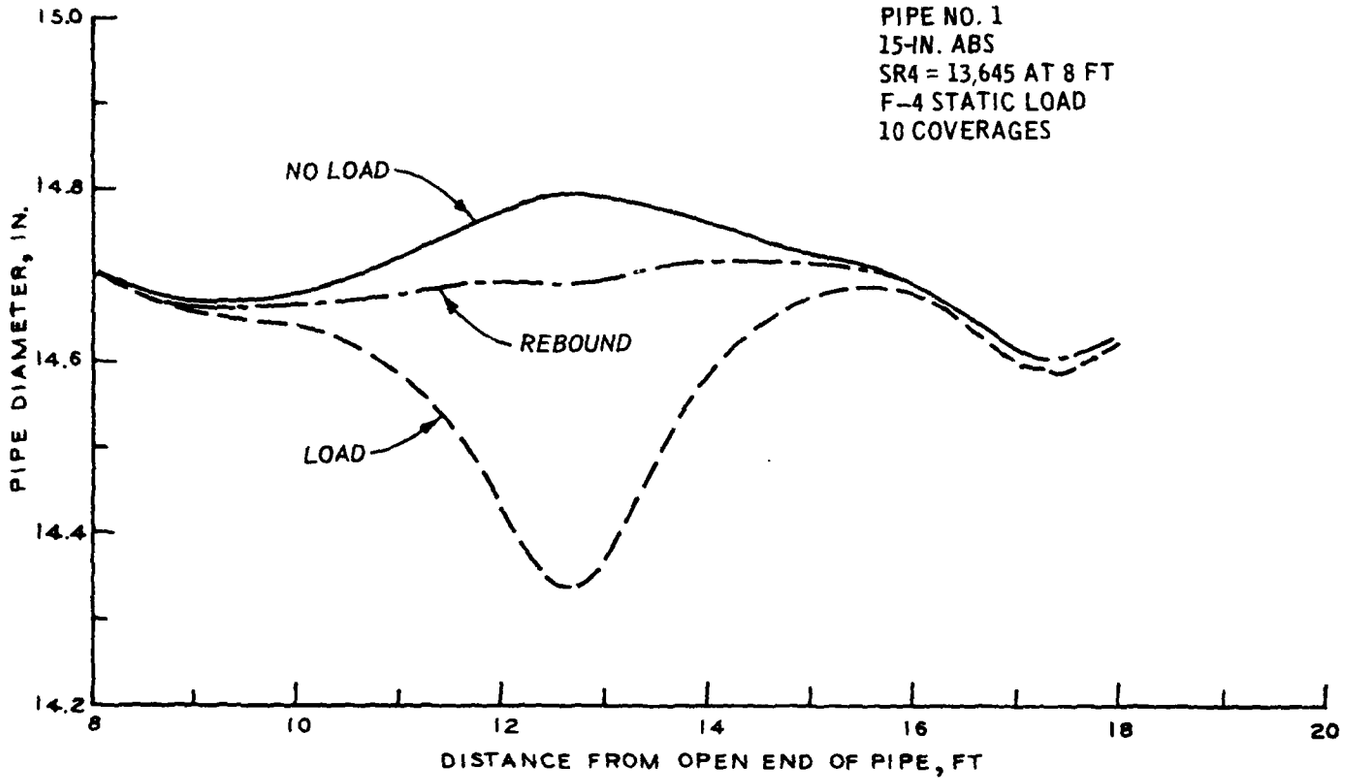

Figure B-2. Measured deflectometer data for pipe No. 1 of Test Site No. 2 (F-4 static load at 10 coverages of F-4 traffic)

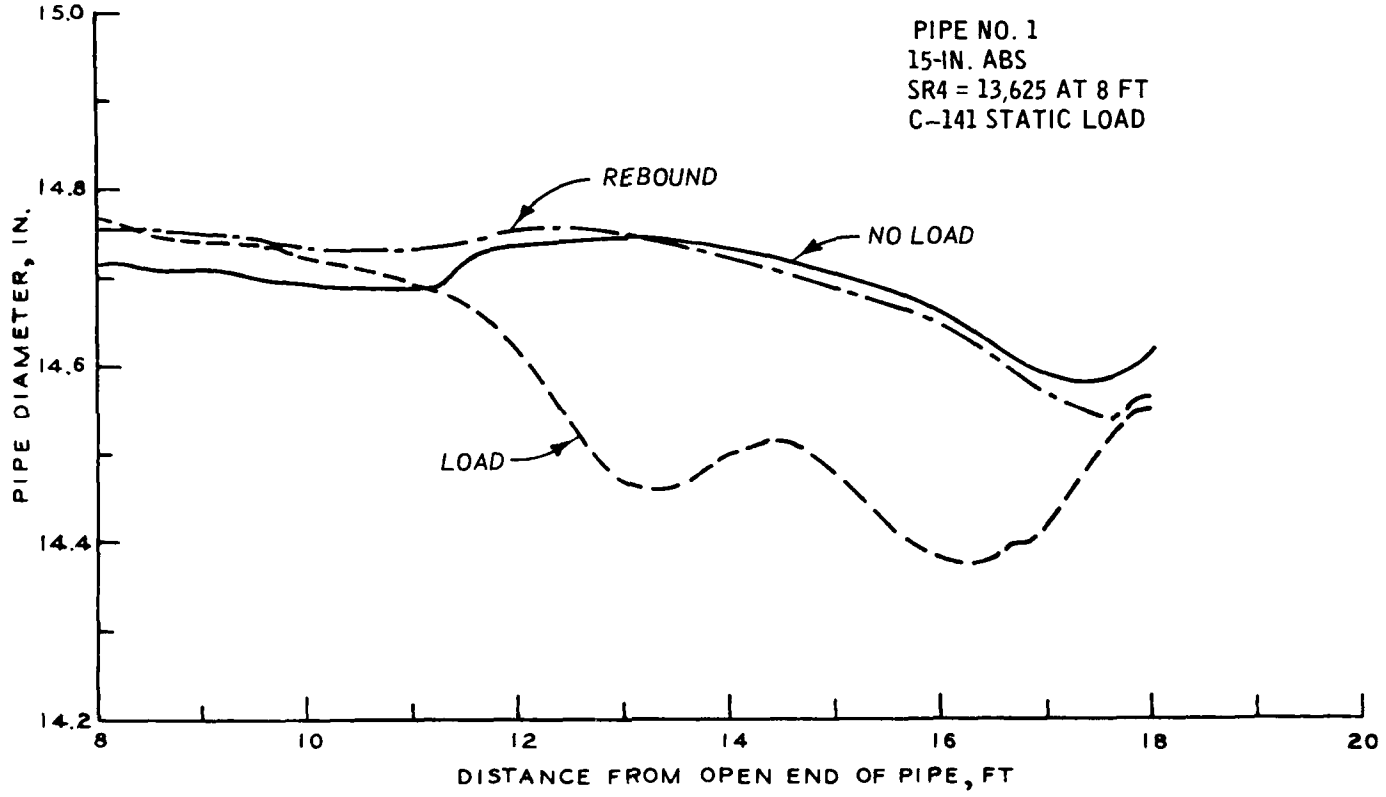

Figure B-3. Measured deflectometer data for pipe No. 1 of Test Site No. 2 (C-141 static load prior to C-141 traffic)

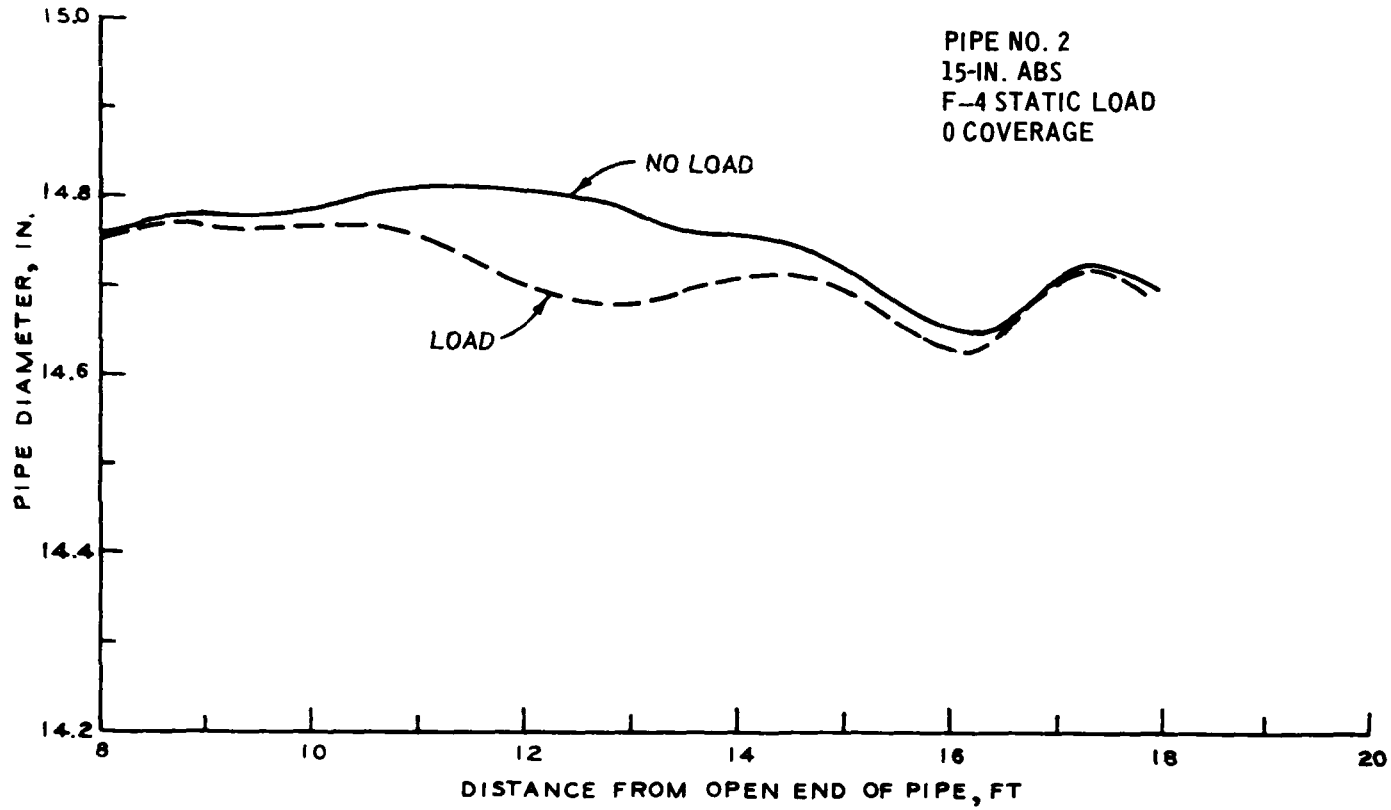

Figure B-4. Measured deflectometer data for pipe No. 2 of Test Site No. 2 (F-4 static load at 0 coverages of F-4 traffic)

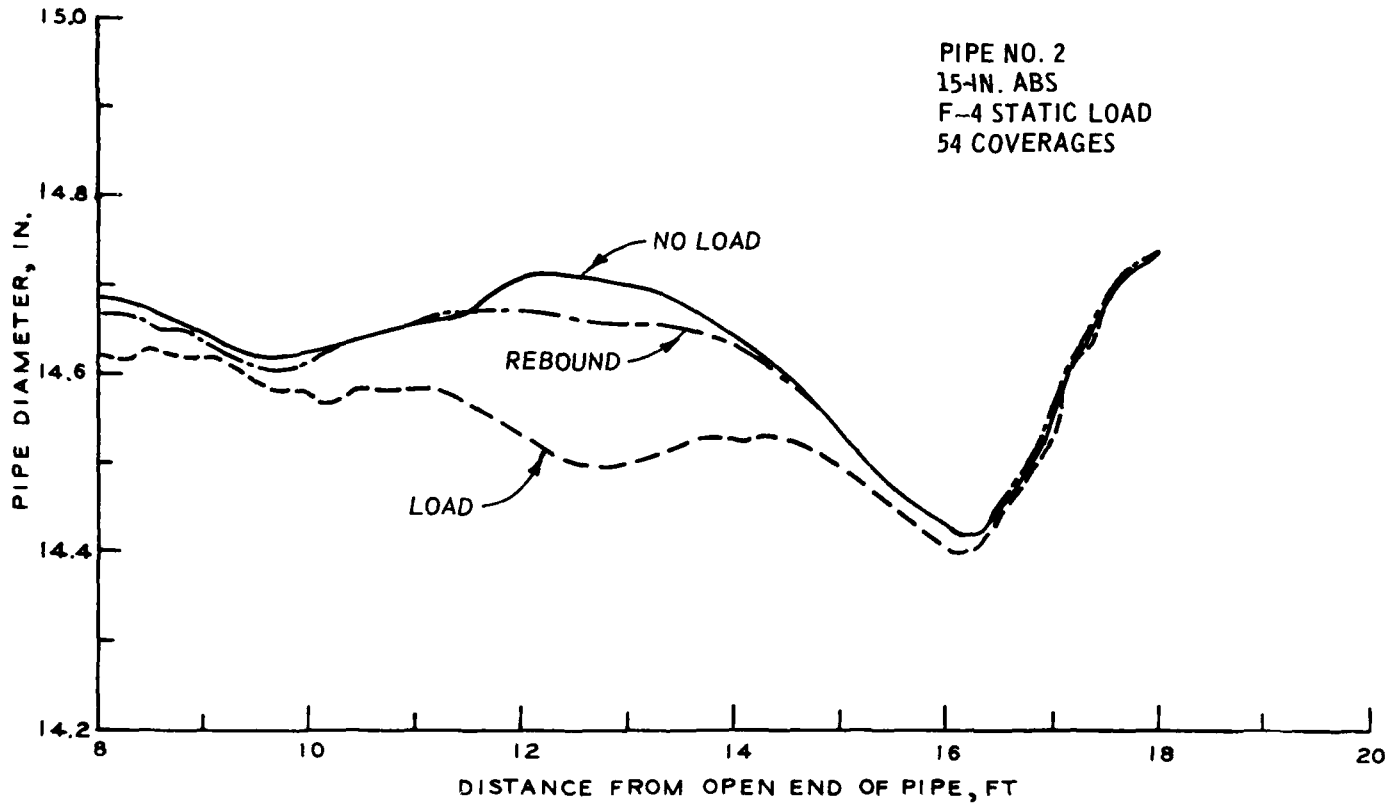

Figure B-5. Measured deflectometer data for pipe No. 2 of Test Site No. 2 (F-4 static load at 54 coverages of F-4 traffic)

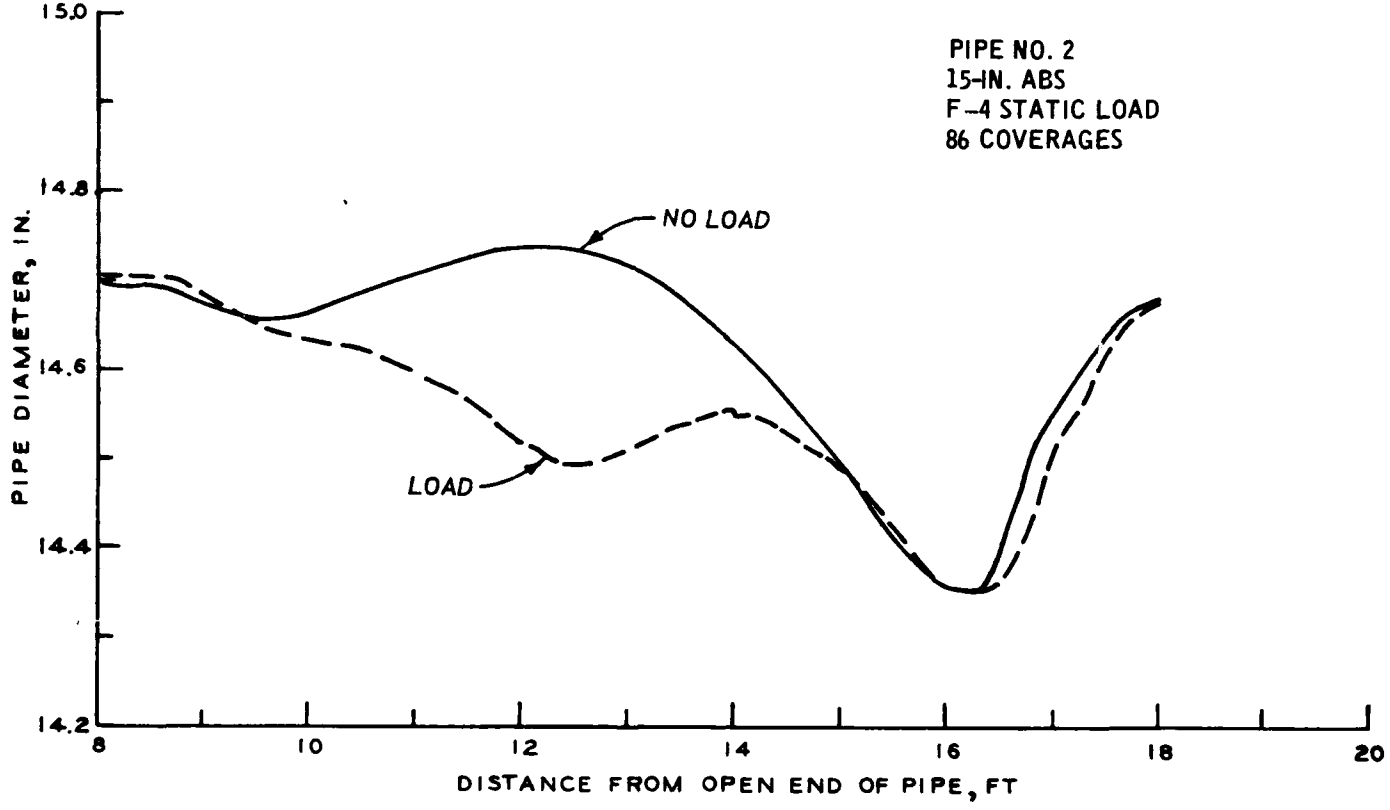

Figure B-6. Measured deflectometer data for pipe No. 2 of Test Site No. 2 (F-4 static load at 86 coverages of F-4 traffic)

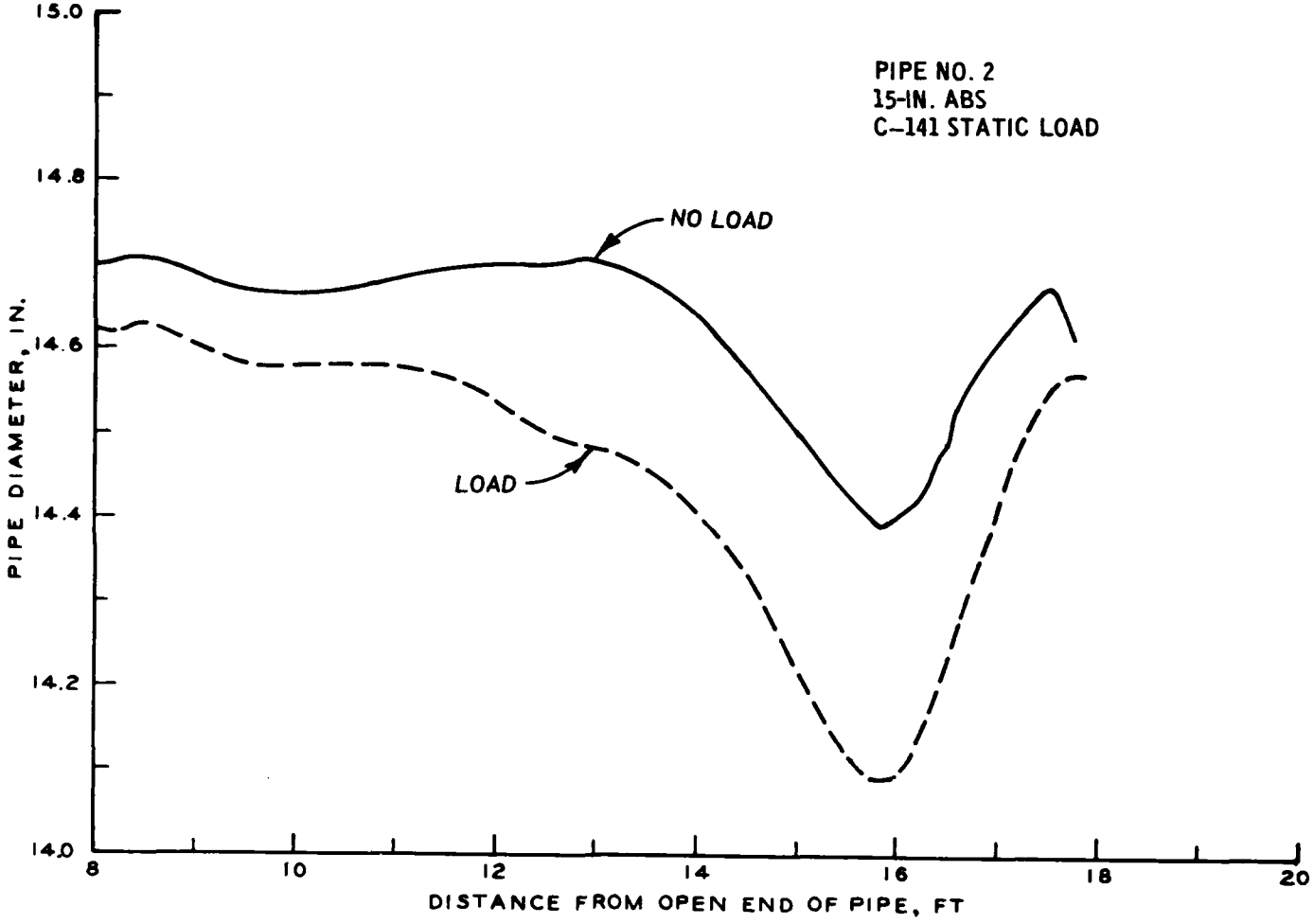

Figure B-7. Measured deflectometer data for pipe No. 2 of Test Site No. 2 (C-141 static load prior to C-141 traffic)

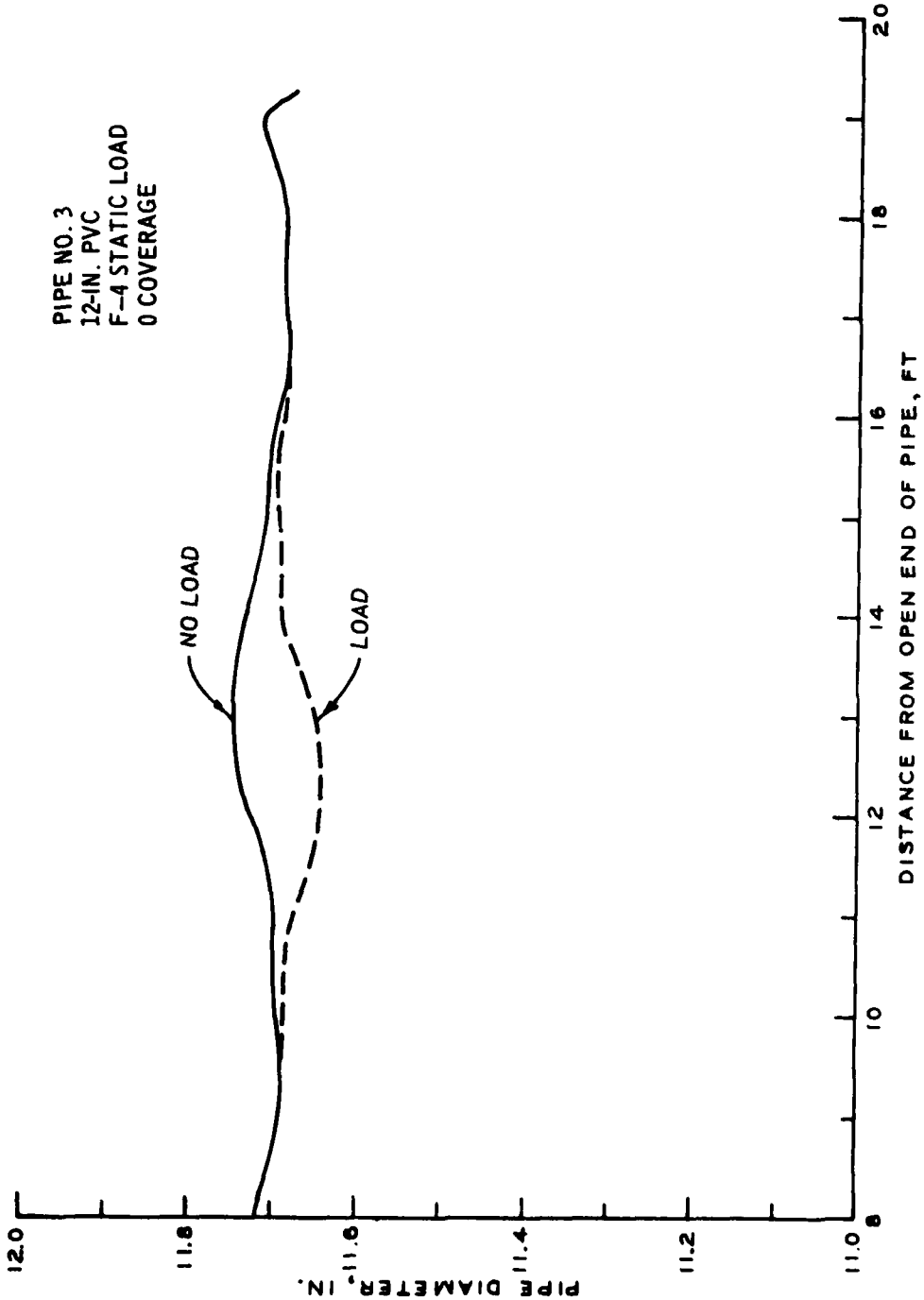

Figure B-8. Measured deflectometer data for pipe No. 3 of Test Site No. 2 (F-4 static load at 0 coverages of F-4 traffic)

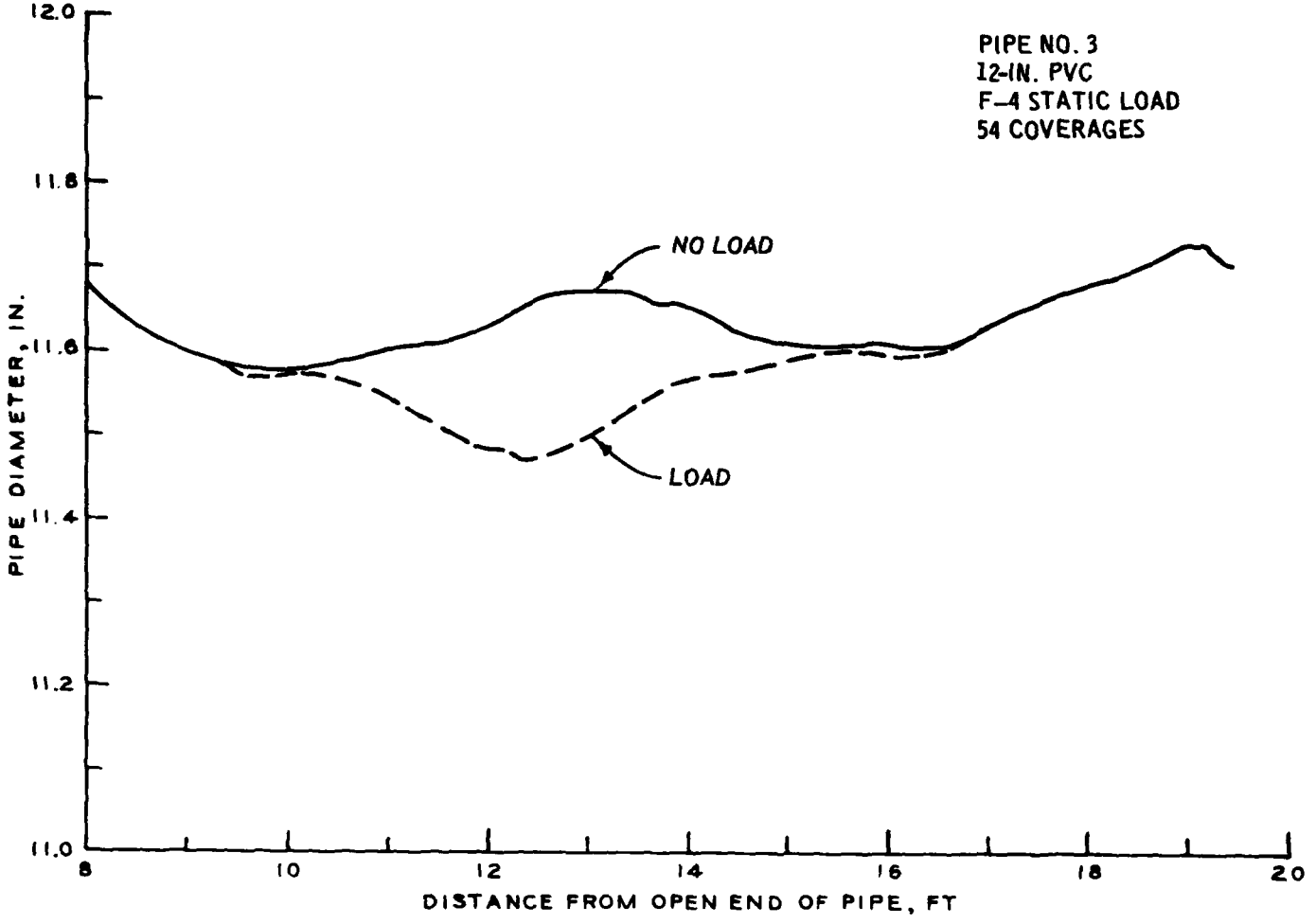

Figure B-9. Measured deflectometer data for pipe No. 3 of Test Site No. 2 (F-4 static load at 54 coverages of F-4 traffic)

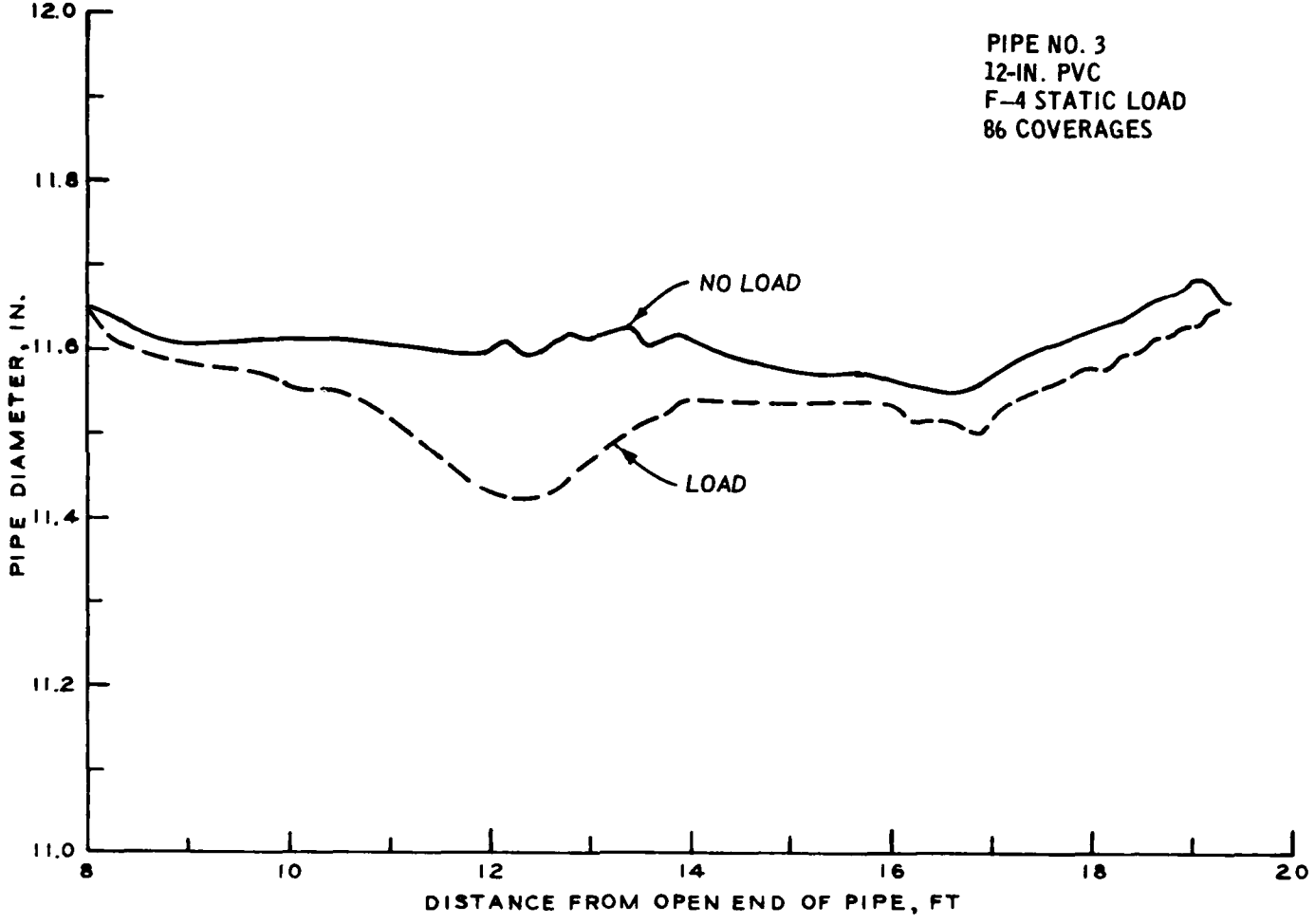

Figure B-10. Measured deflectometer data for pipe No. 3 of Test Site No. 2 (F-4 static load at 86 coverages of F-4 traffic)

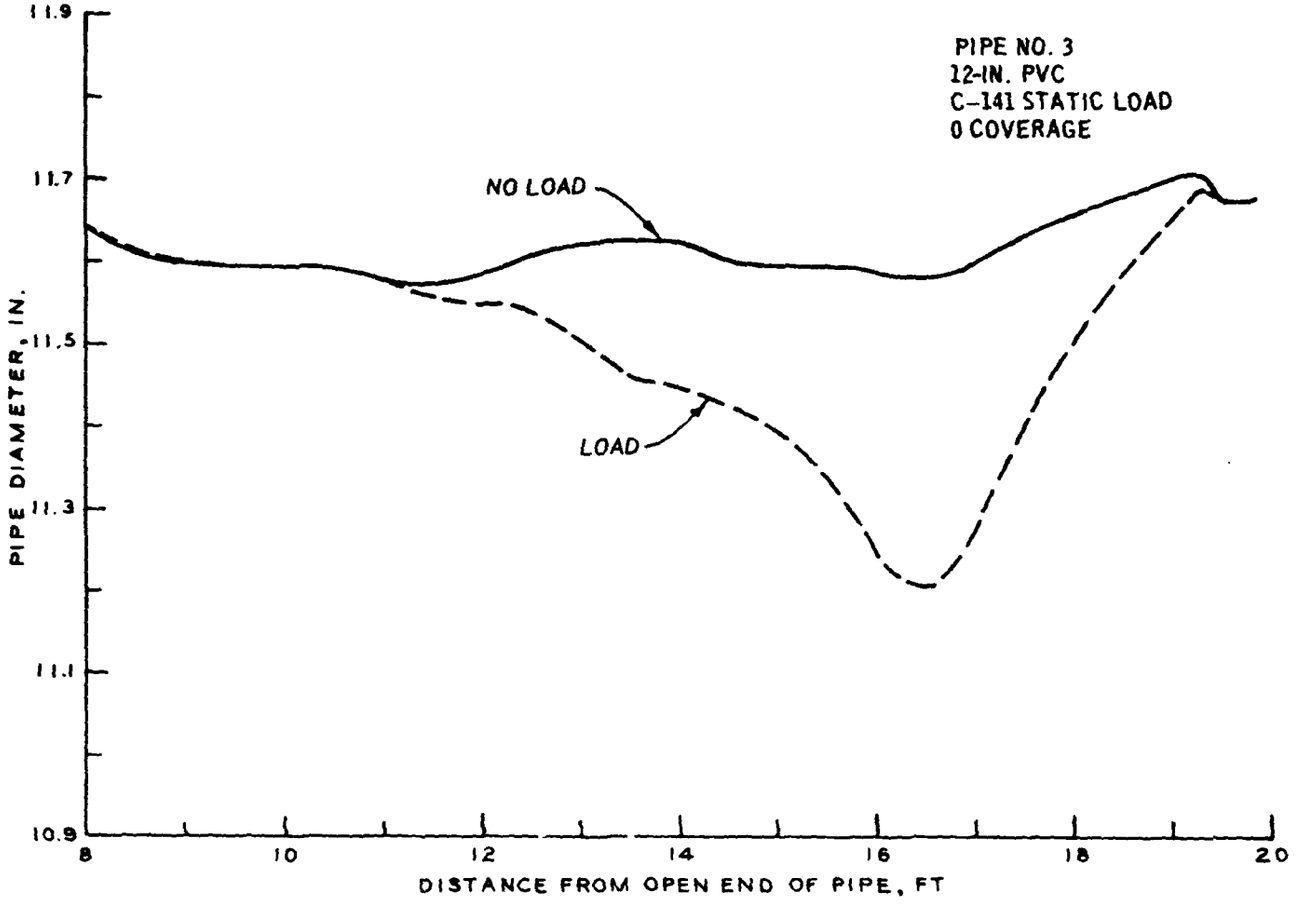

Figure B-11. Measured deflectometer data for pipe No. 3 of Test Site No. 2 (C-141 static load prior to C-141 traffic)

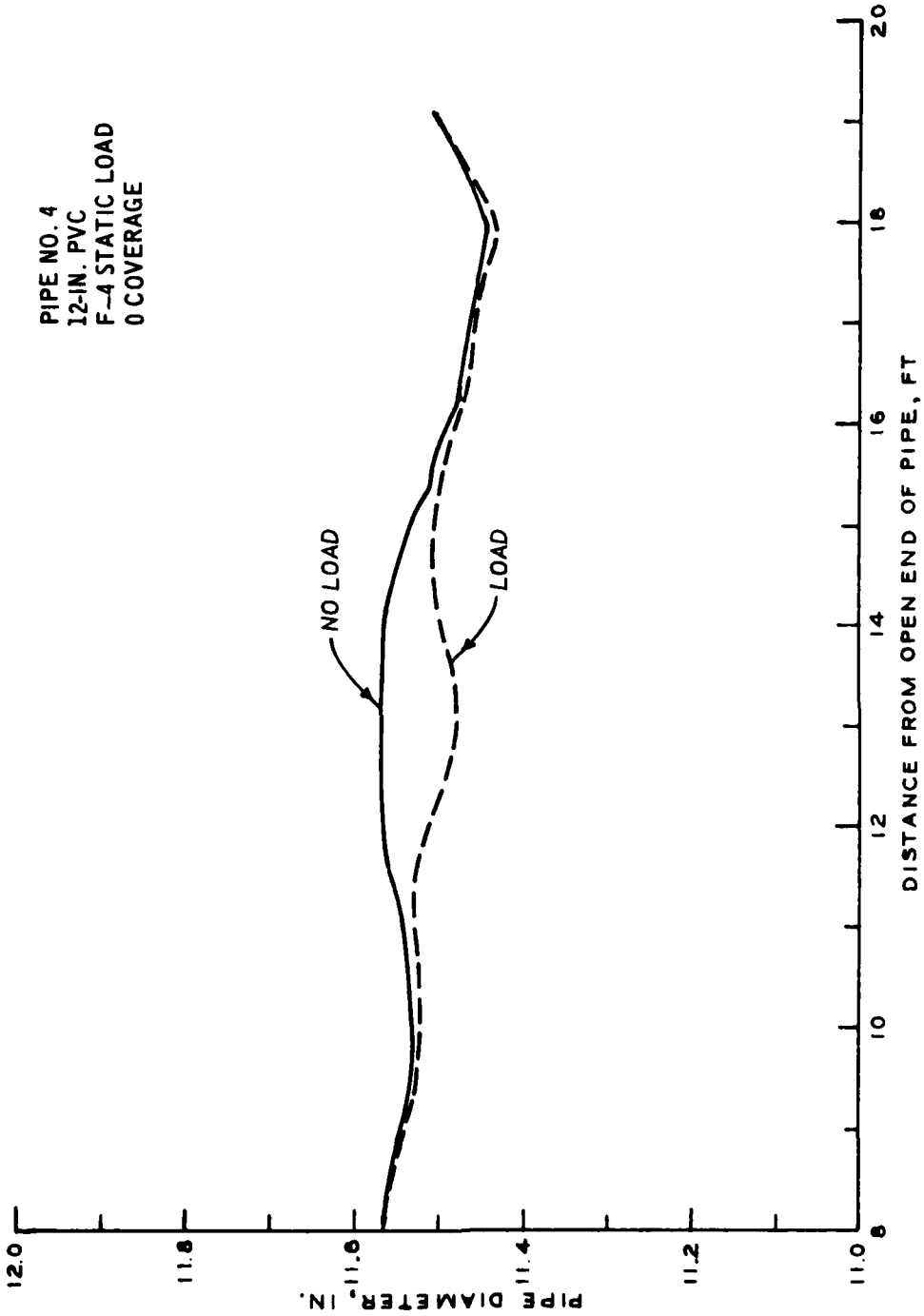

Figure B-12. Measured deflectometer data for pipe No. 4 of Test Site No. 2 (F-4 static load at 0 coverages of F-4 traffic)

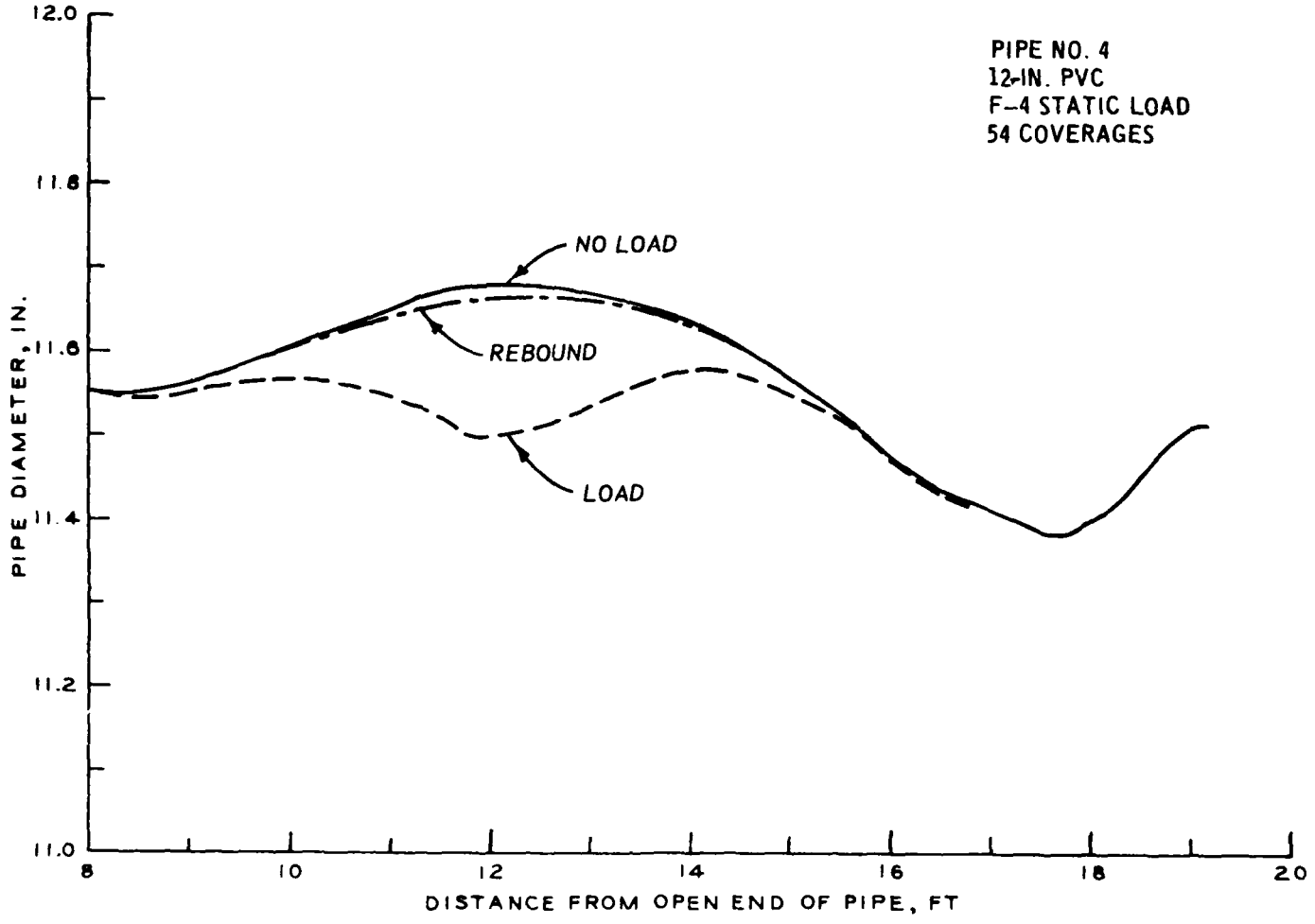

Figure B-13. Measured deflectometer data for pipe No. 4 of Test Site No. 2 (F-4 static load at 54 coverages of F-4 traffic)

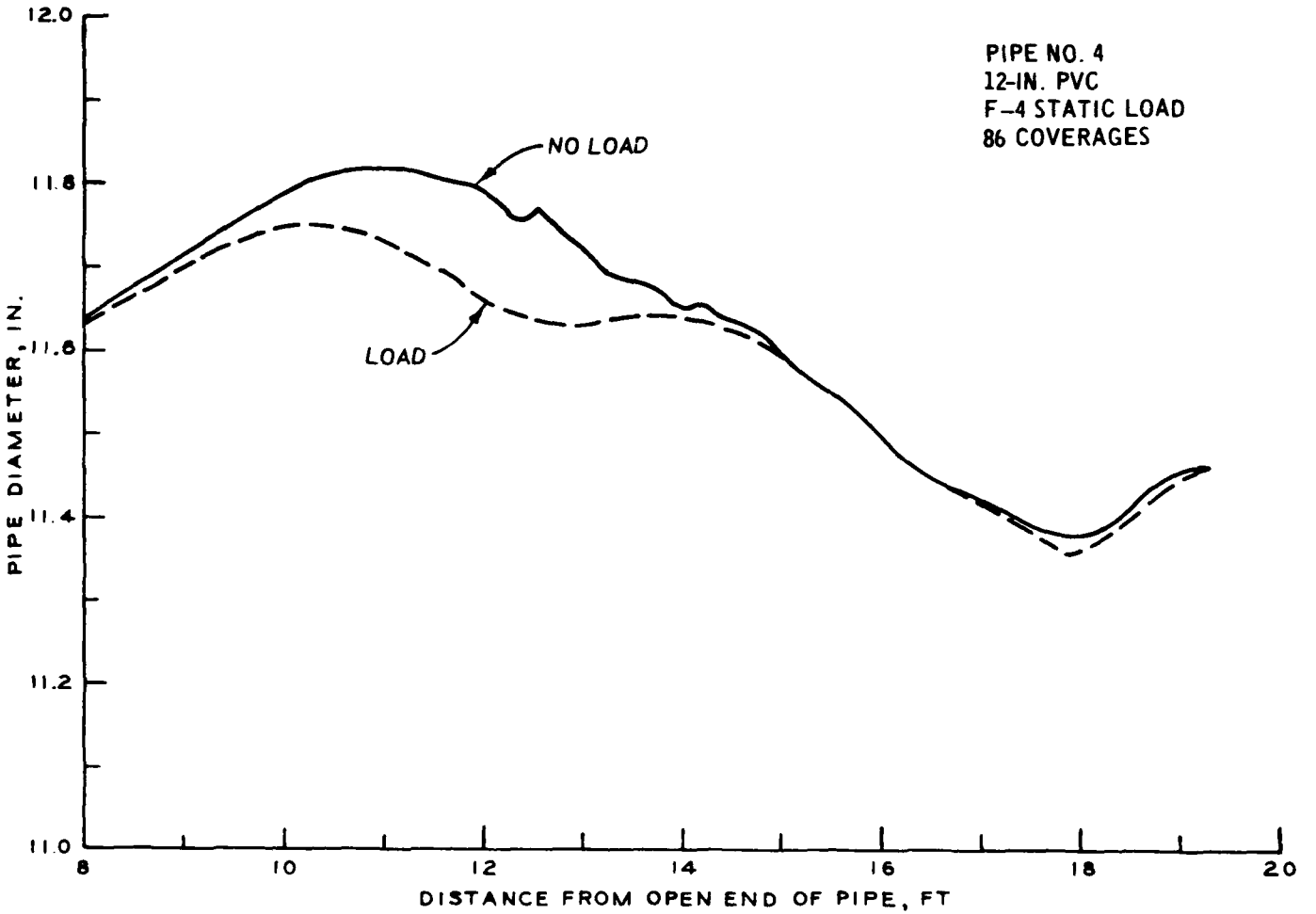

Figure B-14. Measured deflectometer data for pipe No. 4 of Test Site No. 2 (F-4 static load at 86 coverages of F-4 traffic)

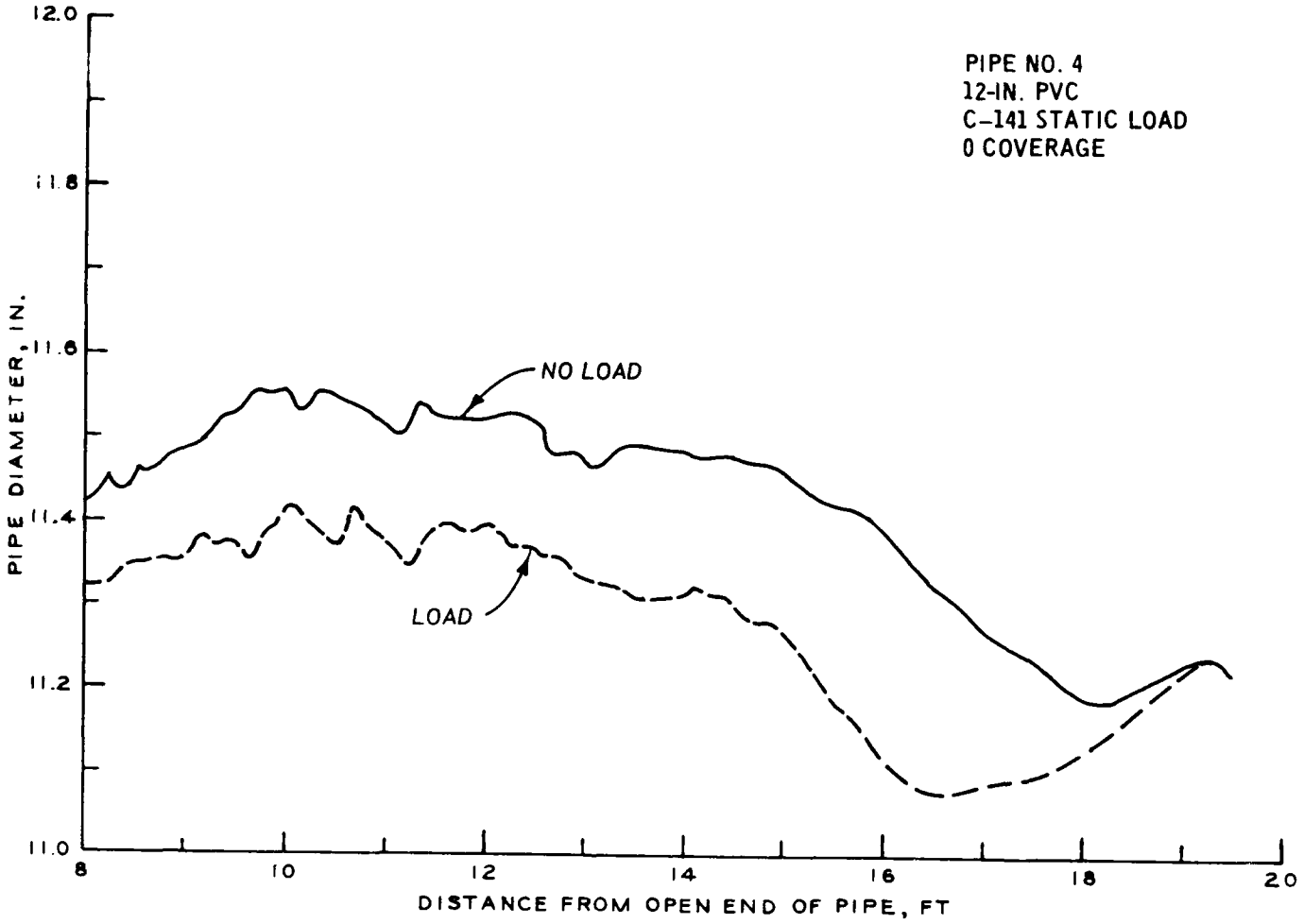

Figure B-15. Measured deflectometer data for pipe No. 4 of Test Site No. 2 (C-141 static load prior to C-141 traffic)

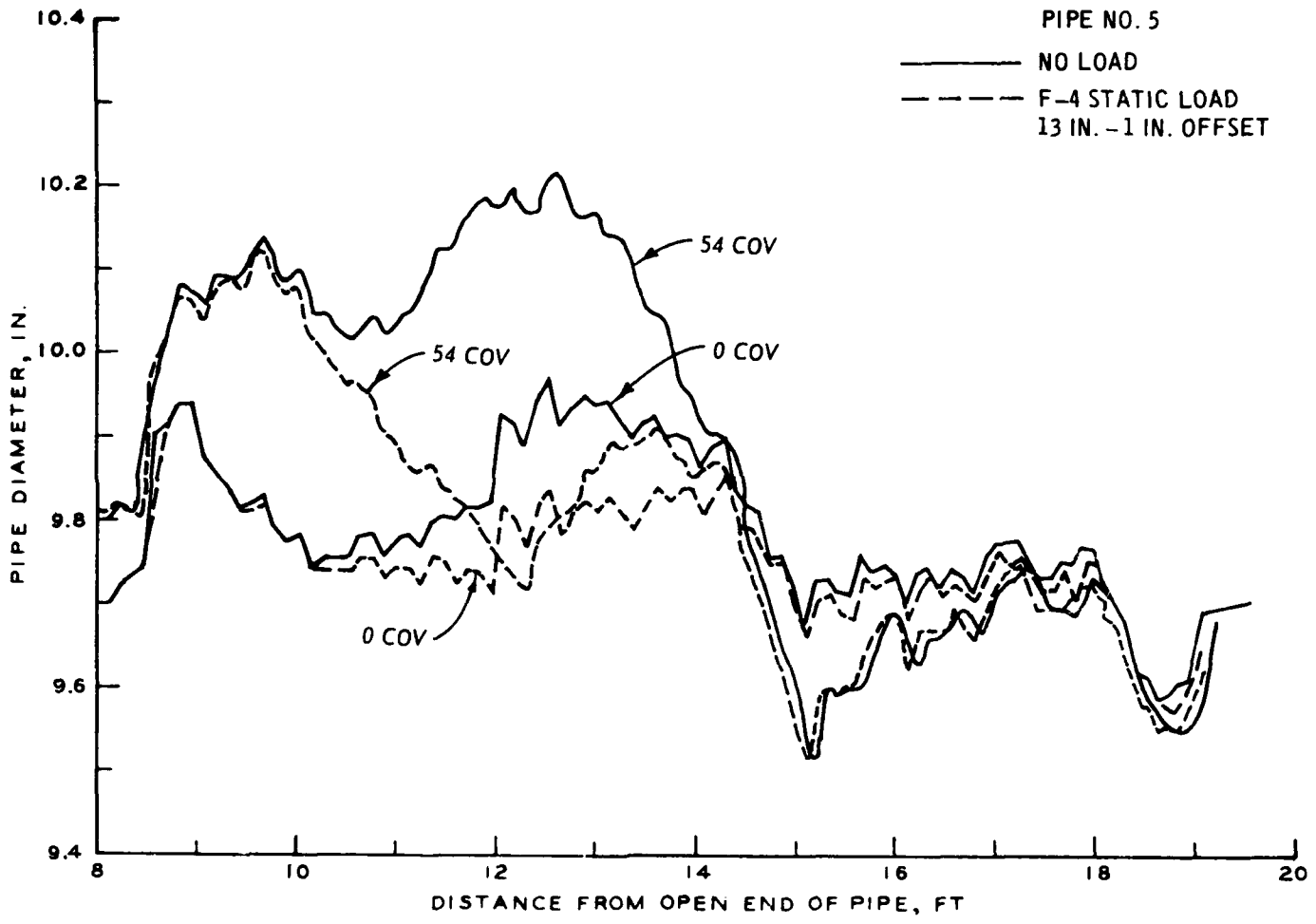

Figure B-16. Measured deflection data for pipe No. 5 of Test Site No. 2 (F-4 static load at 0 and 54 coverages of F-4 traffic)

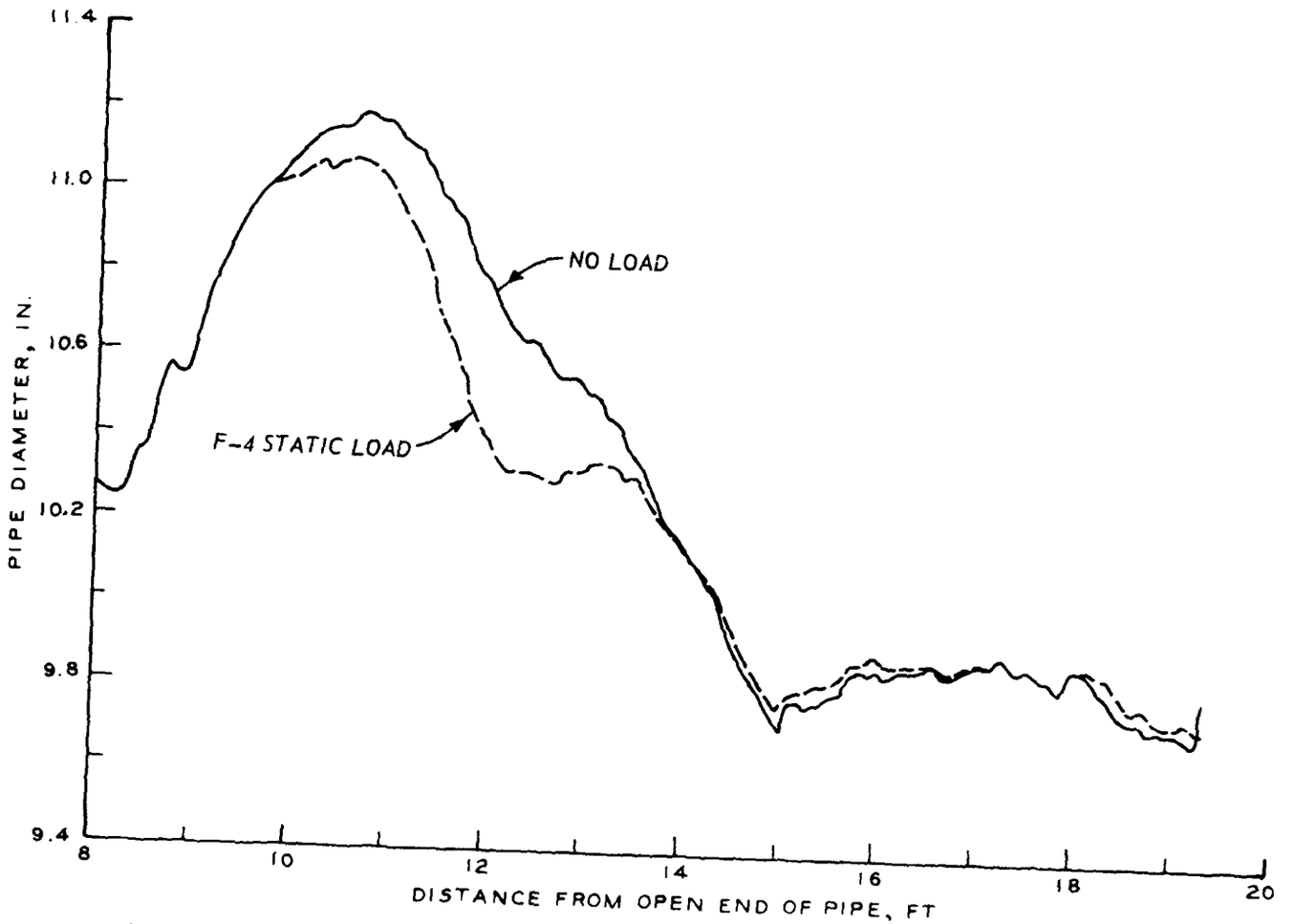

Figure B-17. Measured deflection data for pipe No. 5 of Test Site No. 2 (F-4 static load at 84 coverages of F-4 traffic)

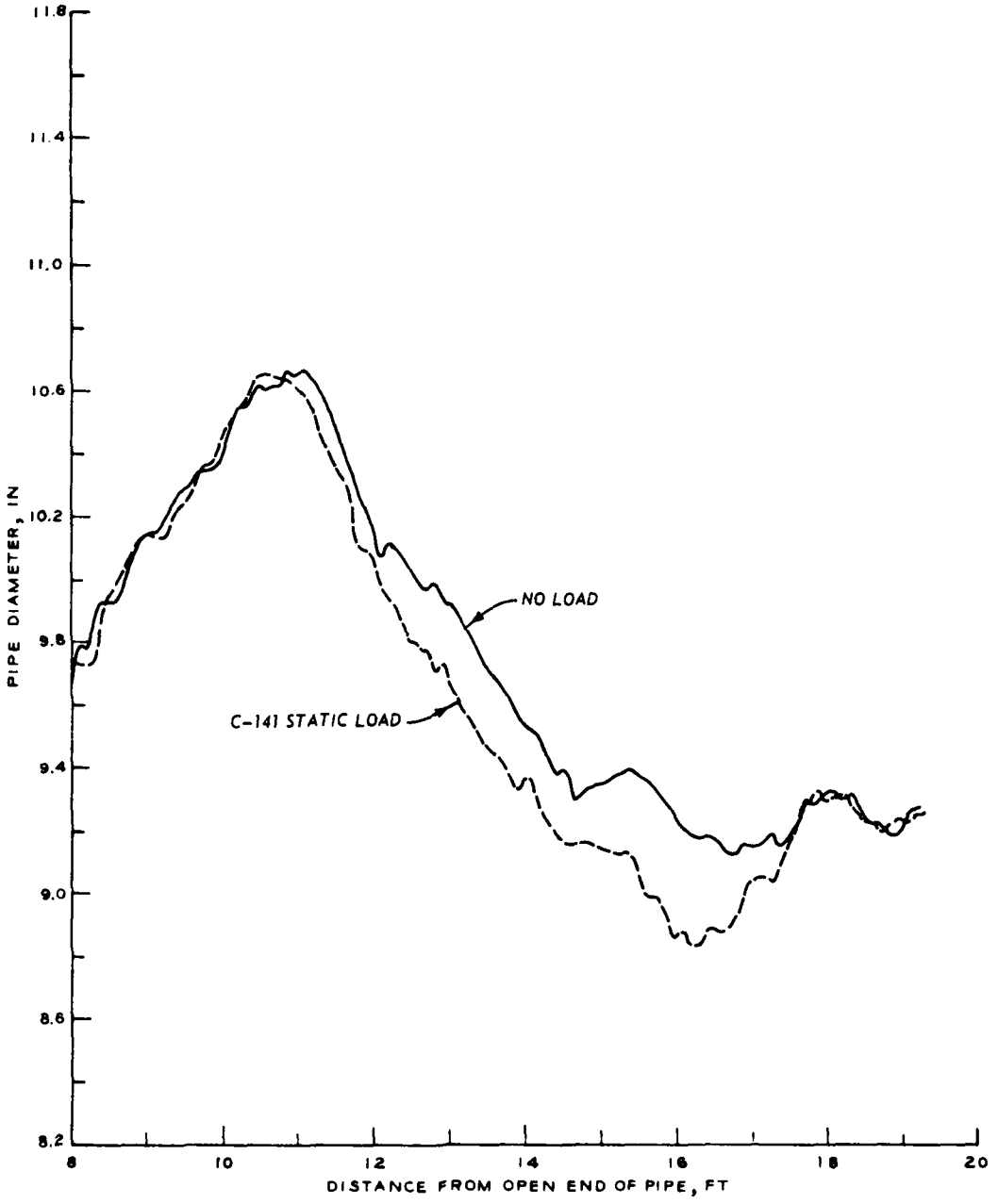

Figure B-18. Measured deflection data for pipe No. 5 of Test Site No. 2 (C-141 static load prior to C-141 traffic)

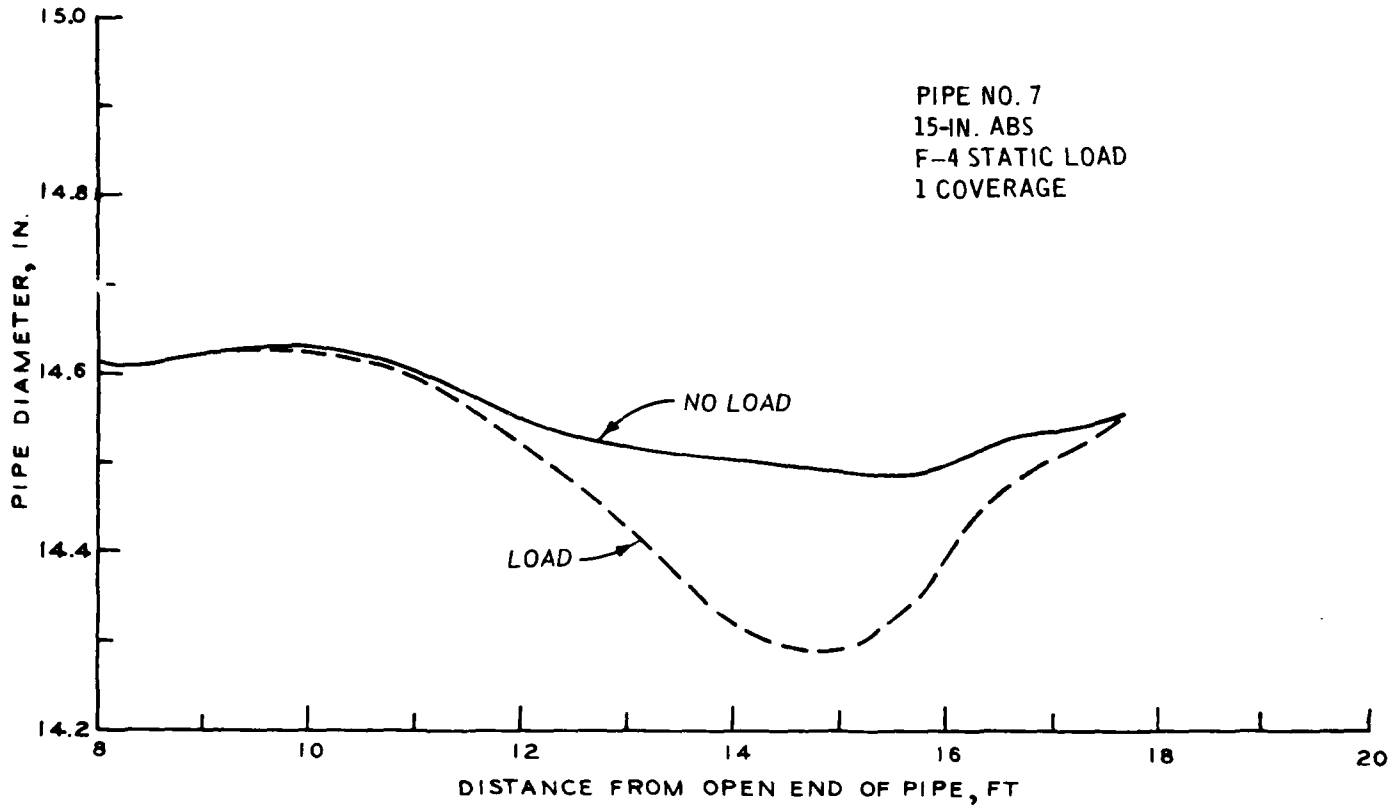

Figure B-19. Measured deflectometer data for pipe No. 7 of Test Site No. 2 (F-4 static load at 1 coverage of F-4 traffic)

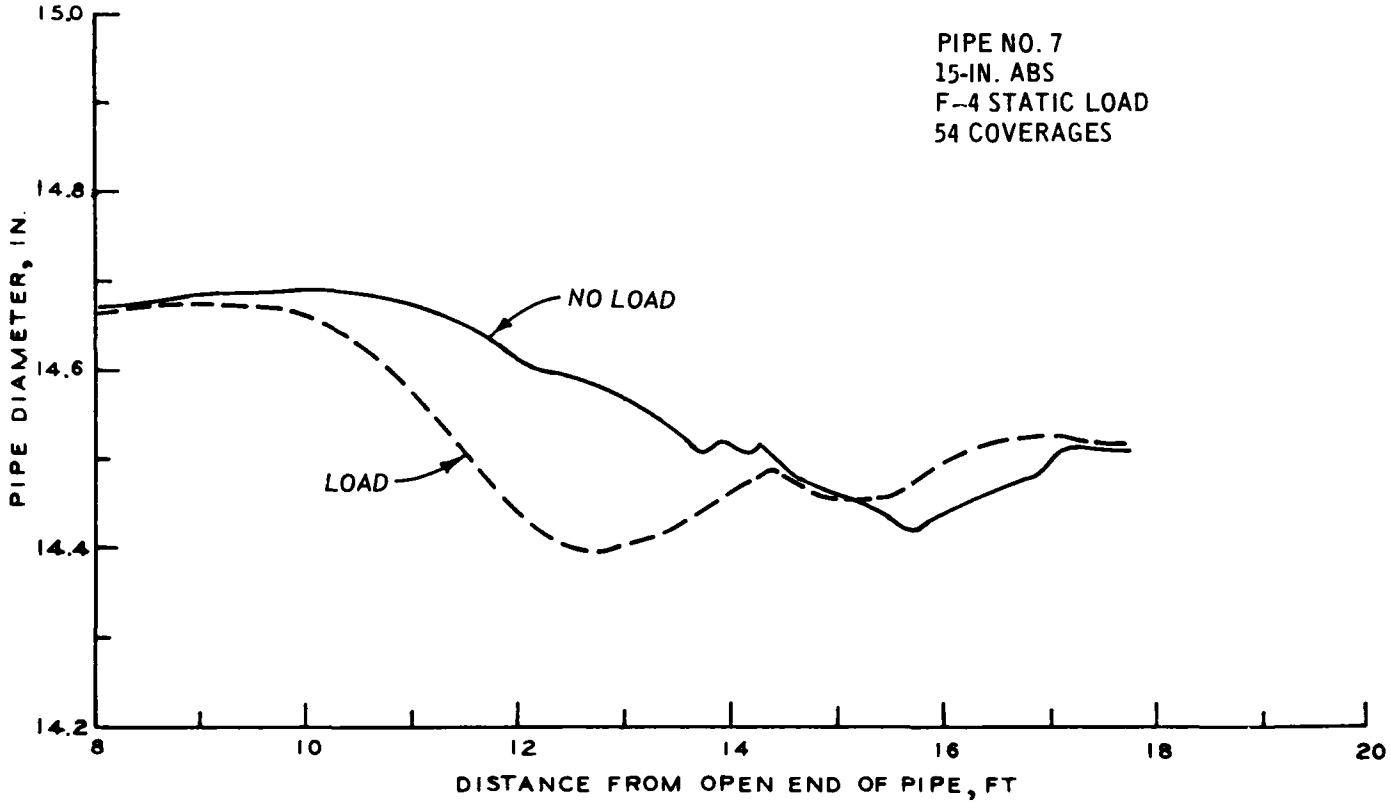

Figure B-20. Measured deflectometer data for pipe No. 7 of Test Site No. 2 (F-4 static load at 54 coverages of F-4 traffic)

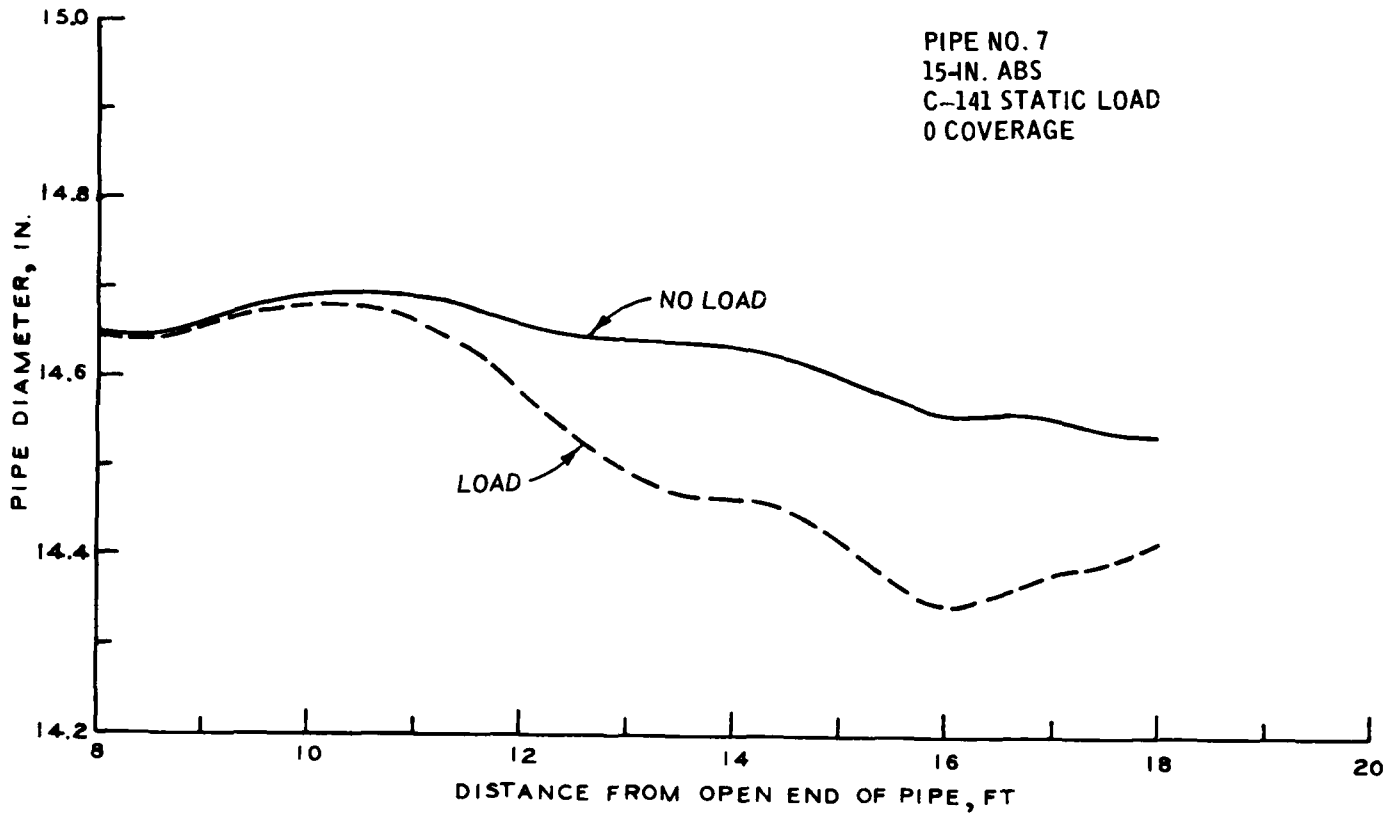

Figure B-21. Measured deflectometer data for pipe No. 7 of Test Site No. 2 (C-141 static load prior to C-141 traffic)

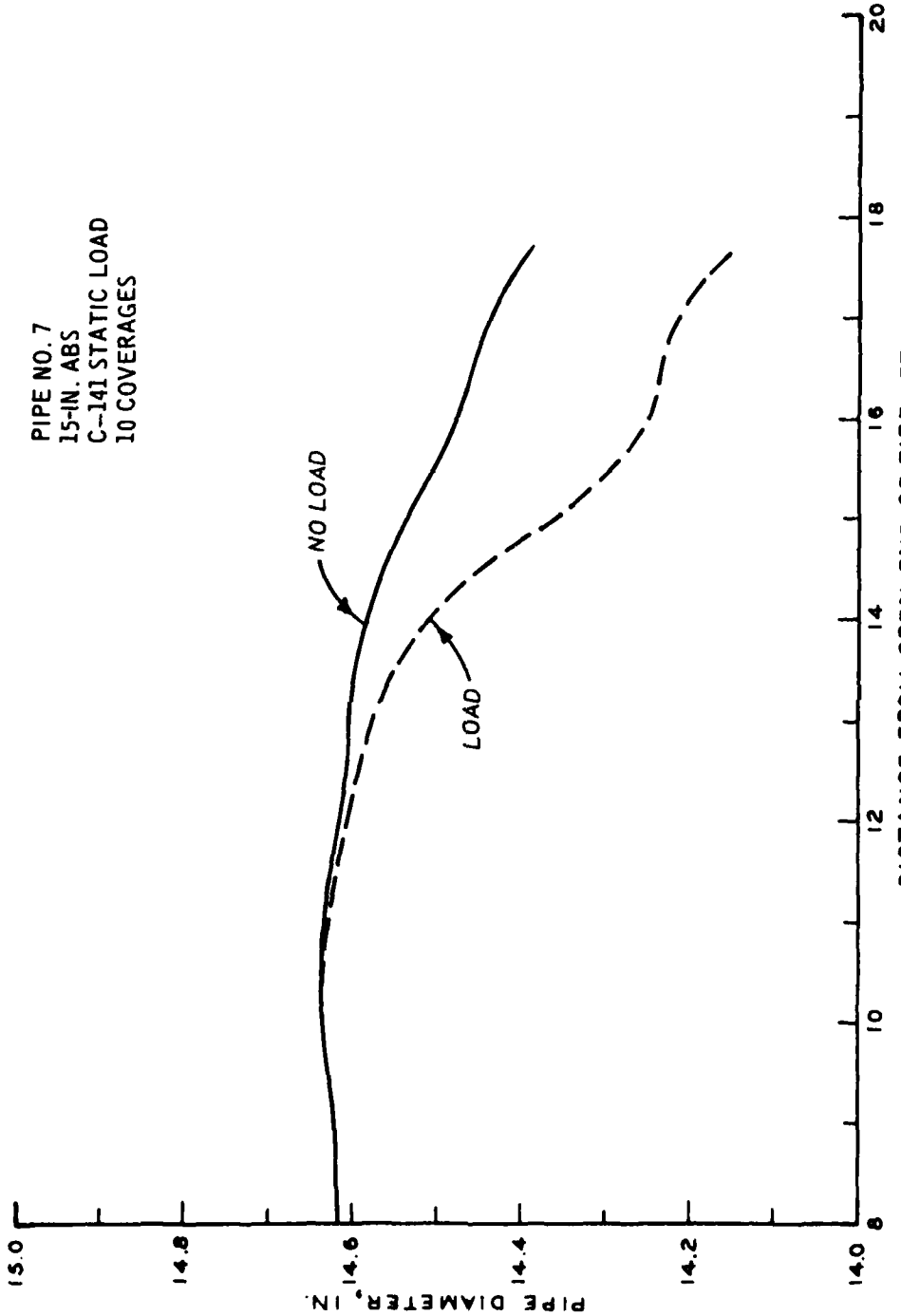

Figure B-22. Measured deflectometer data for pipe No. 7 of Test Site No. 2 (C-141 static load at 10 coverages of C-141 traffic)

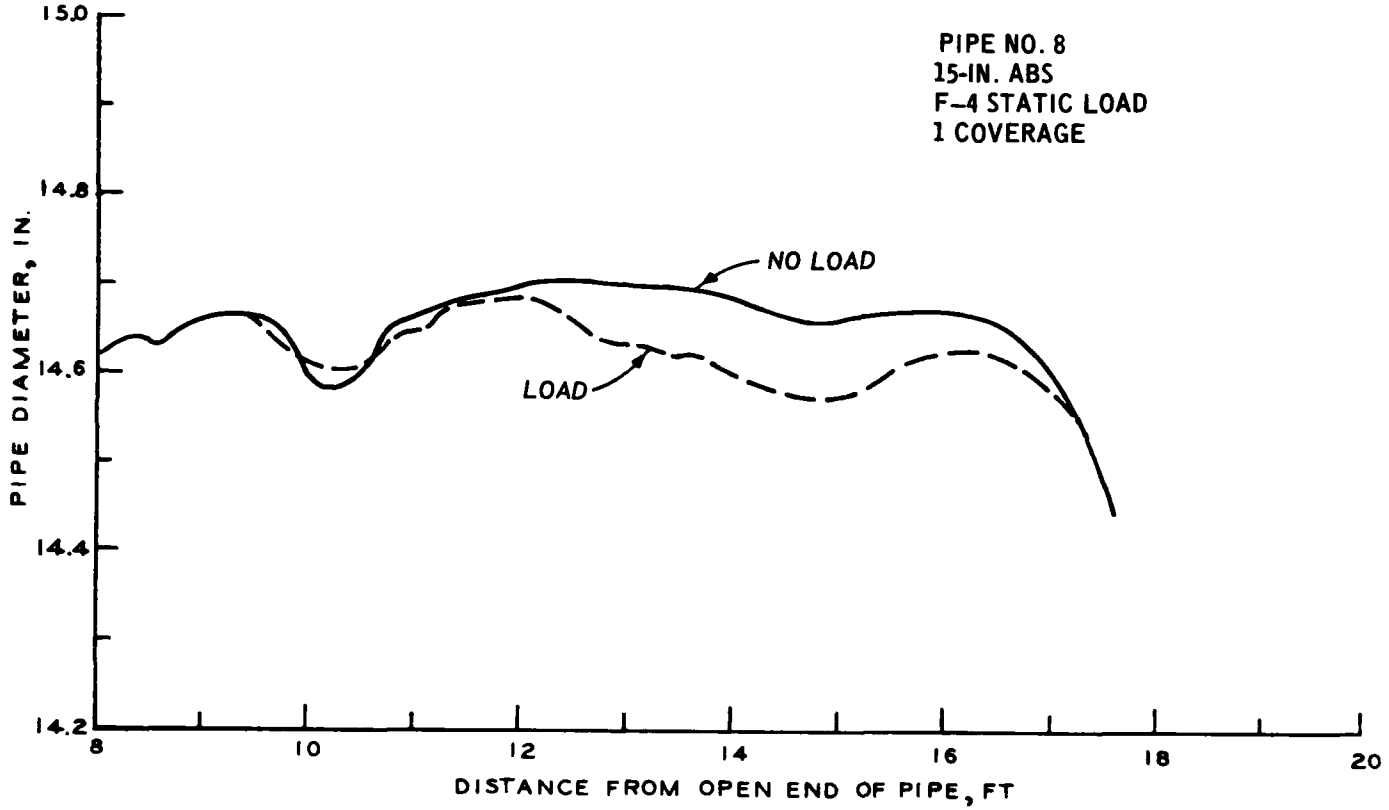

Figure B-23. Measured deflectometer data for pipe No. 8 of Test Site No. 2 (F-4 static load at 1 coverage of F-4 traffic)

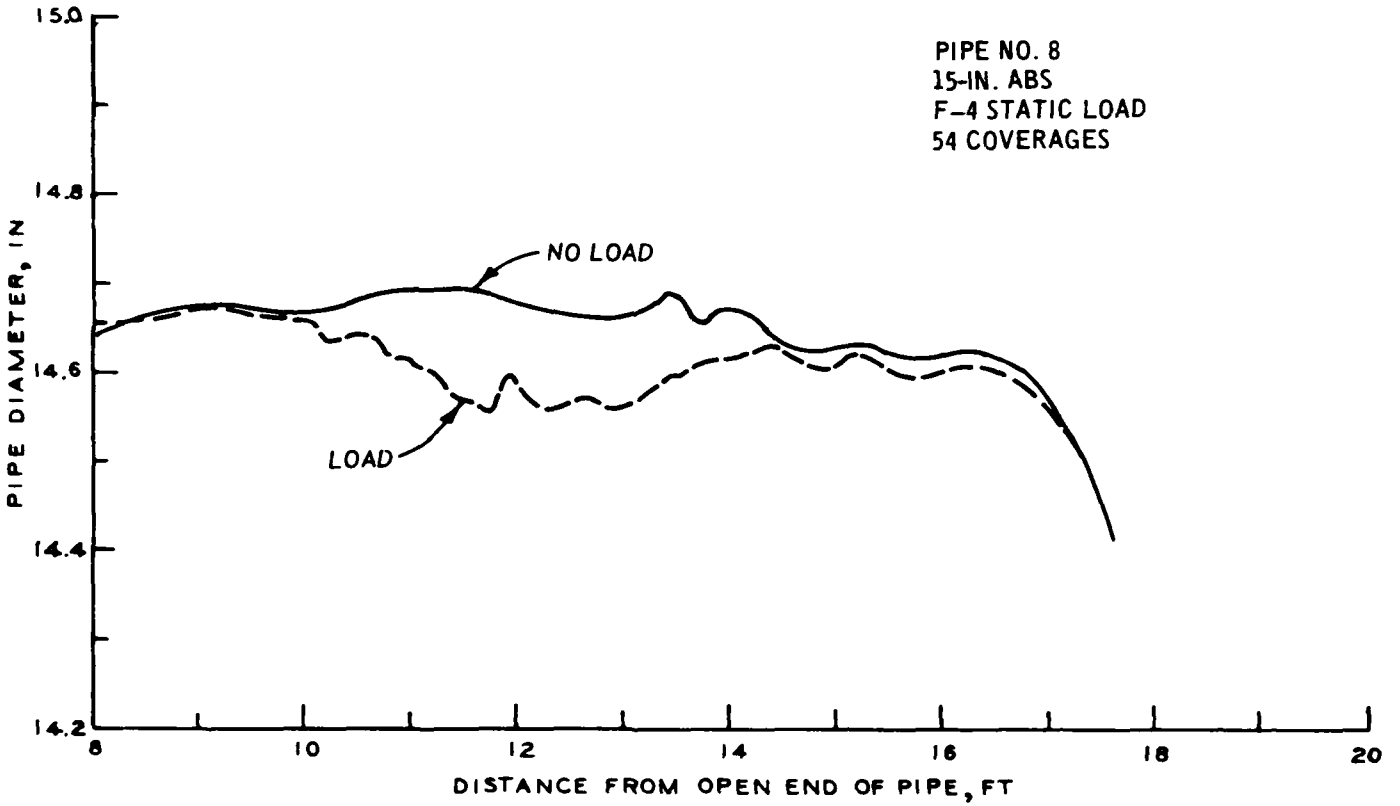

Figure B-24. Measured deflectometer data for pipe No. 8 of Test Site No. 2 (F-4 static load at 54 coverages of F-4 traffic)

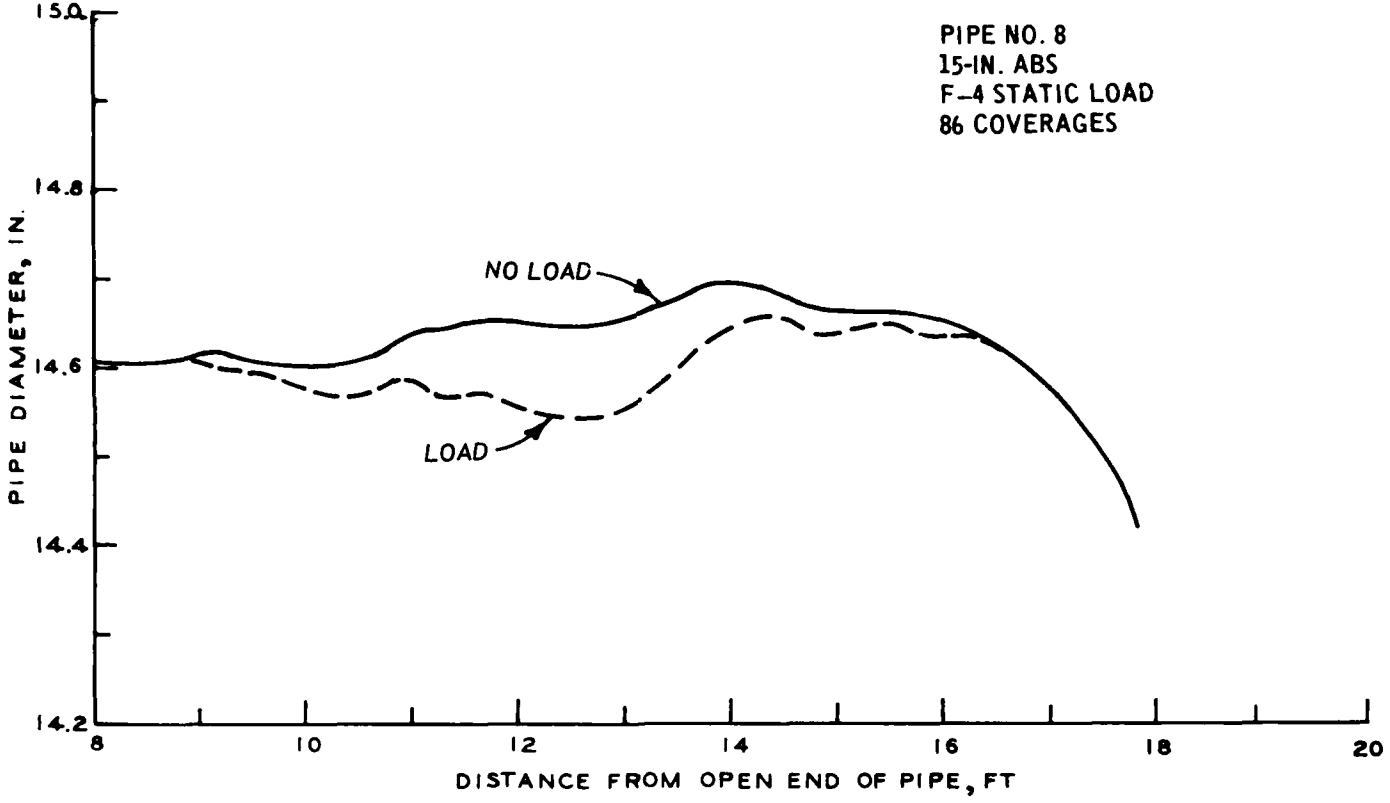

Figure B-25. Measured deflectometer data for pipe No. 8 of Test Site No. 2 (F-4 static load at 86 coverages of F-4 traffic)

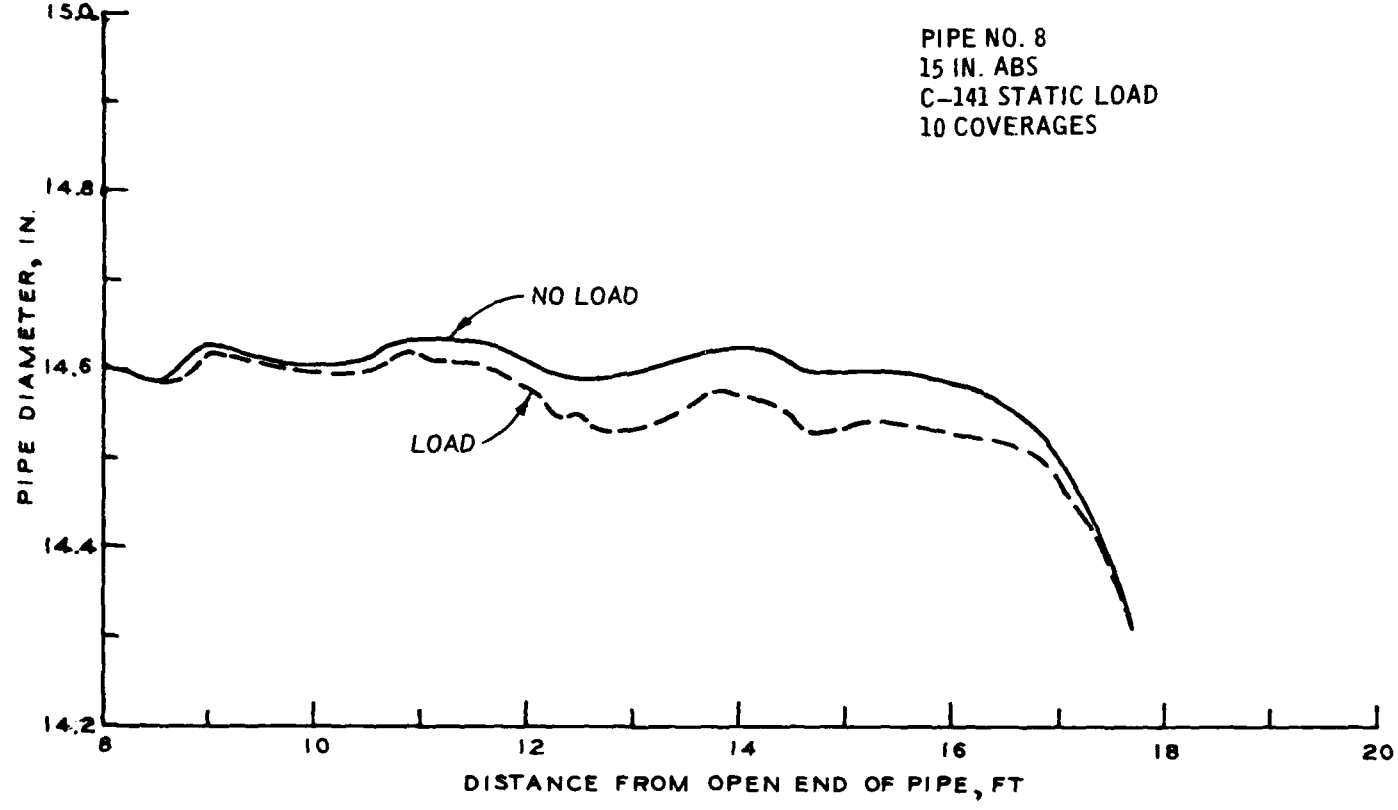

Figure B-26. Measured deflectometer data for pipe No. 8 of Test Site No. 2 (C-141 static load at 10 coverages of C-141 traffic)

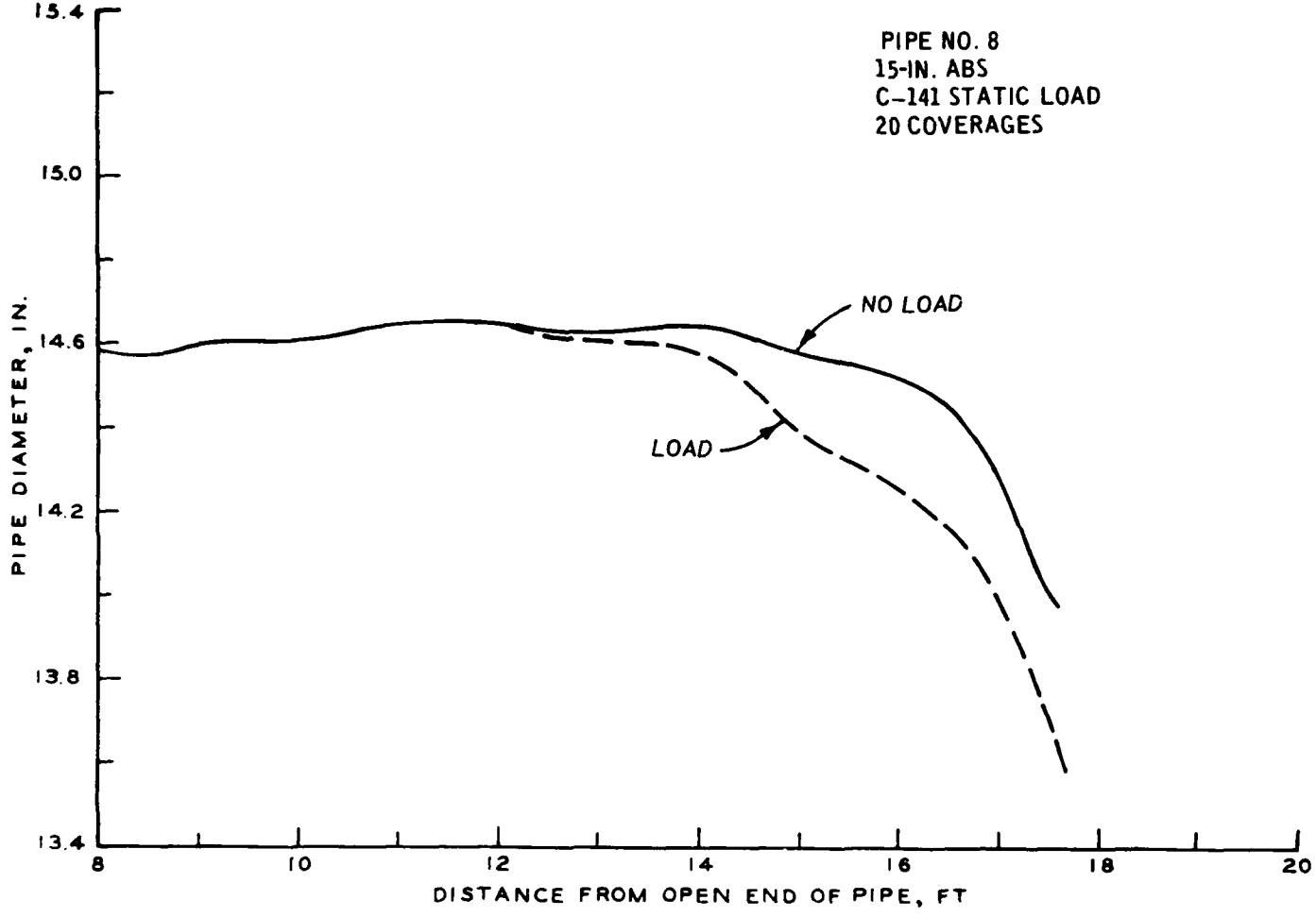

Figure B-27. Measured deflectometer data for pipe No. 8 of Test Site No. 2 (C-141 static load at 20 coverages of C-141 traffic)

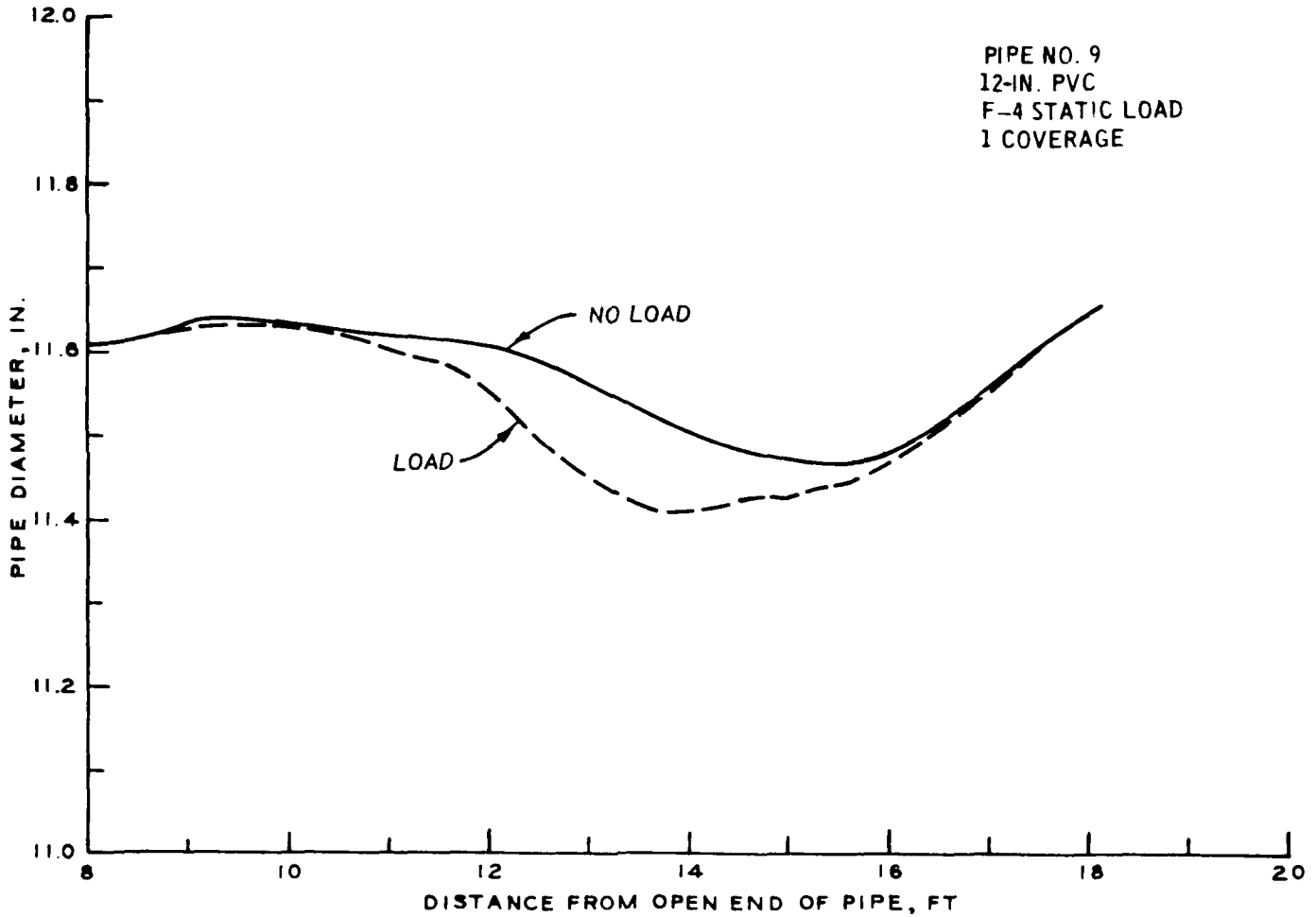

Figure B-28. Measured deflectometer data for pipe No. 9 of Test Site No. 2 (F-4 static load at 1 coverage of F-4 traffic)

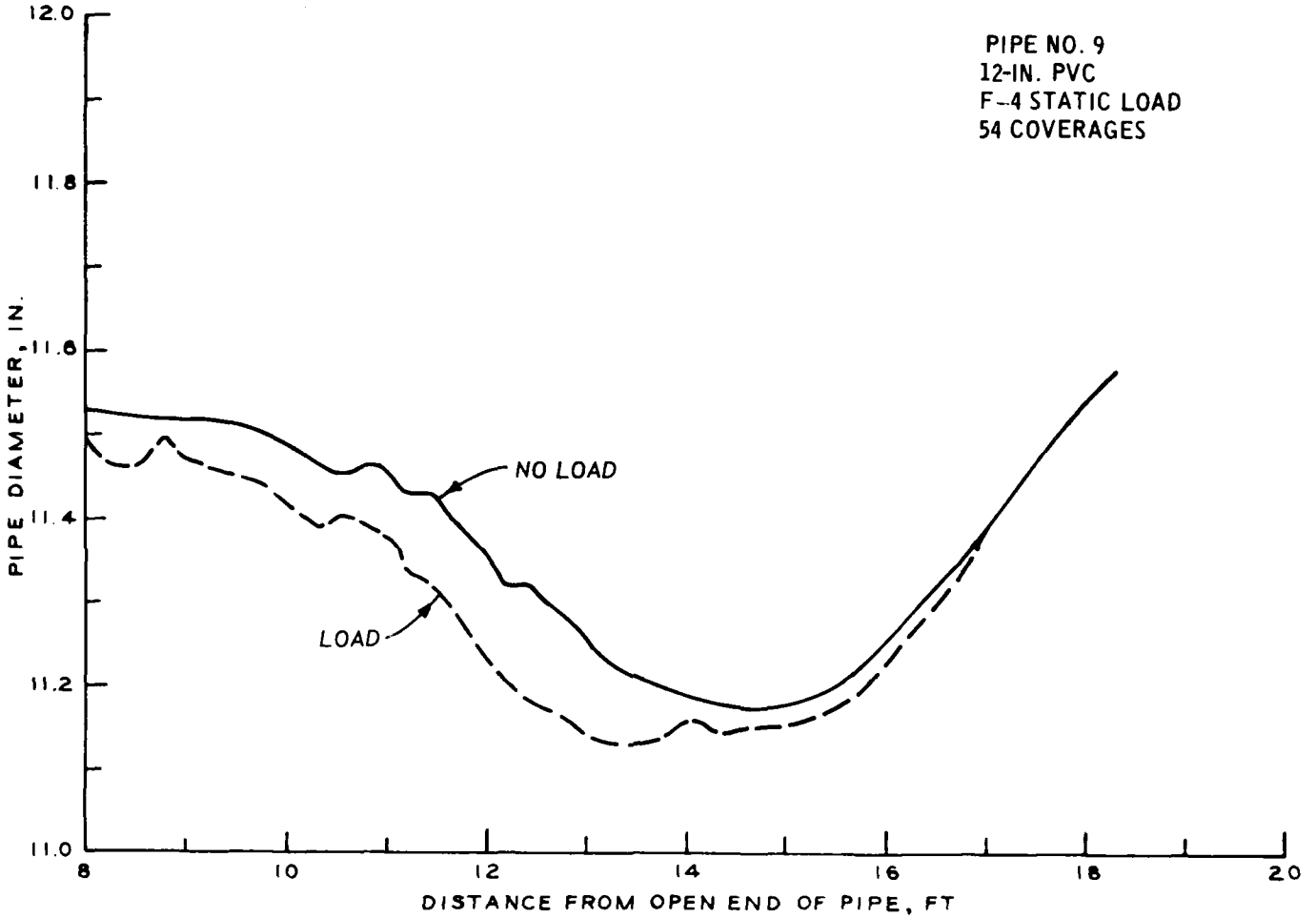

Figure B-29. Measured deflectometer data for pipe No. 9 of Test Site No. 2 (F-4 static load at 54 coverages of F-4 traffic)

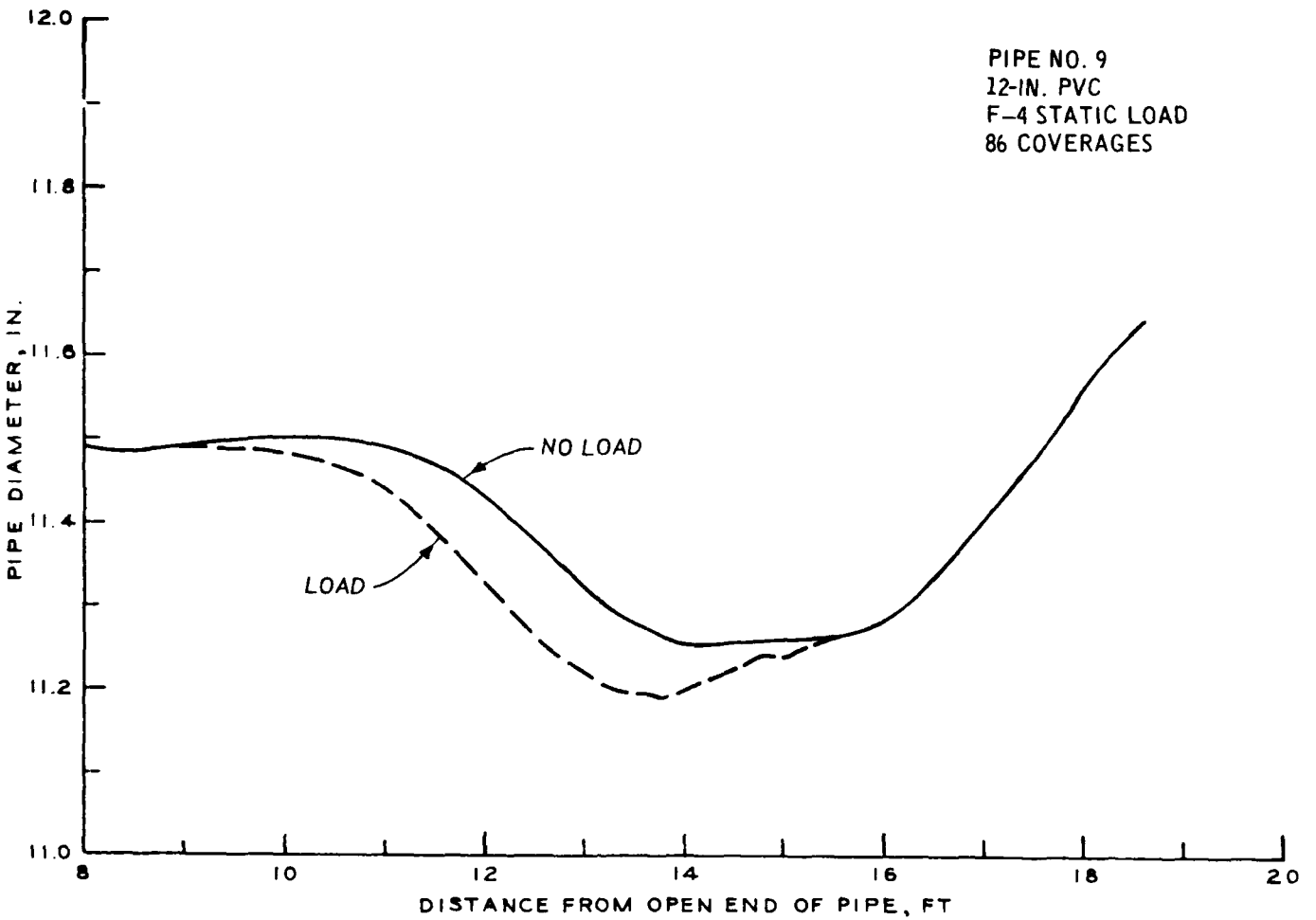

Figure B-30. Measured deflectometer data for pipe No. 9 of Test Site No. 2 (F-4 static load at 86 coverages of F-4 traffic)

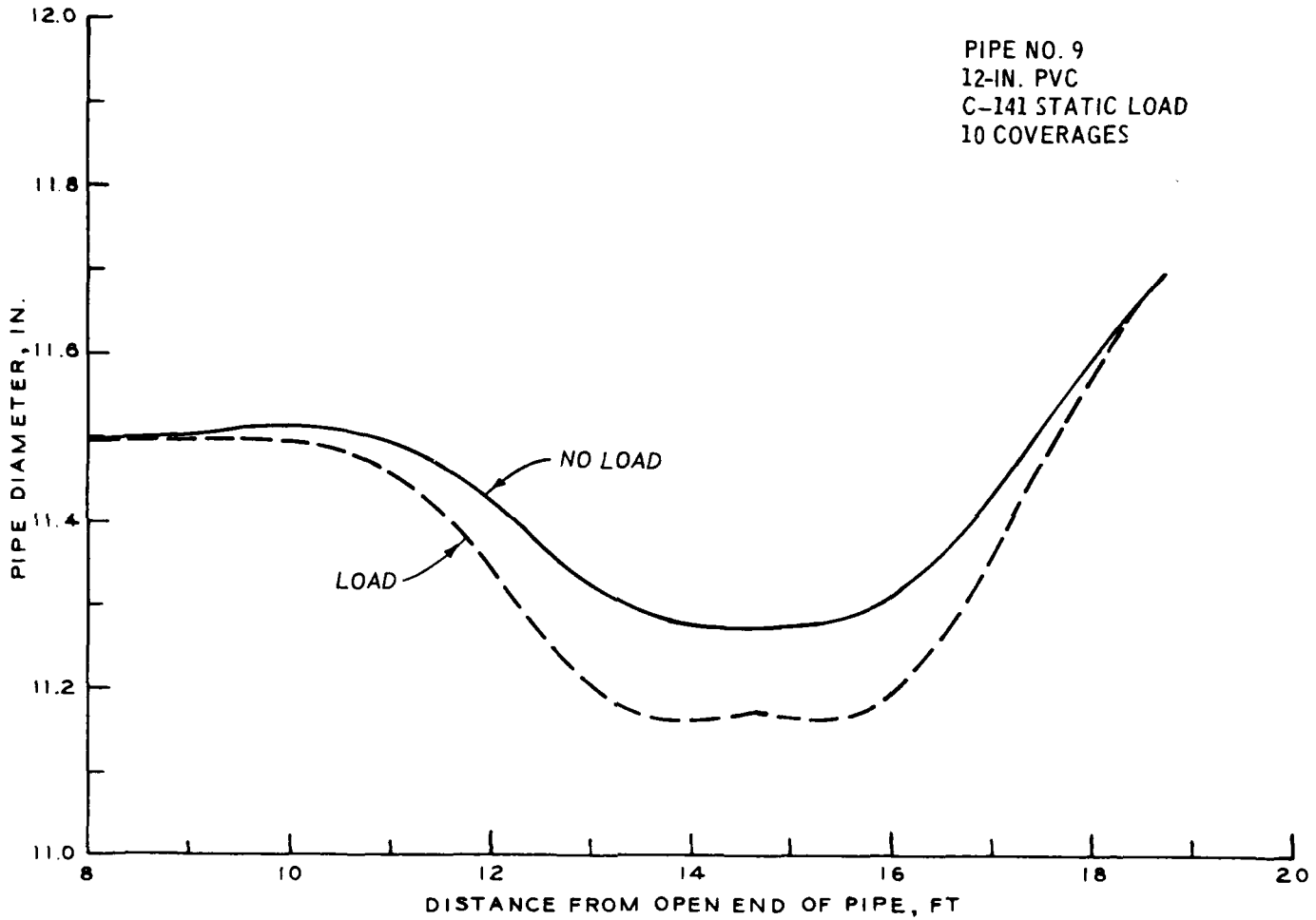

Figure B-31. Measured deflectometer data for pipe No. 9 of Test Site No. 2 (C-141 static load at 10 coverages of C-141 traffic)

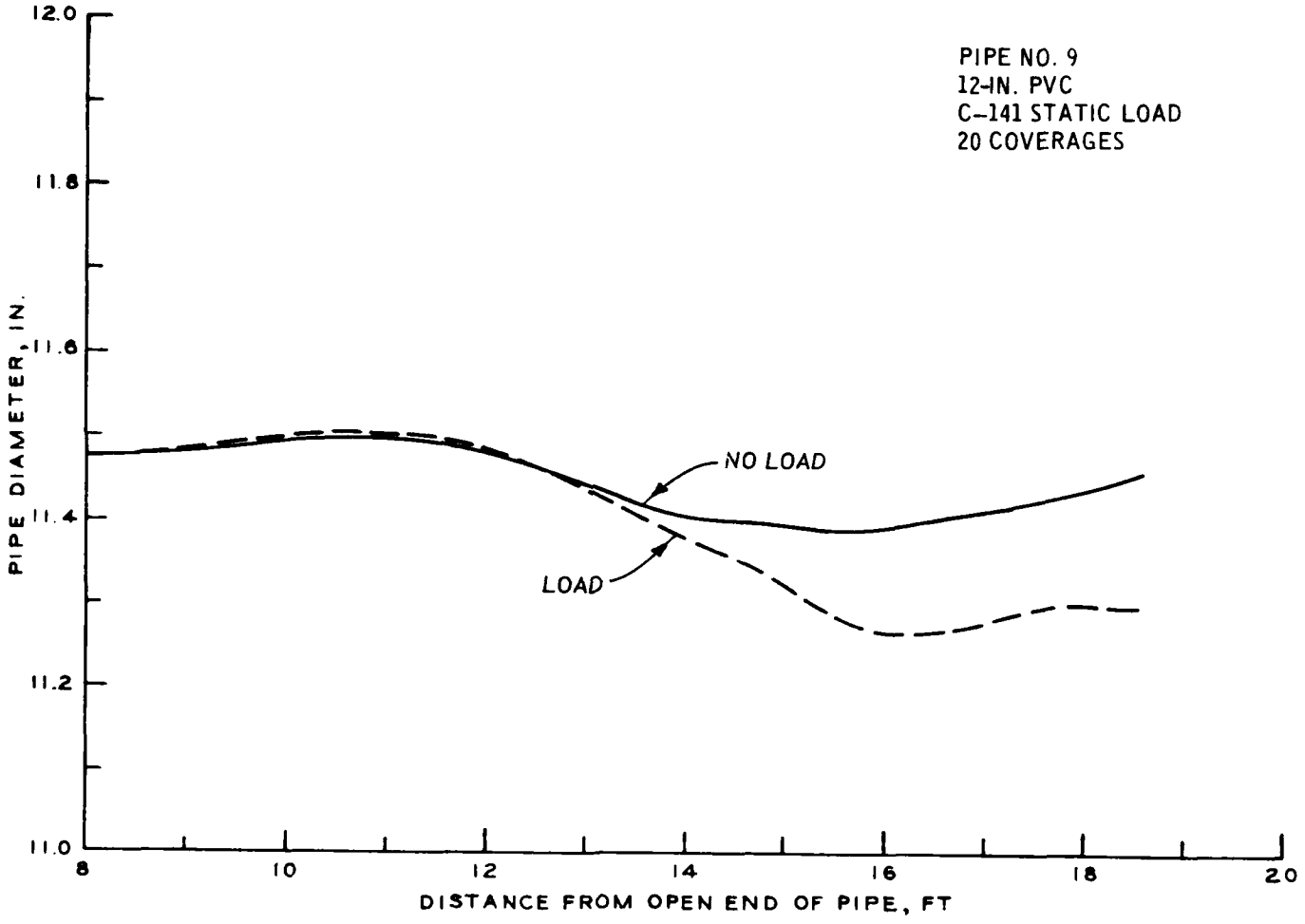

Figure B-32. Measured deflectometer data for pipe No. 9 of Test Site No. 2 (C-141 static load at 20 coverages of C-141 traffic)

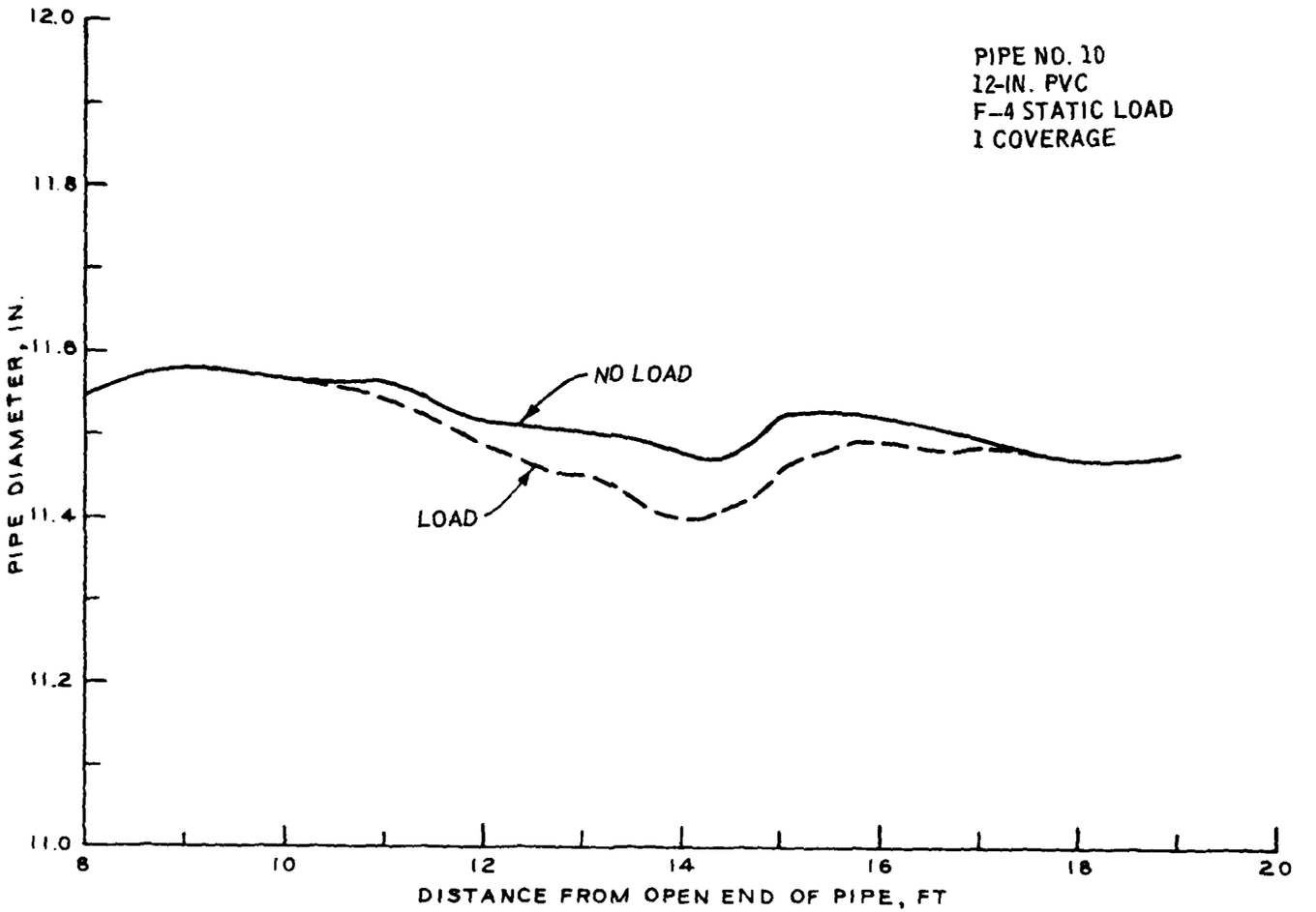

Figure B-33. Measured deflectometer data for pipe No. 10 of Test Site No. 2 (F-4 static load at 1 coverage of F-4 traffic)

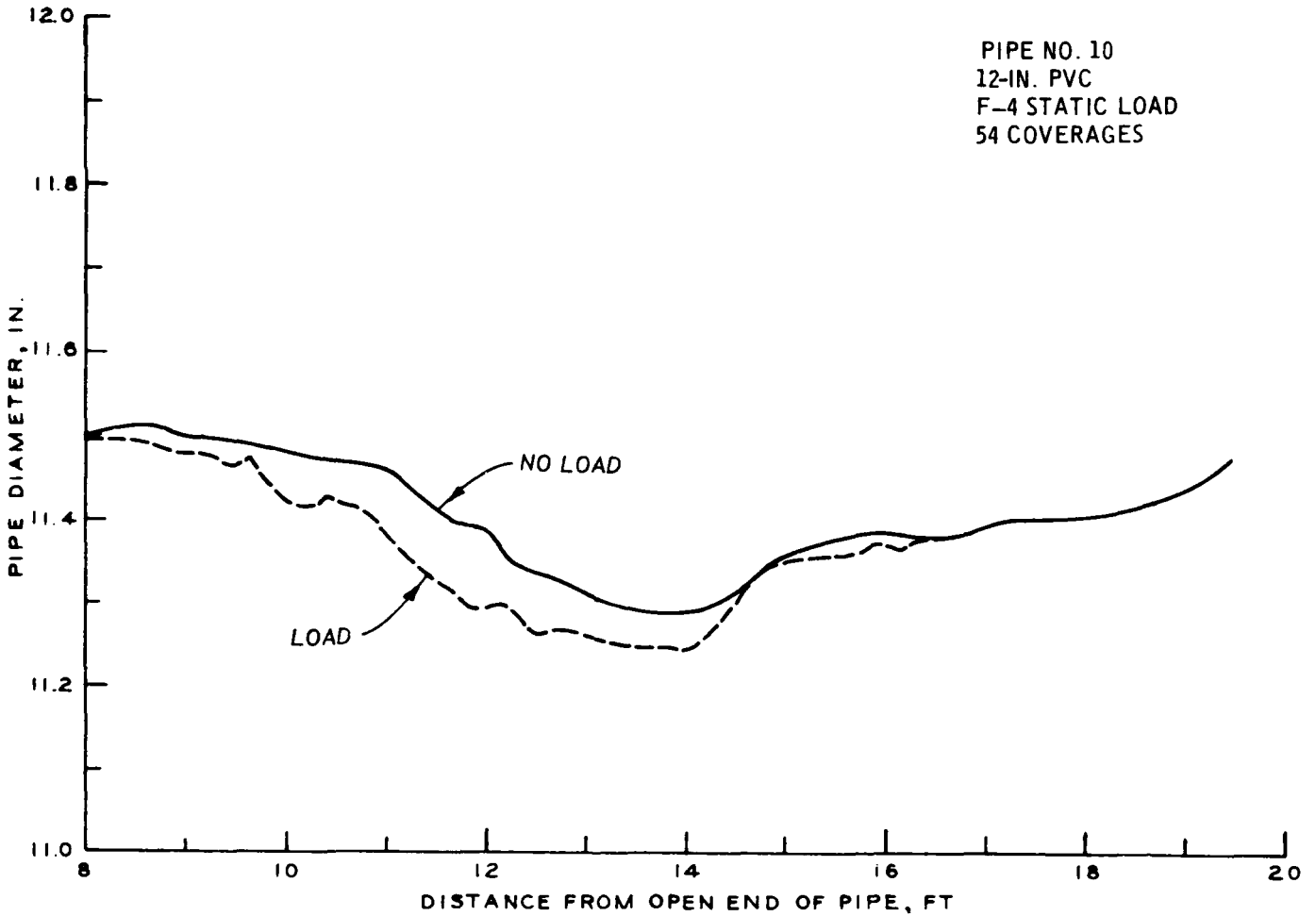

Figure B-34. Measured deflectometer data for pipe No. 10 of Test Site No. 2 (F-4 static load at 54 coverages of F-4 traffic)

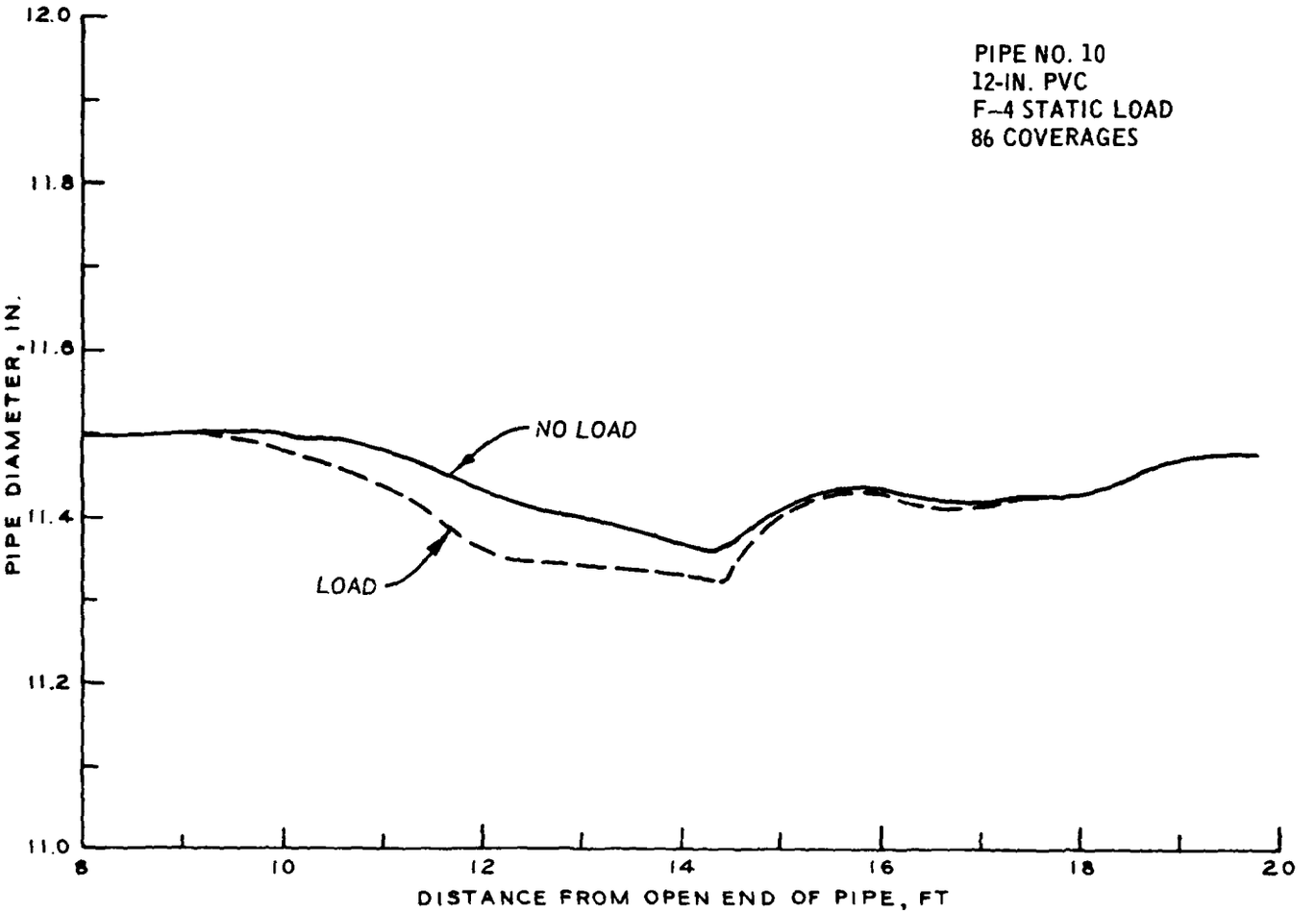

Figure B-35. Measured deflectometer data for pipe No. 10 of Test Site No. 2 (F-4 static load at 86 coverages of F-4 traffic)

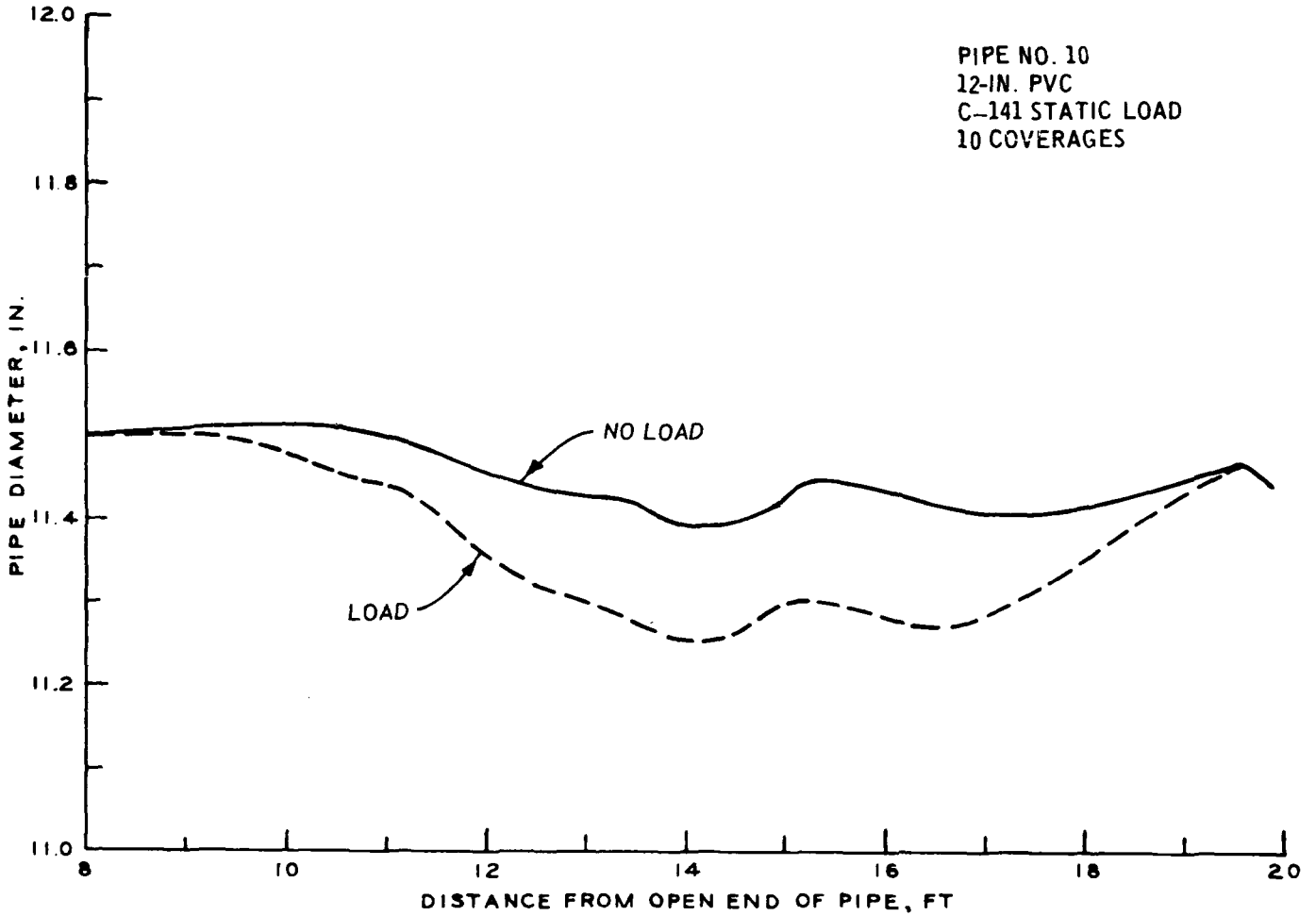

Figure B-36. Measured deflectometer data for pipe No. 10 of Test Site No. 2 (C-141 static load at 10 coverages of C-141 traffic)

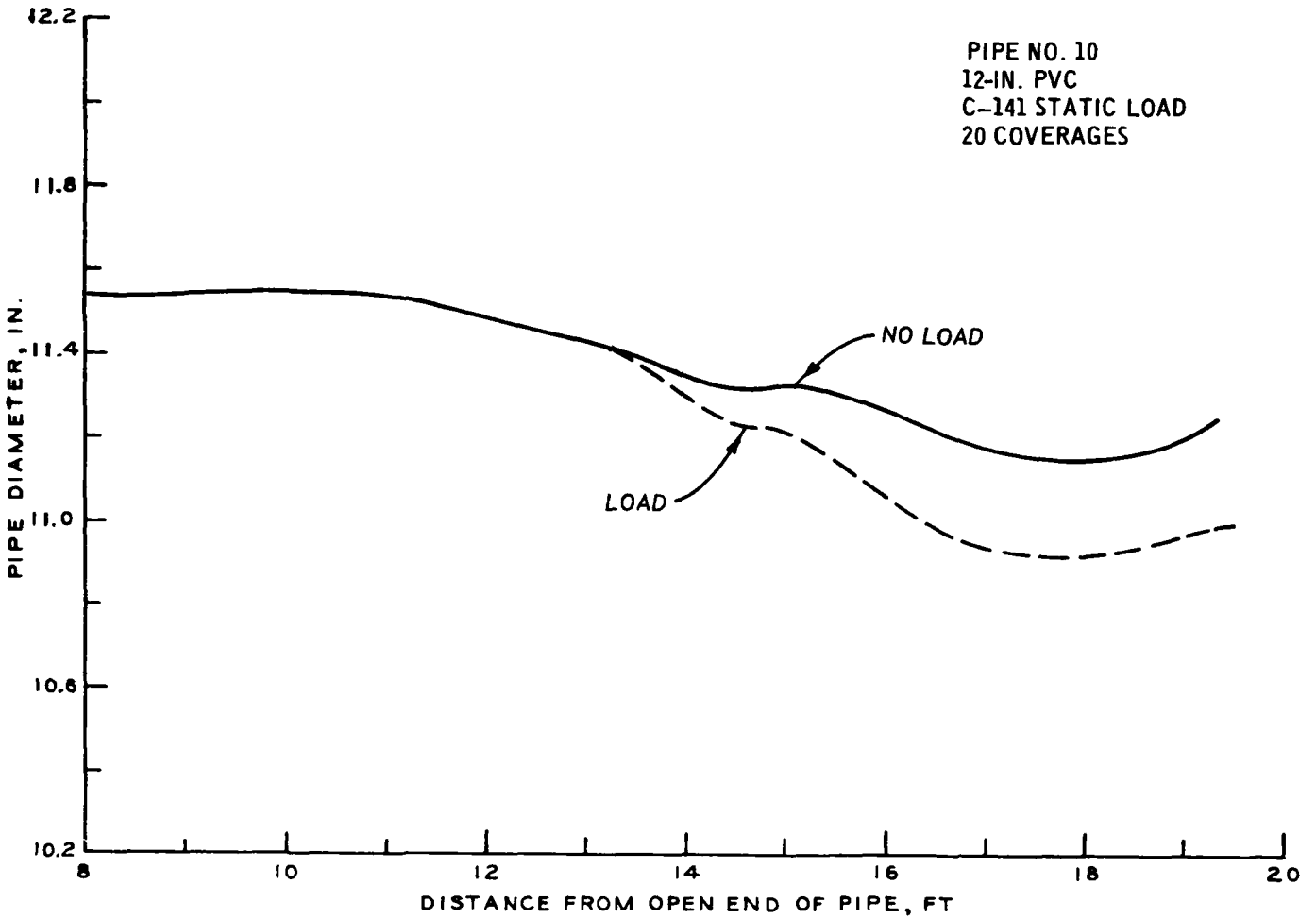

Figure B-37. Measured deflectometer data for pipe No. 10 of Test Site No. 2 (C-141 static load at 20 coverages of C-141 traffic)

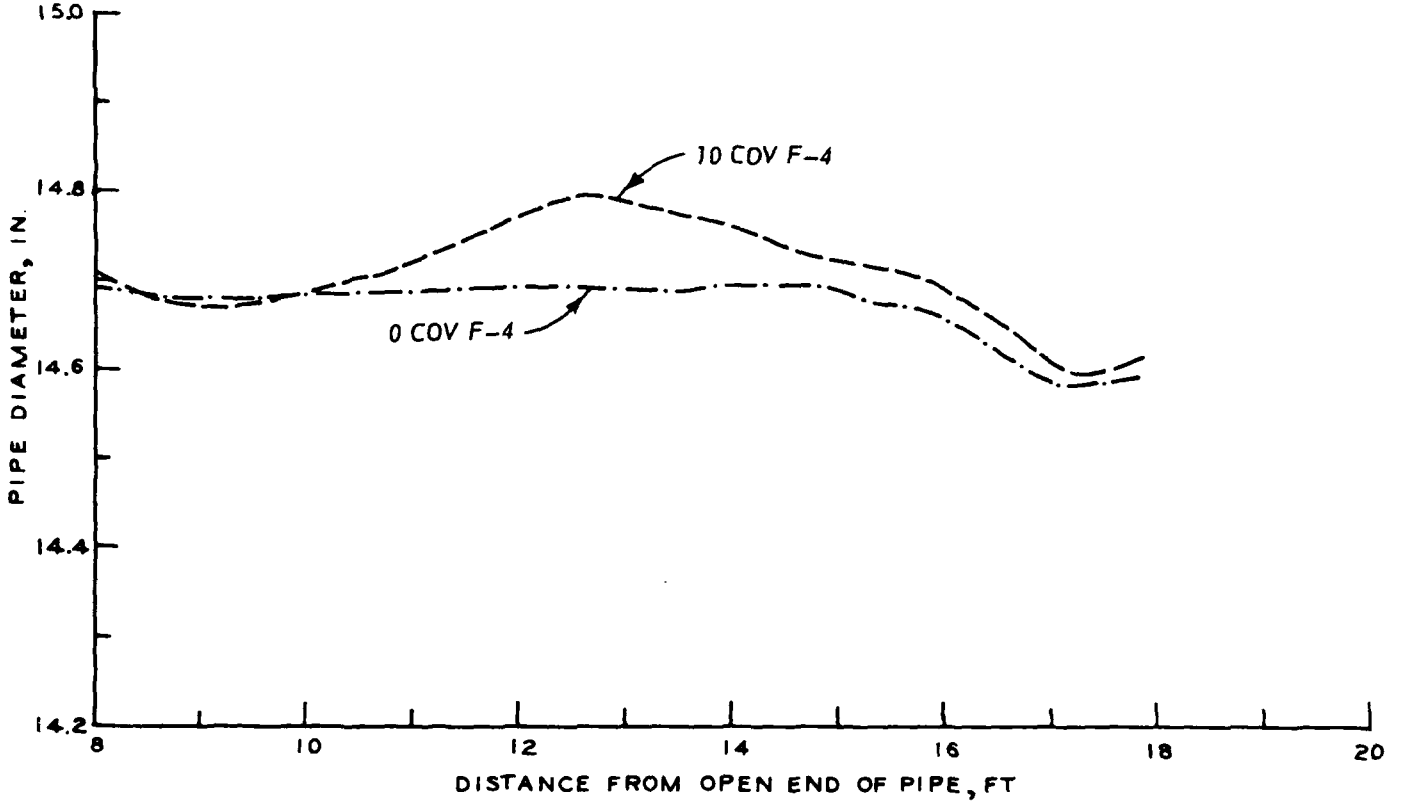

Figure B-38. Comparison of permanent deflection in pipe No. 1 of Test Site No. 2 after 10 coverages with the initial deflection (15-in. ABS with 15.5-in. depth of cover)

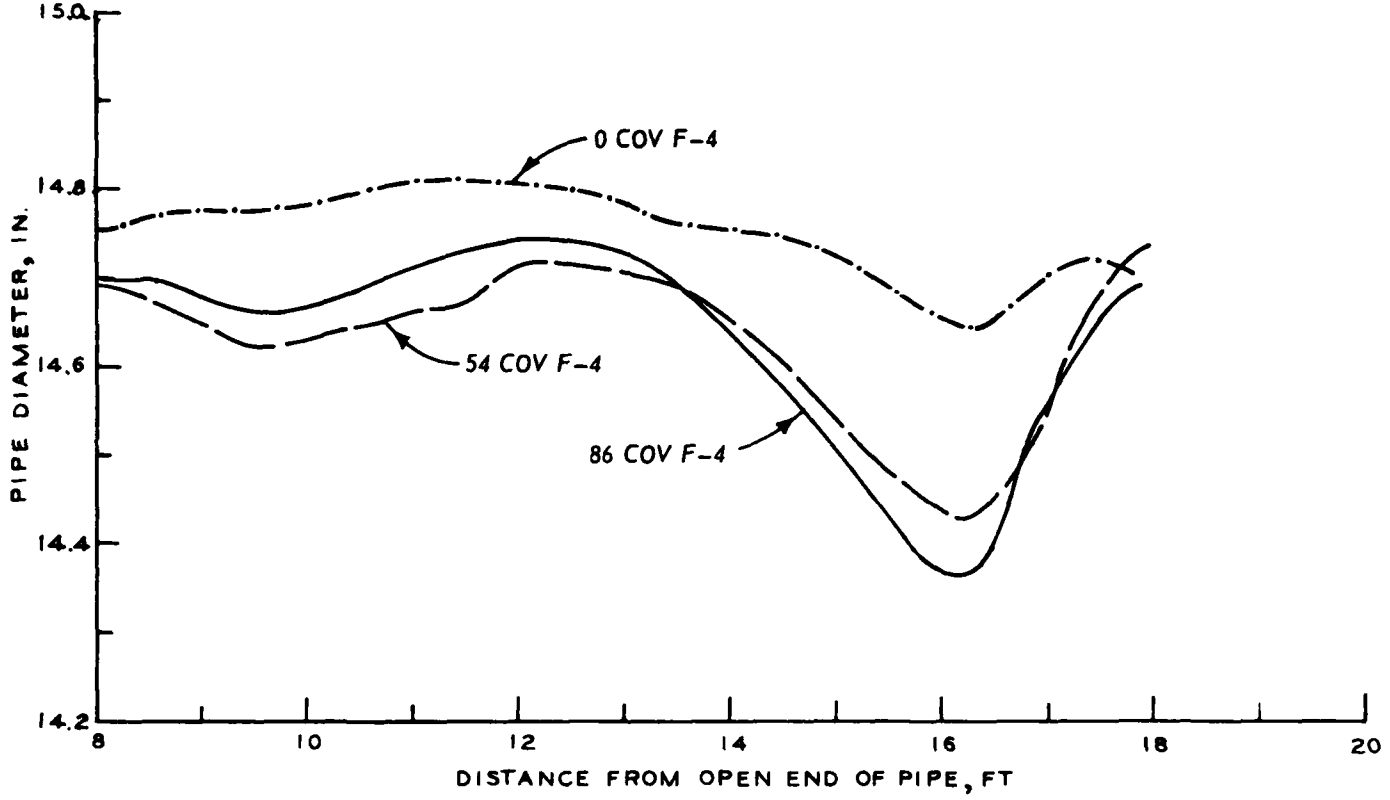

Figure B-39. Comparison of permanent deflection of pipe No. 2 of Test Site No. 2 at different coverage levels of F-4 traffic (15-in. ABS with 20.5-in. depth of cover)

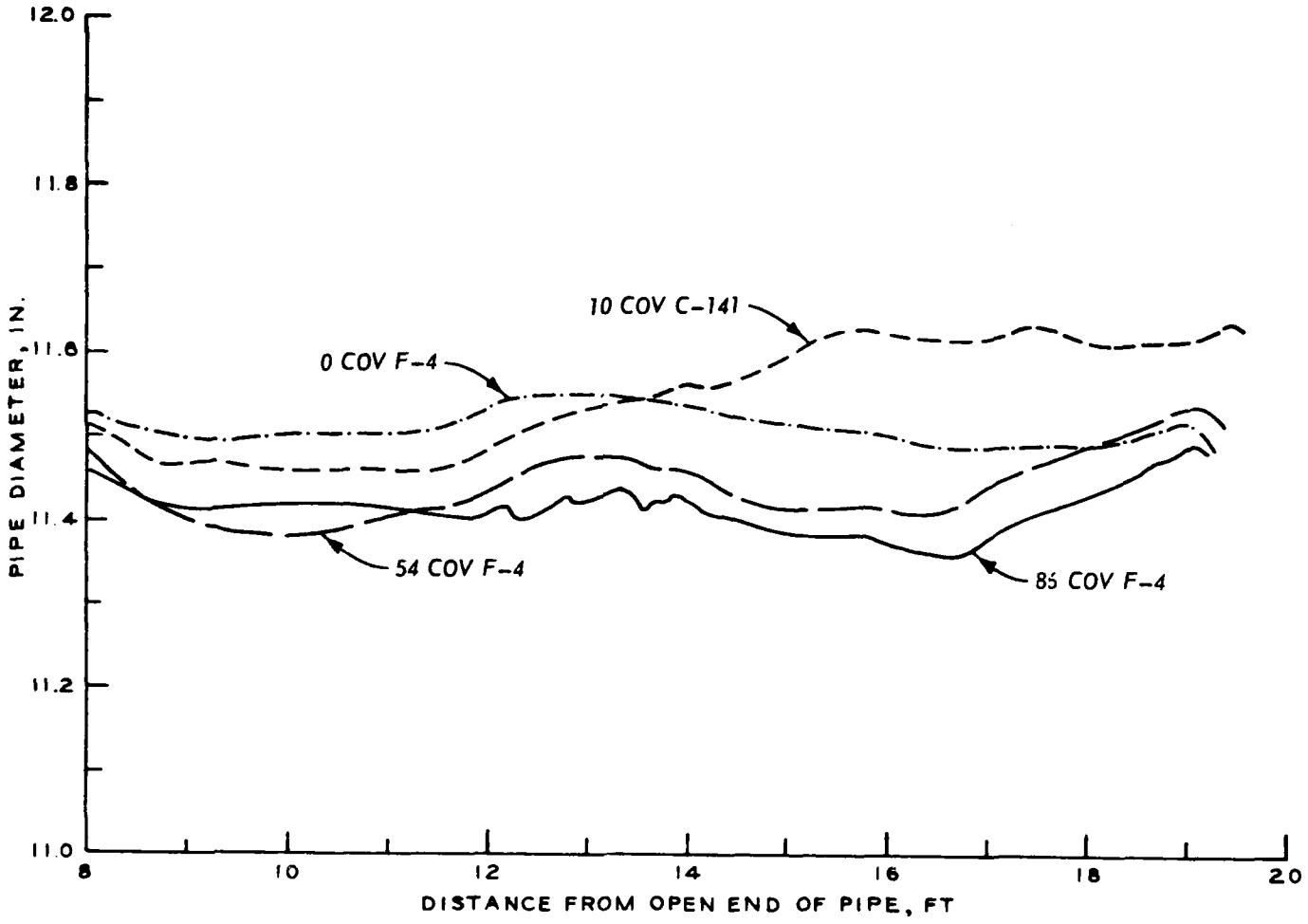

Figure B-40. Comparison of permanent deflection of pipe No. 3 of Test Site No. 2 at different coverage levels of F-4 and C-141 traffic (12-in. PVC with 17-in. depth of cover)

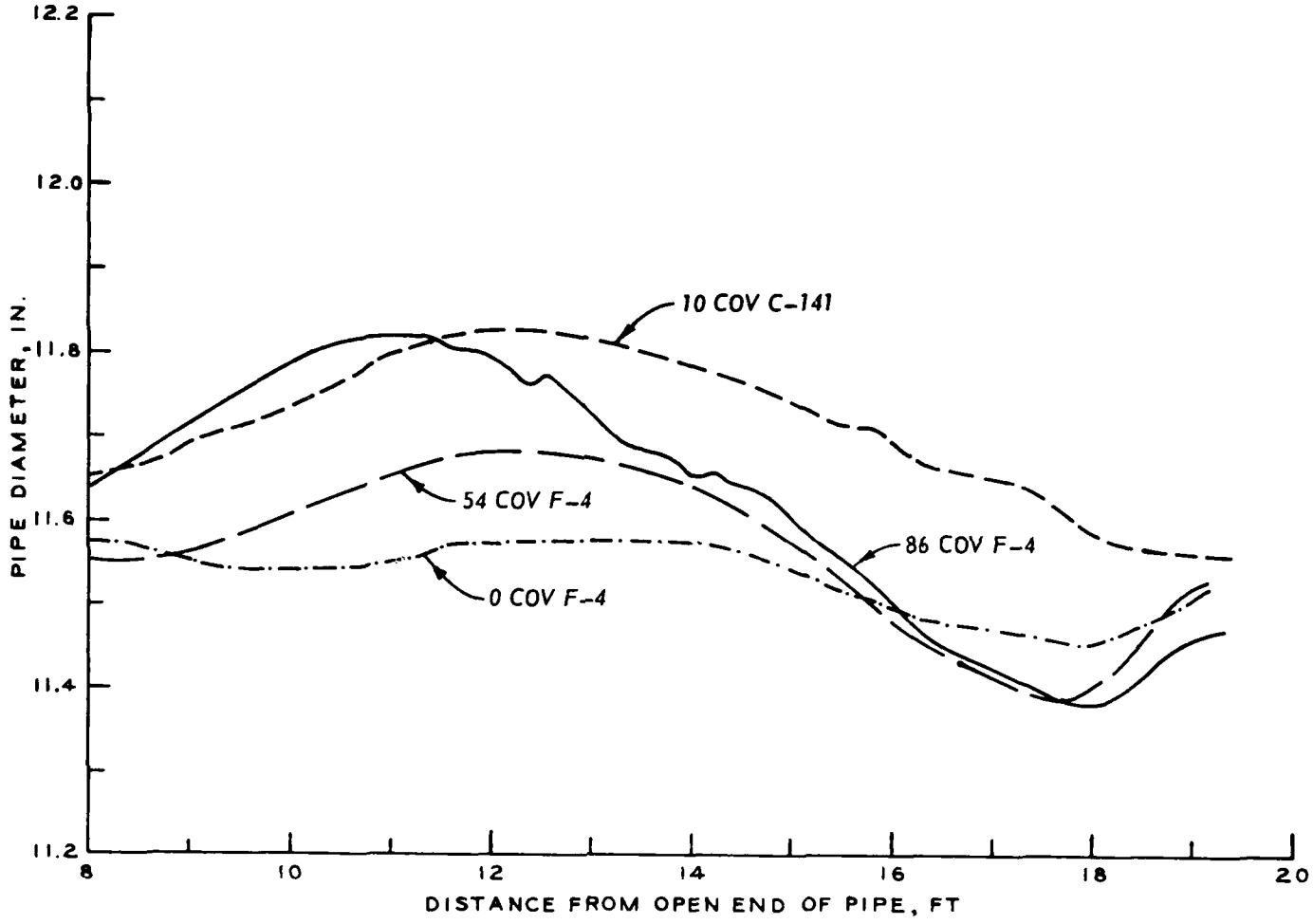

Figure B-41. Comparison of permanent deflection of pipe No. 4 of Test Site No. 2 at different coverage levels of F-4 and C-141 traffic (12-in. PVC with 20.5-in. depth of cover)

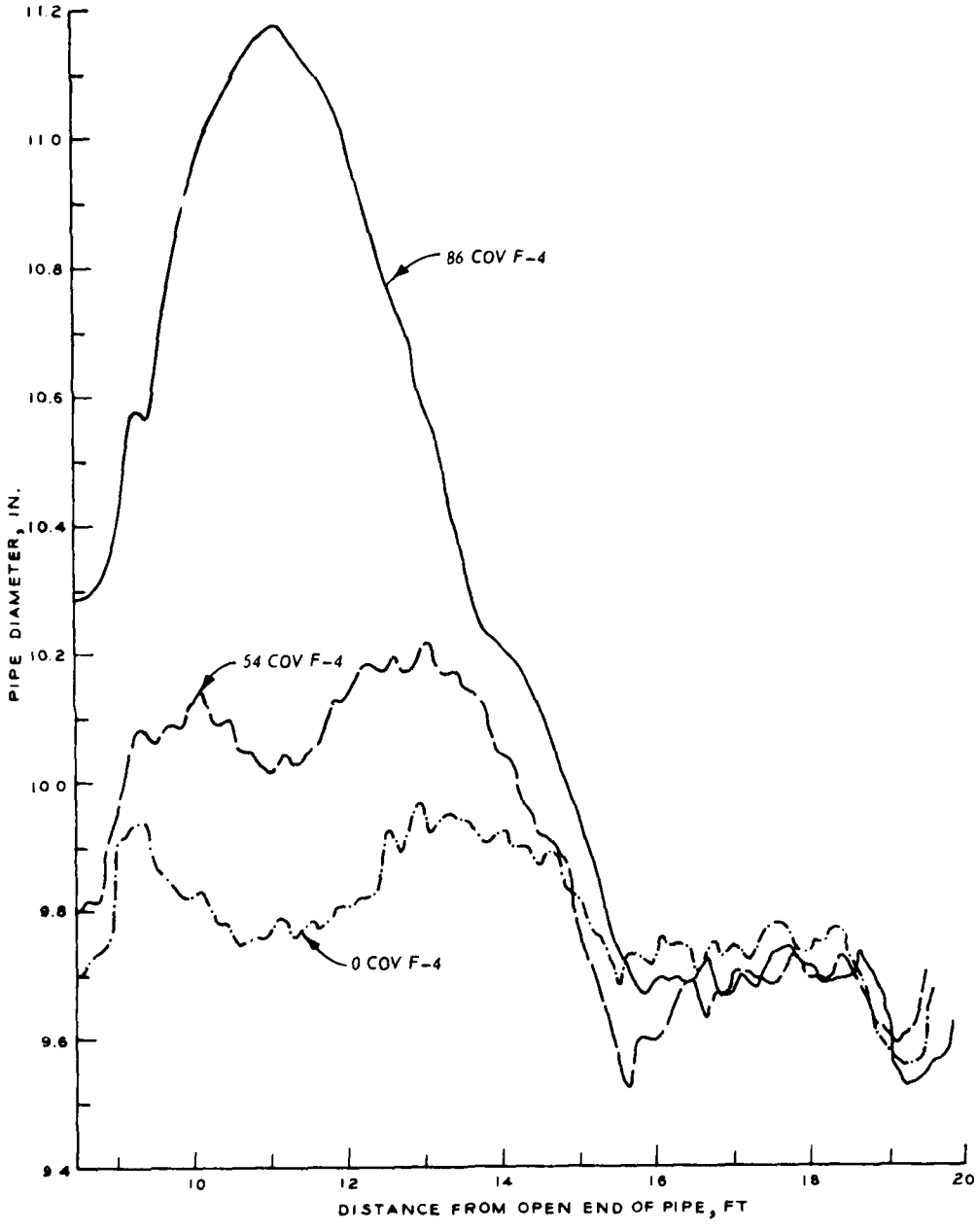

B-42. Comparison of permanent deflection of pipe No. 5 of Test Site No. 2 at different coverage levels of F-4 traffic (10 PE at 15-in.. depth of cover)

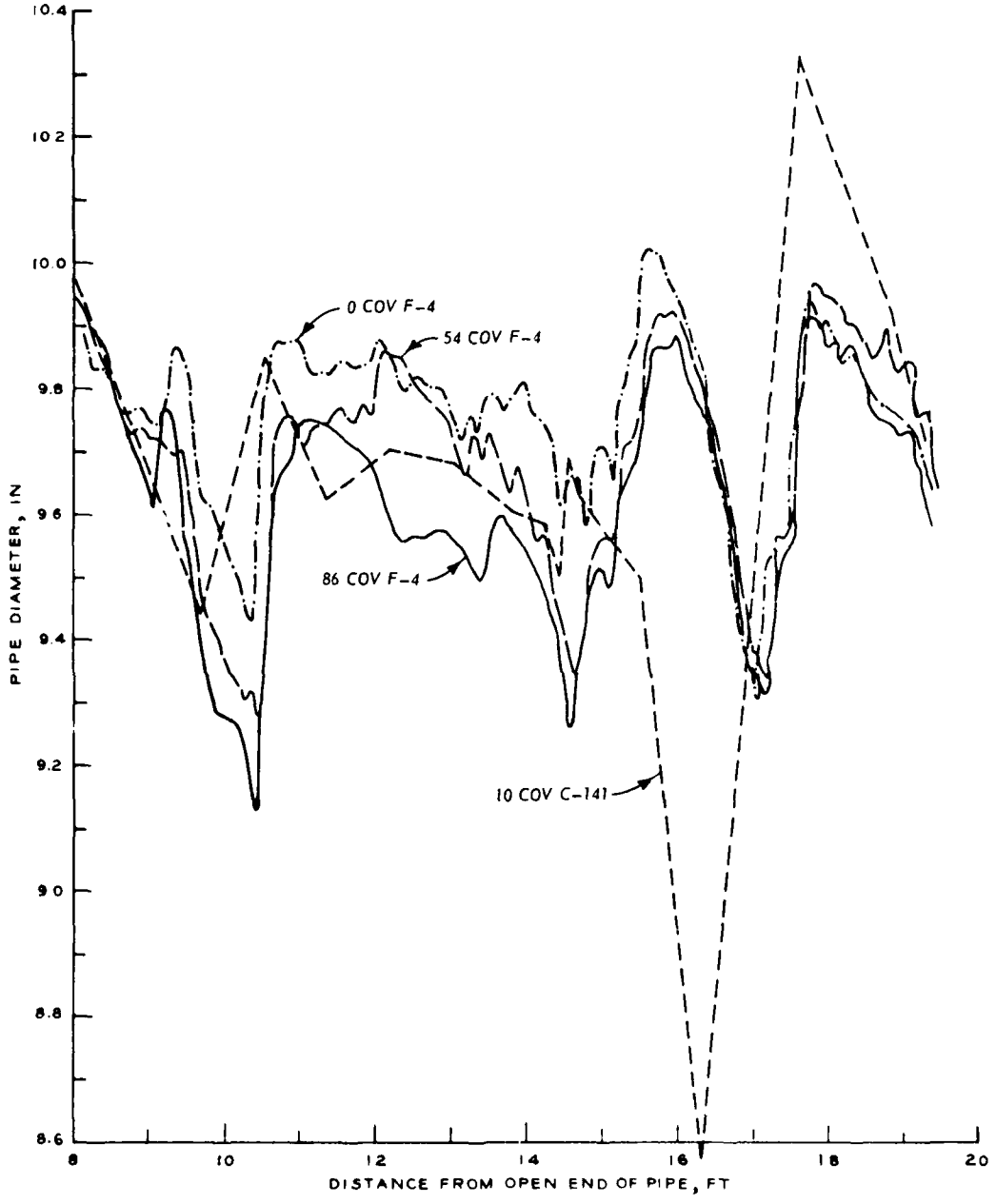

Figure B-43. Comparison of permanent deflections of pipe No. 6 of Test Site No. 2 at different levels of F-4 and C-141 traffic (10-in. PE at 18-in. depth of cover)

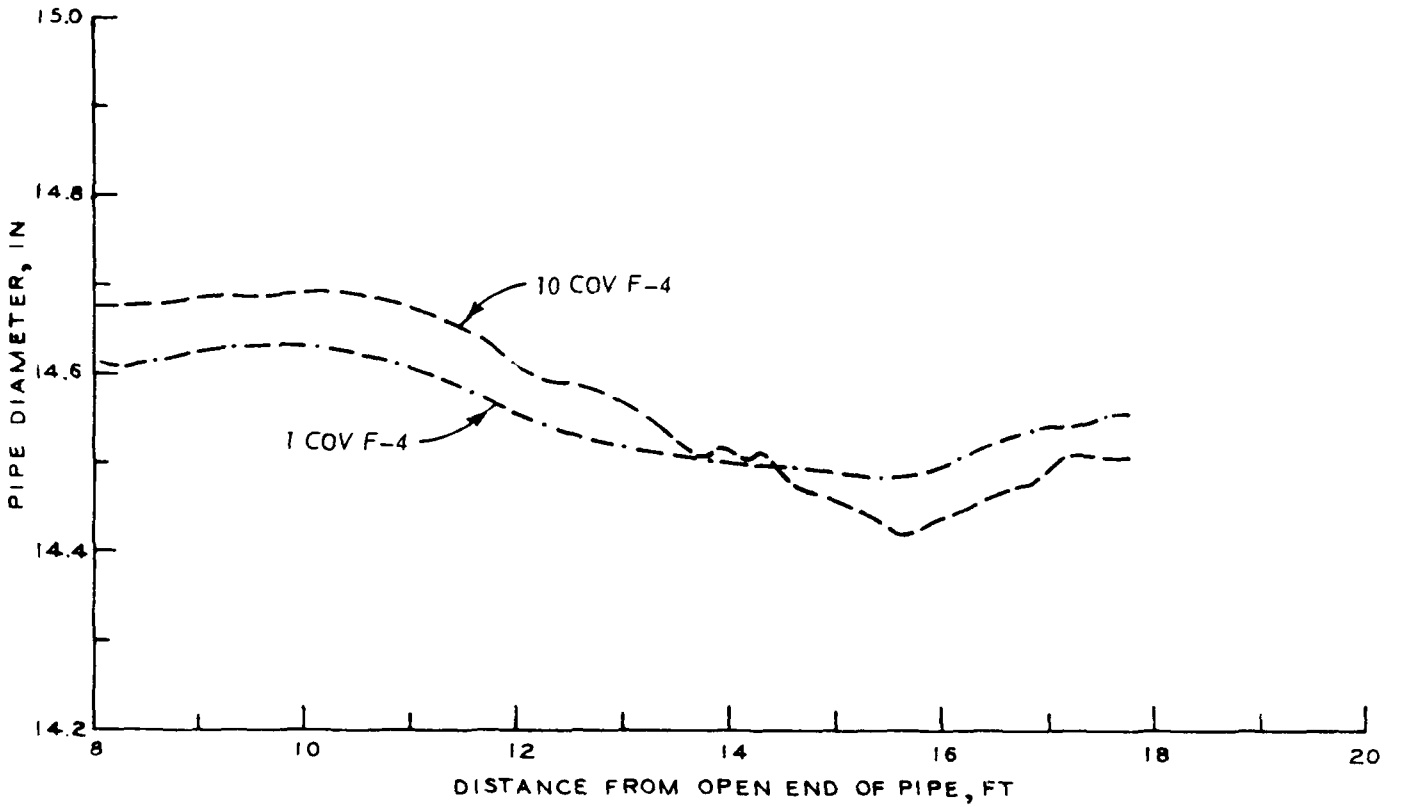

Figure B-44. Comparison of permanent deflections of pipe No. 7 of Test Site No. 2 at different levels of F-4 traffic (15-in. ABS at 24-in. depth of cover)

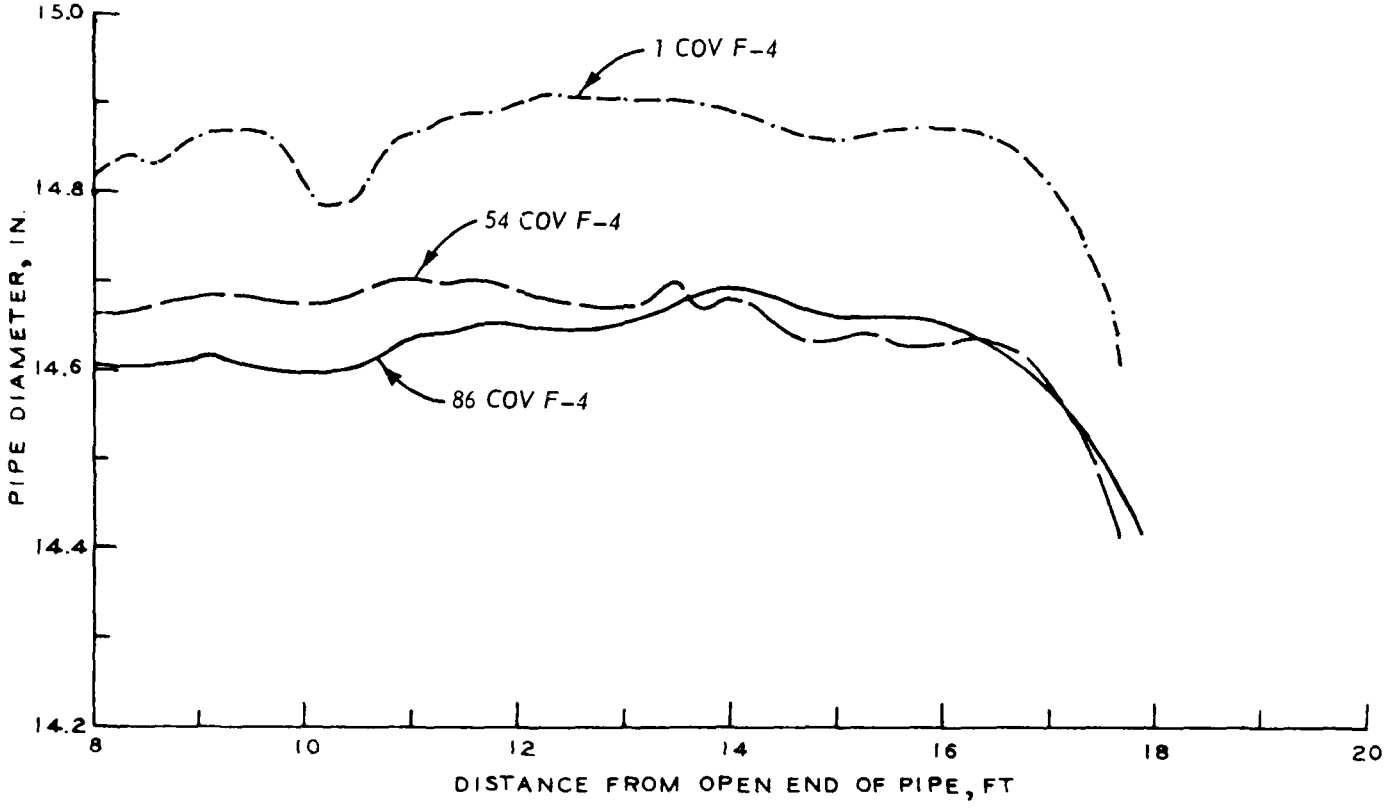

Figure B-45. Comparison of permanent deflection of pipe No. 8 at different levels of F-4 traffic (15-in. ABS at 28-in. depth of cover)

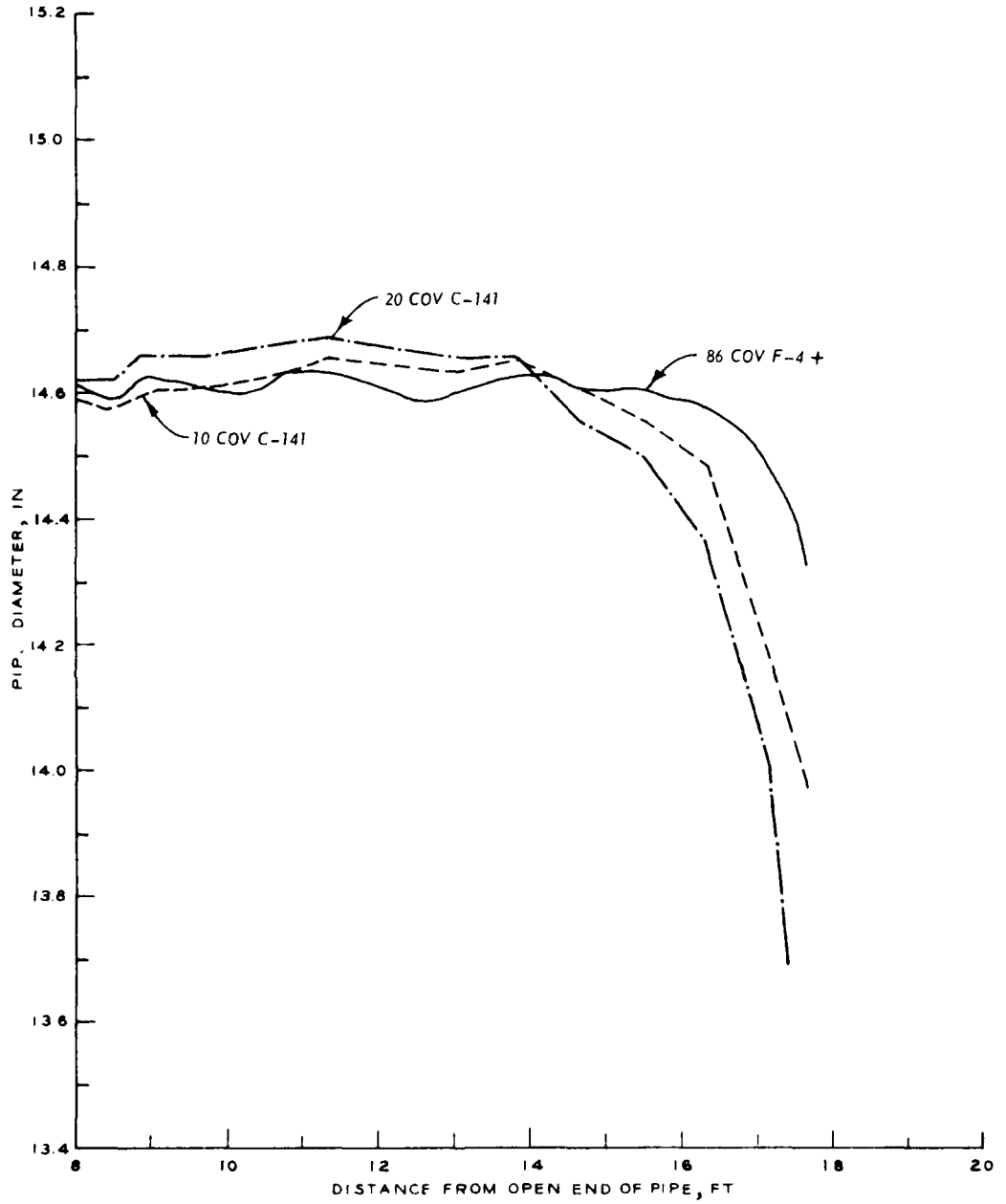

Figure B-46. Comparison of permanent deflection of pipe No. 8 of Test Site No. 2 at different levels of C-141 traffic (15-in. ABS at 28-in. depth of cover)

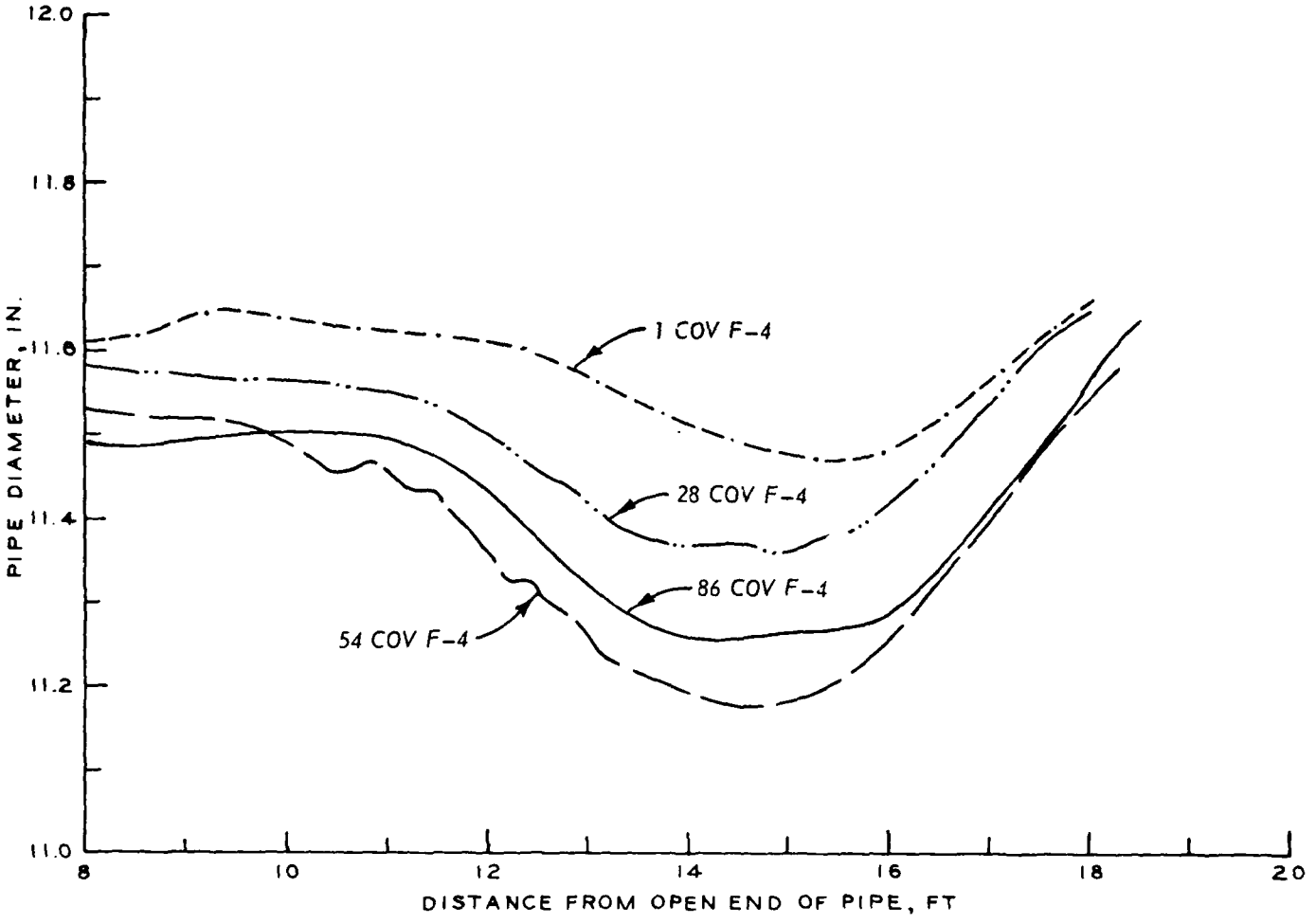

Figure B-47. Comparison of permanent deflection of pipe No. 9 of Test Site No. 2 at different levels of F-4 traffic (12-in. PVC at 24-in. depth of cover)

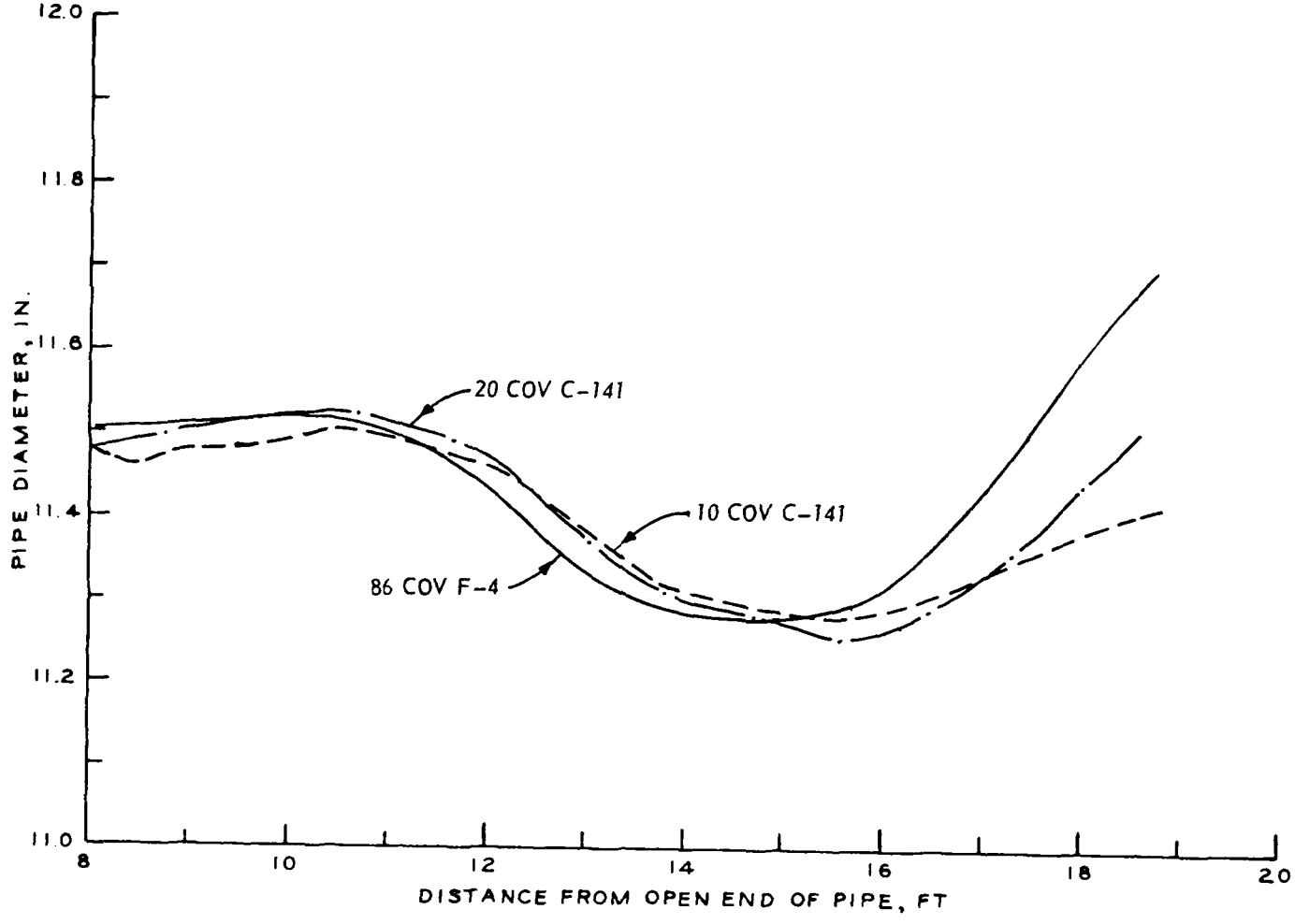

Figure B-48. Comparison of permanent deflections of pipe No. 9 of Test Site No. 2 at different levels of C-141 traffic (12-in. PVC at 24-in. depth of cover)

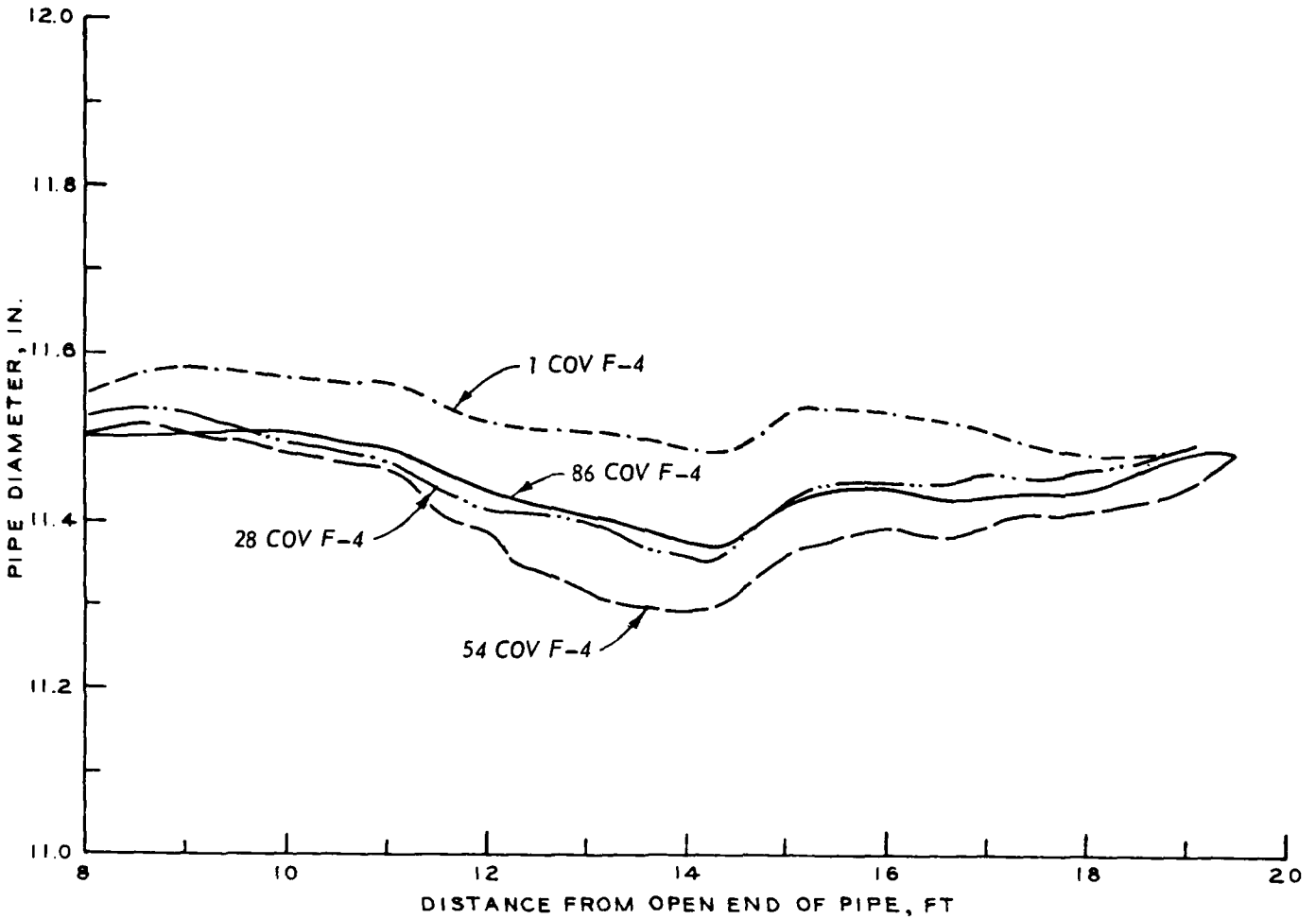

Figure B-49. Comparison of permanent deflections of pipe No. 10 of Test Site No. 2 at different levels of F-4 traffic (12-in. PVC at 30.5-in. depth of cover)

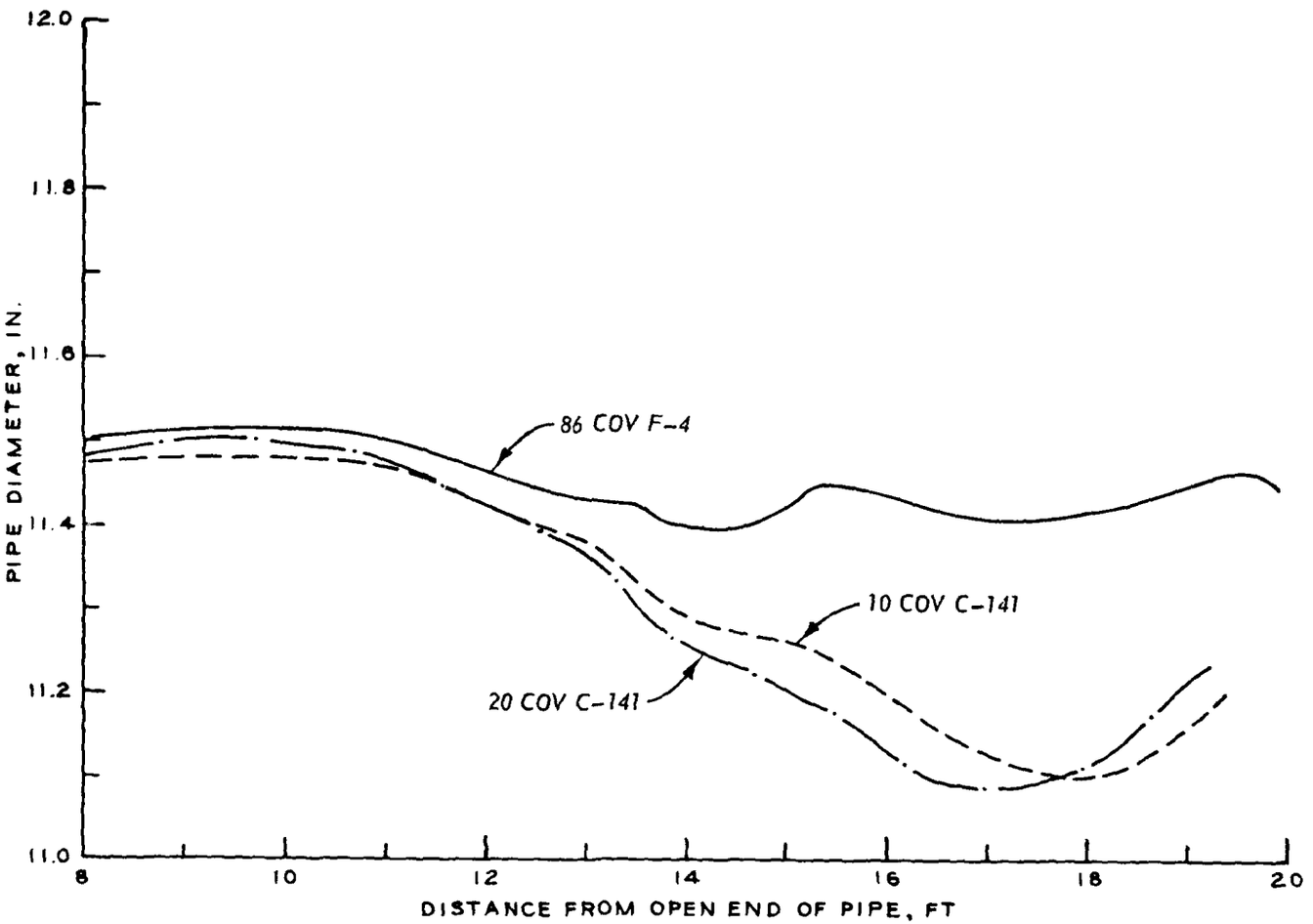

Figure B-50. Comparison of the permanent deflections of pipe No. 10 of Test Site No. 2 at different levels of C-141 traffic (12-in. PVC with 30.5-in. depth of cover)

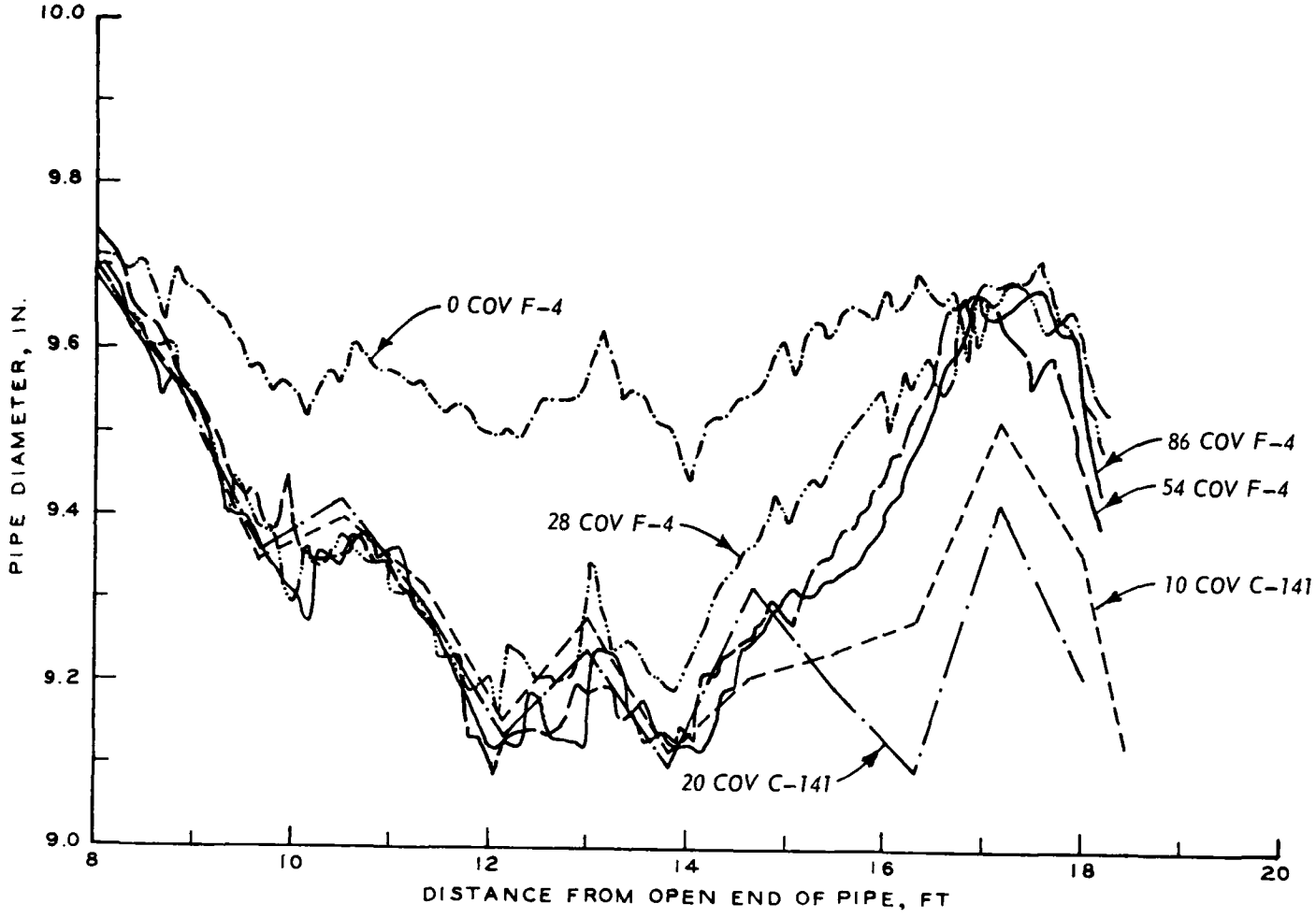

Figure B-51. Comparison of permanent deflection of pipe No. 11 of Test Site No. 2 at different levels of F-4 and C-141 traffic (10-in. PE with 24-in. depth of cover)

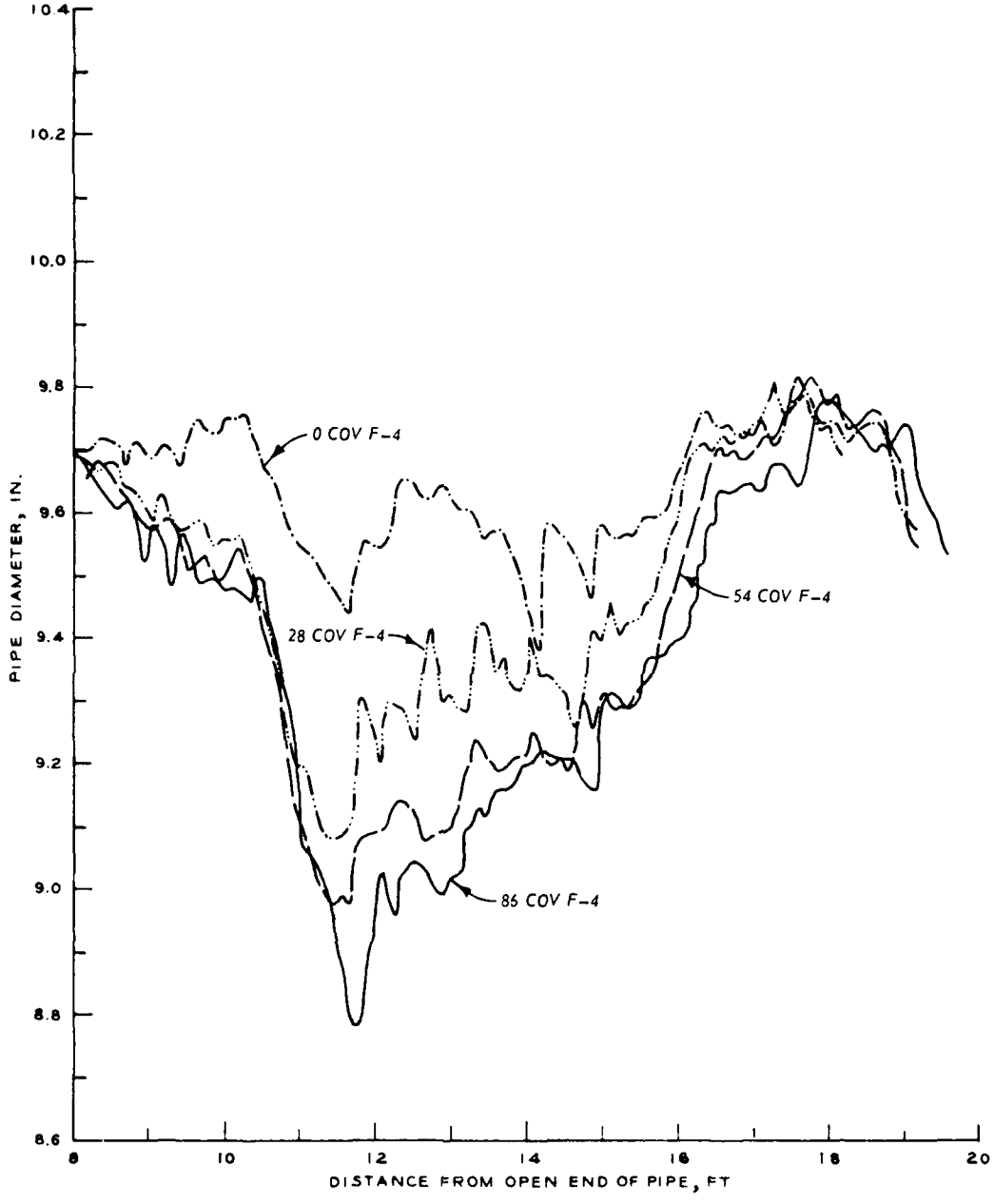

Figure B-52. Comparison of permanent deflections of pipe No. 12 of Test Site No. 2 at different levels of F-4 traffic (10-in. PE with 28-in. depth of cover)

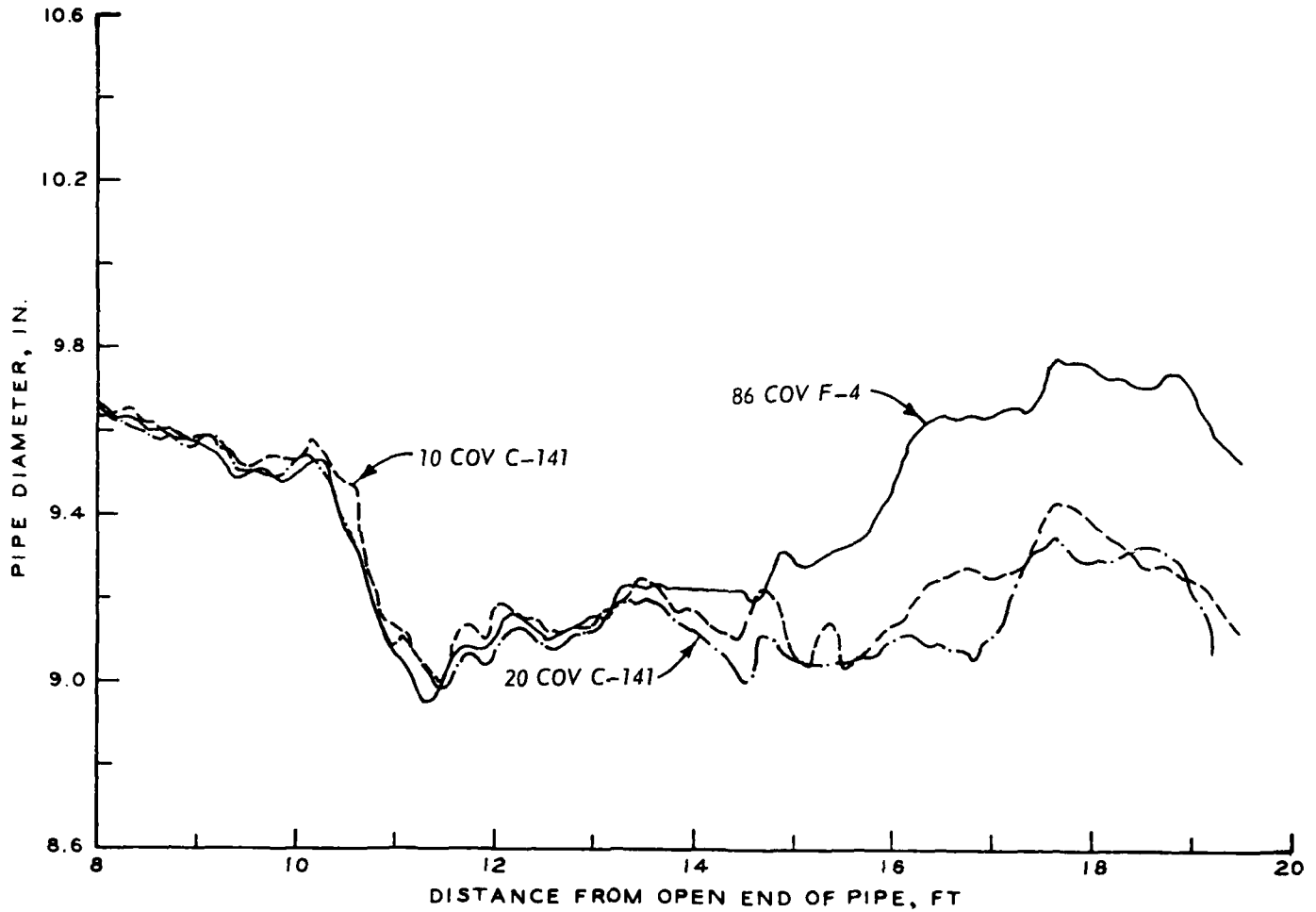

Figure B-53. Permanent deflection of pipe No. 12 of test site No. 2 at different levels of C-141 traffic (10-in. PE with 28-in. depth of cover)